Synthetic Explorations into Carbon-Carbon and Carbon-Nitrogen Bond Forming Reactions

Thesis Submitted to AcSIR For the Award of

the Degree of

DOCTOR OF PHILOSOPHY

In Chemical Sciences

By

Jayant Bhagvanji Rathod

(Registration Number: 10CC14J26003)

Under the guidance of

Dr. Pradeep Kumar

Co-guidance of

Dr. Santosh B. Mhaske

Division of Organic Chemistry

CSIR-National Chemical Laboratory,

Pune - 411 008, INDIA

August 2019

This dissertation is dedicated to

-My family-

Whose constant love, trust, and support

helped me reach this stage of my life

सीएसआईआर - राष्ट्रीय रासायनिक प्रयोगशाला
(वैज्ञानिक तथा औद्योगिक अनुसंधान परिषद)
डॉ. होमी भाभा मार्ग, पुणे - 411 008, भारत
CSIR - NATIONAL CHEMICAL LABORATORY
(Council of Scientific & Industrial Research)
Dr. Homi Bhabha Road, Pune - 411 008, India

CERTIFICATE

This is to certify that the work incorporated in this Ph.D. thesis entitled ***Synthetic Explorations into Carbon-Carbon and Carbon-Nitrogen Bond Forming Reactions*** submitted by Mr. ***Jayant Bhagvanji Rathod*** to Academy of Scientific and Innovative Research (AcSIR) in fulfillment of the requirements for the award of the Degree of ***Doctor of Philosophy***, embodies original research work under my/our supervision/guidance. I/We further certify that this work has not been submitted to any other University or Institution in part or full for the award of any degree or diploma. Research material obtained from other sources has been duly acknowledged in the thesis. Any text, illustration, table etc., used in the thesis from other sources, have been duly cited and acknowledged.

It is also certified that this work done by the student, under my supervision, is plagiarism free.

Jayant Bhagvanji Rathod	**Dr. Santosh B Mhaske**	**Dr. Pradeep Kumar**
(Research Student)	**(Co-guide)**	**(Research Supervisor)**
(Reg. No. 10CC14J26003)		

Date: 27th August 2019

Place: CSIR-NCL, Pune.

Communication Channels
NCL Level DID : 2590
NCL Board No. : +91-20-25902000
EPABX : +91-20-25893300
: +91-20-25893400
FAX
Director's Office : +91-20-25902601
COA's Office : +91-20-25902660
SPO's Office : +91-20-25902664
WEBSITE
www.ncl-india.org

Declaration by the Candidate

I hereby declare that the original research work embodied in this thesis entitled **"Synthetic Explorations into Carbon-Carbon and Carbon-Nitrogen Bond Forming Reactions"** submitted to Academy of Scientific and Innovative Research (AcSIR) for the award of the degree of Doctor of Philosophy (Ph.D.) is the outcome of experimental investigation carried out by me under the supervision of **Dr. Pradeep Kumar,** FNA, INSA Sr. Scientist, Former Head, Division of Organic Chemistry, CSIR-National Chemical Laboratory, Pune. I affirm that the work incorporated is original and has not been submitted to any other academy, university or institute for the award of any degree or diploma.

Jayant Bhagvanji Rathod

Senior Research Fellow,
(CSIR-SRF)
Organic Chemistry Division,
CSIR-National Chemical Laboratory,
Pune-411008

August 2019

It is a matter of immense privilege for me to express my deep sense of indebtedness to all those personalities whose guidance and support helped me in diversified ways. I am very contented to look back with a sense of contentment at the long journey of Ph.D., to be able to recapture some of the little moments with the number of peoples, some who were with me from the beginning, joined at different stages this beautiful voyage. Whose kindness, love, and blessings have brought me to this day. I wish to thank each of them from the bottom of my heart.

I would like to express my sincere gratitude to my research supervisor ***Dr. Pradeep Kumar*** *(Former Head, OCD, CSIR-NCL) for his continuous encouragement and support which helped me to complete this dissertation successfully. He provided me the freedom for work and his scientific brilliance, valuable guidance, and the motivation benefited me to overcome the faltered in this work. His traits, like perfectionism, self-discipline, and personal kindness, always inspired me, and it will benefit my career immeasurably.*

I take this opportunity to express my gratitude to my co-supervisor, Dr. Santosh B Mhaske, for his encouragement, and suggestions throughout my Ph.D. tenure.

I would like to express my sincere thanks to my doctoral Advisory Committee members, Dr. A.T. Biju, Dr. Nitin Patil, Dr. D. Srinivas, Dr. Utpal Das, Dr. M. Muthukrishnan and Dr. C. S. Gopinath for their continuous evaluation of my work and suggestions.

In fact, words fail to express my sincere feelings of gratitude to ***Prof. Anamik Shah,*** *(The Vice-Chancellor, Gujarat Vidyapith, Ahmedabad) for his endless encouragement, support and keen interest for shaping my career. Of course, training under him is my lifetime achievement at Department of Chemistry, Saurashtra University.*

I am thankful to Dr. Ashwini Nangia, Director, CSIR-NCL, Dr. Sourav Pal, Former Director, CSIR-NCL. I would also like to acknowledge the support from the Head, Dr. S. P. Chavan, and Former HODs, Division of Organic Chemistry for providing all the research facilities necessary to carry out my research work.

I have been privileged to interact with many eminent organic chemists, especially Dr. M. Sashidhar, Dr. C. V. Ramana, Dr. D. S. Reddy, Dr. R. Kontham, Dr. Pradip Maity, Dr. A. K. Bhattacharya, Dr. Monisha Fernandes, Dr. Smita Gadre.

I wish to thank OCD office staff Catherine madam, Deepika, Thangaraj, and Fernandes for their paper work & other documentation related assistance.

I express my gratitude towards Dr. P. R. Rajamohanan for their timely help in NMR analysis, Pramod, Dinesh, and Kavya for recording NMR spectra, Dr. Shantakumari for Mass/HRMS analysis. I would like to extend my sincere thanks to Dr. Rajesh Gonnade, Ekta Sangtani, Samir and Shridhar for their necessary help in X-Ray crystallographic analysis; Mrs. S. S. Kunte for HPLC analysis; Mrs. R. R. Damse for recording FTIR spectra and the support from Dr. Borikar for recording GCMS is highly acknowledged.

I would also like to extend my special thanks to Dr. A. P. Singh and Dr. Priti for their help in the synthesis and characterization of solid supported catalysts.

I especially thank my senior Dr. Brijesh Sharma, for his high-spirited discussion, training, and help to drive my research forward.

I gratefully acknowledge the training and support extended by my senior colleagues Dr. Ankush, Dr. Krishanu, Dr. Vishwajeet, Dr. Shruti, Dr. Nookaraju, and Kiran. I would also like to thank my lab colleagues Rohini, Arjun, Sunil, Dr. Shruti (NPDF), Nilesh, and Madhukar for maintaining a warm and cheerful atmosphere in the lab.

It is a pleasure to thank my departmental colleagues present and past Dr. Valmik, Dr. Yogesh, Dr. Paresh, Dr. Avinash, Dr. Pradip, Amol, Shom, Manjur, Indra, Ravindra, Virat, Balu, Sagar. I have been fortunate to be friends and roommate with Popat Shinde, Anil Yadav, Anil Mahida and Mahesh Neralkar; I always enjoyed the company for sharing our joys and sorrows.

I extend my thanks to the technical and office staff of NCL Mr. S. Mane, Atul Mahajan, Ashok Mahajan, K. D. Deshpande, P. V. Iyer sir and Kohle madam for their assistance.

I am also thankful to Council of Scientific & Industrial Research (CSIR), New Delhi for the financial assistance in the form of fellowship for JRF and SRF.

I would like to bow my head with utter respect to my parents; my expression fails to express my feelings in acknowledging the incredible debt that I owe to my beloved mother, Smt. Damyantiben and most esteemed father Shri Bhgvanjibhai. This study is only possible because of their blessings, love, inspiration, and sacrifice that I have been able to steer through my life.

Jayant Rathod

Contents

Chapter 3: Section A

Brønsted acid catalysed C-C bond formation via Michael addition of Vinyl azide to *p*-Quinone methides

Chapter 3: Section B

Gold catalysed C-C bond formation via 1,6-conjugate addition of *in situ* generated allenol acetate to *p*-Quinone methides

Units

°C	Degree centigrade
mg	Milligram
h	Hour
Hz	Hertz
µg	Microgram
mL	Millilitre
min	Minutes
MHz	Mega hertz
mmol	Millimole
nm	Nanometre
ppm	Parts per million

Chemical Notations

Ac	Acetyl
AcOH	Acetic Acid
Ar	Aryl
MeCN	Acetonitrile
n-BuLi	*n*-Butyl lithium
DMAP	N,N'-Dimethylaminopyridine
Et_2O	Diethyl Ether
t-BuOH	*tert*-Butyl alcohol
BINAP	(2,2'-bis(Diphenylphosphino)-1,1'-binaphthyl)
DCE	1,2-Dichloroethane
MeOH	Methanol
C_6D_6	Deuterated Benzene
$CDCl_3$	Deuterated Chloroform
CD_3OD	Deuterated Methanol
DDQ	2,3-Dichloro-5,6-dicyano-1,4-benzoquinone
Me	Methyl
Ph	Phenyl

DMF	N, N'-Dimethylformamide
EtOH	Ethanol
Et	Ethyl
EtOAc	Ethyl Acetate
THF	Tetrahydrofuran
K_2CO_3	Potassium carbonate
$Pd(OAc)_2$	Palladium acetate
Et_3N	Triethylamine
*i*Pr	Isopropyl
t-Bu	*tert*-Butyl
Cy	Cyclohexyl
KO*t*Bu	Potassium *tert*-butoxide
TBAB	Tetrabutyl ammonium bromide
DMSO	Dimethyl sulfoxide
NMP	N-Methyl-2-pyrrolidone
Tf_2NH	Triflimide
p-QMs	*p*-Quinone methides

Other Notations

calcd	Calculated
δ	Chemical shift
J	Coupling constant
equiv.	Equivalents
ESI	Electrospray ionization Mass spectrometry
HRMS	High Resolution Mass Spectrometry
IR	Infra Red
m/z	Mass-to-charge ratio
mp	Melting Point
NMR	Nuclear Magnetic Resonance
rt	Room temperature
SBA	Santa Barbara Amorphous
PMO	Periodic Mesoporous Organosilica

- ^{1}H and ^{13}C NMR analysis was done with Bruker 200, 300, 400, and 500 MHz spectrometer. Chemical shift are expressed in ppm relative to TMS, using the residual solvent peak of deuterated solvents as a reference. Coupling constants were calculated in Hertz. To represent the splitting pattern of NMR signal following abbreviations are used s = singlet, d = doublet, t = triplet, q = quartet, m = multiplet, br =broad. All deuterated solvents were used as received.
- Mass Spectra of known compounds were recorded on Polaris-Q Thermoscientific spectrometer and for new compounds HRMS spectra were recorded at UHPLC-MS (Q-exactive-Orbitrap Mass Spectrometer) using electron spray ionization (ESI+, +/− 5kV).
- Melting points were recorded on Buchi M-535, M-560 melting point apparatus by open capillary are uncorrected and the temperature measured in degree centigrade.
- All reactions were monitored by Thin layer chromatography (TLC) with 0.25 mm pre-coated silica gel on aluminium sheets 20 x 20cm, Silica gel 60 F_{254}, Merck grade. Using various visualizing agents such as UV light, Iodine adsorbed on silica gel, ethanolic solution of phosphomolybdic acid (PMA), *p*-anisaldehyde or $KMnO_4$ followed by heating with a hot air gun for ~10 sec.
- All solvents and reagents were purified and dried by according to documented procedures. All reactions were performed under inert atmosphere using nitrogen or argon gas.
- The synthesized compounds were purified by Column chromatography using silica gel (100-200 or 230-400 mesh size).
- Chemical name (IUPAC) and structures were drawn using ChemDraw Professional 15.1 software.
- The compound, scheme, figure and table numbers given in each section of chapter refer to the particular section of chapter only.
- All reagents, starting materials, and solvents were obtained from commercial suppliers and used as such without further purification.

Synopsis

AcSIR	**Synopsis of the Thesis to be Submitted to the Academy of Scientific and Innovative Research for Award of the Degree of Doctor of Philosophy in Chemical Science**
Name of the Candidate	**Jayant Bhagvanji Rathod**
AcSIR Enrolment No. & Date	**10CC14J26003; January 2014**
Faculty	**Chemical Sciences**
CSIR Lab Affiliated With	**Division of Organic Chemistry, CSIR-NCL, Pune**
Title of the Thesis	**Synthetic Explorations into Carbon-Carbon and Carbon-Nitrogen Bond Forming Reactions**
Research Supervisor/ Co-guide	**Dr. Pradeep Kumar / Dr. Santosh Mhaske**

Key words: *Biaryl Phosphine, Cross coupling, Heterogeneous catalyst, SBA 15, Gold, propargylic acetate, Click reaction, p-Quinone Methides, 1,6-conjugate addition, [3,3]-Sigmatropic rearrangement.*

The thesis mainly deals with the explorations of homogeneous palladium and heterogeneous Ruthenium catalyzed Carbon–Nitrogen bond forming reaction of aryl halide with amine and alkyne with sodium azide and benzyl bromide. Heterogeneous palladium, Gold and Brønsted acid catalysed C-C bond forming reaction is investigated by using cross coupling and Michael addition reaction of *p*-Quinone methide with nucleophile. The work demonstrated in this thesis has been divided into three chapters as described below.

***Chapter 1*: Development of Microwave assisted Pd catalysed C-N cross coupling reaction using C-1 symmetric biaryl phosphine ligands**

In last decade there has been tremendous upsurge of interest among the synthetic chemists in developing diverse methods for palladium-catalyzed C–N bond-forming reactions. Consequently, this synthetic transformation has gained utmost importance with its widespread use across various disciplines, such as the synthesis of key intermediates for fine chemicals, building blocks for pharmaceuticals, conducting polymers, and photographic materials. In this chapter, development of a new catalyst system and Microwave assisted C – N cross coupling of aryl halide and primary and secondary amine are described (Scheme 1), The method was found to be highly efficient and reaction completion time was reduced to the 10 -15 min from 24 h to 48 h

Scheme 1:

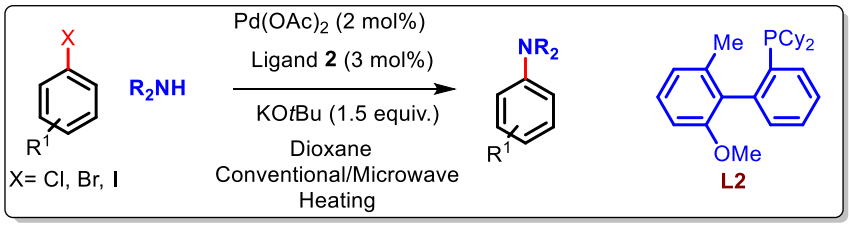

***Chapter 2*: Section A: Synthesis of SBA-15 supported heterogeneous Ru(II)-1,2,3-Triazole catalyst: Application to the 1,4-selective click reaction for C-N bond formation**

In this section we have demonstrated a simple and efficient method for ligand formation and covalent anchoring to heterogeneous support via click reaction. The complex tris(triphenylphosphine) ruthenium(II) dichloride [$RuCl_2(PPh_3)_3$] anchored over the click modified ligand of SBA-15, forms a new highly efficient heterogeneous SBA-15-Tz-Ru(II)TPP catalyst. Solid state ^{13}C, ^{29}Si, & ^{31}P CP-MAS NMR spectra provide evidence for the formation of the heterogeneous catalyst. SBA-15-Tz-Ru(II)TPP catalyst was screened for the multi component click cycloaddition reaction in water medium as green solvent, exhibited unusual and excellent selectivity for the formation of 1,4-disubstituted triazole product under mild reaction condition. In addition, SBA-15-Tz-Ru(II)TPP catalyst also catalyzed the hydrogen transfer reaction of various carbonyl compounds with excellent catalytic activity to give the corresponding alcohols. The heterogeneous catalyst can be recycled and reused several times (five) without the loss in reactivity.

Scheme 2:

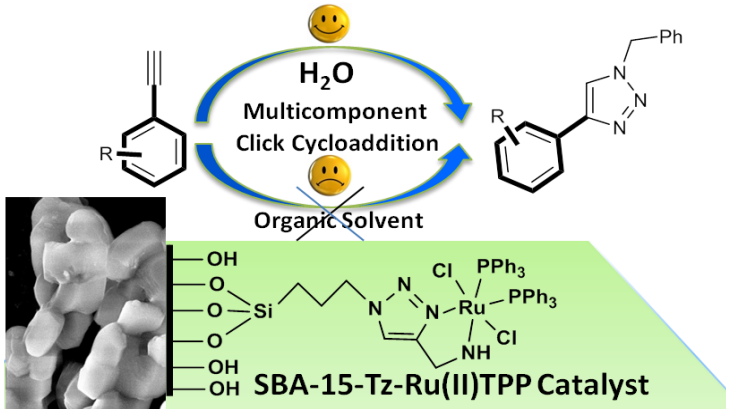

Section B: PMO silica supported Pd complex as heterogeneous catalyst: The recyclable tool for C-C bond forming reactions

Palladium catalyzed cross-coupling reactions are the most fundamental and practical method for carbon-carbon bond formation of aryl halides with various nucleophiles in organic synthesis. Various supported heterogeneous palladium catalysts have been reported in the literature which includes palladium supported over polymer/dendrimer, on carbon, supported on metal oxides, clays, molecular sieves, mesopores and nanopores etc. For the heterogeneous support ordered mesoporous material SBA-15; high surface areas, easily accessible surface sites, uniform pore sizes and good stability constitute the basis of promising suitable substitute as mesoporous support. Heterogeneous surfaces should be modified by organic functional groups for anchoring metals and complexes. In this section, catalytic activity of heterogeneous SBA-15-EDTA-Pd(11) catalyst was screened for Heck, Stille & Kumada cross-coupling reactions (Scheme 3). Catalytic system exhibited excellent activity (Pd loading is 0.87 mmol %) with excellent yields. Covalently anchored heterogeneous SBA-15-EDTA-Pd(11) catalyst can be recycled for more than five times without noticeable loss in activity & selectivity.

Scheme 3:

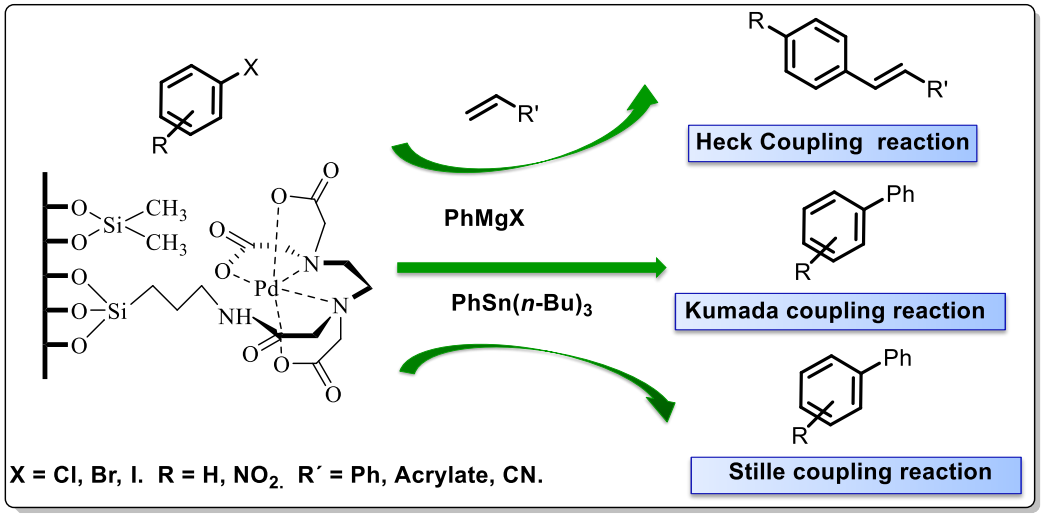

***Chapter 3*: Section A: Brønsted acid catalysed C-C bond formation via Michael addition of Vinyl azide to *p*-Quinone methides**

In recent years, the *p*-Quinone methide derivatives gained attraction among synthetic organic chemistry, due to its unique reactivity and its ability for 1,6-conjugate addition with a variety

of nucleophiles. *p*-Quinone methide motif serves as an important reactive intermediate in various natural product syntheses and biosynthetic transformations. Recently, *p*-quinone methides (*p*-QMs) were extensively studied for addition reaction, using the Lewis acid, organocatalytic, and transition-metal-catalyzed transformations. In this section, Tf_2NH-catalyzed tandem 1,6-conjugate addition/Schmidt type rearrangement using vinyl azides and p-quinone methides to access a variety of *β*-bis-arylated amides is described (Scheme 4). The method is quick, efficient, mild, and high yielding with broad substrate scope.

Scheme 4:

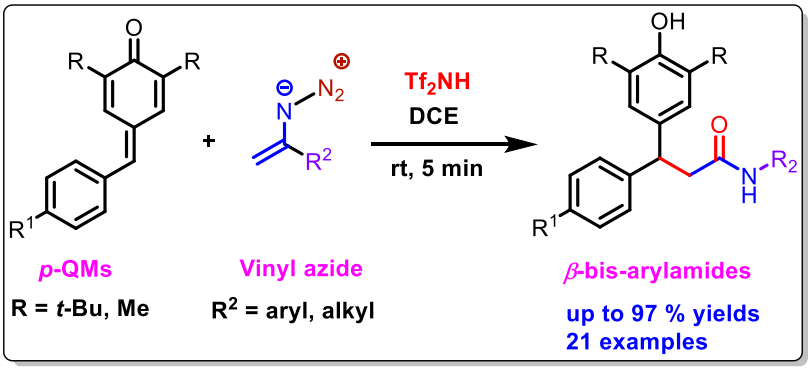

Section B: Gold catalysed C-C bond formation via 1,6-conjugate addition of *in situ* generated allenol acetate to *p*-Quinone methides

In recent years, there has been tremendous upsurge of interest in the homogeneous gold catalyzed activation of C–C triple bond and allenes for constructing novel molecular architectures or structural core of natural products/analogs in a cascade fashion. The gold catalyzed [3,3]-sigmatropic rearrangement of propargylic acetate to allenol ester followed by electrophilic activation by gold (I)/(III) complexes towards nucleophilic attack, encompassing both inter- and intramolecular variants, are among the most exploited reactions. However, till date, there are only few reports which deal with inherent nucleophilicity of *in situ* generated allenol ester towards intermolecular electrophilic addition through gold catalyzed [3,3]-sigmatropic rearrangement reaction in C–C bond formation. In this section, A gold (I) catalyzed protocol for intermolecular 1,6-conjugate addition of nucleophilic allenol ester generated *in situ* through [3,3]-sigmatropic rearrangement with *p*-quinone methides (*p*-QMs) has been developed. The gold catalyst plays a dual role by the π-acid-triggered activation of alkynes; and at the same time as a Lewis acid for activation of *p*-QMs towards nucleophilic

attack. This method enables rapid access to wide range of densely functionalized diarylmethine-substituted enones, a Morita-Baylis-Hillman (MBH) product with high selectivity, excellent yields, and broad substrate scope.

Scheme 4:

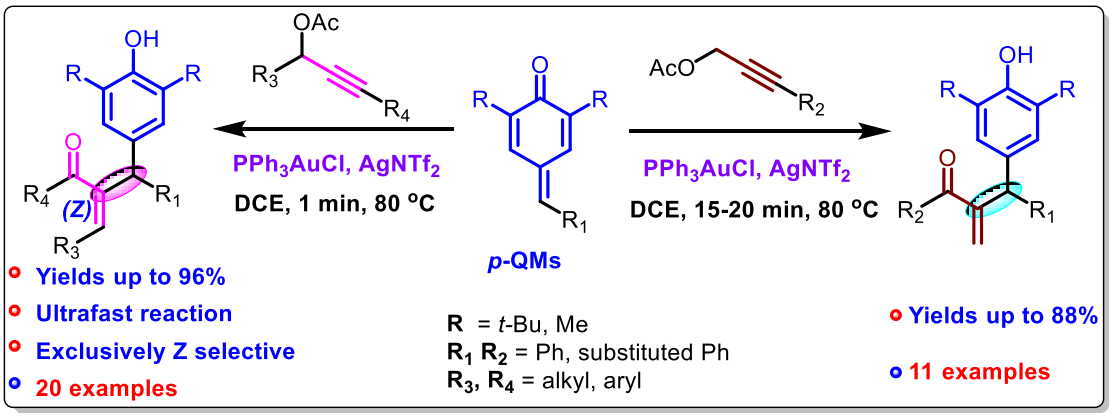

<u>Noteworthy Findings</u>:

- Developed, Microwave assisted Pd catalysed C-N coupling reaction using C-1 symmetric biaryl phosphine ligand, The developed catalyst was useful for the primary and secondary aromatic and aliphatic amines.

- Developed, SBA 15 suppored Ru and Pd heterogeneous catalyst: and its further application for the multicomponant click reaction with the unusual highly selective outcome, and for the various C – C bond forming reaction respectively.

- Developed, Brønsted acid and Gold catalyzed 1,6-conjugate addition reaction of vinyl azide and propargylic acetate with variety of *p*-Quinone methides, which yielded interesting organic framework like *β*-bis aryl amide and *α*-substituted enones.

Chapter 1

Development of Microwave-assisted Pd catalyzed C-N cross-coupling reaction using C-1 symmetric biaryl phosphine ligands

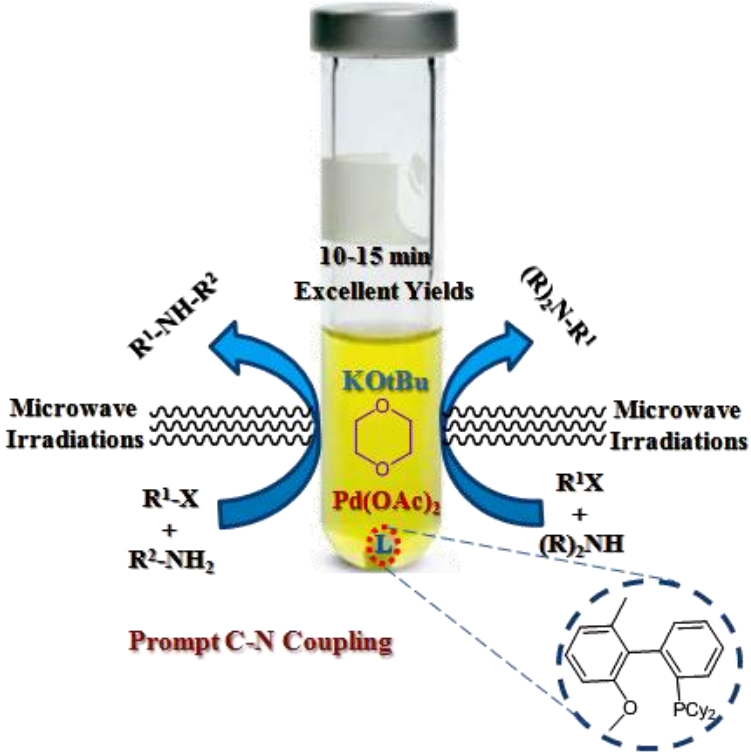

1.1 Introduction

In the last few years, the Palladium-catalyzed coupling of an aryl halide and pseudo-halide with amines has been exploited well in the development of the diverse synthetic strategy to construct the C–N bonds. Consequently, this cross-coupling transformation emerged as an exceedingly methods with its utmost applications in numerous disciplines of fundamental and industrial research like the production of fine chemicals intermediate, pharmaceutical building blocks, synthesis of various polymers and photographic materials, etc.[1]

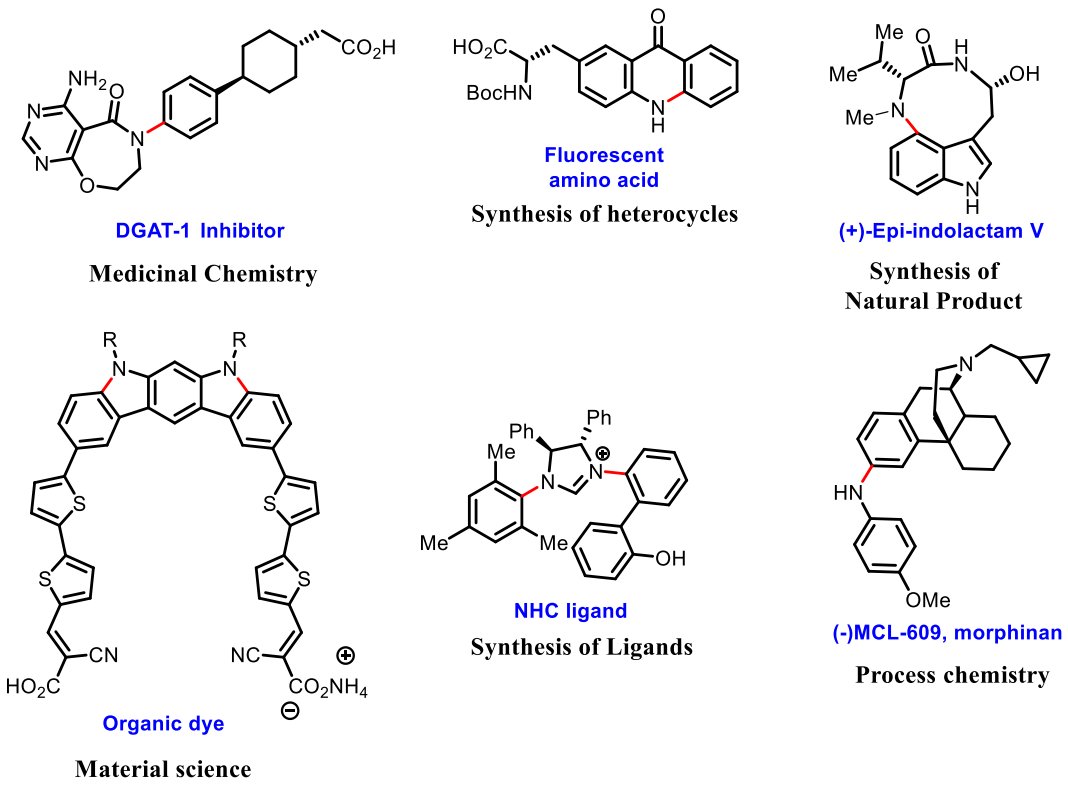

Figure 1: Important organic molecules containing aromatic C-N bonds

Due to the extensive occurrence of substituted arylamines in the natural product, API, Organic materials and Ligands/ catalysts (figure 1); the stitching of the C-N bond finds widespread applications in chemical industries, despite continuous development in palladium catalyzed C-N coupling reactions for the improvement in ligands and catalysts activity.[2] Several reported catalyst systems suffer from limitations such as reaction time, functional group tolerance, sensitive and expensive catalyst, etc. Therefore a versatile, consistent and user-friendly synthetic method to access the functionalized aromatic amine via C-N cross coupling is highly desirable.

The initial reports for the C-N coupling including copper catalyzed Ullmann coupling and nucleophilic aromatic substitution revealed either of them suffer from the substrate scope. Subsequently, Pd-catalyzed coupling reaction was extensively investigated for the designing the ligand and mechanistic studies led the reaction conditions to significantly general with the wide range of coupling substrates and evolved as an exciting alternative to the traditional methods for the coupling.[3]

Development and identification of broad classes of phosphine ligands with broad applicability have a contribution to the rapid growth in the Pd-catalysed C-N coupling reaction.[4] Typically, MOP-type mono phosphine containing biaryl skeleton with either aryl or alkyl group as substituents, N-Heterocyclic carbenes (NHC) have been extensively studied for these transformations. [5, 6]

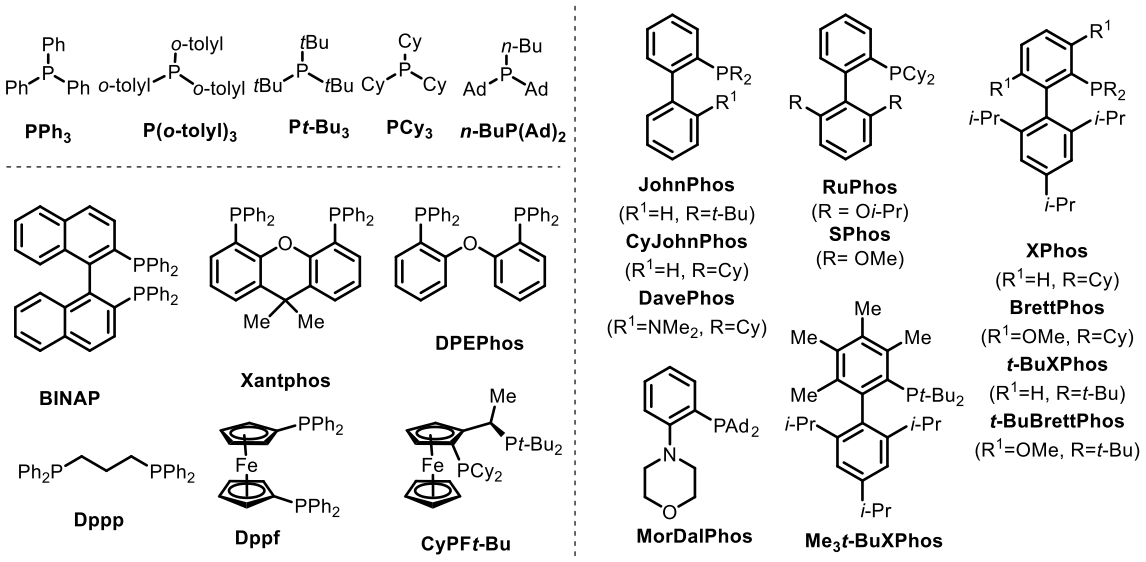

Figure 2: The family of the most frequently used phosphine ligand in the C-N coupling reaction

The most commonly considered class of compounds for the C-N coupling transformations are summarised in figure 2. These could be classified mainly as, symmetric monodentate phosphine ligands such as PR_3 type ligands containing same or different aryl and alkyl substituents,[7] symmetric bidentate ligands such as BINAP,[7, 8] DPEPhose,[7] Dppf,[9] Dppp, [7] Hantphos[10] and the third class of ligands is asymmetric monodentate phosphine compounds such as CyPFt-Bu,[11] MorDalPhos,[12] BippyPhos,[13] etc. Asymmetric dialkyl biaryl phosphines[14] class is profoundly explored for C-N bond making reactions using the benefit of structural variability. To overcome the limitation of the catalyst system, and achieve the desired reactivity as well as selectivity, the phosphine ligand can be tuned by

changing the electronic parameter with substituents. Since last decade Buchwald and co-workers have been working for the development of the improved biaryl monophosphine based catalyst/ligand (figure 2) system for the cross-coupling transformation.[15] In order to develop improved and the more versatile method, many other groups have thoroughly investigated by employing the various palladium source, and ligands also studied the mechanistic pathway of the reaction to understand the mechanism.[16, 17]

1.2 Literature reports:

1.2.1 Applications of C−N Coupling in the Synthesis of Heterocycles:

The heterocycles with N-heteroatom are widely spread structural motif in the pharmaceuticals,[18] natural products, and other organic materials. The construction of N-heterocyclic compounds using palladium catalyzed C-N cross-coupling reaction gives essential advantages to the traditional procedures. In 2008, Troels Dahl *et al.* reported the process for the construction of *N*-heterocycles using Pd-catalyzed cross-coupling. It was the first one-pot method to construct the tricyclic biologically important N-substituted phenothiazines via multiple coupling of amine, 2-bromothiophenol and functionalized 1-bromo-2-iodobenzene using only one catalyst system (Scheme 1).[19] Other groups of chemist, Willis and co-worker[20] and Buchwald *et al.*,[21] have developed the tandem processes for the coupling of aromatic halide and urea, the critical precursor for the synthesis of a variety of heterocycles.

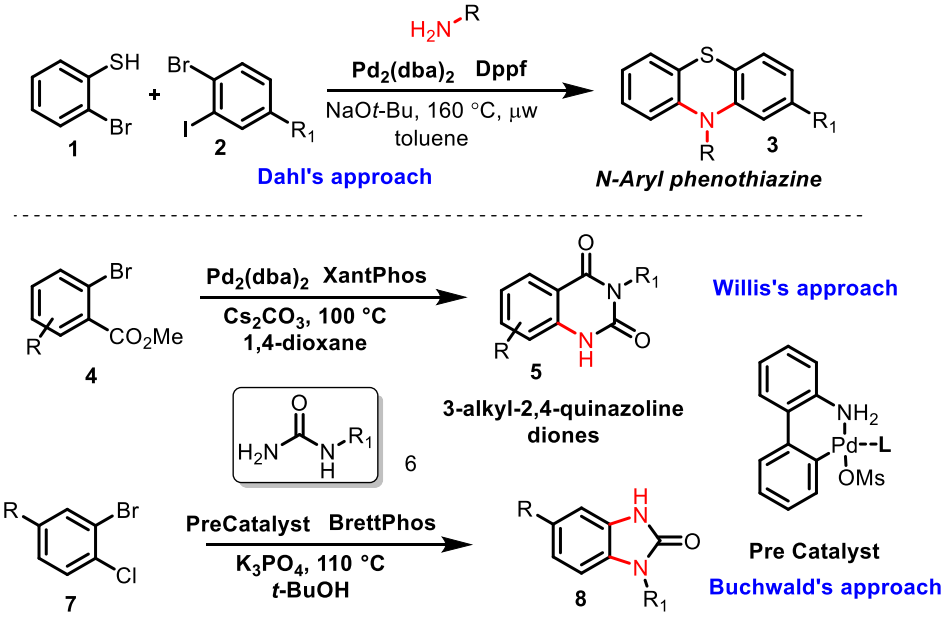

Scheme 1: Synthesis of N-heterocycles via C-N cross coupling

They have reported the alternative method for the sequential functionalization of N1 and N3 which leads to the formation of single region isomer. Using these approach an array of the complex and polycyclic framework with several heteroatoms have been constructed from simple organic precursors.

1.2.2 Applications of C−N Coupling in Medicinal Chemistry

Nitrogen-containing important biologically active compounds occur widely in our Mother Nature. To study these compounds for the applicability for the society, the integration of synthesis of N-heterocycle in the pharmaceutical industries is rapidly growing. Since last decade, Palladium-catalysed C-N cross-coupling reaction becomes an essential tool in the medicinal chemistry for the development of the libraries of a variety of biologically active organic molecules.[22] Jensen and co-workers reported tandem N-arylation for the synthesis 3,7-substituted analogs of dibenzazepines, the antidepressant drug molecule Imipramine[23] by cross-coupling using palladium catalyst under microwave condition (Scheme 2). Grøtli and co-worker have reported the synthesis of chromone analogs via cross-coupling reaction of chloride derivative with a primary amine under the microwave conditions, using Dppp and CyJhonPhos ligand with palladium catalyst. The prepared chromone derivatives were found active against human breast cancer.[24] Many other scientists also reported the synthesis of biologically essential N-heterocycles by employing the Pd-catalysed cross-coupling reaction using supporting ligands.[25]

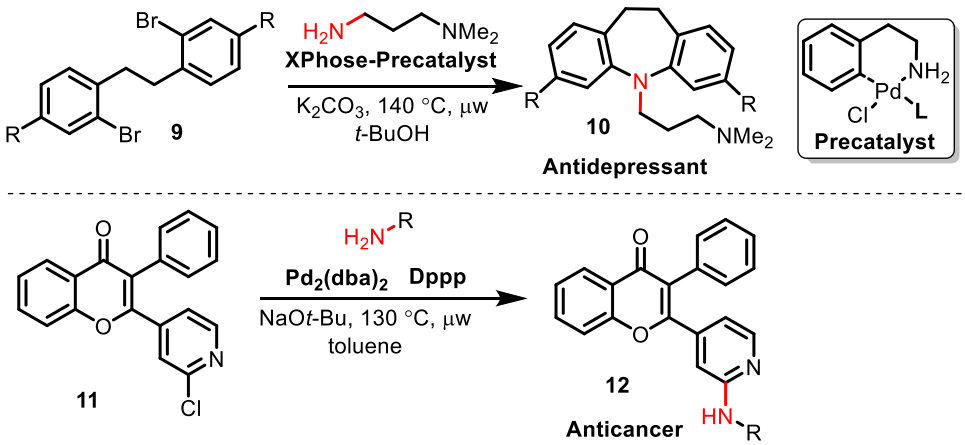

Scheme 2: Applications of C−N Coupling in medicinal chemistry

1.2.3 Applications of C−N Coupling in Process Chemistry

Due to the various important feature of the C-N coupling reaction, application in the large scale production became attractive. Since last few years, N-arylation reaction is quickly growing to the process chemistry due to the low catalyst loading and high activity.[26]

The exciting finding in the catalyst development like large scale metal scavenger [27] using functionalized organosilica [28] and fixed bed absorption method,[29] gear up the scalability of the medicinal chemistry route for N-arylation reactions for the synthesis of pharmaceutically active compounds. These new technologies could achieve a lower level of the residual palladium content according to the regulatory guidelines for the API. Leahy and co-workers have developed large scale synthesis of intermediate **15** of CGRP receptor antagonists compound **16** used for the curing from migraine. The established route is significantly improved from the earlier reports in aspects of cost-cutting by enabling the use of cheap starting materials, and the overall yield also improved (Scheme 3). Previously, the NH_2 group incorporated in the molecule using LHMDS or NH_3 gas which led to the generation of by-products and reduced the yield of desired products. The reported method is highly efficient with over two steps 80% yield and overcomes the limitation of by-products formation. Further, generation of primary amine group in the biologically active core molecules has been reported using Pd-catalysed cross-coupling reaction.[30]

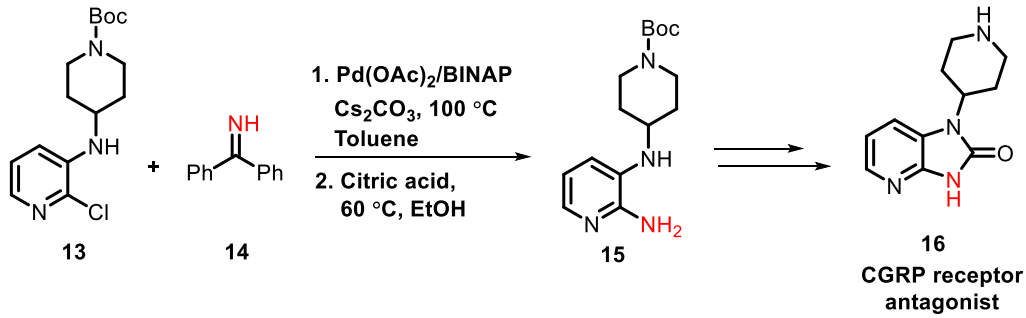

Scheme 3: Process-scale coupling of benzophenone imine

1.2.4. Applications in the Synthesis of Natural Products.

N-Arylation reaction has a vital role in challenging transformations for the construction of the core structure of natural product in total synthesis. The versatility of the C-N coupling reaction enables the late-stage construction of the complex structure by making new C-N bond and generation of N-centre with protection which can be used for further functionalization to achieve the target molecule. Many scientists have completed the total synthesis of nitrogen-containing complex natural product using the C-N cross-coupling protocol,[31] few of them are shown in scheme 4. Piersanti and co-workers have constructed the natural product (+)-*epi*-indolactam-V **19** via Pd catalyzed intramolecular C-N coupling reaction of intermediate **17** (Scheme 4).[32] Macro-cyclization was accomplished using the XPhos ligand in combination with pre-catalyst with 72% yield. Chida and co-workers have

reported the construction of N-substituted carbazole framework present in the biologically active alkaloid murrayazoline **23**, using double C-N coupling reaction of bromo derivative of biphenyl (compound **20**) with the other primary amine-containing coupling partner **21** (Scheme 4).[33]

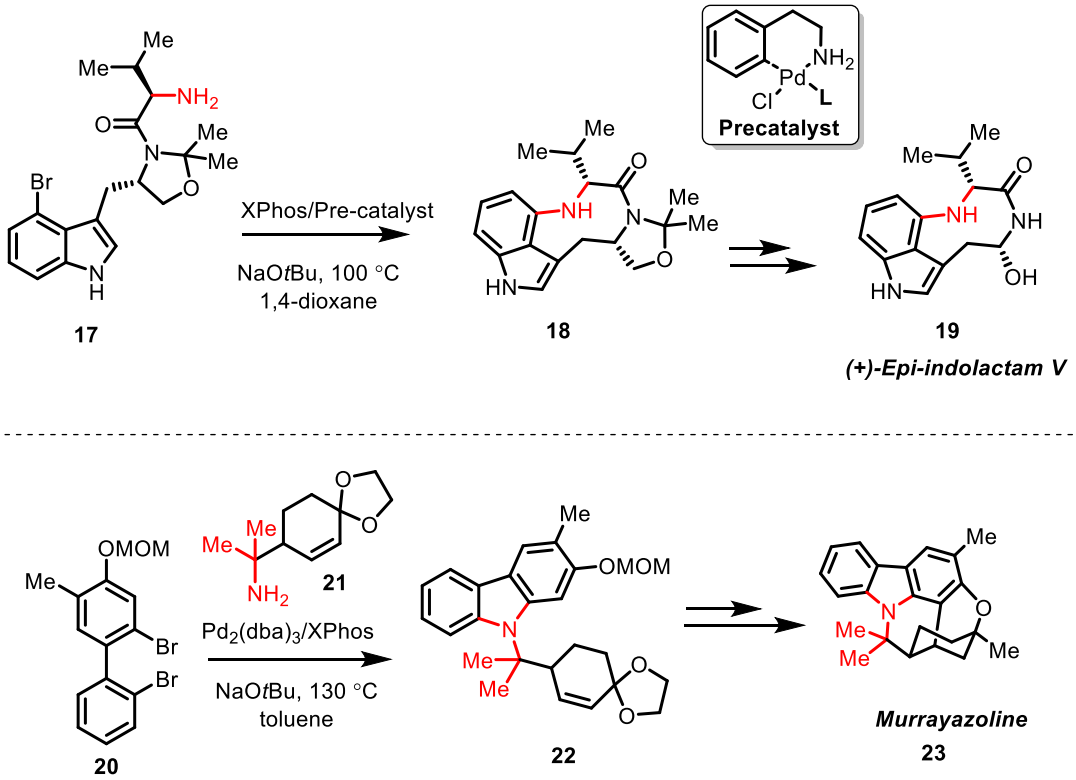

Scheme 4: N-Arylation in the synthesis of natural products.

1.2.5. Applications in Materials Chemistry and Chemical Biology

The organic materials with a highly conjugated system with electron donating functional group with nitrogen atom are widely used in material sciences research. Multiple N-arylation reactions were carried out with numerous functionalities on aryl halide and with more than one nucleophilic nitrogen atom is employed for the synthesis of target materials.[34] Mata and Luedtke have developed a fluorescent probe for proton-coupled DNA folding detection. The advanced intermediate **25** of ^{DMA}C Nucleoside **26** was synthesized by coupling of deoxycytidine **24** and dimethylaniline using JohnPhos/$Pd_2(dba)_3$ catalyst system (Scheme 5).[35] Edkins and Marder et al. have developed the general method for the functionalization of pyrenes, which has multiple applications in material science. Pyrene was sequentially functionalized with electron withdrawing nucleophile ($^{-}$CN) and secondary alkyl amine at 2 and 7 positions as a 2-cyano-7-(N, N-diethylamino) pyrene **28** (Scheme 5).[36] This method enables to prepare the donor and acceptor functional group at the opposite side of the conjugated system; the

material is useful in the optoelectronics. Nazir and co-workers developed the fluorescent molecule by attaching the dialkyl amines with thioxanthone as an electron donor group, which increased the quantum yield of the synthesized fluorescent molecule **30** (Scheme 5).[37]

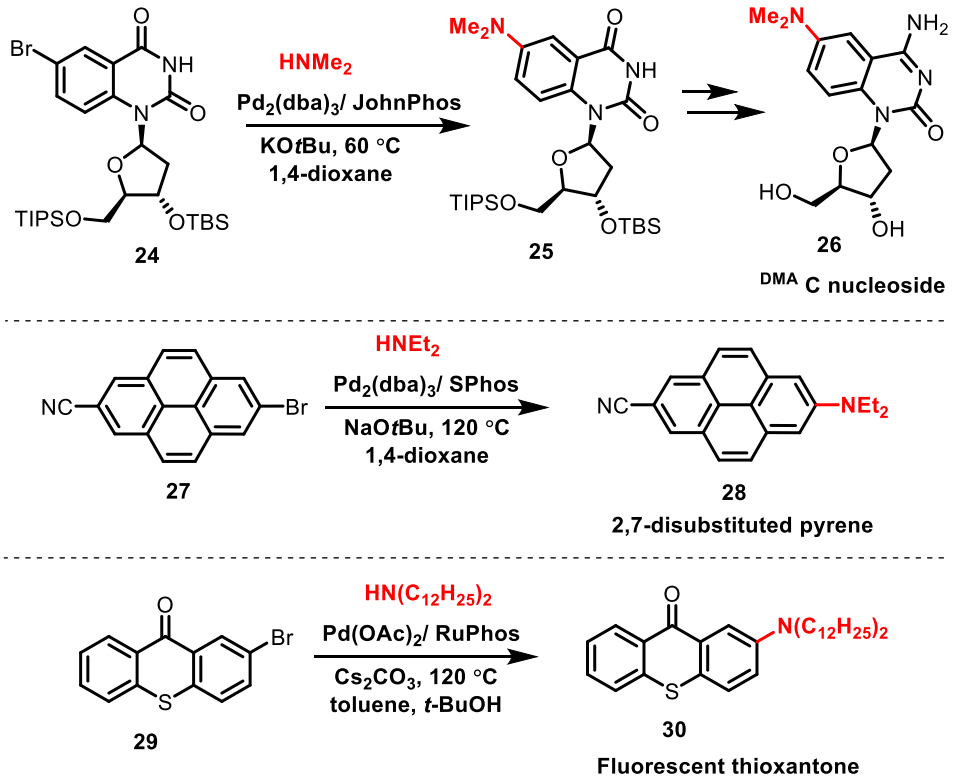

Scheme 5: C-N cross-coupling in materials chemistry and chemical biology

1.3 Present Work:

The recently Buchwald and co-workers extensively studied the catalyst system for Pd-catalysed N-arylation reaction to make it versatile. By carefully observing the reported catalyst system the structure of supporting ligand and the substituents present on the ligands play crucial role in the catalyst activity. With above literature background, it was envisioned that the new C-1 symmetric phosphine ligands (figure 3) synthesized by our French collaborator as a part of the on-going research program, could be employed for the N-arylation reaction. We have screened the ligands for the C-N cross-coupling with a primary and secondary amine with various aryl halides under microwave condition. The proposed ligands system L2/L5 with $Pd(OAc)_2$ was found to be the best in catalyst activity and reaction time.

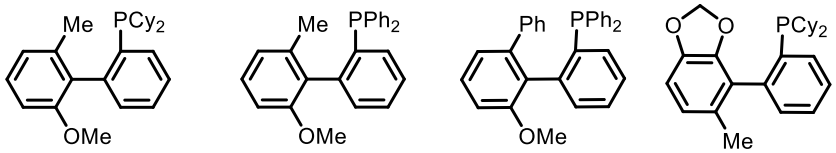

Ligand **L**

Figure 3: The new C-1 symmetric ligands for N-arylation reaction

1.4 Results and discussion:

1.4.1 Optimization of reaction conditions

Having biaryl phosphine ligands with substituents on the phosphorus atom and also in the phenyl rings in hand, we have examined the influence of electronic and steric factor of these substituents by careful ligand screening for optimization of efficient reaction conditions.

Table 1: Optimization of reaction conditions for coupling of dibutyl amine with bromobenzene under conventional heating.

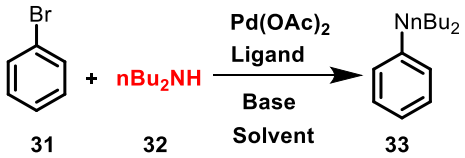

Entry	Ligand	Solvent	Temp/ °C	Base	Time (h)	Yield/ %[b]
1	**2**	DME	85	Cs_2CO_3	18	12 %[b]
2	**4**	DME	85	Cs_2CO_3	18	10 %
3	**5**	DME	85	Cs_2CO_3	18	16 %
4	**3**	DME	85	Cs_2CO_3	18	12 %
5	**2**	THF	66	KOtBu	16	40%
6	**2**	**toluene**	**110**	**KO*t*Bu**	**14**	**90 %**
7	**2**	*m*-xylene	139	KO*t*Bu	24	68%
8	**2**	*p*-xylene	140	KO*t*Bu	24	60%
9	**2**	mesitylene	145	KO*t*Bu	8	48%
10	**2**	**dioxane**	**110**	**KO*t*Bu**	**6**	**90%**
11	**5**	dioxane	110	KO*t*Bu	6	85 %
12	-	toluene	110	KO*t*Bu	24	n.r.
13	**3**	toluene	110	KO*t*Bu	14	8 %

[a]Reaction Conditions: bromobenzen (1.2 equiv.), *n*-Bu_2NH (1 equiv.), base (1.5 eq.), $Pd(OAc)_2$ (2 mol%), ligand (3 mol%); DME = Dimethoxy ethane. [b] Isolated yield after column chromatography.

Toward this end, we then decided to screen different Pd/ligand systems to find the most suitable one for the N-arylation of both primary and secondary amines with various aryl halides. Bromobenzene and di-*n*-butylamine were chosen as a model substrate for the coupling reaction. Initially, we have examined the influence of the requisite components for the catalyst activity. Solvents also play an important role during the reaction as it stabilizes the intermediate and provides the homogeneity for the reactant, the obtained results are illustrated in Table-1

At the beginning of the optimization, various solvents were screened for the reaction. The N-arylation reaction was firstly performed in dimethoxyethane as solvent under reflux conditions, even on prolonged reaction up to 18-24 h and also on changing the new ligands L2 to L5, the desired product was obtained only in meager yields (10-16%, Table-1, entries 1-4). When we switched the solvent to THF the yield of the desired compound was increased up to 40% (Table-1, entry 5). Further to optimize the condition, the reaction was performed in toluene using $Pd(OAc)_2$/Ligand(L2) as a catalyst system and KO*t*Bu as a base, the reaction was completed on prolongation up to the 14h under reflux condition and to our delight the desired product **33** was obtained in 90% yield (Table 1, entry 6).

In order to reduce the time, further, the coupling reaction was performed with high boiling solvents like *m*- or *p*- xylene and mesitylene at elevated temperature with the same catalyst system used in reaction condition of entry 6. However the desired compound **33** was obtained in the lower yield as compared to the reaction in toluene (Table-1, 68%, entry 7; 60%, entry 8; and 48%, entry 9). Further to reduce the reaction time, the solvent 1, 4-dioxane was used with $Pd(OAc)_2$/Ligand(L2) and KO*t*Bu as base which afforded the maximum yield of the coupled product and the reaction time was considerably reduced to 6 h (Table-1, entry 10). Further, we have tested the other ligand L5 under the optimized condition which was also found to be effective with almost comparable catalytic activity (Table-1, entry 11). The ligand L3 and L4 were used for coupling reaction but ended up with a lower yield (Entry 13). Without any ligand, the coupling reaction did not proceed at all (Table 1, entry 12). So, from these observations, we could conclude that aliphatic substitution present on the phosphorus atom of ligand plays a role in the ease of C-N cross-coupling reaction. Among various bases and ligands screened for the C-N coupling reactions, the potassium *tert*-butoxide, ligand L2 and L5 using $Pd(OAc)_2$ as a source for palladium in 1, 4-dioxane was found to be the best.

1.4.2 Scope of the C-N cross coupling reaction

Encouraged by the above results, additionally, we have investigated the N-arylation reaction of an aryl halide and primary amines. To obtain the best possible results under the above-optimized conditions, we commenced our study with model substrate aniline as primary amine and halo source as iodobenzene, the obtained results are illustrated in table 2.

Table 2: Optimization of reaction conditions for C-N cross-coupling of aniline with iodobenzene

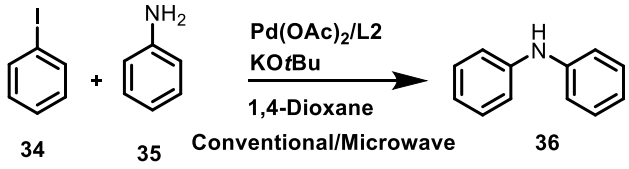

Entry	Catalyst	Ligand	Solvent	Base	Reaction time	% Yield
1[a]	$Pd(OAc)_2$	L2	1,4-Dioxane	KOtBu	2h	trace
2[b]	$Pd(OAc)_2$	L2	1,4-Dioxane	KOtBu	1h	15
3[c]	$Pd(OAc)_2$	L2	1,4-Dioxane	KOtBu	2h	75

a) Reaction at room temperature. **b)** Reaction at 100^{o}C. **c)** Reaction at 100^{o}C, before heating, Argon gas was purged for 10 min.

Even at room temperature within 2 h the aniline was completly consumed and formed the azobenzene as major by-product (Table 2 entry 1), the almost same result was obtained while the reaction was heated at 100 ^{o}C for 1-2 h in the presence of KO*t*Bu in 1,4-dioxane with lower yields (15%) of the desired diphenyl amine **36** (Table 2, entry 2). A significant amount of azobenzene was formed as a by-product due to the aerobic oxidation of aniline. To prevent the aerobic oxidation and increase the yield of diarylamine **36**, before heating the reaction mixture was purged with inert gas for 10 minutes in the reaction vessel to maintain inert condition. To our delight, the required diphenyl amine **36** was obtained in 75% yield (Table- 2, entry 3). Thus, from these observations it was clear, the primary amine is highly susceptible for the air oxidation so, we decided to carry out all the N-arylation reaction under the inert atmosphere.

As indicated in Table 1, the coupling of secondary amine and aryl halide requires long time (6 h) to complete the reaction, we envisioned that the reaction could be done under

microwave heating in place of conventional heating in order to reduce the time period. The Anton par Monowave-400, (Glass vial-G10**)** was used to perform the reactions. The coupling of bromobenzene with dibutylamine was carried out under the optimized condition with the assistance of microwave irradiation and heated up to the 160°C; delightfully the reaction time drastically reduced to 10 minutes furnishing the desired product in 90% yield (Table 3, entry 1). Similarly, the coupling of iodobenzene with primary amine aniline under the same reaction condition was also completed within 10 minutes affording the product in excellent yield (Table 3, entry 2).

Table 3 Optimization of reaction conditions for C-N coupling of the primary & secondary amine with aryl halide under the Microwave irradiation

Entry	Catalyst	Ligand	Solvent	Base	Reaction time	% Yield[c]
1	$Pd(OAc)_2$	1	1,4-Dioxane	KOtBu	10 min	90 %[a]
2	$Pd(OAc)_2$	1	1,4-Dioxane	KOtBu	10 min	85%[b]

a) The reaction of bromobenzene with dibutylamine, b) Reaction of iodobenzene with aniline, c) Isolated Yield (Anton par Monowave-400, Glass vial-G10)

After the best-optimized catalyst system in hand, to prove the versatility of it, we carried out systematic screening of N-arylation reaction employing the variety of primary and secondary amines with various aryl halides using the developed catalyst system. It should be noted that the coupling of primary amines and aryl halides is the most challenging in N-arylation reaction. Reductive dehalogenation of aryl halides is usually encountered with primary amines, and the product is often contaminated with tertiary amines which could result due to competing mono- and diarylation reactions. Buchwald and co-workers have developed the monodentate biaryl phosphine based ligands BrettPhos and RuPhos for the C-N cross-coupling reaction. The BrettPhos[38] ligand efficiently worked for the monoarylation of primary amines but was not suitable for coupling of secondary amines. While another ligand RuPhos[39] was effectively useful only for the N-arylation of secondary amines but ineffective with the coupling of primary amine. Because of this, a multi-ligand based Pd catalyst for C-N coupling reactions was also reported for both primary and secondary amines by combining the activity of both the ligands.[40]

In the backdrop of literature reports, we became interested in scrutinizing the efficacy of our monodentate biaryl phosphine ligand L2 for the N-arylation of both primary and

secondary amines with a variety of aryl halides under the optimized conditions. As illustrated in Table 4, various secondary amines underwent coupling reaction efficiently using our developed protocol. Firstly, the developed catalyst system was employed with conventional heating for the reaction of dibutyl amine with aryl halide, such as chloro, bromo, and iodobenzene furnishing the coupled products in excellent yields. The reaction becomes sluggish when chlorobenzene was used for the N-arylation. Similarly, under microwave irradiation, the reaction was completed within 10 minutes irrespective of the aryl halide used for the coupling, affording the desired products in comparable yields (**39a**). The N-arylation reaction with multi substituted aryl halide was found to be highly selective for aryl iodides compared to the lighter halogens.

Table 4: Pd/L2 catalyzed C-N Cross-coupling reaction of aryl halide and secondary amine

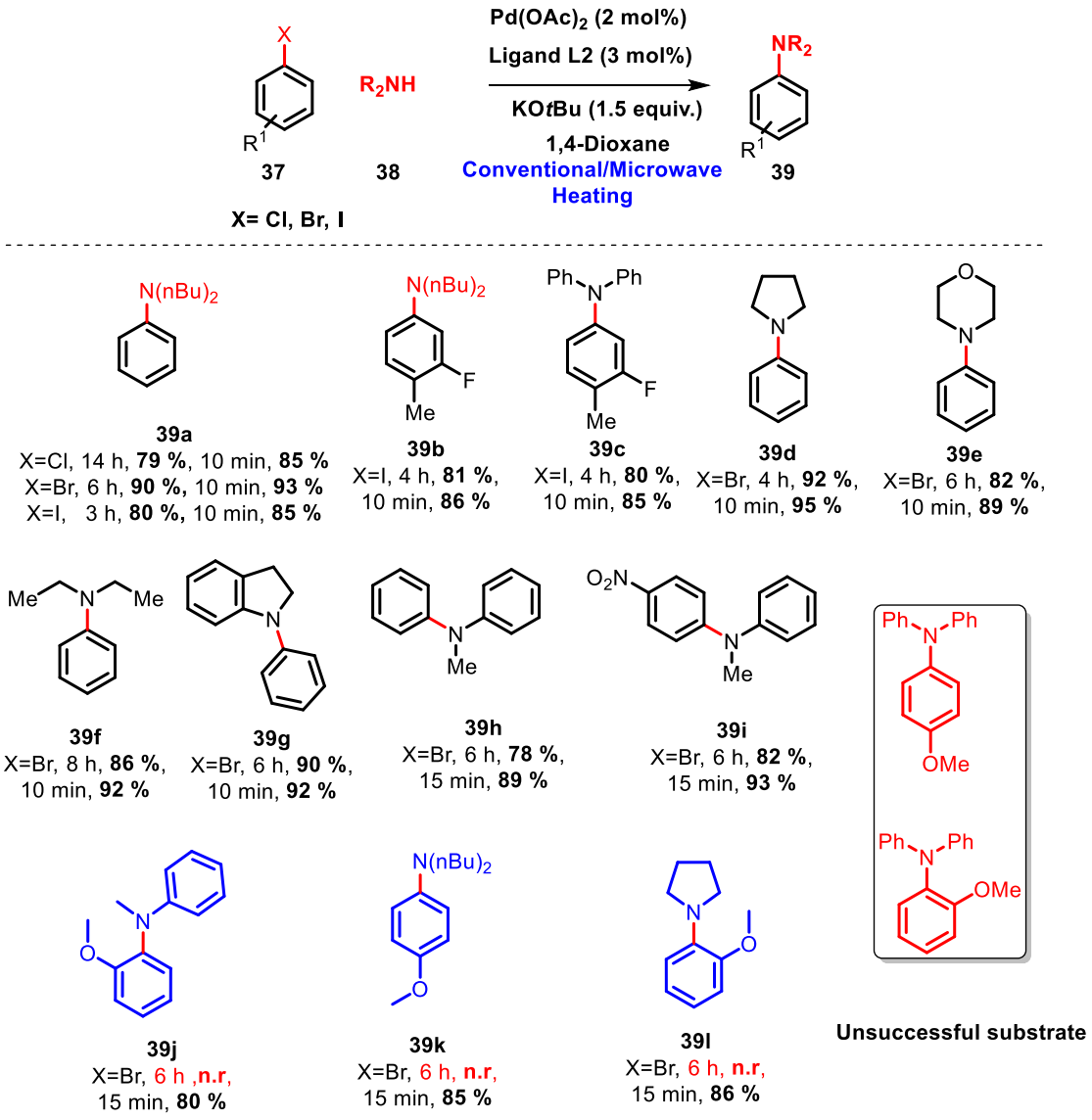

The aminated product was formed in excellent yield in both the heating conditions and the fluorine atom remained intact in the coupled product (**39b, 39c**). The scope of secondary amine for N-arylation was investigated. Various aliphatic, aromatic and mixed secondary amines were employed under both reaction conditions. Cyclic aliphatic amine pyrrolidine, morpholine, and dihydroindole were successfully coupled with bromobenzene (**39d, 39e, 39g**). Acyclic diethyl amine also smoothly delivered the desired couple product in excellent yields under both conditions (**39f**). The mixed secondary amine N-methyl aniline successfully coupled with bromobenzene and 4-nirtrobromobenzene smoothly to deliver the desired product (**39h, 39i**). It is worth mentioning that few aryl halide 2- and 4-methoxybromobenzene were unsuccessful for coupling with pyrrolidine, dibutyl amine and N-methylaniline under the conventional heating condition but successfully delivered the coupled product in good to excellent yields within 10 minute (**39j, 39k, 39l**) under microwave condition. It is evident from these results that microwave irradiations not only accelerate the rate of reaction but also overcomes the problem of steric hindrance and decomposition of products. On the contrary, the N-arylation reaction was unsuccessful of 2- and 4-bromoanisole with diphenylamine under the both conventional and microwave heating conditions. This observation could probably be attributed to the steric hindrance caused by two phenyl groups resulting in the blockage and decomposition of the reactive site.

After a successful investigation of the substrates scope of secondary amine further, we have investigated the scope of a catalytic system for a variety of primary amines. As depicted in Table-5, the aniline was coupled with various aryl halides such as chloro, bromo, and iodobenzene under both conventional and microwave conditions affording the coupled products in excellent yields (**42a**). As anticipated, the reaction time for primary amine coupling was also drastically reduced to 1-2 h for conventional heating and 10 minutes for the microwave conditions. Further, we also studied the effect of both the electronic and steric factors on the reactions by using substituted aniline and aryl halides. e.g., when *p*-methoxyaniline was coupled either with bromobenzene and *p*-bromoanisole, it furnished the expected products in 90% yield under both the conditions (**42b, 42c**). Interestingly, aniline with the bulkier tertiary group at the ortho position to NH_2 group reacted with bromobenzene or substituted aryl halides smoothly to afford the desired compounds in the excellent yields (**42d, 42h, 42i, 42j**). The catalyst system shows the

excellent activity and selectivity for all these reactions, as it delivered the selective monoarylation product of primary amine.

It is worthwhile mentioning that, generally, tuning of selectivity for mono N-arylation is quite difficult for the primary amine in palladium-catalyzed arylation reactions. To achieve selective monoarylation, fine-tuning of the catalyst with bulky ligands is required.[41] However, when aniline (1 equiv) was reacted with 1.2 equivalent aryl halides, the mixture of both mono- and diarylated products was observed. In contrast, when primary amines were used in small excess (1.2 equiv.) compared to the aryl halide (1 equiv.), only mono-arylation was observed.

Table 5: Pd/L2 catalyzed C-N cross-coupling reaction of an aryl halide and a primary amine

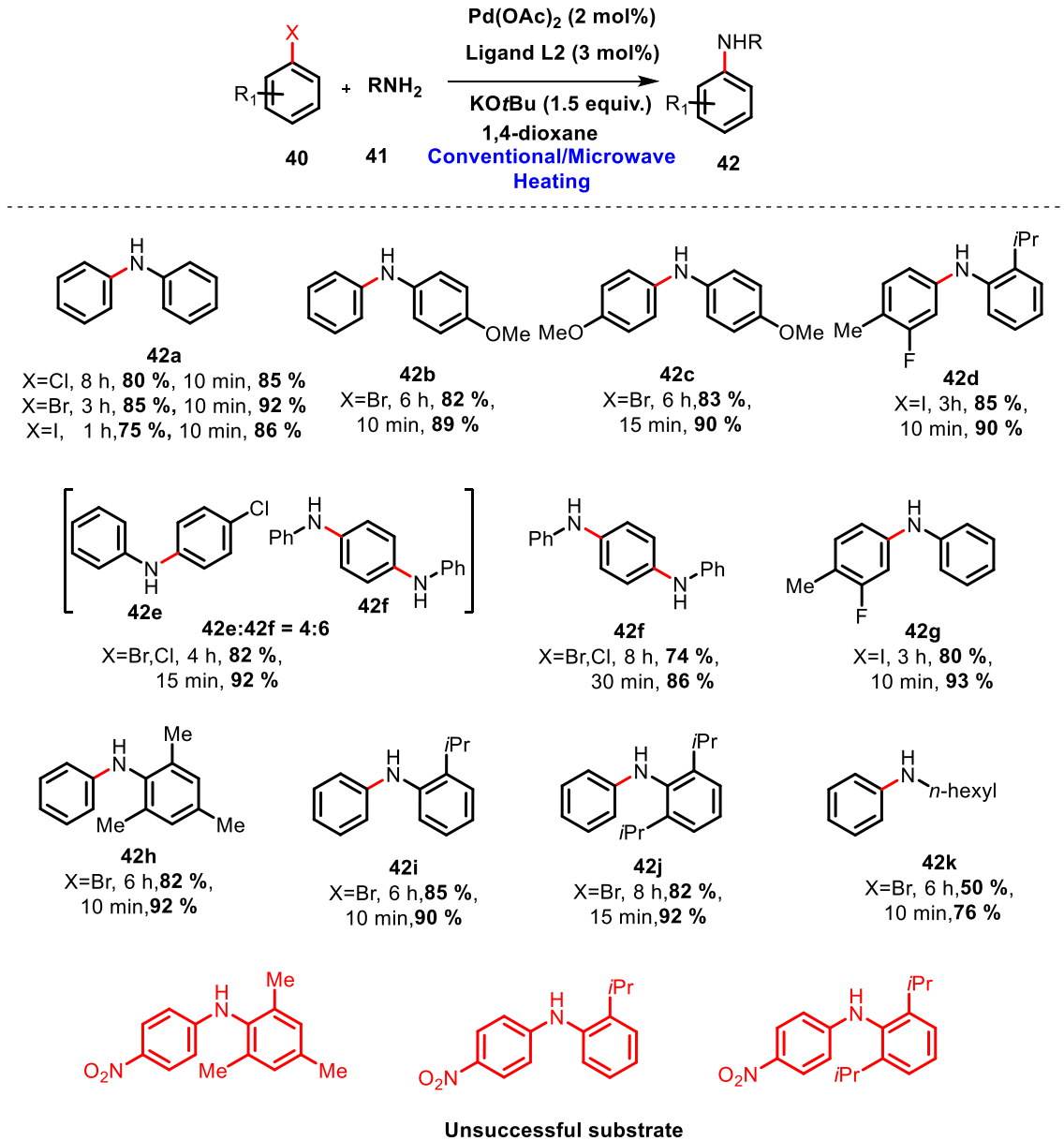

The reaction of aniline with *p*-bromo chlorobenzene either under conventional heating or microwave conditions led to a mixture of fully aminated product and *p*-chloro diphenylamine in a 6:4 (**42e:42f**) ration, respectively. On prolongation under heating or under microwave conditions it furnished only the bis-aminated product in good yield (**42f**).

1.4.3 The plausible mechanism of C-N Cross-Coupling reaction

A plausible reaction mechanism for the N-arylation is well studied in literature[42] as shown in figure 4. The first stage is the oxidative addition of active Pd catalyst in the C-X bond, followed by the coordination with the amine to form a complex. Further, the base-mediated palladium amide bond formation, followed by reductive elimination affords N-arylated product.

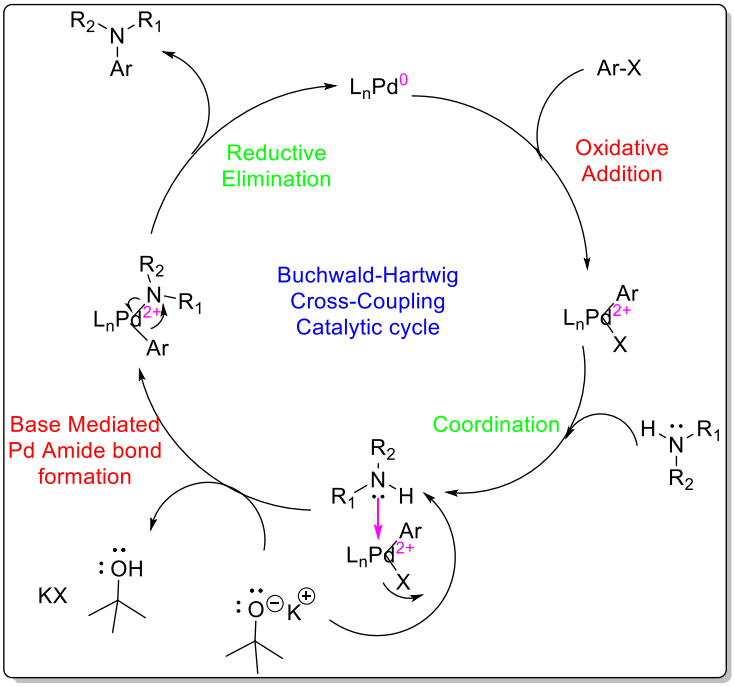

Figure 4: Plausible mechanism of C-N Cross-Coupling reaction

1.5 Conclusions

In conclusion, we have designed and developed a new Pd catalyst based on biaryl phosphine ligands which displayed broad substrate scope and catalytic activity in C-N cross-coupling reactions. The broad range of primary and secondary amines was successfully coupled with an array of substituted aryl halides. The developed catalyst system was found highly selective for the coupling of primary amines and provided the single monoarylated products. Several sterically hindered substrates were smoothly coupled in the C-N cross-coupling reactions. Several aromatic amines such as anilines and

substituted anilines including aliphatic amines were successfully coupled using our catalytic system. Another noteworthy feature of this method is the development of optimal microwave- assisted conditions for the coupling of different halo compounds with primary and secondary amines with the drastic reduction in the reaction time. We believe our catalytic system will find a widespread use especially for the industry in pharmaceutical research and may be potentially useful in other cross-coupling reactions.

1.6 Experimental Procedures

General procedure for the palladium-catalyzed C-N coupling reactions:

1.6.1 Coupling reaction of secondary amines and aryl halides under conventional heating:

In an oven dried two neck round bottom flask $Pd(OAc)_2$ (2 mol%), ligand (3 mol%) and the base (1.5 eq.) were purged with argon 3 times under high vacuum. Subsequently, the aryl halide (1 eq.), secondary amine (1.2 eq.) and solvent were added via syringe through a septum and the reaction mixture heated to reflux in the preheated oil bath. Completion of the reaction was monitored by TLC using ethyl acetate and pet ether. After completion of the reaction, diethyl ether (5 ml) was added and the reaction mixture filtered through a pad of celite. The filtrate was concentrated under vacuum. Purification by column chromatography gave the pure compound.

1.6.2 Coupling reaction of primary amines and aryl halides under conventional heating:

In an oven dried two neck round bottom flask $Pd(OAc)_2$ (2 mol%), ligand (3 mol%), base (1.5 eq.), aryl halide (1 eq.), primary amine (1.2 eq.) and the solvent were degassed with argon. The reaction mixture was heated to reflux in a preheated oil bath for the given time. Completion of the reaction was monitored by thin layer chromatography using ethyl acetate and pet ether as eluent. After completion of the reaction, diethyl ether (5 ml) was added and the reaction mixture filtered through a pad of celite. The filtrate was concentrated under vacuum. Purification by column chromatography gave the pure compound.

1.6.3 C-N coupling reaction under microwave irradiation:

A flame dried microwave reaction vial was charged with $Pd(OAc)_2$ (2 mol %), ligand (3mol %), base (1.5 eq.), aryl halide (1 eq.), amine (1.2 eq.) and solvent (2 mL). The reaction mixture was degassed with argon and the vial heated up to 160 °C for the given time in a microwave reactor. After completion of the reaction, diethyl ether (5 ml) was

added and the reaction mixture filtered through a pad of celite. The filtrate was concentrated under vacuum. Purification by column chromatography gave the pure compound.

1.6.4 Characterization data of the synthesized compounds

***N,N*-Dibutylaniline (39a):**[43]

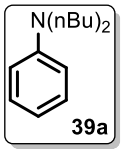

Colourless oil;

^{1}H NMR (200MHz, $CDCl_3$) δ = 7.08 - 7.27 (m, 2 H), 6.51 - 6.73 (m, 3 H), 3.10 - 3.39 (m, 4 H), 1.46 - 1.68 (m, 4 H), 1.20 - 1.46 (m, 4 H), 0.81 - 1.07 ppm (m, 6 H);

^{13}C-NMR (50MHz, $CDCl_3$) δ = 148.2, 129.1, 115.1, 111.7, 77.6, 76.4, 50.8, 29.4, 20.4, 14.0 ppm;

GC-MS (*m/z*) = 205.18 $[M]^+$.

***N,N*-Dibutyl-3-fluoro-4-methylaniline (39b**):

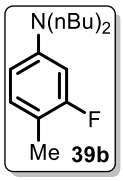

Colourless liquid;

^{1}H NMR (400MHz, DMSO-d_6) δ = 6.98 (t, *J* = 8.9 Hz, 1 H), 6.27 - 6.40 (m, 2 H), 3.16 - 3.25 (m, 4 H), 2.07 (s, 3 H), 1.46 (quin, *J* = 7.5 Hz, 4 H), 1.26 - 1.36 (m, 4 H), 0.91 ppm (t, *J*=7.3 Hz, 6 H);

^{13}C NMR (101MHz, DMSO-d_6) δ = 131.6, 131.6, 107.4, 98.3, 98.0, 49.9, 28.9, 19.6, 13.9, 13.1 ppm;

HRMS (ESI^+) *m/z* = Calcd. for $C_{15}H_{25}NF$ $[M+H]^+$ 238.1967; found 238.1966.

3-Fluoro-4-methyl-*N,N*-diphenylaniline (39c):

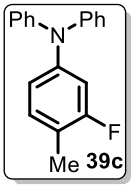

White solid; mp = 93-94 ^{o}C;

^{1}H NMR (500MHz, $CDCl_3$) δ = 7.26 - 7.22 (m, 4 H), 7.07 (d, J = 7.6 Hz, 4 H), 7.04 - 6.99 (m, 3 H), 6.77 - 6.71 ppm (m, 2 H);

^{13}C NMR (126MHz, $CDCl_3$) δ = 162.6, 160.6, 147.5, 131.5, 131.5, 129.3, 124.3, 123.0, 119.2, 118.8, 118.6, 110.7, 110.5, 14.0 ppm;

HRMS (ESI^+) *m/z* = Calcd. for $C_{19}H_{17}NF$ $[M+H]^+$ 278.1340; found 278.1310.

1-Phenylpyrrolidine (39d):[43]

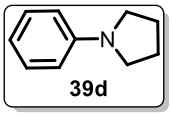

Colourless liquid;

^{1}H NMR (400MHz, C_6D_6) δ = 7.25 - 7.38 (m, 2 H), 6.76 - 6.87 (m, 1 H), 6.48 - 6.59 (m, 2 H), 2.82 - 2.98 (m, 4 H), 1.47 ppm. (dt, J = 6.6, 3.3 Hz, 4 H);

^{13}C NMR (101MHz, C_6D_6) δ = 148.5, 129.6, 128.2, 127.9, 116.1, 112.3, 47.6, 25.6 ppm;

GC-MS (*m/z*) = 147.10 $[M]^+$.

4-Phenylmorpholine (39e):[44]

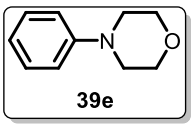

White Solid, mp = 53-54 °C; (repored mp = 51-54 °C);

^{1}H NMR (500MHz, CD_3OD) δ = 7.25 (t, J = 7.0 Hz, 2 H), 6.97 (d, J = 7.9 Hz, 2 H), 6.86 (t, J = 6.7 Hz, 1 H), 3.83 (br. s., 4 H), 3.12 ppm (br. s., 4 H);

^{13}C NMR (126MHz, CD_3OD) δ = 153.0, 130.2, 121.4, 117.2, 68.1, 49.3 ppm;

GC-MS (*m/z*) = 163.09 $[M]^+$.

***N,N*-Diethylaniline (39f):**

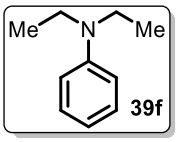

Colourless Liquid;

^{1}H NMR (400MHz, DMSO-d_6) δ = 7.06 - 7.19 (m, 2 H), 6.64 (d, J = 8.1 Hz, 2 H), 6.54 (t, J = 7.2 Hz, 1 H), 3.31 (q, J = 7.0 Hz, 4 H), 1.07 ppm (t, J = 7.0 Hz, 6 H);

^{13}C NMR (101MHz, DMSO-d_6) δ = 147.4, 129.1, 114.8, 111.5, 43.5, 12.4 ppm;

GC-MS (*m/z*) = 149.12 $[M]^+$.

1-**Phenylindoline (39g):**[43]

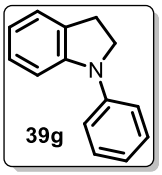

White Solid; mp = 50-52 °C;

^{1}H NMR (200MHz, $CDCl_3$): δ = 7.46 - 7.60 (m, 1 H), 7.30 - 7.46 (m, 2 H), 6.91 - 7.25 (m, 5 H), 6.67 - 6.84 (m, 1 H), 3.97 (t, J = 8.5 Hz, 2 H), 3.14 ppm (t, J = 8.4 Hz, 2 H);

^{13}C NMR (126MHz, CD_3OD): δ = 156.0, 153.2, 140.8, 138.7, 136.5, 134.6, 130.2, 128.3, 126.8, 117.2, 61.1, 37.0 ppm;

GC-MS (*m/z*) = 195.10 $[M]^+$.

***N*-Methyl-*N*-phenylaniline (39h):**[44]

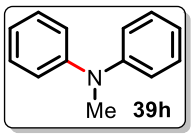

Colourless Liquid;

^{1}H NMR (500MHz, C_6D_6) δ = 7.11 (t, J = 7.9 Hz, 4 H), 6.93 (d, J = 7.9 Hz, 4 H), 6.85 (t, J = 7.3 Hz, 2 H), 2.91 ppm (s, 3 H);

^{13}C NMR (126MHz, C_6D_6) δ = 149.9, 129.8, 128.7, 128.6, 128.3, 128.2, 121.9, 121.2, 40.4 ppm;

GC-MS (*m/z*) = 183.10 $[M]^+$.

***N*-Methyl-4-nitro-*N*-phenylaniline (39i):**

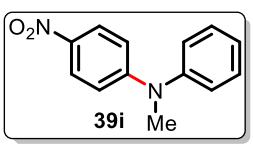

Yellow solid; mp = 152-154 °C;

^{1}H NMR (400MHz, DMSO-d_6) δ = 8.53 (br. s., 1 H), 8.41 (d, J = 9.0 Hz, 1 H), 7.58 (d, J = 9.0 Hz, 1 H), 7.23 - 7.45 (m, 2 H), 6.96 - 7.23 (m, 3 H), 3.47 ppm (s, 3 H);

^{13}C NMR (50MHz, $CDCl_3$) δ = 147.3, 146.2, 130.0, 127.8, 126.1, 123.3, 123.1, 121.1, 42.5 ppm;

GC-MS (*m/z*) = 228.07 $[M]^+$.

2-Methoxy-*N*-methyl-*N*-phenylaniline (39j):[45]

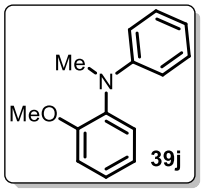

Colourless liquid;

^{1}H NMR (500MHz, $CDCl_3$) δ = 7.25 - 7.43 (m, 5 H), 7.02 - 7.12 (m, 2 H), 6.82 (t, *J* = 7.3 Hz, 1 H), 6.76 (d, *J* = 8.2 Hz, 2 H), 3.88 (s, 3 H), 3.33 ppm (s, 3 H);

^{13}C NMR (126MHz, $CDCl_3$) δ = 156.0, 149.4, 136.8, 129.1, 128.7, 126.9, 121.3, 117.1, 113.4, 112.6, 77.3, 76.7, 55.6, 55.6, 39.0 ppm;

GC-MS (*m/z*) = 213.11 $[M]^+$.

***N,N*-Dibutyl-4-methoxyaniline (39k):**[46]

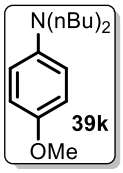

Colourless Liquid;

^{1}H NMR (400MHz, CD_3OD) δ = 6.65 - 6.84 (m, 4 H), 3.71 (s, 3 H), 3.07 - 3.19 (m, 4 H), 1.40 - 1.52 (m, 4 H), 1.21 - 1.39 (m, 8 H), 0.88 - 0.95 ppm (m, 6 H);

^{13}C NMR (101MHz, CD_3OD) δ = 117.7, 115.8, 56.3, 53.6, 30.7, 21.6, 14.5 ppm;

GC-MS (*m/z*) = 235.19$[M]^+$.

1-(2-Methoxyphenyl)pyrrolidine (39l):[47]

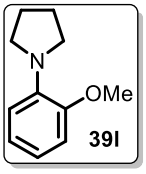

Colourless liquid;

^{1}H NMR (500MHz, CD_3OD) δ = 6.93 (d, *J* = 4.9 Hz, 1 H), 6.81 - 6.90 (m, 3 H), 3.84 (s, 3 H), 3.24 (ddd, *J* = 6.6, 4.1, 2.7 Hz, 4 H), 1.94 ppm (dt, *J* = 6.7, 3.4 Hz, 4 H);

^{13}C NMR (126MHz, CD_3OD) δ = 152.5, 141.1, 122.3, 122.0, 117.3, 113.3, 56.2, 51.9, 25.5 ppm;

GC-MS (*m/z*) = 177.11 $[M]^+$.

Diphenylamine (42a):

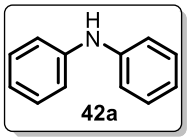

White solid; mp = 48-50 °C; (reported mp = 53°C);

^{1}H NMR (200MHz, $CDCl_3$) δ = 7.25 - 7.43 (m, 4 H), 7.07 - 7.20 (m, 4 H), 6.93 - 7.04 (m, 2 H), 5.86 ppm (br. s., 1 H);

^{13}C NMR (50MHz, $CDCl_3$) δ = 142.96, 129.25, 120.91, 117.13 ppm;

GC-MS (m/z) = 169.08$[M]^+$.

4-Methoxy-*N*-phenylaniline (42b):

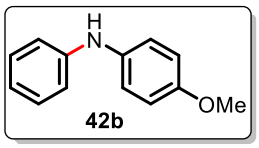

White solid; mp = 98-99 °C; (reported mp = 104-106 °C);

^{1}H NMR (400MHz, DMSO-d_6) δ = 7.82 (s, 1 H), 7.15 (t, *J* = 7.8 Hz, 2 H), 6.99 - 7.07 (m, 2 H), 6.82 - 6.94 (m, 4 H), 6.70 (t, *J* = 7.2 Hz, 1 H), 3.71 ppm (s, 3 H);

^{13}C NMR (101MHz, DMSO-d_6) δ = 153.8, 145.1, 136.1, 129.1, 120.4, 118.2, 114.8, 114.5, 55.2, ppm;

HRMS (ESI$^+$) *m/z* = Calcd. for $C_{13}H_{14}ON$ $[M+H]^+$ 200.1070; found 200.1069.

***Bis*(4-methoxyphenyl)amine (42c):**[48]

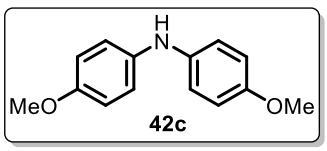

White solid; mp = 99-100 °C; (reported mp = 101-104 °C);

^{1}HNMR (500MHz, $(CD_3)_2SO$) δ = 7.51 (s, 1 H), 6.87 - 6.95 (m, 4 H), 6.77 - 6.84 (m, 4 H), 3.68 ppm (s, 6 H);

^{13}C NMR (126MHz, $(CD_3)_2SO$) δ = 152.8, 138.0, 118.0, 114.5, 55.2 ppm;

GC-MS (*m/z*) = 229.11 $[M]^+$.

3-Fluoro-*N*-(2-isopropylphenyl)-4-methylaniline (42d):

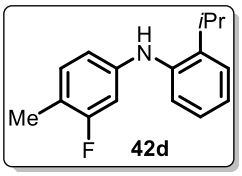

Yellow liquid;

^{1}H NMR (200MHz, $CDCl_3$) δ = 7.29 - 7.41 (m, 1 H), 6.91 - 7.26 (m, 4 H), 6.48 - 6.63 (m, 2 H), 3.14 (quin, *J* = 6.9 Hz, 1 H), 2.19 (d, *J* = 1.5 Hz, 3 H), 1.25 ppm (d, *J* = 6.8 Hz, 6 H);

^{13}C NMR (50MHz, $CDCl_3$) δ = 159.4, 140.9, 139.1, 131.7, 131.6, 126.5, 126.1, 123.8, 122.3, 111.8, 103.2, 102.7, 27.6, 23.0, 13.8 ppm;

HRMS (ESI^+) *m/z* = Calcd. for $C_{16}H_{19}NF$ $[M+H]^+$ 244.1496; found 244.1497.

4-Chloro-*N*-phenylaniline (42e):[49]

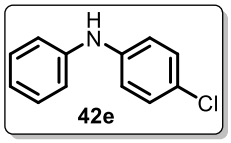

White solid; mp = 68-69 °C; (reported mp = 72 °C);

^{1}H NMR (500MHz, C_6D_6) δ = 7.15 (br. s., 1 H), 7.08 (t, *J* = 7.9 Hz, 2 H), 6.83 (t, *J* = 7.5 Hz, 1 H), 6.70 - 6.76 (m, *J* = 8.5 Hz, 2 H), 6.39 - 6.48 (m, *J* = 8.5 Hz, 2 H), 4.78 ppm (br.s., 1 H);

^{13}C NMR (126MHz, C_6D_6) δ =143.1, 143.0, 132.7, 129.9, 122.1, 119.7, 118.9, 113.1 ppm;

GC-MS (*m/z*) = 203.05 $[M]^+$: 205.03 $[M]^+$ (3:1).

***N*^{1},*N*^{4}-Diphenylbenzene-1,4-diamine (42f):**[50]

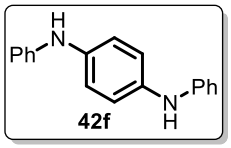

White solid; mp = 144-146 °C; (reported mp = 143-145 °C);

^{1}H NMR (400MHz, C_6D_6) δ = 7.09 - 7.15 (m, 4 H), 6.71 - 6.89 (m, 10 H), 4.92 ppm (br. s., 2 H);

^{13}C NMR (101MHz, C_6D_6) δ = 145.3, 137.9, 121.5, 120.5, 117.1 ppm;

GC-MS (*m/z*) = 260.15 $[M]^+$.

3-Fluoro-4-methyl-*N*-phenylaniline (42g):

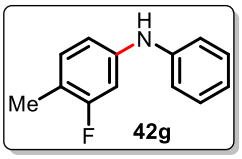

Colourless liquid;

^{1}H NMR (500MHz, $(CD_3)_2SO$) δ = 8.24 (s, 1 H), 7.20 - 7.28 (m, 2 H), 7.05 - 7.13 (m, 3 H), 6.75 - 6.89 (m, 3 H), 2.14 ppm (s, 3 H);

^{13}C NMR (126MHz, $CD_3)_2SO$) δ = 162.5, 160.6, 143.9, 143.8, 143.7, 143.4, 132.3, 132.2, 129.7, 129.6, 120.6, 120.1, 117.6, 117.2, 114.8, 114.6, 112.8, 112.8, 103.4, 103.2, 13.9, 13.9 ppm;

HRMS (ESI^+) *m/z* = Calcd. for $C_{13}H_{13}NF$ $[M+H]^+$ 202.1027; found 202.1028.

2,4,6-Trimethyl-*N*-phenylaniline (42h):

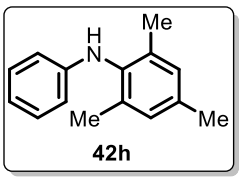

Brown crystalline solid; mp = 48-50 °C;

^{1}H NMR (400MHz, $CDCl_3$) δ = 7.17 (t, *J* = 7.5 Hz, 2 H), 6.97 (s, 2 H), 6.75 (t, *J* = 7.0 Hz, 1 H), 6.52 (d, *J* = 8.3 Hz, 2 H), 5.13 (br. s., 1 H), 2.34 (s, 3 H), 2.21 ppm (s, 6 H);

^{13}C NMR (101MHz, $CDCl_3$) δ = 146.6, 135.9, 135.5, 135.4, 129.2, 117.8, 113.2, 20.9, 18.2 ppm;

GC-MS (*m/z*) = 211.13 $[M]^+$.

2-Isopropyl-*N*-phenylaniline (42i):[51]

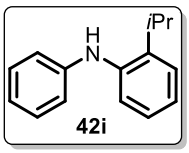

Yellow liquid;

^{1}H NMR (200MHz, $CDCl_3$) δ = 6.99 - 7.36 (m, 6 H), 6.79 - 6.90 (m, 3 H), 5.39 (br. s., 1 H), 3.15 (spt, *J* = 6.8 Hz, 1 H), 1.24 ppm (d, *J* = 6.9 Hz, 6 H);

^{13}C NMR (50MHz, $CDCl_3$) δ = 145.2, 140.6, 139.5, 129.2, 126.4, 126.0, 123.4, 121.9, 119.7, 116.3, 27.6, 23.0 ppm;

GC-MS (*m/z*) = 211.13$[M]^+$.

2,6-Diisopropyl-*N*-phenylaniline (42j):

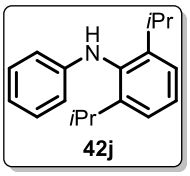

Brown crystalline solid; mp = 45-46 °C;

^{1}H NMR (200MHz, $CDCl_3$) δ = 7.02 - 7.38 (m, 5 H), 6.63 - 6.78 (m, 1 H), 6.41 - 6.53 (m, 2 H), 5.11 (br. s., 1 H), 3.20 (spt, *J* = 6.8 Hz, 2 H), 1.14 ppm (d, *J* = 6.8 Hz, 12 H);

^{13}C NMR (50MHz, $CDCl_3$) δ = 148.1, 147.5, 135.1, 129.2, 127.2, 123.8, 117.7, 113.0, 28.2, 23.8 ppm;

GC-MS (**m/z**) = 253.18 $[M]^+$.

***N*-Hexylaniline (42k):**

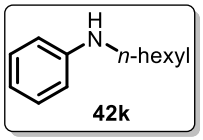

Colourless Liquid;

^{1}H NMR (200MHz, $CDCl_3$) δ = 7.04 - 7.30 (m, 2 H), 6.37 - 6.87 (m, 3 H), 2.98 - 3.23 (m, 2 H), 1.52 - 1.73 (m, 2 H), 1.29 - 1.46 (m, 6 H), 0.87 - 0.94 ppm (m, 3 H);

^{13}C NMR (50MHz, $CDCl_3$) δ = 147.9, 129.2, 117.6, 113.2, 44.4, 31.6, 29.3, 26.8, 22.6, 14.0 ppm;

GC-MS (*m/z*) = 177.29 $[M]^+$.

1.7 Selected NMR Spectra:

^{1}H NMR of *N,N*-dibutylaniline (39a) (200MHz, $CDCl_3$):

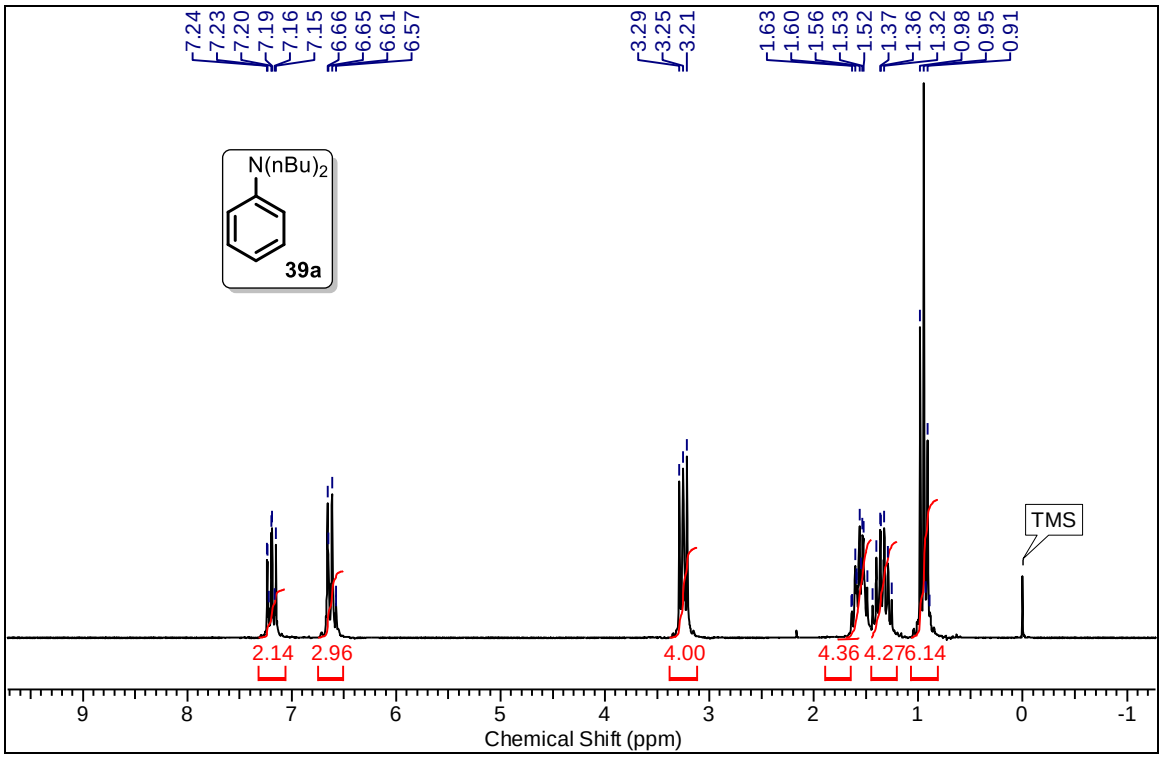

^{13}C NMR of *N,N*-dibutylaniline (39a) (50MHz, $CDCl_3$):

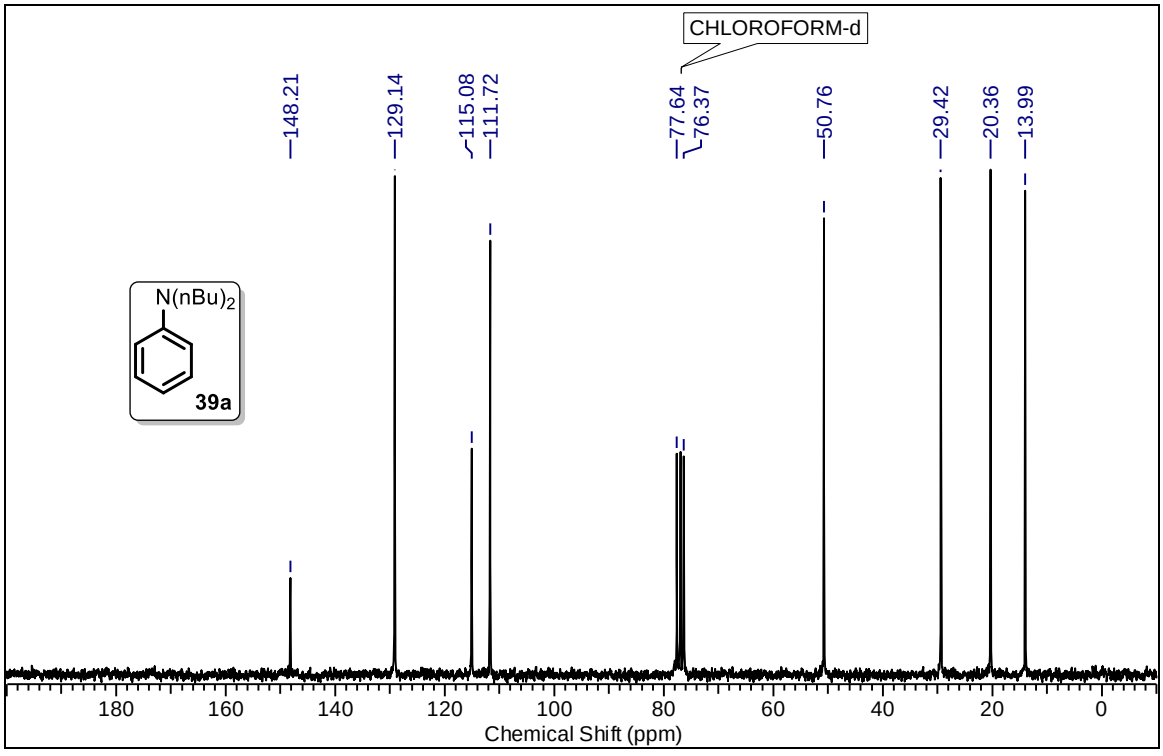

^{1}H NMR of 3-fluoro-4-methyl-*N*,*N*-diphenylaniline (39c) (500MHz, $CDCl_3$):

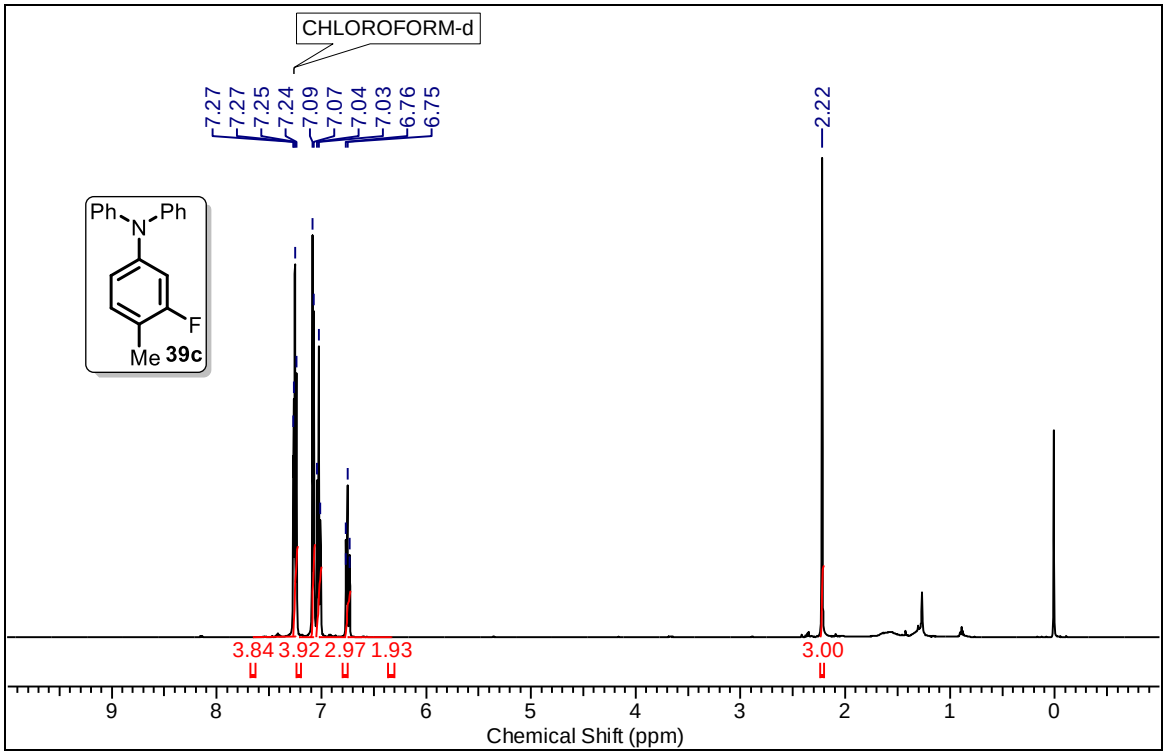

^{13}C NMR of 3-fluoro-4-methyl-*N*,*N*-diphenylaniline 39c (126MHz, $CDCl_3$):

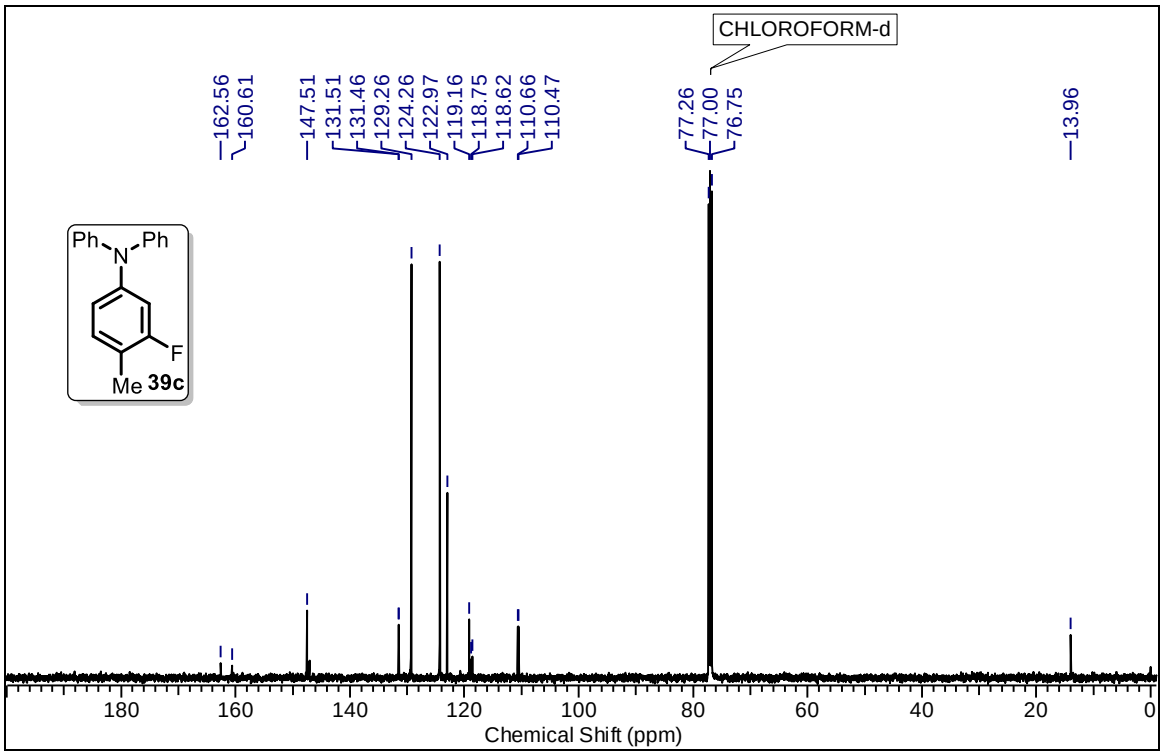

^{1}H NMR of 1-phenylpyrrolidine (39d) (400MHz, C_6D_6):

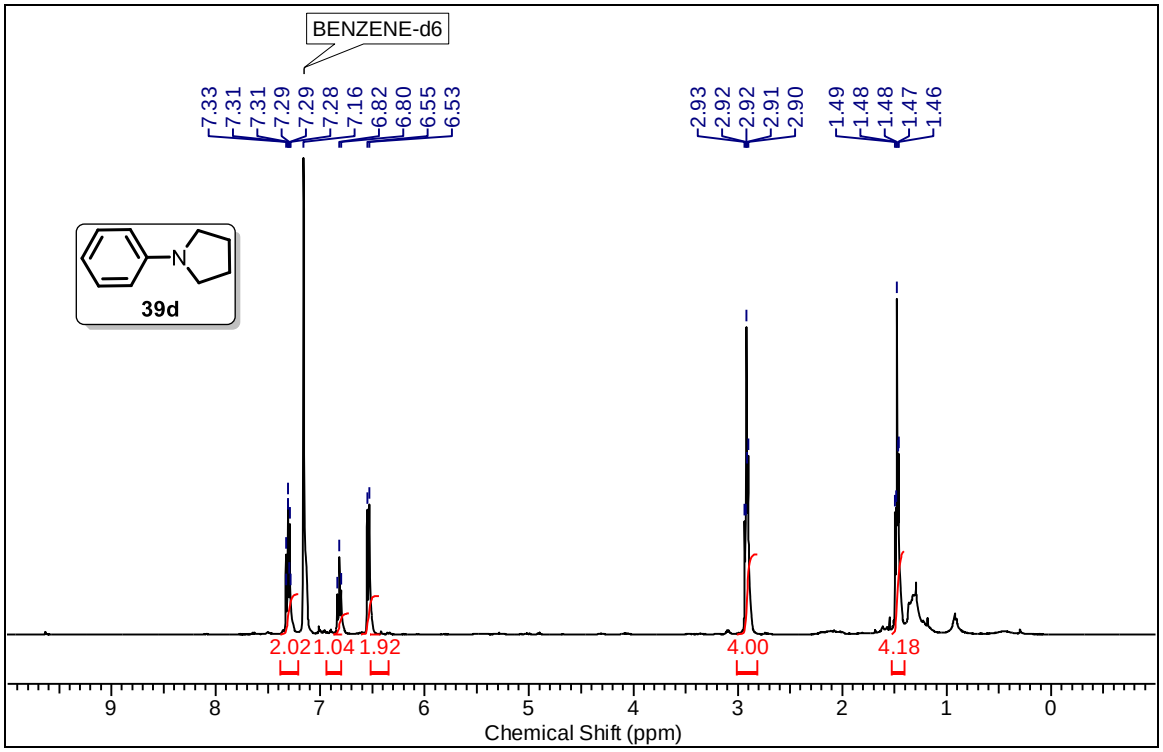

^{13}C NMR of 1-phenylpyrrolidine (39d) (101MHz, C_6D_6):

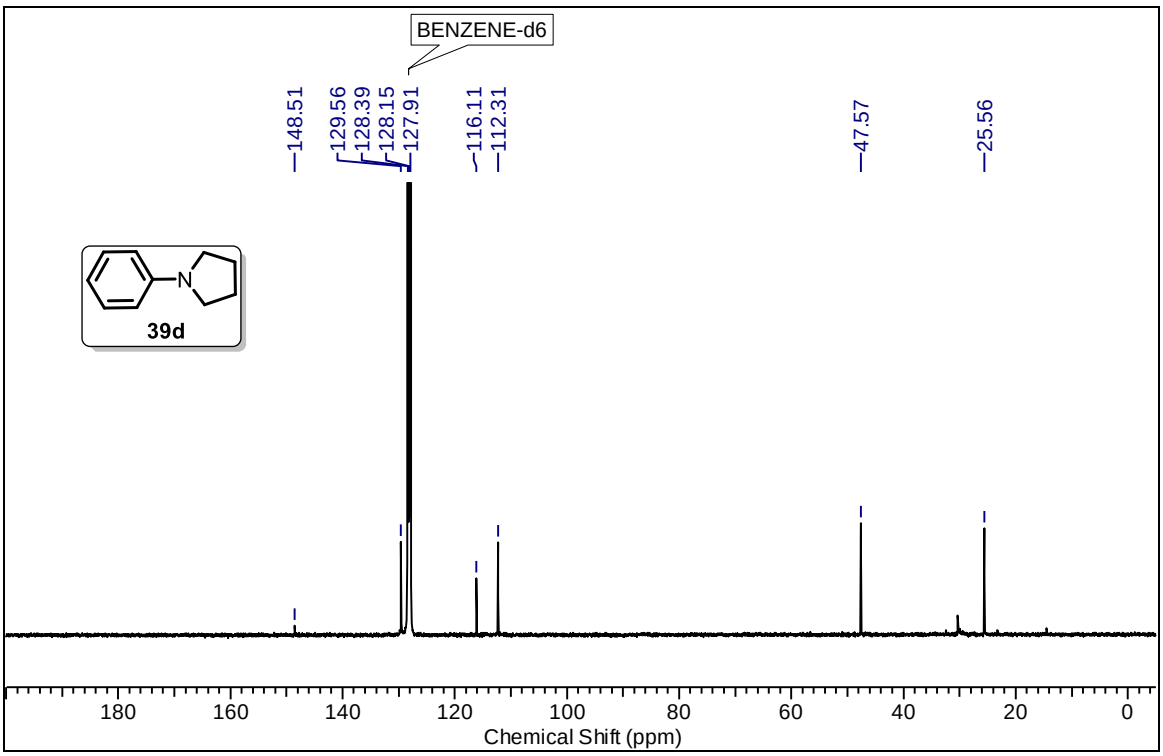

^{1}H NMR 4-phenylmorpholine (39e) (500MHz, CD_3OD):

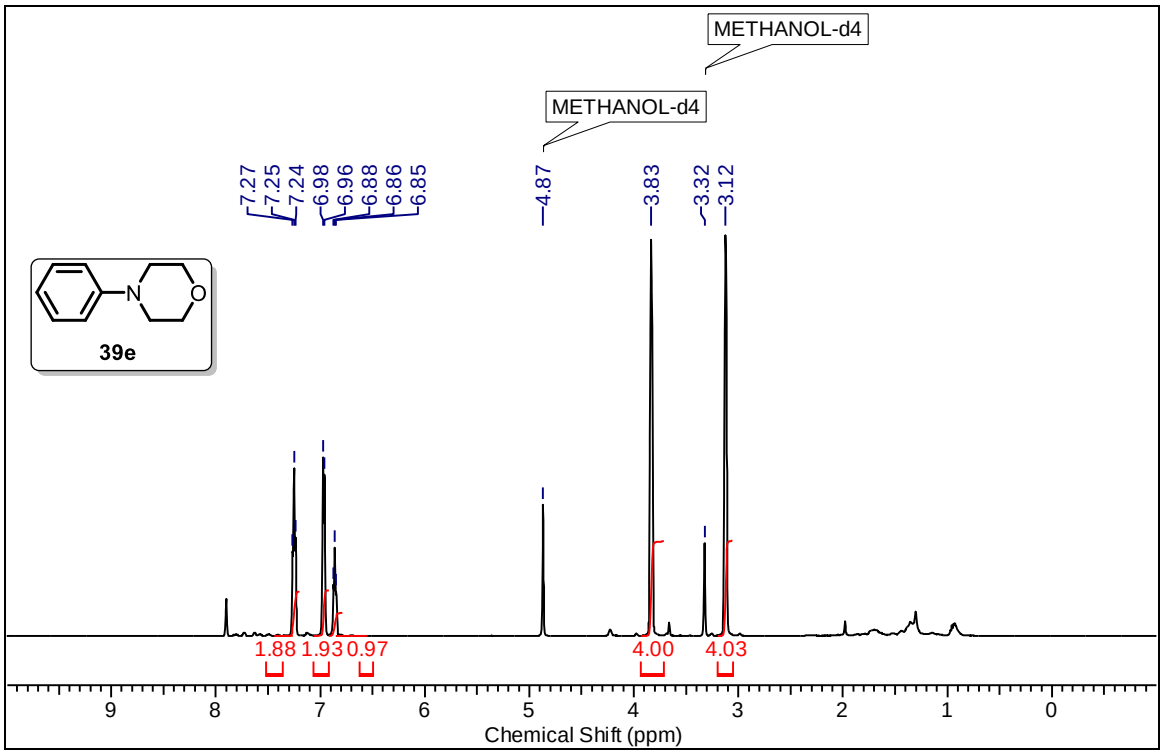

^{13}C NMR 4-phenylmorpholine (39e) (126MHz, CD_3OD):

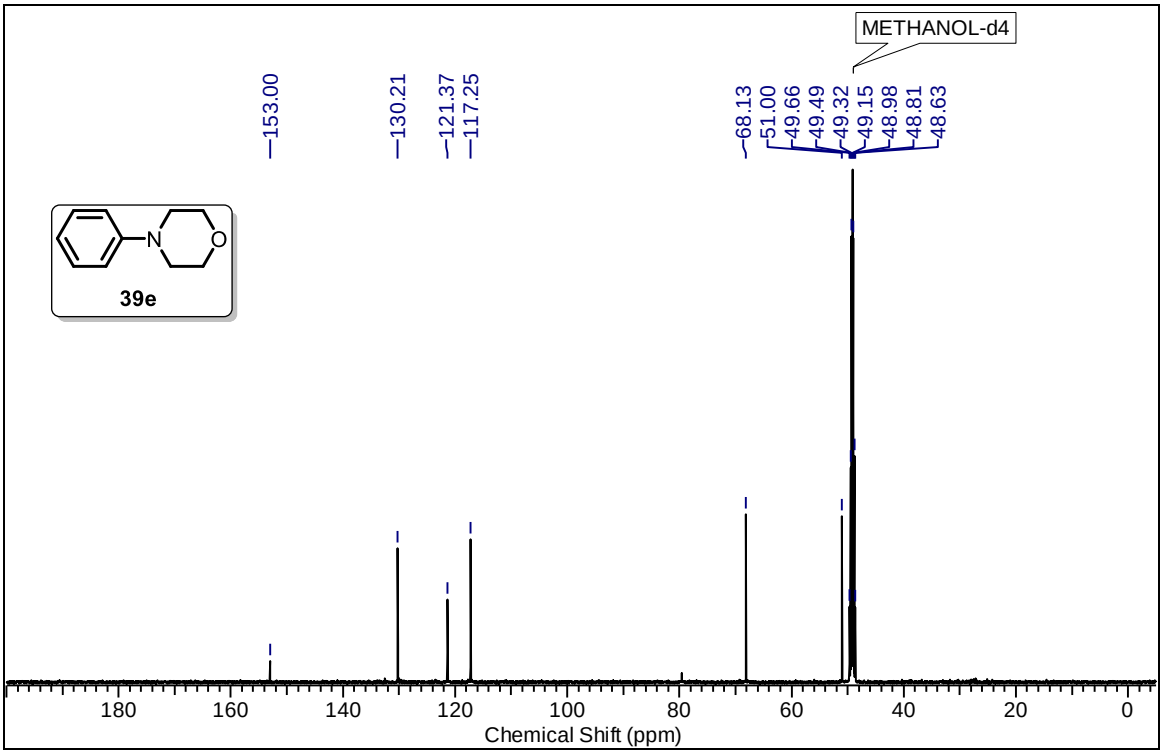

^{1}H NMR of *N*-methyl-*N*-phenylaniline (39h) (500MHz, C_6D_6):

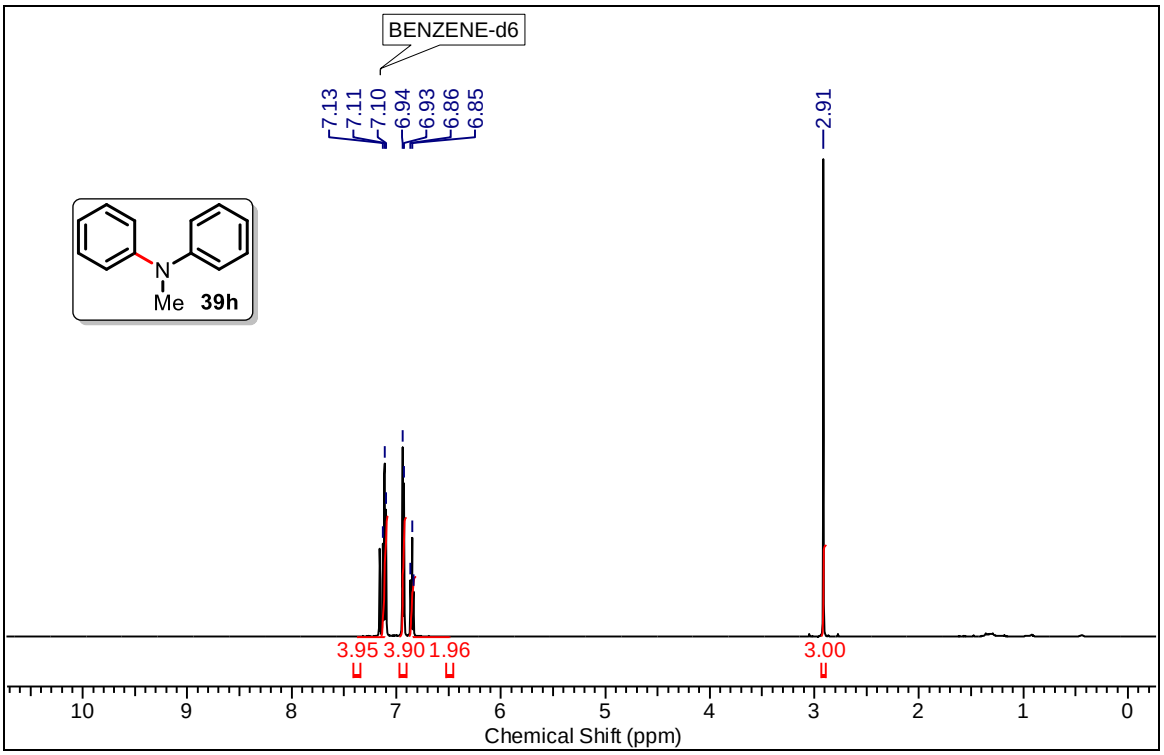

^{13}C NMR of *N*-methyl-*N*-phenylaniline (39h) (126MHz, C_6D_6):

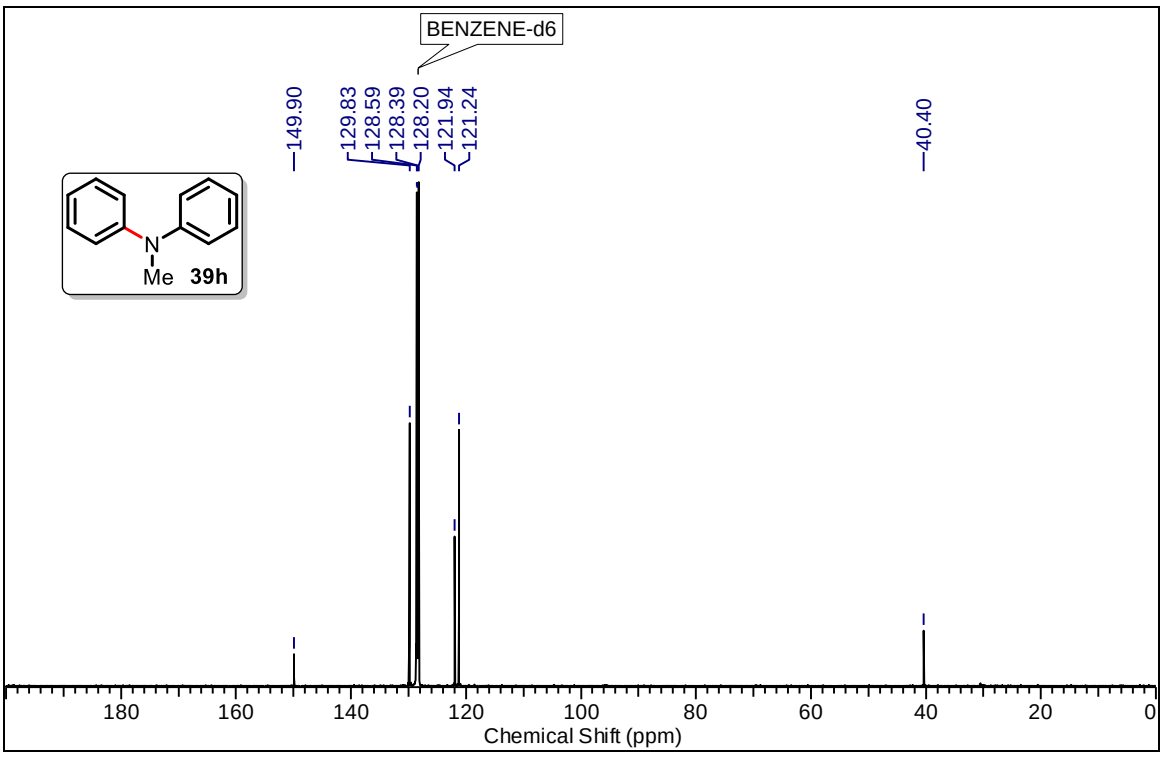

^{1}H NMR of *N*-methyl-4-nitro-*N*-phenylaniline (39i) (400MHz, DMSO-d$_6$):

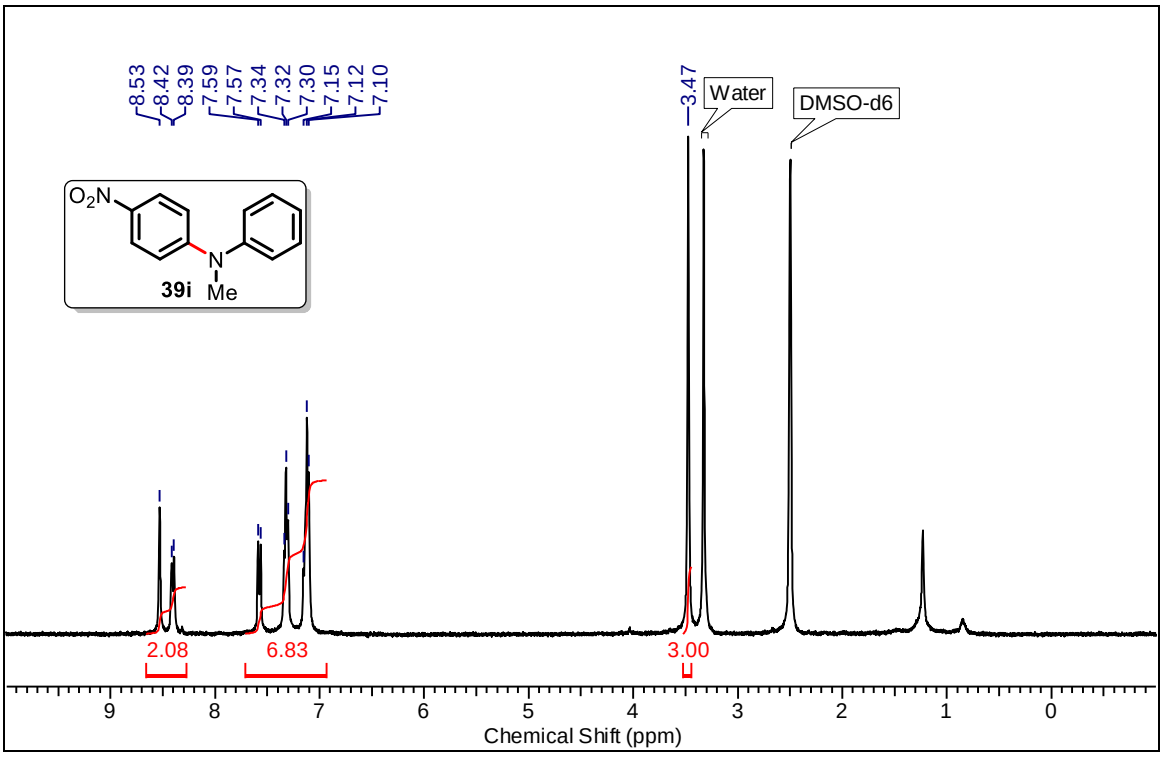

^{13}C NMR of *N*-methyl-4-nitro-*N*-phenylaniline (39i) (101MHz, DMSO-d$_6$):

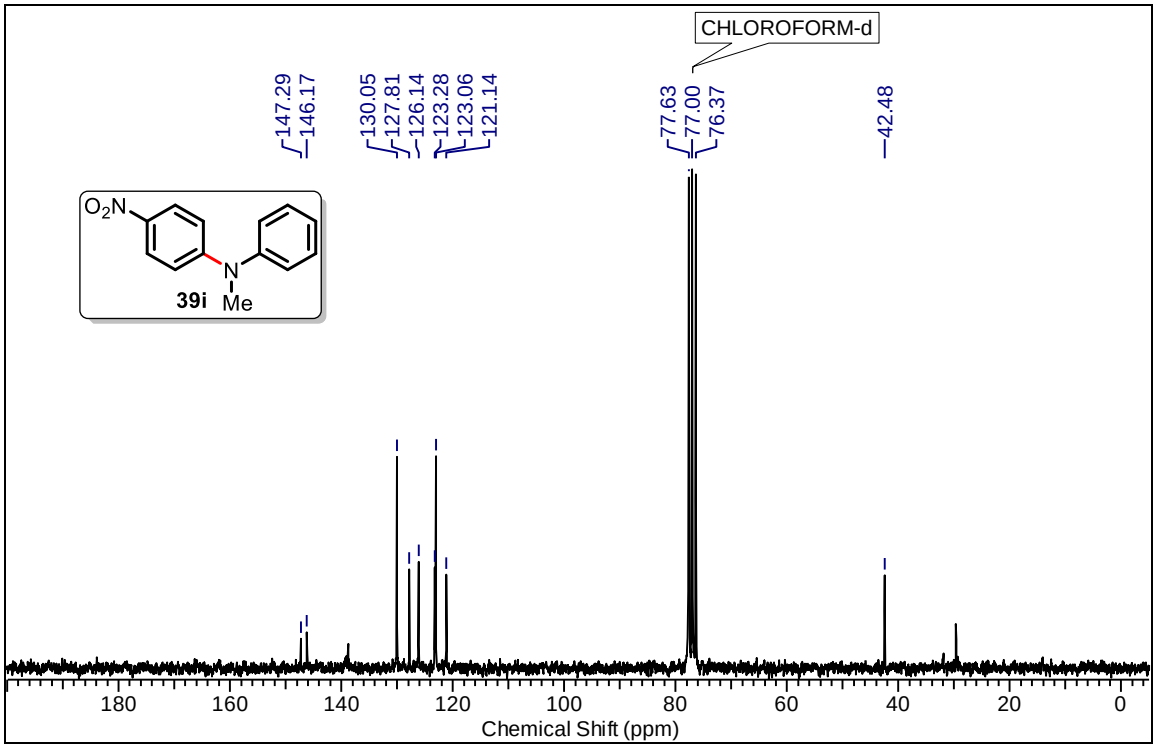

^{1}H NMR of 4-methoxy-*N*-phenylaniline (42b) (400MHz, DMSO-d$_6$):

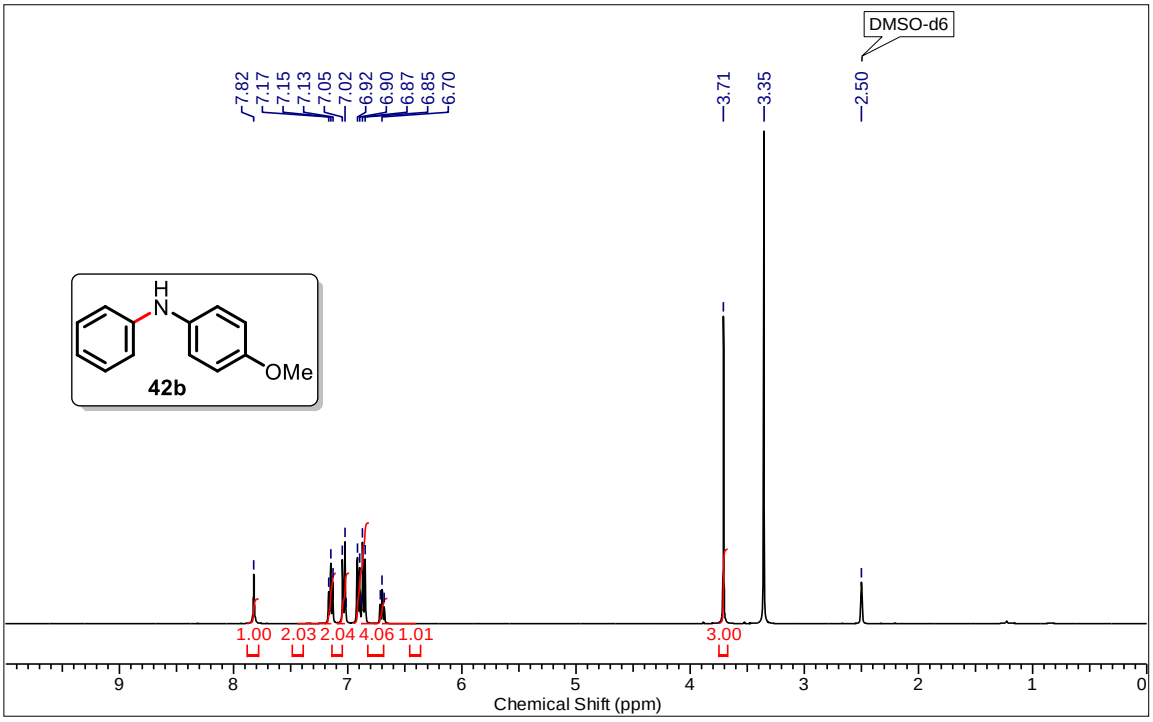

^{13}C NMR of 4-methoxy-*N*-phenylaniline (42b) (101MHz, DMSO-d$_6$):

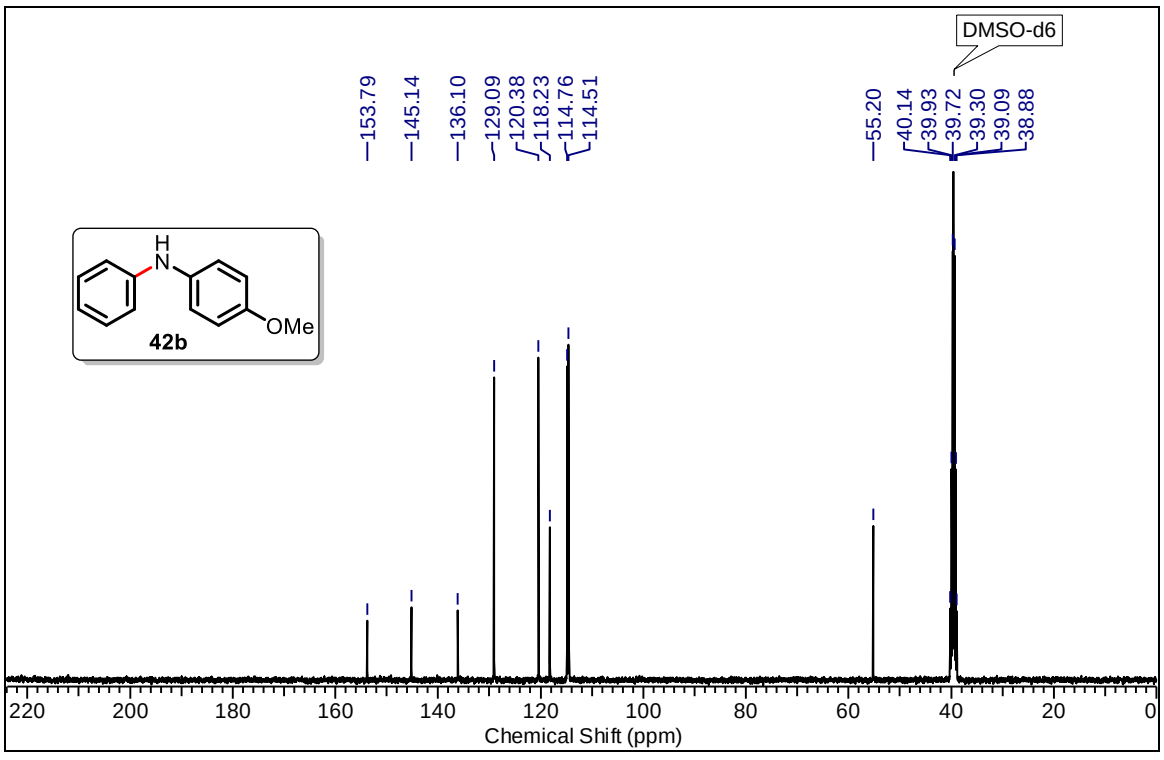

^{1}H NMR of 4-chloro-N-phenylaniline (42e) (400MHz, C_6D_6):

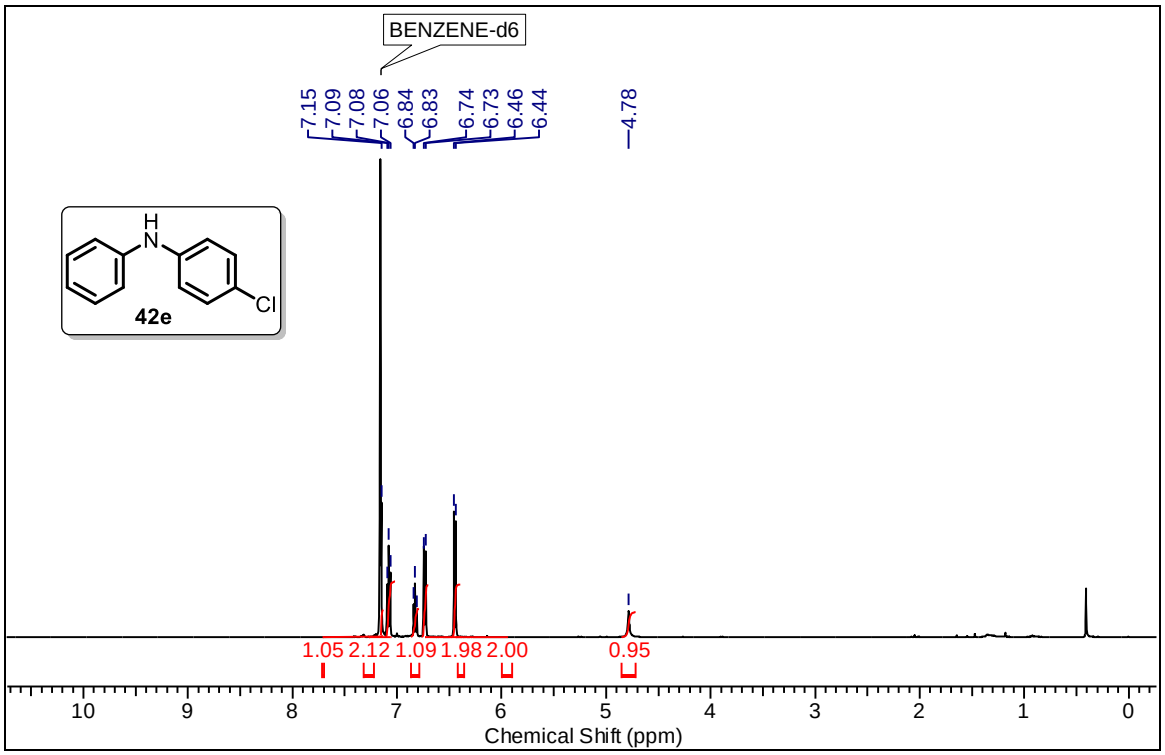

^{13}C NMR of 4-chloro-N-phenylaniline (42e) (101MHz, C_6D_6):

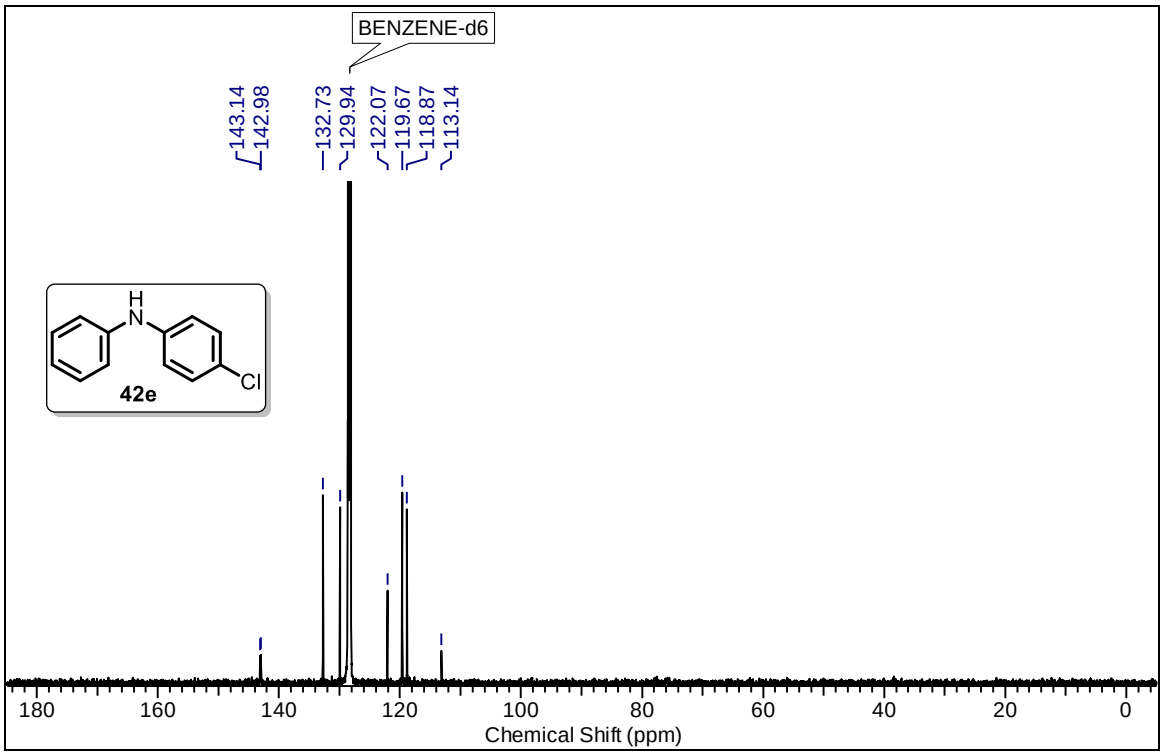

^{1}H NMR of N^{1},N^{4}-diphenylbenzene-1,4-diamine (42f) (400MHz, C_6D_6):

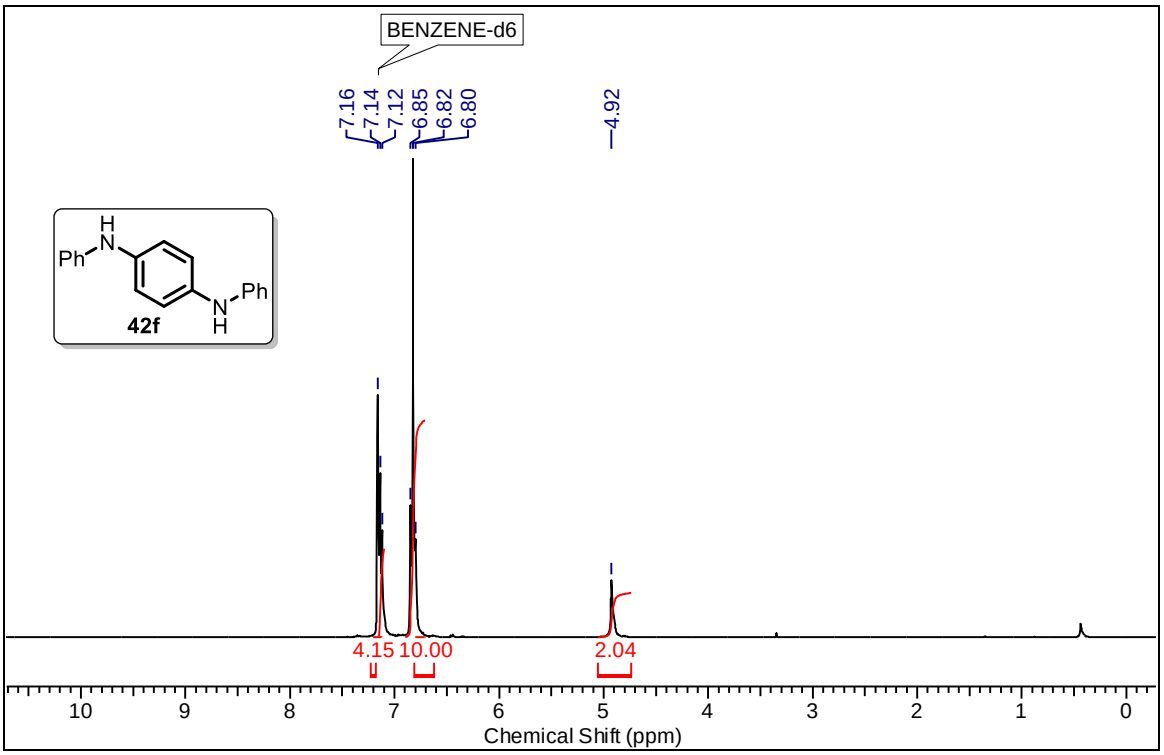

^{13}C NMR of N^{1},N^{4}-diphenylbenzene-1,4-diamine (42f) (101MHz, C_6D_6):

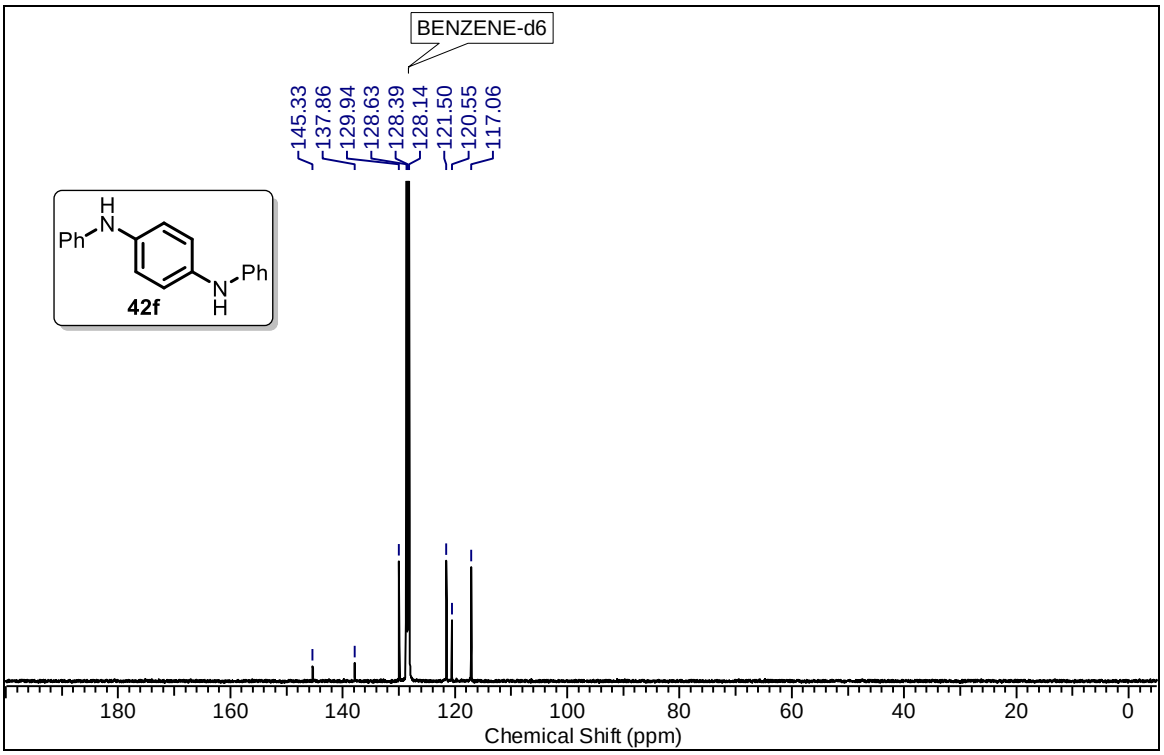

^{1}H NMR of 2,4,6-trimethyl-*N*-phenylaniline (42h) (400MHz, $CDCl_3$):

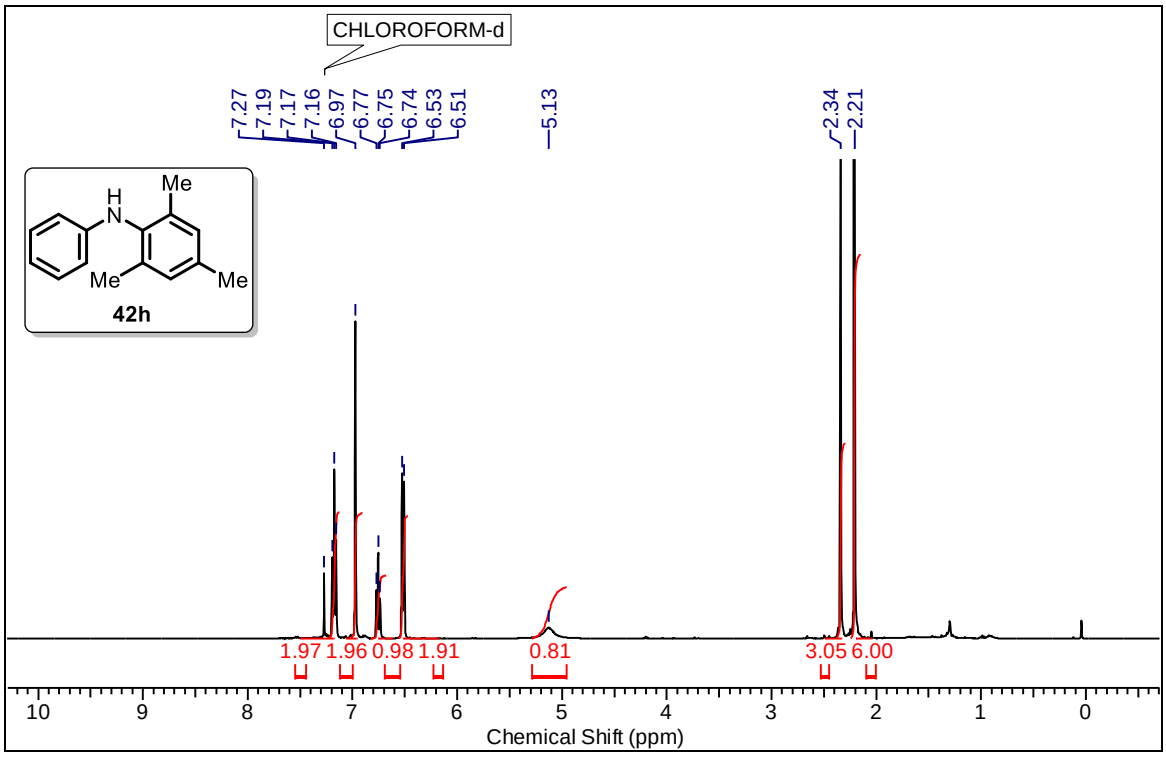

^{13}C NMR of 2,4,6-trimethyl-*N*-phenylaniline (42h) (101MHz, $CDCl_3$):

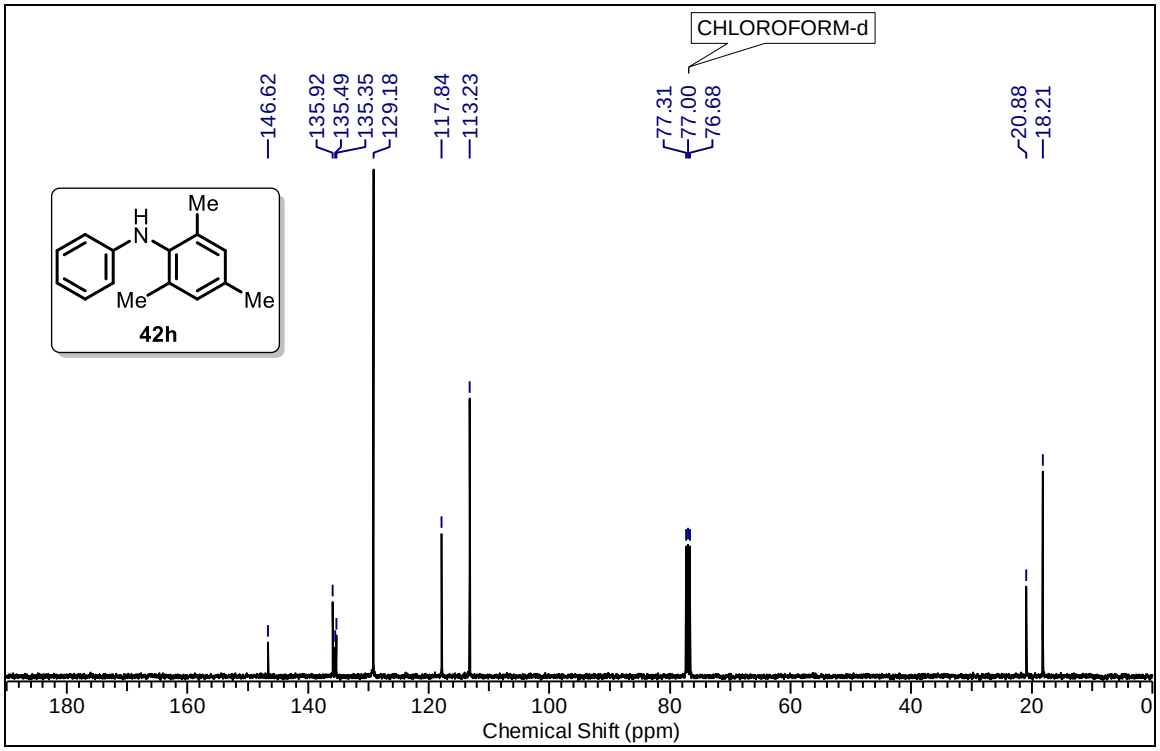

^{1}H NMR of 2-isopropyl-*N*-phenylaniline (42i) (200MHz, $CDCl_3$):

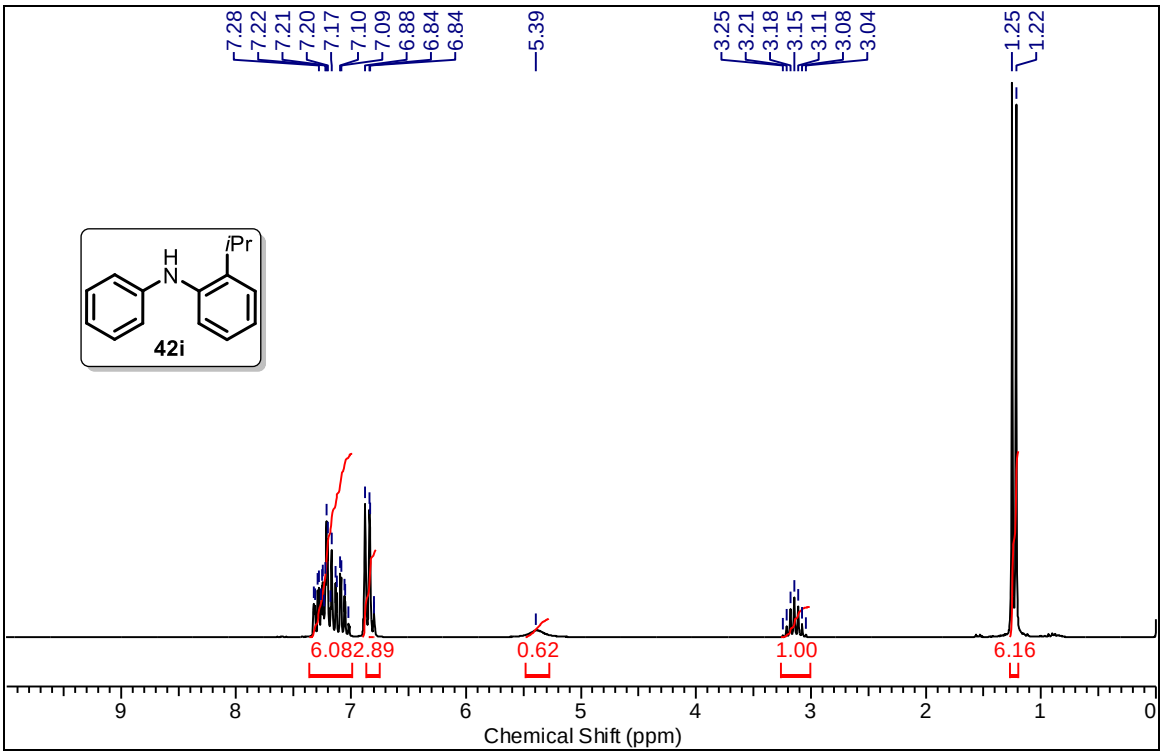

^{13}C NMR of 2-isopropyl-*N*-phenylaniline (42i) (50MHz, $CDCl_3$):

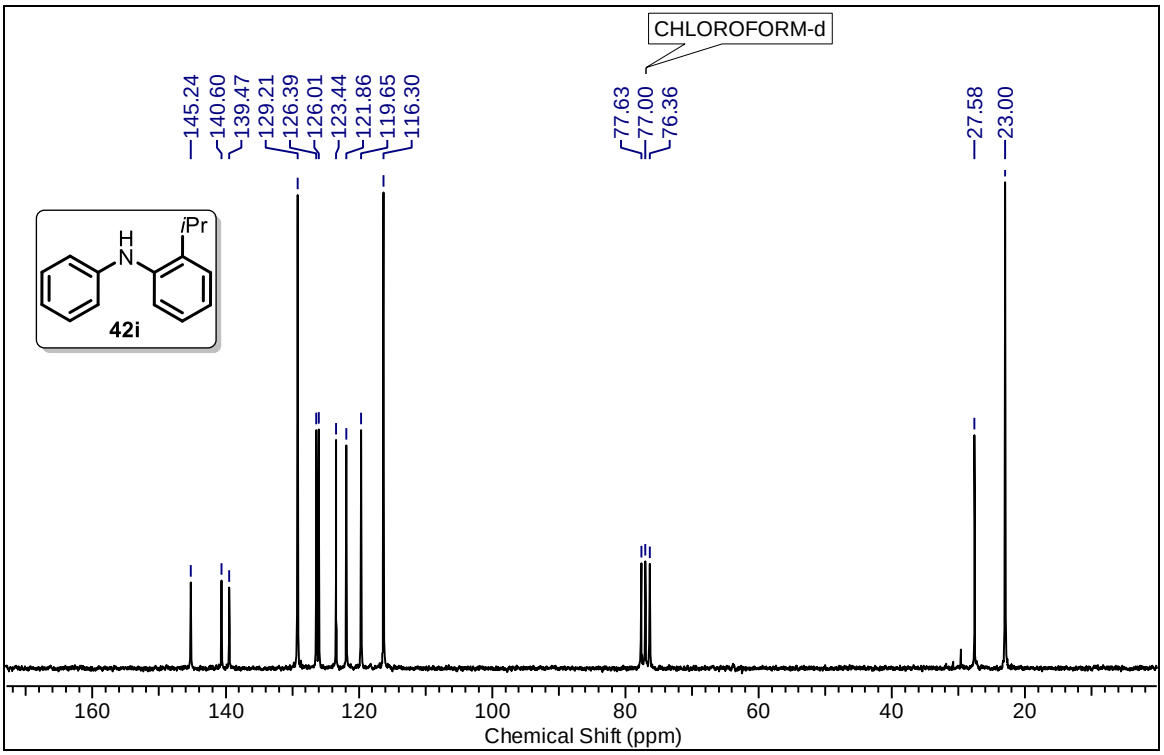

^{1}H NMR of *N*-hexylaniline (42k) (200MHz, $CDCl_3$):

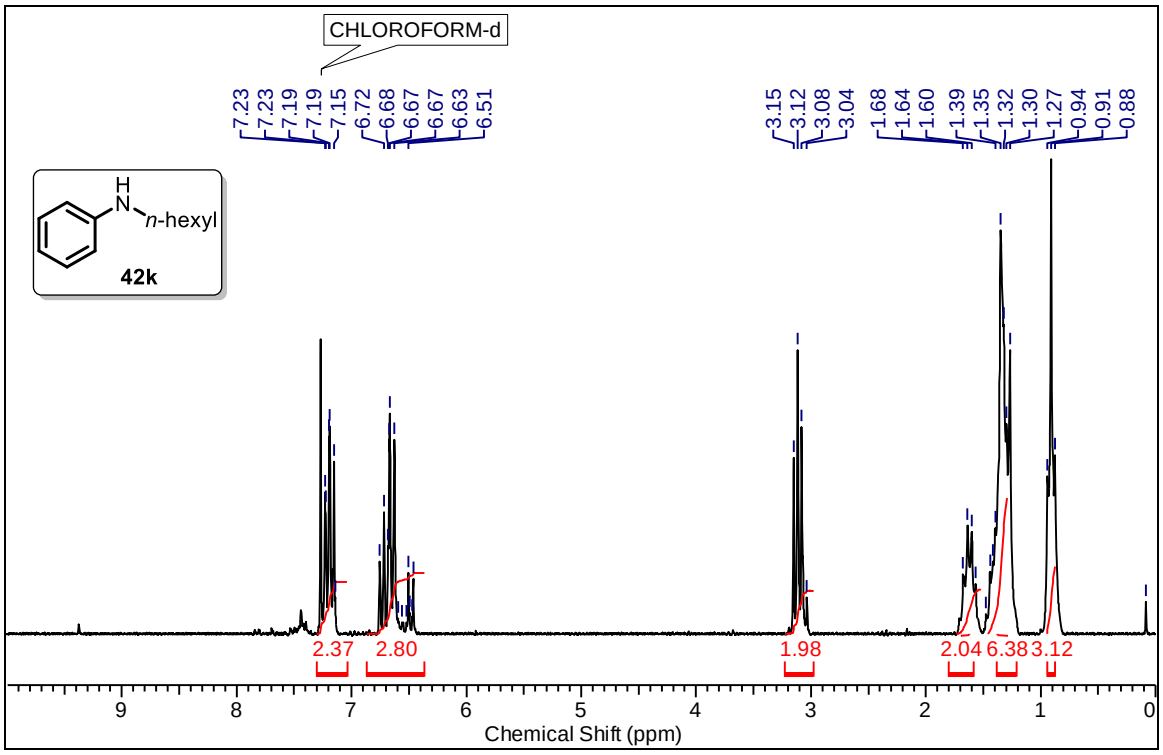

^{13}C NMR of *N*-hexylaniline (42k) (50MHz, $CDCl_3$):

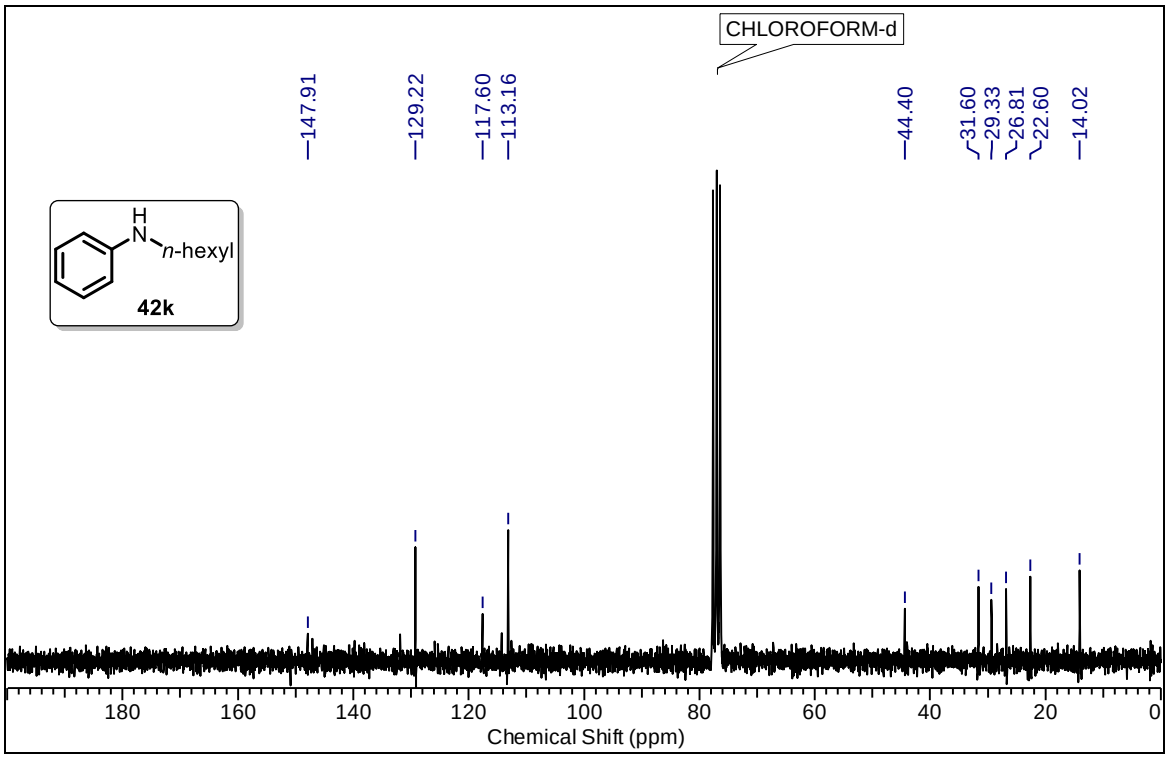

1.8 References:

[1] a) Torborg, C.; Beller, M. *Adv. Synth. Catal.* **2009**, *351*, 3027−3043; b) Corbet, J.-P.; Mignani, G. *Chem. Rev.* **2006**, *106*, 2651−2710; c) Schlummer, B.; Scholz, U. *Adv. Synth. Catal.* **2004**, *346*, 1599−1626.

[2] a) Surry, D. S.; Buchwald, S. L. *Chem. Sci.* **2011**, *2*, 27−50; b) Hartwig, J. F. *Nature* **2008**, *455*, 314−322; c) Bariwal, J.; Van der Eycken, E. *Chem. Soc. Rev.* **2013**, *42*, 9283−9283; d) Lundgren, R. J.; Stradiotto, M. *Chem. Eur. J.* **2012**, *18*, 9758−9769.

[3] Beletskaya, I. P.; Cheprakov, A. V. *Organometallics* **2012**, *31*, 7753−7808; b) Fischer, C.; Koenig, B. *Beilstein J. Org. Chem.* **2011**, *7*, 59−74.

[4] a) Fleckenstein, C. A.; Plenio, H. *Chem. Soc. Rev*. **2010**, *39*, 694−711; b) Hicks, J. D.; Hyde, A. M.; Alberto Martinez, C.; Buchwald, S. L. *J. Am. Chem. Soc.* **2009,** *131*, 16720; c) Klinkenberg, J. L.; Hartwig, J. F. *Angew. Chem., Int. Ed.* **2011,** *50*, 86; d) Doherty, S.; Knight, J.G.; McGrady, J. P.; Ferguson, A. M.; Ward, N. A. B.; Harrington, R. W.; Clegg, W. *Adv. Synth. Catal.* **2010**, *352*, 201; e) Lundgren, R. J.; Peters, B. D.; Alsabeh, P. G.; Stradiotto, M. *Angew. Chem., Int. Ed.* **2010**, *49*, 4071.

[5] a) Díez-González, S.; Marion, N.; Nolan, S. P. *Chem. Rev.* **2009**, *109*, 3612−3676; b) Fortman, G. C.; Nolan, S. P. *Chem. Soc. Rev.* **2011**, *40*, 5151−5169; c) Kantchev, E. A. B.; O'Brien, C. J.; *Angew. Chem., Int. Ed.* **2007**, *46*, 2768−2813.

[6] a) Tu, T.; Fang, W.; Jiang, J. *Chem. Commun.* **2011**, *47*, 12358. b) Zhu, L.; Ye, Y.; Shao, L. *Tetrahedron* **2012**, *68*, 2414; c) Chartoire, A.; Frogneux, X.; Nolan, S.P. *Adv. Synth. Catal.* **2012**, *354*, 1897; d) Valente, C.; Çalimsiz, S.; Hoi, K. H.; Mallik, D.; Sayah, M.; Organ, M. *Angew. Chem., Int. Ed.* **2012**, *51*, 3314; e) Fang, W.; Jiang, J.; Xu, Y.; Zhou, J.; Tu, T. *Tetrahedron* **2013**, *69*, 673; f) Huang, P.; Wang, Y.; Yu, H.; Lu, J. *Organometallics* **2014**, *33*, 1587.

[7] a) Wolfe, J. P.; Wagaw, S.; Marcoux, J.-F.; Buchwald, S. L. *Acc. Chem. Res.* **1998**, *31*, 805−818; b) Hartwig, J. F. *Angew. Chem., Int. Ed.* **1998**, 37, 2046−2067; c) Hartwig, J. F.; Kawatsura, M.; Hauck, S. I.; Shaughnessy, K. H.; Alcazar-Roman, L. M. *J. Org. Chem.* **1999**, *64*, 5575−5580.

[8] Wolfe, J. P.; Buchwald, S. L. *J. Org. Chem.* **2000**, *65*, 1144−1157.

[9] Mann, G.; Hartwig, J. F.; Driver, M. S.; Fernández-Rivas, C. *J. Am. Chem. Soc.* **1998**, *120*, 827−828.

[10] a) Yin, J.; Buchwald, S. L. *Org. Lett.* **2000**, *2*, 1101−1104; b) Artamkina, G. A.; Sergeev, A. G.; Beletskaya, I. P. *Tetrahedron Lett.* **2001**, *42*, 4381−4384.

[11] Hartwig, J. F. *Acc. Chem. Res.* **2008**, *41*, 1534−1544.

[12] Tardiff, B. J.; McDonald, R.; Ferguson, M. J.; Stradiotto, M. *J. Org. Chem.* **2012**, *77*, 1056−1071.

[13] Crawford, S. M.; Lavery, C. B.; Stradiotto, M. *Chem. – Eur. J.* **2013**, *19*, 16760−16771.

[14] Surry, D. S.; Buchwald, S. L. *Angew. Chem., Int. Ed.* **2008**, *47*, 6338−6361.

[15] a) Old, D. W.; Wolfe, J. P.; Buchwald, S. L. *J. Am. Chem. Soc.* **1998**, *120*, 9722; b) Surry, D. S.; Buchwald, S. L. *J. Am. Chem. Soc.* **2007**, *129*, 10354; c) Martin, R.; Buchwald, S. L. *Acc. Chem. Res.* **2008**, 41, 1461.

[16] a) Percec, V.; Golding, G. M.; Smidrkal, J.; Weichold, O. *J. Org. Chem.* **2004**, *69*, 3447; b) Yang, Q.; Ney, J. E.; Wolfe, J. P. *Org. Lett.* **2005**, *7*, 2575; c) Reetz, M. *Angew. Chem., Int. Ed.* **2008**, *47*, 2556; d) Cao, P.; Qu, J.; Burton, G.; Rivero, R. A. *J. Org. Chem.* **2008**, *73*, 7204; e) Moldoveanu, C.; Wilson, D. A.; Wilson, C. J.; Corcoran, P.; Rosen, B. M.; Percec, V. *Org. Lett.* **2009**, *11*, 4974; f) D. A.; Wilson, Wilson, C. J.; Moldoveanu, C.; Resmerita, A. M.; Corcoran, P.; Hoang, L. M.; Rosen, B. M.; Percec, V. *J. Am. Chem. Soc.* **2010**, *132*, 1800.

[17] a) Espinet, P.; Echavarren, A. M. *Angew. Chem., Int. Ed.* **2004**, *43*, 4704; b) Hartwig, J. F. *Acc. Chem. Res.* **2008**, *41*, 1534.

[18] Vitaku, E.; Smith, D. T.; Njardarson, J. T. *J. Med. Chem.* **2014**, *57*, 10257−10274.

[19] Dahl, T.; Tornøe, C. W.; Bang-Andersen, B.; Nielsen, P.; Jørgensen, M. *Angew. Chem. Int. Ed.* **2008**, *47*, 1726−1728.

[20] Willis, M. C.; Snell, R. H.; Fletcher, A. J.; Woodward, R. L. *Org. Lett.* **2006**, *8*, 5089−5091.

[21] a) Ernst, J. B.; Tay, N. E. S.; Jui, N. T.; Buchwald, S. L. *Org. Lett.* **2014**, *16*, 3844−3846; b) McLaughlin, M.; Palucki, M.; Davies, I. W. *Org. Lett.* **2006**, *8*, 3311−3314.

[22] a) Tasler, S.; Mies, J.; Lang, M. *Adv. Synth. Catal*. **2007**, *349*, 2286−2300; b) Roughley, S. D.; Jordan, A. M. *J. Med. Chem.* **2011**, *54*, 3451−3479; c) Cooper, T. W. J.; Campbell, I. B.; Macdonald, S. J. F. *Angew. Chem. Int. Ed.* **2010**, *49*, 8082−8091.

[23] a) Christensen, H.; Schjøth-Eskesen, C.; Jensen, M.; Sinning, S.; Jensen, H. H. *Chem. - Eur. J.* **2011**, 17, 10618−10627; b) Wolfe, J. P.; Rennels, R. A.; Buchwald, S. L. *Tetrahedron* **1996**, *52*, 7525−7546.

[24] Dyrager, C.; Möllers, L. N.; Kjäll, L. K.; Alao, J. P.; Dinér, P.; Wallner, F. K.; Sunnerhagen, P.; Grøtli, M. *J. Med. Chem.* **2011**, *54*, 7427−7431.

[25]a) Gopalsamy, A.; Shi, M.; Golas, J.; Vogan, E.; Jacob, J.; Johnson, M.; Lee, F.; Nilakantan, R.; Petersen, R.; Svenson, K.; Chopra, R.; Tam, M. S.; Wen, Y.; Ellingboe, J.; Arndt, K.; Boschelli, F. *J. Med. Chem.* **2008**, *51*, 373−375; b) Dow, R. L.; Li, J.-C.; Pence, M. P.; Gibbs, E. M.; LaPerle, J. L.; Litchfield, J.; Piotrowski, D. W.; Munchhof, M. J.; Manion, T. B.; Zavadoski, W. J.; Walker, G. S.; McPherson, R. K.; Tapley, S.; Sugarman, E.; Guzman-Perez, A.; DaSilva-Jardine, P. *ACS Med. Chem. Lett.* **2011**, *2*, 407−412; c) George, D. M.; Breinlinger, E. C.; Friedman, M.; Zhang, Y.; Wang, J.; Argiriadi, M.; Bansal-Pakala, P.; Barth, M.; Duignan, D. B.; Honore, P.; Lang, Q.; Mittelstadt, S.; Potin, D.; Rundell, L.; Edmunds, J. J. *J. Med. Chem.* **2015**, *58*, 222−236; d) Griffin, A. M.; Brown, W.; Walpole, C.; Coupal, M.; Adam, L.; Gosselin, M.; Salois, D.; Morin, P.-E.; Roumi, M. *Bioorg. Med. Chem. Lett*. **2009**, *19*, 5999−6003; e) Gosmini, R.; Nguyen, V. L.; Toum, J.; Simon, C.; Brusq, J.-M. G.; Krysa, G.; Mirguet, O.; Riou-Eymard, A. M.; Boursier, E. V.; Trottet, L.; Bamborough, P.; Clark, H.; Chung, C.-w.; Cutler, L.; Demont, E. H.; Kaur, R.; Lewis, A. J.; Schilling, M. B.; Soden, P. E.; Taylor, S.; Walker, A. L.; Walker, M. D.; Prinjha, R. K.; Nicodème, E. *J. Med. Chem.* **2014**, *57* , 8111−813.

[26] a) Magano, J.; Dunetz, J. R. *Chem. Rev*. **2011**, *111*, 2177−2250; b) Buchwald, S. L.; Mauger, C.; Mignani, G.; Scholz, U. *Adv. Synth. Catal.* **2006**, *348*, 23−39; c) Carey, J. S.; Laffan, D.; Thomson, C.; Williams, M. T. *Org. Biomol. Chem.* **2006**, *4*, 2337−2347.

[27] Reginato, G.; Sadler, P.; Wilkes, R. D. *Org. Process Res. Dev*. **2011**, *15*, 1396−1405.

[28] Galaffu, N.; Man, S. P.; Wilkes, R. D.; Wilson, J. R. H. *Org. Process Res. Dev.* **2007**, *11*, 406−413.

[29] Girgis, M. J.; Kuczynski, L. E.; Berberena, S. M.; Boyd, C. A.; Kubinski, P. L.; Scherholz, M. L.; Drinkwater, D. E.; Shen, X.; Babiak, S.; Lefebvre, B. G. *Org. Process Res. Dev.* **2008**, *12* 1209−1217.

[30] a) Leahy, D. K.; Desai, L. V.; Deshpande, R. P.; Mariadass, A. V.; Rangaswamy, S.; Rajagopal, S. K.; Madhavan, L.; Illendula, S. *Org. Process Res. Dev.* **2012**,*16*, 244−249; b) Alabanza, L. M.; Dong, Y.; Wang, P.; Wright, J. A.; Zhang, Y.; Briggs, A. J. *Org. Process Res. Dev*. **2013**, *17*, 876−880; c) Goodyear, A.; Linghu, X.; Bishop, B.; Chen, C.; Cleator, E.; McLaughlin, M.; Sheen, F. J.; Stewart, G. W.; Xu, Y.; Yin, J. *Org. Process Res. Dev*. **2012**, *16*, 605−611; d) Airey, J.; Barrague, M.; Edwards, M.; Ferro, M.; Friedrich, D.; Gillespy, T.; Jurcak, J.; Musick, K.; Weintraub, P. M. *Synthesis* **2014**, *46*, 96−100; e) Hill, G. B.; Mortlock, A. A. *Synthesis* **2007**, *2007*, 1697−1701.

[31] a) Bringmann, G.; Gulder, T.; Hertlein, B.; Hemberger, Y.; Meyer, F. *J. Am. Chem. Soc.* **2010**, *132*, 1151−1158; b) Foo, K.; Newhouse, T.; Mori, I.; Takayama, H.; Baran, P. S. *Angew. Chem. Int. Ed.* **2011**, *50*, 2716−2719; c) Schmidt, A. W.; Reddy, K. R.; Knölker, H.-J. *Chem. Rev.* **2012**, *112*, 3193−3328; d) Schuster, C.; Julich-Gruner, K. K.; Schnitzler, H.; Hesse, R.; Jager, A.; Schmidt, A. W.; Knölker, H.-J. *Org. Chem.* **2015**, *80*, 5666−5673; e) Börger, C.; Schmidt, A. W.; Knölker, H.-J. *Synlett* **2014**, *25*, 1381−1384; f) Konkol, L. C.; Guo, F.; Sarjeant, A. A.; Thomson, R. J. *Angew. Chem. Int. Ed*. **2011**, *50*, 9931−9934; g) Liang, J.; Hu, W.; Tao, P.; Jia, Y. *Org. Chem.* **2013**, *78*, 5810−5815; h) Aigret, B. M.; Jacobs, J.; Van Meervelt, L.; De Borggraeve, W. M. *Synlett* **2013**, *24*, 1097−1100.

[32] Mari, M.; Bartoccini, F.; Piersanti, G. *J. Org. Chem.* **2013**, *78*, 7727−7734.

[33] Ueno, A.; Kitawaki, T.; Chida, N. *Org. Lett.* **2008**, *10*, 1999−2002.

[34] a) Benedetti, E.; Kocsis, L. S.; Brummond, K. M. *J. Am. Chem. Soc*. **2012**, *134*, 12418−12421; b) Ito, A.; Yokoyama, Y.; Aihara, R.; Fukui, K.; Eguchi, S.; Shizu, K.; Sato, T.; Tanaka, K. *Angew. Chem. Int. Ed.* **2010**, *49*, 8205−8208; c) Yokoyama, Y.; Sakamaki, D.; Ito, A.; Tanaka, K.; Shiro, M. A. *Angew. Chem. Int. Ed*. **2012**, *51*, 9403−9406; d) Terazono, Y.; Kodis, G.; Bhushan, K.; Zaks, J.; Madden, C.; Moore, A. L.; Moore, T. A.; Fleming, G. R.; Gust, D. *J. Am. Chem. Soc.* **2011**, *133*, 2916−2922; e) Fa, S.-X.; Wang, L.-X.; Wang, D.-X.; Zhao, L.; Wang, M.-X. *J. Org. Chem.* **2014**, *79*, 3559−3571.

[35] Mata, G.; Luedtke, N. W. *J. Am. Chem. Soc.* **2015**, *137*, 699−707.

[36] Ji, L.; Lorbach, A.; Edkins, R. M.; Marder, T. B. *J. Org. Chem.* **2015**, *80*, 5658−5665.

[37] Nazir, R.; Balčiūnas, E.; Buczyńska, D.; Bourquard, F.; Kowalska, D.; Gray, D.; Maćkowski, S.; Farsari, M.; Gryko, D. T. *Macromolecules* **2015**, *48*, 2466−2472.

[38] Fors, B. P.; Watson, D. A.; Biscoe, M. R.; Buchwald, S. L. *J. Am. Chem. Soc.* **2008**, *130* , 13552.

[39] Fors, B. P.; Davis, N. R.; Buchwald, S. L. *J. Am. Chem. Soc.* **2009**, *131*, 5766.

[40] Fors, B. P.; Buchwald, S. L. *J. Am. Chem. Soc.* **2010**, *132*, 15914–15917.

[41] a) Surry, D. S.; Buchwald, S. L. *Chem. Sci.* **2011**, *2*, 27-50; b) Klinkenberg, J. L.; Hartwig, J. F. *Angew. Chem. Int. Ed*. **2011**, *50*, 86; c) Cai, L.; Qian, X.; Song, W.; Liu, T.; Tao, X.; Li, W.; Xie, X. *Tetrahedron* **2014**, *70*, 4754.

[42] Guram, A. S.; Buchwald, S. L. *J. Am. Chem. Soc.* **1994**, *116*, 7901–7902.

[43] Xie, X.; Zhang, T.; Zhang, Z. *J. Org. Chem.* **2006**, *71*, 6522-6529.

[44] Huang, P.; Wang, Y.; Yu, H.; Lu, J. *Organometallics* **2014**, *33*, 1587-1593.

[45] Hill , L.; Crowell, J.; Tutwiler, S.; Massie, N.; Hines, C.; Griffin, S.; Rogers, R.; Shaughnessy, K. *J. Org. Chem.* **2010**, *75*, 6477-6488.

[46] Barker, T. J.; Jarvo, E. R. *Angew. Chem. Int. Ed*. **2011**, *50*, 8475 –8478.

[47] Shim, S.; Huh, K.; Park, W. *Tetrahedron* **1986**, *42*, 259-263.

[48] Zhou, C.; Yang, D.; Jia, X.; Zhang, L.; Cheng, J. *Synlett* **2009**, *19*, 3198-3200.

[49] Fors, B. P.; Davis, N. R.; Buchwald, S. L. *J. Am. Chem. Soc.* **2009**, *131*, 5766-5768.

[50] Alsabeh , P. G.; Stradiotto , M. *Angew. Chem. Int. Ed*. **2013**, *52*, 7383-7387.

[51] Matsubara, K.; Ueno, K.; Koga, Y.; Hara, K. *J. Org. Chem.* **2007**, *72* , 5069-5076.

Chapter 2: Section A

Synthesis of SBA-15 supported heterogeneous Ru(II)-1,2,3-Triazole catalyst: Application to the 1,4-selective click reaction for C-N bond formation

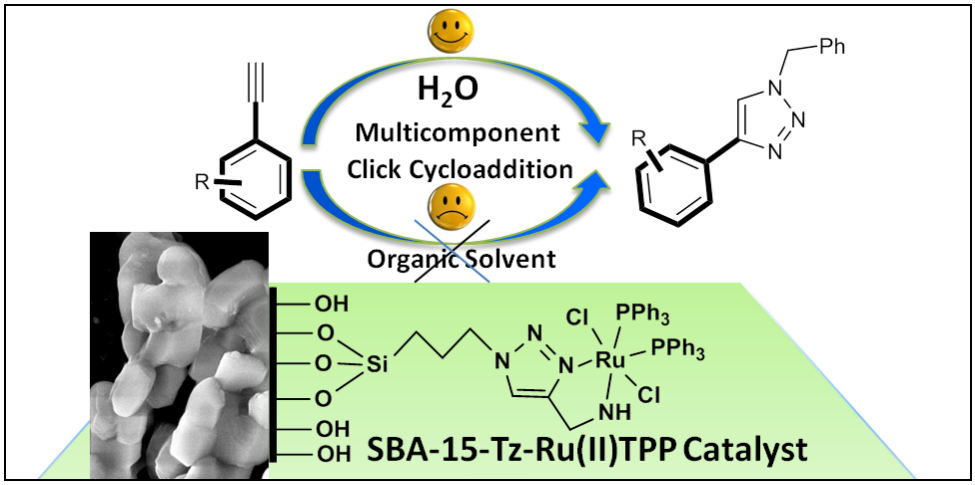

2.1.1 Introduction:

Since the development of the heterogeneous catalysts, SBA-15 serves as the crucial solid support for the catalyst due to its inherent chemical and physical morphology. After the first reports of the periodic mesoporous silica, MCM 41 (Mobil Crystalline Materials)[1] and SBA-15 (Santa Barbara Amorphous)[2] (Figure-1) with highly regularised narrow hexagonal pores have boosted the research for the modification and control of morphology and surface of silica. The properties of SBA 15 such as tuneable pore size (2 to 30 nm), very high surface area (400 to 900 m^2/g), and higher hydrothermal and mechanical stability attracted much attention in academic research for the important applications for the welfare of people. Mesoporous materials could be used as support for catalyst,[3] in adsorption and separation,[4] advanced optics,[5] drug delivery,[6] biosensor,[7] thermal energy storage,[8] etc.

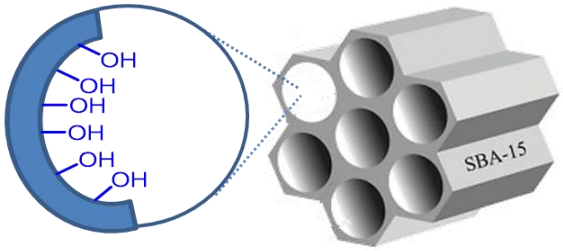

Figure 1: 3D structure of SBA-15

SBA-15 contains the free hydroxyl group inside the pore, plays a crucial role for the properties useful for the application. The main goal of recent research is to modify the surface via functionalization on free –OH group with organic molecules of these materials and could be useful for various applications.

2.1.2 Literature reports:

Yusoff and co-workers [9] have developed heterogeneous Pd- catalyst by modifying the surface of SBA-15. They have covalently anchored the organic silane molecules containing alkyl chain with thiol, which serves as a ligand for the binding with palladium metal. The developed heterogeneous Pd- catalyst was screened for Sonogashira and Suzuki-Miyaura cross-coupling reactions (Scheme 1). The catalyst was found to be the highly active catalyst for these coupling reactions of aryl halide. The catalyst works for Sonogashira cross-coupling without copper and solvent and could be recovered directly from the reaction mixture without significant loss of its activity.

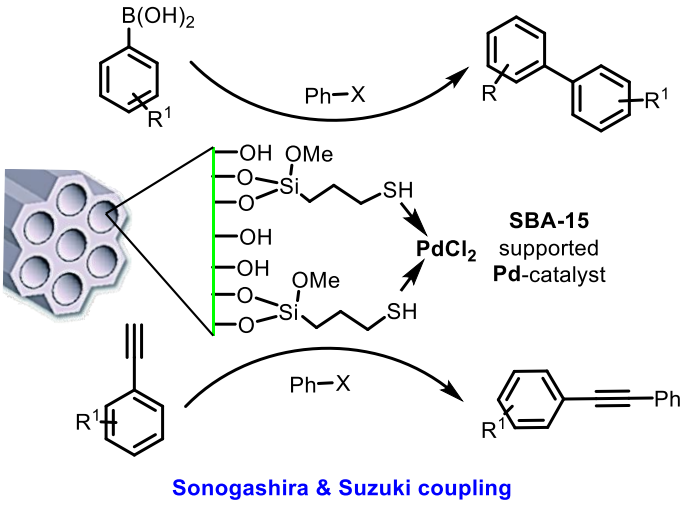

Scheme 1: Heterogeneous Pd-catalyst for Suzuki & Sonogashira coupling reactions

Burri and co-workers [10] have prepared the heterogeneous gold catalyst by immobilizing the gold nanoparticles on the lipoic acid grafted SBA-15 (SBA-LAG) mesoporous silica. SBA-LAG was synthesized via grafting of propyl amine linker over SBA-15, followed by the tethering of lipoic acid and at last the gold nanoparticle anchored over the ligand site. The catalyst is found to be an efficient heterogeneous catalyst for one pot multi-components reaction of aldehyde, amine, and alkyne (scheme 2).

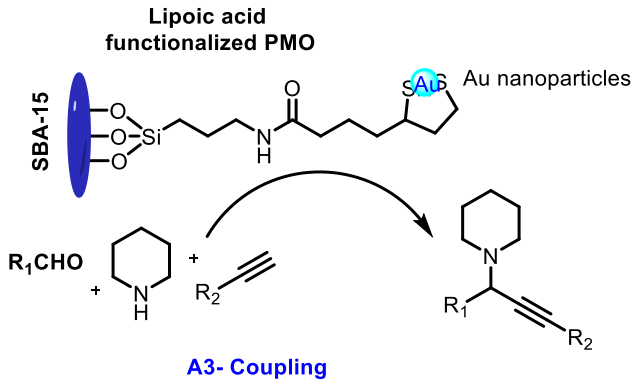

Scheme 2 One-pot synthesis of propargylamines over SBA-LAG catalyst

Bao and co-worker[11] have synthesized modified solid surfaces of SBA-15 by encoring the phosphine containing organic chain with linker template (Ph-SBA-15-PPh_3), followed by the anchoring of palladium metal via ligand-exchange to obtain the solid supported Pd catalyst Ph-SBA-15-PPh_3-Pd. They have displayed the catalytic activity for the Suzuki reaction with a wide range of aryl bromides with aryl boronic acids in supercritical carbon dioxide (Scheme 3). They have reported the 7-time catalyst to recycle without loss of activity.

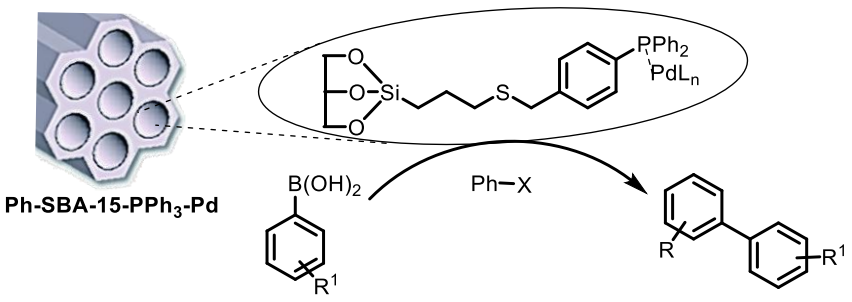

Scheme 3: Suzuki reaction in supercritical CO_2 with Ph-SBA-15-PPh_3-Pd

Paul *et al.* [12] have developed heterogeneous nickel catalyst supported over modified silica SBA-15-NH_2-DAMO. The modified surface has been synthesized via functionalization with linker 3-aminopropyl-triethoxysilane and followed by the Schiff base condensation with diacetyl monoxime, followed by the reaction with the nickel perchlorate ($Ni(ClO_4)_2$) to obtain functionalized nickel catalyst SBA-15-NH_2-DAMO-Ni. The catalyst was screened for the oxidation of a wide range of olefin using *tert*-butyl hydroperoxide as oxidant (scheme 4).

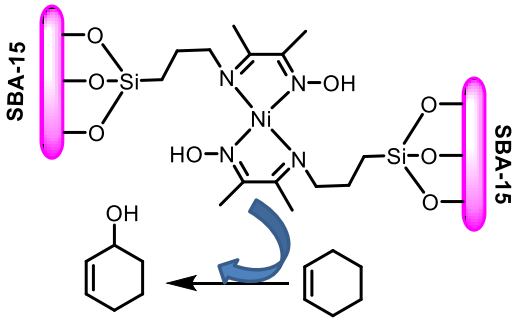

Scheme 4: Catalytic oxidation of olefin following a concerted mechanism

Most recent literature reports for the functionalization of SBA-15 and its applications are based on the controlled drug-delivery systems (DDSs).[13] It could serve as an ideal system in health care; it enables the constant rate of release of the drug and to maintain the optimum concentration of medicine in the blood. Deng[14] has reported preparation, characterization of amino-functionalized mesoporous silica (A-SBA-15) as drug delivery agents. They have investigated the efficacy of SBA-15 and modified A-SBA-15 for the controlled release of baicalin (SBA-15/baicalin and A-SBA-15/baicalin). A-SBA-15/baicalin was found as a better delivery system than SBA-15/baicalin due to the faster dissolution rate in the modified surface and therefore more favorable for the drug absorption (Scheme 5).

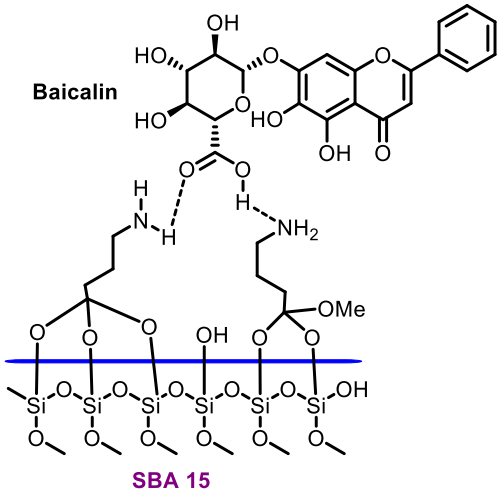

Scheme 5: Interaction of Baicalin with the surface of SBA-15–Pr–NH_2

2.1.2.1 Click reaction:

The click reaction has attracted the researcher because, it enables the synthesis of a wide range of triazole heterocycles with convenient reaction conditions, atom economy, high selectivity and wide range of functional group tolerance[15] which dignified importance in the area of medicinal chemistry, polymer[16] and material sciences.[17] Apart from this, click reaction has a vital role in the field of coordination chemistry for designing the new ligand and modification based on 1,2,3-triazole.[18] Generally click reaction is two components cycloaddition reaction of organic azide and an alkyne in the presence of metal catalysts. However, most of the methods suffer from the limitation such as stability of reactant, tedious procedure and long reaction time which leads to the formation of other side product.[19]

Apart from the copper, other metals complexes are also reported for catalyzing the click cycloaddition reaction of terminal alkyne and organic azides and selectively delivered the 1,4- and 1,5-substituted 1,2,3-triazoles (Scheme 6).[20]

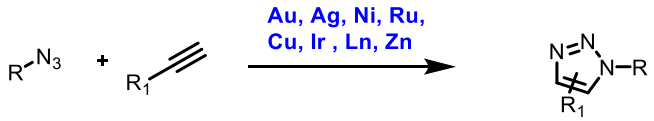

Scheme 6: Metal complex reported for the click cycloaddition reaction

Catalyst dependent regioselectivity in Ru-catalyst click reaction is unambiguously documented in the literature.[21] The ligands present in the Ru-metal complex and the oxidation state of Ru influence the selectivity of the click cyclo-addition reaction. The Ru-metal complex with cyclopentadienyl (Cp and Cp*) ligand and Ru(I) metal favor the

formation of 1,5-disubstituted triazoles, while without Cp/Cp* ligand and Ru(II) complexes favor the formation of 1,4-disubstituted triazoles (scheme 7).

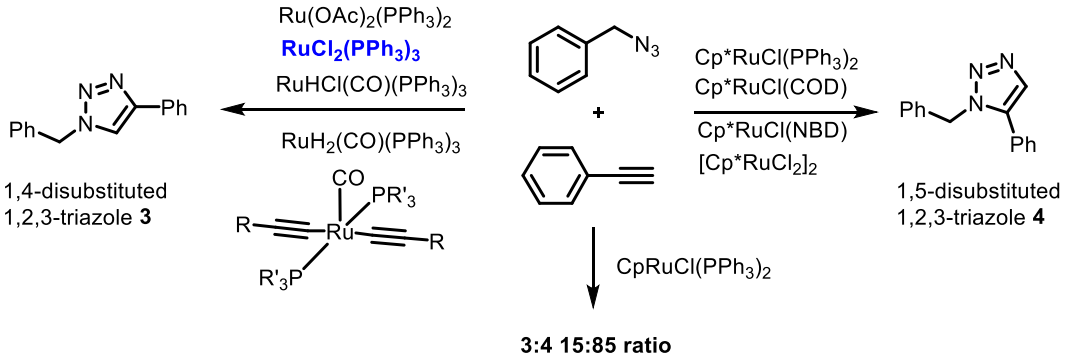

Scheme 7: Catalyst dependent regioselectivity in click reaction

Molla *et al.*[22] have reported recoverable polymer supported Ru(III) complex and first time displayed catalytic activity for the multicomponent azide-alkyne cycloaddition reaction of an alkyne, benzyl bromide and sodium azide in water as the heterogeneous medium. The click reaction was highly regioselective for 1,4-disubstituted 1,2,3-triazoles (Scheme 8)

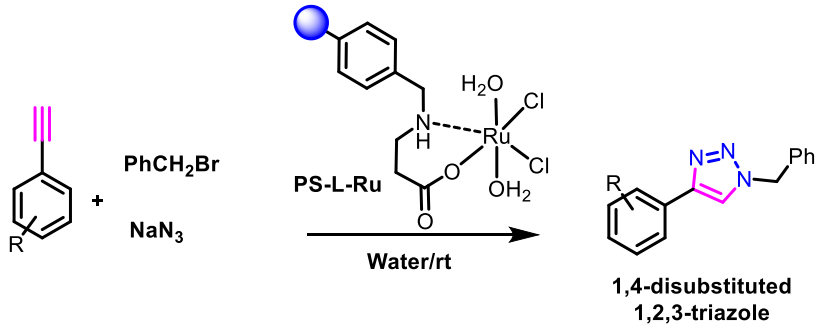

Scheme 8: Polymer-supported Ru(III) catalyzed cycloaddition reactions

In 2012, remarkable work was reported by Funk and co-workers,[23] the method for distinguishing between two regioisomers of 1,2,3-triazoles by using ^{13}C NMR analysis. 1,4-Disubstituted triazoles show the proton-decoupled ^{13}C NMR signal of secondary carbon of triazole at δ 119.5 ppm and proton-coupled ^{13}C NMR shows the doublet of triplet signal with coupling constant J = 191 and 2.7 Hz. While 1,5-disubstituted triazole showed signal at 133.3 ppm and coupled ^{13}C NMR shows doublet signal with coupling constant J = 195 Hz (Figure 2).

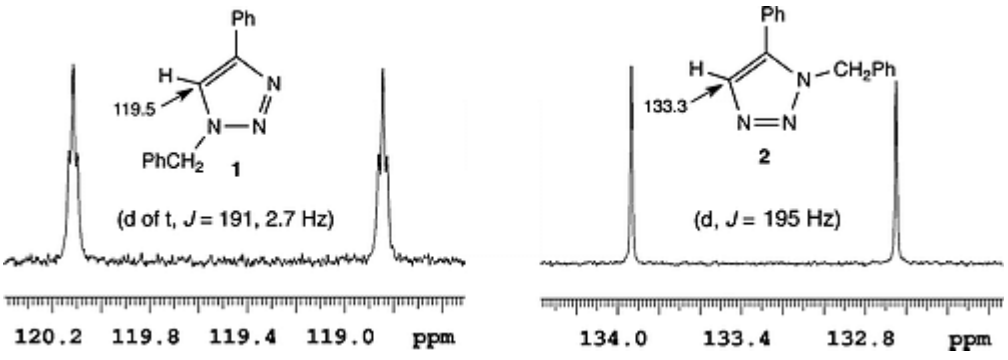

Figure 2: Distinguished ^{13}C NMR signal of 1,4- and 1,5- triazoles

However, these catalytic system suffers from certain drawbacks, such as it requires additive, sodium ascorbate, functional group tolerance, limited substrate scope and use of high boiling organic solvents like DMF, DMSO, dioxane, acetonitrile, etc. reactions.

2.1.3 Present work and Hypothesis:

Considering the literature report, we have designed a new ligand SBA-15-Tz covalently anchored over mesoporous silica SBA-15. The Ru-metal could be easily bound with the silica supported ligand to obtain the catalyst named as SBA-15-Tz-Ru(II)TPP (Figure 3):

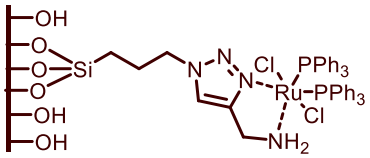

SBA-15-Tz-Ru(II)TPP

Figure 3: Proposed supported Ru-catalyst

We envisioned multi-component click cycloaddition of alkyne, azide and alkyl halide for the catalytic application of the synthesized solid supported Ru(II) catalyst SBA-15-Tz-Ru(II)TPP (Scheme 9).

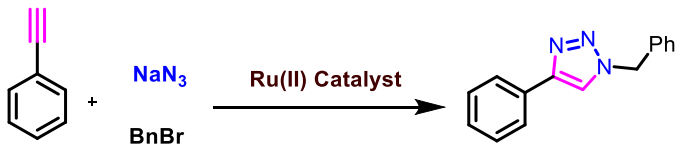

Scheme 9: Proposed catalytic organic transformation using SBA-15-Tz-Ru(II)TPP

Synthesis of SBA-15-Tz-Ru(II)TPP

The synthesis strategy for the preparation of solid supported Ru catalyst SBA-15-Tz-Ru(II)TPP is briefly shown in scheme 10. SBA-15 silica was modified by

functionalizing the free hydroxyl group, the azido linker 3-Az-PTMS covalently anchored, followed by the click reaction with propargylamine to obtain 1,2,3-triazole as SBA-15 supported ligand (SBA-15-Tz). Further, functionalized SBA-15-Tz was treated with $[RuCl_2(PPh_3)_3]$ complex in DMF and refluxed for 12h, and the Ru-metal successfully immobilized over the synthesized solid support (Scheme 10).

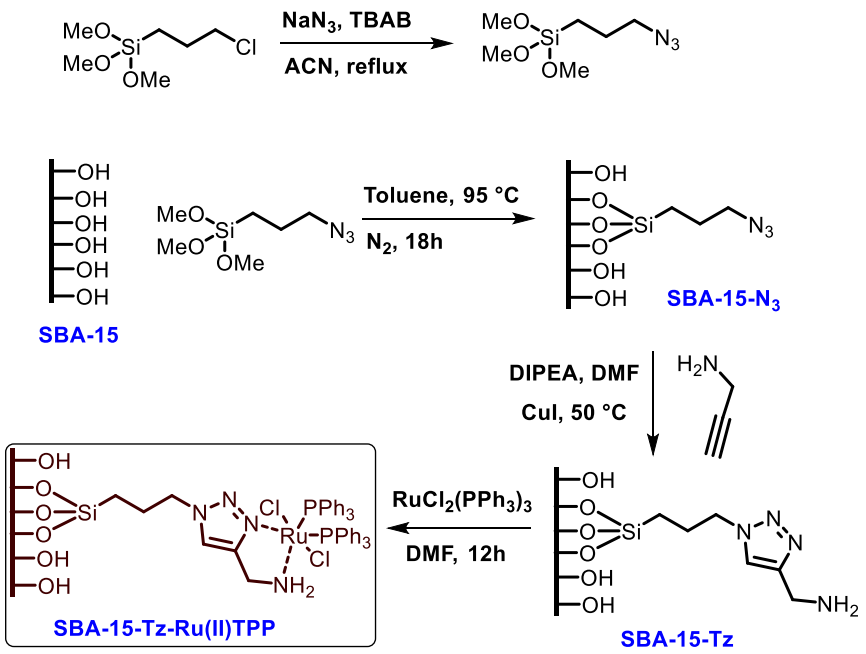

Scheme 10: Synthesis of SBA-15-Tz-Ru(II)TPP

The catalyst was prepared and characterized with the help of our collaborator Dr. A.P. Singh and his group in catalysis division. The structure of catalyst was confirmed by using various analysis techniques like small angle powder XRD, comparative IR analysis for each step of the synthesis. ^{13}C, ^{31}P, and ^{29}Si solid-state CP-MAS NMR analysis, the pore size of modified SBA-15 were analyzed by N_2 adsorption-desorption isotherm. The Ru XPS binding energy analysis confirmed the presence of Ru metal and the oxidation state of the metal. The morphology of the solid supported after the synthesis was analyzed by TEM and SEM. The amount of Ru metal present in the catalyst SBA-15-Tz-Ru(II)TPP was analyzed by ICP-OES technique. The characterization data of catalyst could be easily accessed from online publication.[24] After having the SBA-15 supported Ru catalyst and to prove our hypothesis, we screened the efficacy of this catalyst for the multi-component click reaction. The obtained results are illustrated in following section.

2.1.4 Results and discussion:

2.1.4.1 Optimization of reaction conditions:

Phenylacetylene, sodium azide and benzyl bromide were chosen as a model substrate for the optimisation of the reaction conditions and reacted in the presence of various Ru catalyst for the click reaction.

Table 1: Optimization for multi-component cycloaddition reaction in homogeneous and heterogeneous medium.[a]

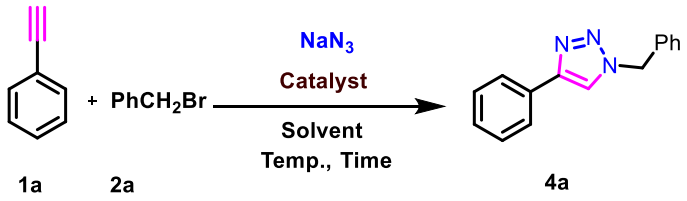

Sr. No.	Catalyst	Ligand	Temp. (°C)	Solvent	Yield (%)
1	$RuCl_3$	PPh_3	90	DMF	6
2	$RuCl_3$	PPh_3	90	DMSO	24
3	$RuCl_3$	PPh_3	90	Dioxane	26
4	$RuCl_3$	PPh_3	90	Toluene	5
5	$RuCl_3$	PPh_3	90	Water	48
6	$RuCl_3$	DMAP	90	Water	32
7	$RuCl_3$	2-amino-6-picoline	90	Water	10
8	$[Ru(p\text{-}cym)Cl]_2$	--	90	Water	26
9	SBA-15-Tz-Ru(II)TPP	--	90	Water	88
10	SBA-15-Tz-Ru(II)TPP	--	RT	Water	NR
11	SBA-15-Tz-Ru(II)TPP	--	90	DMSO	46
12	SBA-15-Tz-Ru(II)TPP	--	90	DMF	63
13	SBA-15-Tz-Ru(II)TPP	--	90	*t*-BuOH	35
14	SBA-15-Tz-Ru(II)TPP	--	80	EtOH	50
15	SBA-15-Tz-Ru(II)TPP	--	66	THF	20

[a]**Reaction conditions:** Phenylacetylene (1 mmol), Benzyl bromide (1.2 mmol), Sodium azide (1.2 mmol), Catalyst (Ruthenium 5 mol %)/ SBA-15-Tz-Ru(II)TPP Catalyst (15 mg, Ruthenium metal 0.445 mol %) and solvent (3 mL). The reaction mixture was refluxed for 18 h, NR= No reaction;

To find the best optimized reaction conditions, in the beginning the homogeneous $RuCl_3/PPh_3$ catalyst was screened with various organic solvents such as DMF, DMSO, Dioxane and toluene and refluxed at 90 °C for the 18 h, the reaction ended up with lower yield of product up to 26% only and with 1,4-selectivity (1,4-disubstituted triazole, Table 1 entry 1-4). Interestingly, when water was used as a solvent with $RuCl_3/PPh_3$ catalyst system, the yield of triazole was increased up to 48% with 1,4-selectivity (Table 1 entry 5). Further, to optimize the yield, the reaction was carried out by changing the ligand DMAP and 2-amino-6-picoline in place of TPP in an aqueous medium, but the reaction was poor yielding (Table 1. entry 6, 7). $[Ru(p\text{-}cym)Cl]_2$ was also not found efficient to improve the yield of desired product **4a**. Next to improve the yield of product we switched over to heterogeneous conditions, when the reaction was performed with our developed solid supported catalyst SBA-15-Tz-Ru(II)TPP in aqueous medium, delightfully the click reaction worked very smoothly and delivered the excellent yield (88%) of the desired product with 1,4-selectivity (Table 1, entry 9).

To optimize best reaction conditions further we have screened the click reaction using SBA-15-Tz-Ru(II)TPP as a catalyst with wide variety of solvents like DMSO, DMF, EtOH, *t*-BuOH and THF at reflux temperature, the results only showed decrease in the yields (20-63%) of desired product **4a** (Table 1, entries 11 to 15). Besides these when the reaction was performed at room temperature using our catalyst (SBA-15-Tz-Ru(II)TPP) in the aqueous medium, the reaction did not trigger even on prolongation for 24 h (Table 1, entry 10). The green solvent water as medium and other conditions was found the most suitable for the click reaction with solid supported SBA-15-Tz-Ru(II)TPP catalyst (Table 1, entry 9).

2.1.4.2 The substrate scope

After the best-optimized condition in hand, further to establish the generality for the catalytic activity of synthesized silica supported SBA-15-Tz-Ru(II)TPP, we employed the catalyst for a variety of substituted phenylacetylenes and benzyl halides with sodium azide to obtain the corresponding 1,4-disubstituted 1,2,3-triazole, the results are illustrated in Table 2.

Table 2: The substrate scope of alkyne and aryl/alkyl halide

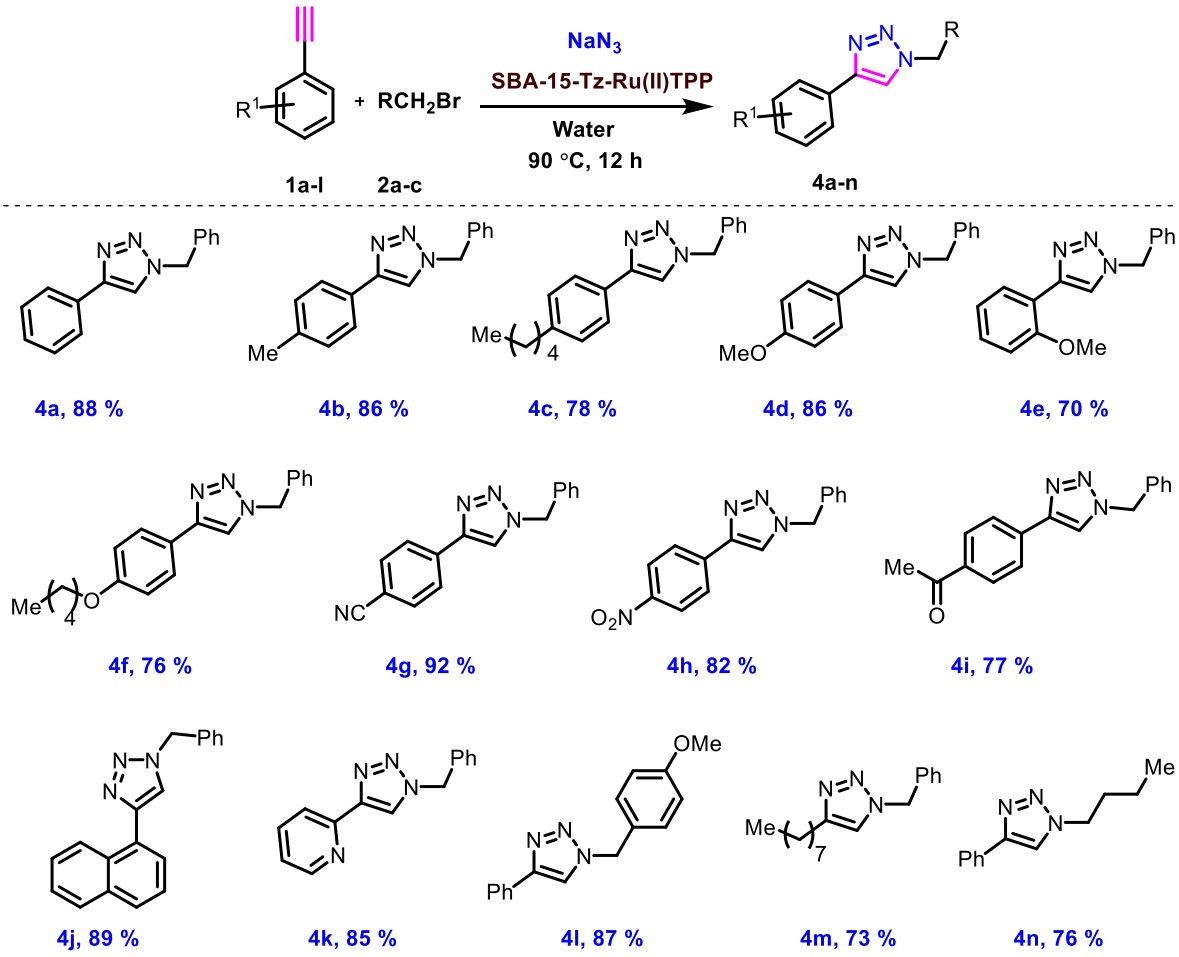

Various substituted phenylacetylenes were smoothly reacted with benzyl bromide and sodium azide under the optimized reaction conditions to afford the desired product **4a-i.** The electronic nature (electron withdrawing or donating) of substitution present on the acetylene such as -Me, -OMe, -NO_2, -CN, -COMe and long aliphatic chain does not have any influence on the rate of reaction, all delivered the respective 1,4-disubstituted 1,2,3-triazole **4** in good to excellent yield. Further the acetylene with heterocyclic ring (pyridine) also readily reacted under the developed catalytic conditions to provide the respective triazole **4k** in excellent yields (87%). Bulky aromatic acetylene also furnished the corresponding product **4j** in excellent yield (89%). Interestingly, aliphatic alkyne and aliphatic halide and *p*-methoxy benzyl chloride also afforded the respective desired product **4m, 4n,** and **4l** in good to excellent yields.

2.1.4.3 Recycle study

After establishing the substrate scope, we proceeded forward for the stability and recyclability study of the developed catalyst, SBA-15-Tz-Ru(II)TPP. The catalyst was consecutively used five times for the one-pot multi-component click cycloaddition reaction. After the completion of the reaction, the catalyst SBA-15-Tz-Ru(II)TPP was removed by filtration through the Whatman filter paper and washed several times with ethyl acetate or DCM and dried overnight under the oven. After each recycle, the considerable change was observed in the conversion and 1,4-selectivity of the corresponding desired product (Figure 4). Finally, after the last cycle, the recovered catalyst was subjected for the ICP-OES analysis, the recycled catalyst showed nearly the same ruthenium metal content as the fresh catalyst. These results revealed that the heterogeneous SBA-15-Tz-Ru(II)TPP catalyst is very stable and the activity can be retained for the several recycles.

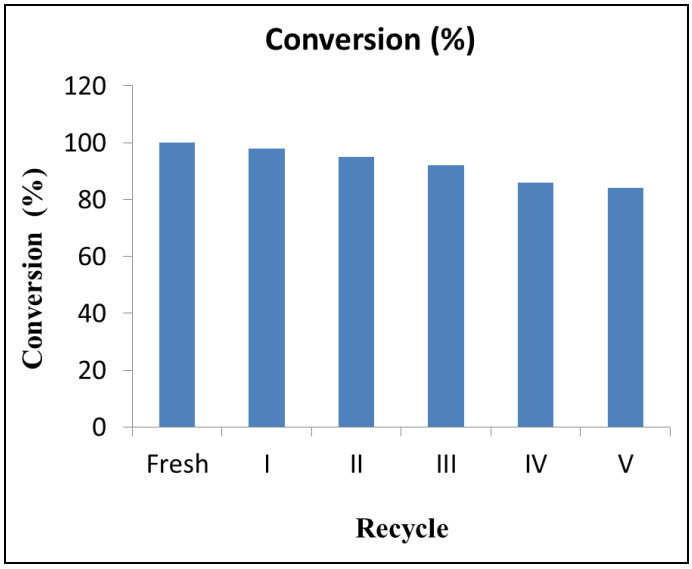

Figure 4: Recycle study of SBA-15-Tz-Ru(II)TPP catalyst

ICP-OES Ru-metal analysis: 1) Fresh Catalyst, 21.078 mg/L, 2) V^{th} Recycle, 17.09 mg/L.

2.1.4.4 Control Experiments and plausible mechanism for click reaction:

To understand the mechanism and to support the regioselective formation of the 1,4-disubstituted 1,2,3-triazole, some controlled experiments were performed. The proposed method is multi-component and the 1,4-regioselectivity could be achieved; if the reaction follows the sequence as initial cycloaddition of azide and alkyne can provide the intermediate 4-phenyl-*1H*-1,2,3-triazole followed by *in situ* substitution with benzyl bromide could form selective 1,4-disubstituted 1,2,3-triazole (Scheme

11A). To prove this hypothesis, first the reaction was performed with phenylacetylene and sodium azide in the absence of benzyl bromide, the reaction was completed in 6h, and the 4-phenyl-*1H*-1,2,3-triazole was isolated with excellent yield (83 %) under the optimized conditions (Scheme 11B).

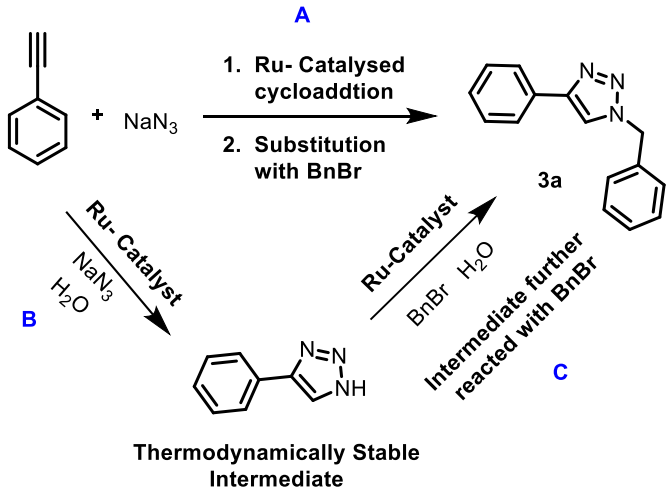

Scheme 11: Control experiments

After purification and analysis, the intermediate 4-phenyl-*1H*-1,2,3-triazole was further subjected for reaction with the benzyl bromide under the similar conditions to obtain the expected 1,4-disubstituted 1,2,3-triazole (Scheme 11C). From these results, we proposed the plausible mechanism for the selective formation of 1,4-disubstituted triazole as shown in Scheme 12.

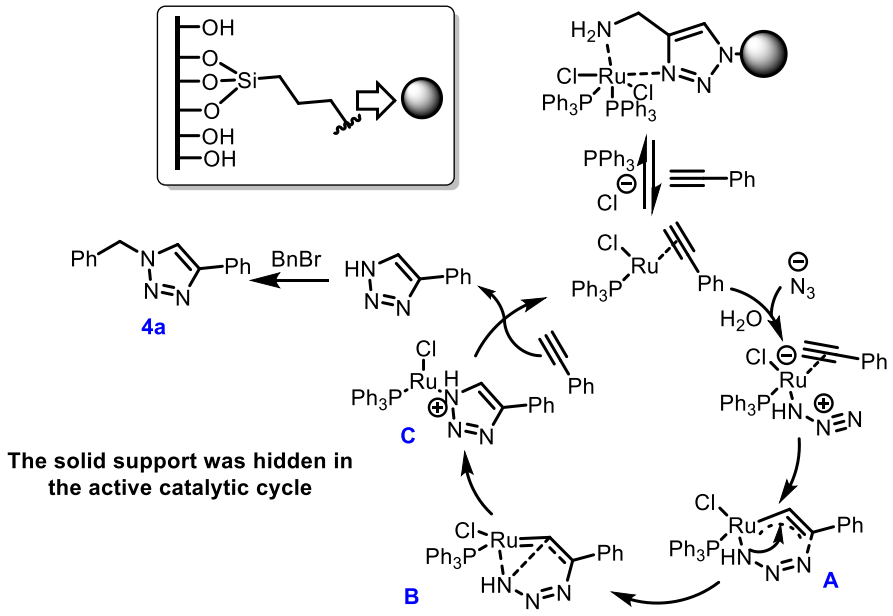

Scheme 12: The plausible mechanism for multicomponent click reaction

2.1.5 Conclusions

In summary, we have demonstrated an efficient method for ligand synthesis and covalent tethering to solid support. A new highly efficient, heterogeneous SBA-15-Tz-Ru(II)TPP catalyst is developed by immobilizing $[RuCl_2(PPh_3)_3]$ complex over triazole functionalized SBA-15. The catalytic efficiency of SBA-15-Tz-Ru(II)TPP was established for multicomponent click cycloaddition. The multi-component cycloaddition reaction exhibits remarkable reactivity in an aqueous medium for the regioselective synthesis of 1,4-disubstituted 1,2,3-triazole in excellent yields. The salient features of the heterogeneous catalyst SBA-15-Tz-Ru(II)TPP are its stability in the water as reaction medium, heterogeneous nature and recyclability without loss of activity.

2.1.6 Experimental

2.1.6.1 General procedure for the Multi-Component Click reaction

In the 50 mL round bottom flask, alkyne (1 mmol), sodium azide (1.2 mmol), benzyl bromide (1.2 mmol) and SBA-15-Tz-Ru(II)TPP catalyst 15 mg were taken followed by addition of 3 ml of water as a solvent. The mixture was stirred at 90°C in the preheated oil bath for a given time. Progress of the reaction was monitored by TLC (2:8 ethyl acetate: pet ether). After the completion of the reaction, 10 mL of ethyl acetate added to the reaction mixture and filtered to recover the SBA-15-Tz-Ru(II)TPP catalyst. The residue was washed with ethyl acetate (5 mL x 3 times). The combined organic layer was dried with anhydrous sodium sulfate and concentrated under the reduced pressure. The crude product was purified by the column chromatography to get the product **4 a-n** (Scheme 3).

2.1.6.2 Analytical Data

1-Benzyl-4-phenyl-*1H*-1,2,3-triazole (4a):[25]

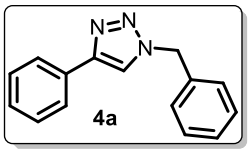

White solid; mp = 126-128 °C (reported mp 127-128 °C);

^{1}H NMR (400MHz, $CDCl_3$) δ = 7.81 (d, *J* = 7.3 Hz, 2 H), 7.68 (s, 1 H), 7.47 - 7.28 (m, 8 H), 5.57 ppm (s, 2 H);

^{13}C NMR (101MHz, $CDCl_3$) δ = 148.1, 134.6, 130.5, 129.1, 128.7, 128.7, 128.1, 128.0, 125.6, 119.5, 54.2 ppm;

MS (EI) m/z = 235.1 [M^+].

1-Benzyl-4-(*p*-tolyl)-*1H*-1,2,3-triazole (4b):[25]

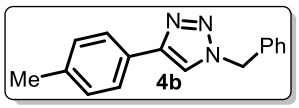

White solid; mp = 142-144 °C (reported 142–146 °C);

^{1}H NMR (400MHz, $CDCl_3$) δ = 7.66 - 7.77 (m, *J* = 7.9 Hz, 2H), 7.64 (s, 1H), 7.35 - 7.43 (m, 3H), 7.31 - 7.35 (m, 1H), 7.30 (br. s., 1H), 7.17 - 7.26 (m, *J* = 7.9 Hz, 2H), 5.56 (s, 2H), 2.37 ppm (s, 3H);

^{13}C NMR (101MHz, $CDCl_3$) δ = 148.2, 137.9, 134.7, 129.4, 129.1, 128.7, 128.0, 127.6, 125.5, 119.1, 54.1, 21.2 ppm;

MS (EI) m/z = 249.2 [M^+].

4-(1-Benzyl-*1H*-1,2,3-triazol-4-yl)benzonitrile (4c):[26]

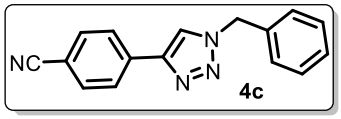

White solid; mp = 140-142 °C;

^{1}H NMR (500MHz, $CDCl_3$) δ = 7.83 - 8.01 (m, *J* = 8.0 Hz, 2 H), 7.77 (s, 1 H), 7.53 - 7.73 (m, *J* = 8.0 Hz, 2 H), 7.40 (br. s., 3 H), 7.28 - 7.37 (m, 2 H), 5.60 ppm (s, 2 H);

^{13}C NMR (126MHz, $CDCl_3$) δ = 146.3, 134.9, 134.2, 132.6, 129.2, 129.0, 128.1, 126.0, 120.6, 118.7, 111.5, 54.4 ppm;

MS (EI) m/z = 260.1 [M^+].

1-Benzyl-4-(4-pentylphenyl)-*1H*-1,2,3-triazole (4d):[27]

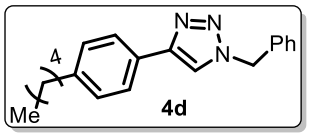

White solid; mp = 92-94 °C (reported m.p. = 92–94 °C);

^{1}H NMR (500MHz, $CDCl_3$) δ = 7.67 - 7.78 (m, *J* = 8.0 Hz, 2H), 7.64 (s, 1H), 7.34 - 7.41 (m, 3H), 7.30 - 7.34 (m, 1H), 7.30 (br. s., 1H), 7.17 - 7.26 (m, *J* = 8.0 Hz, 2H), 5.57 (s, 2H),2.62 (t, *J* = 7.6 Hz, 2H), 1.63 (quin, *J* = 7.3 Hz, 2H), 1.29 - 1.43 (m, 4H), 0.90 ppm (t, *J* = 6.9 Hz, 3H);

^{13}C NMR (126MHz, $CDCl_3$) δ = 148.3, 143.1, 134.7, 129.1, 128.8, 128.7, 128.0, 127.9, 125.6, 119.1, 54.1, 35.6, 31.4, 31.0, 22.5, 14.0 ppm;

MS (EI) m/z = 263.2 [M^+].

1-Benzyl-4-(4-nitrophenyl)-*1H*-1,2,3-triazole (4e):[25]

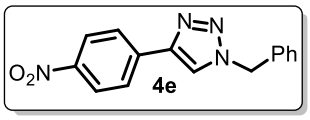

Light yellow solid; mp = 166-168 °C (reported mp 167–168 ºC);

^{1}H NMR (500MHz, $CDCl_3$) δ = 8.18 - 8.35 (m, *J* = 8.8 Hz, , 2H), 7.91 - 8.06 (m, *J* = 8.8 Hz, 2H), 7.83 (s, 1H), 7.29 - 7.52 (m, 5H), 5.61 ppm (s, 2H);

^{13}C NMR (126MHz, $CDCl_3$) δ = 147.3, 146.0, 136.8, 134.1, 129.3, 129.0, 128.2, 126.1, 124.2, 121.0, 54.4 ppm;

MS (EI) m/z = 280.1 [M^+].

1-(4-(1-Benzyl-*1H*-1,2,3-triazol-4-yl)phenyl)ethan-1-one (4f):[28]

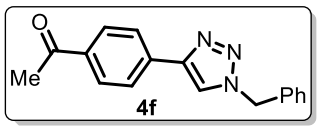

White solid; mp = 160-162 ^{o}C (reported mp = 160-162 ^{o}C);

^{1}H NMR (400MHz, $CDCl_3$) δ = 7.94 - 8.09 (m, *J* = 8.5 Hz, 2H), 7.85 - 7.94 (m, *J* = 7.9 Hz, 2H), 7.77 (s, 1H), 7.36 - 7.51 (m, 3H), 7.33 (d, *J* = 6.7 Hz, 2H), 5.59 (s, 2H), 2.61 ppm (s, 3H);

^{13}C NMR (101MHz, $CDCl_3$) δ = 209.0, 197.5, 147.0, 136.4, 134.9, 134.4, 129.2, 128.9, 128.1, 125.6, 120.4, 54.3, 26.6 ppm;

MS (EI) m/z = 277.2 [M^+].

1-Benzyl-4-(4-methoxyphenyl)-*1H*-1,2,3-triazole (4g):[25]

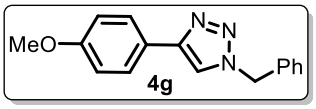

White solid; mp = 138-140 °C (reported mp 139–141 ºC);

^{1}H NMR (400MHz, $CDCl_3$) δ = 7.80 - 7.67 (m, *J* = 8.5 Hz, 2 H), 7.58 (s, 1 H), 7.47 - 7.35 (m, 3 H), 7.31 (d, *J* = 6.7 Hz, 2 H), 7.00 - 6.85 (m, *J* = 8.5 Hz, 2 H), 5.56 (s, 2 H), 3.83 ppm (s, 3 H);

^{13}C NMR (101MHz, $CDCl_3$) δ = 159.6, 148.1, 134.7, 129.1, 128.7, 128.0, 127.0, 123.2, 118.7, 114.2, 55.3, 54.2 ppm;

MS (EI) m/z = 265.1 [M^+].

1-Benzyl-4-(2-methoxyphenyl)-*1H*-1,2,3-triazole (4h):[29]

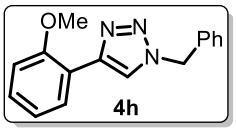

White solid; mp = 168-170 °C (reported mp = 167.5–169.5 °C);

^{1}H NMR (500MHz, $CDCl_3$) δ = 8.34 (d, *J* = 7.6 Hz, 1H), 7.96 (s, 1H), 7.21 - 7.40 (m, 6H), 7.05 (t, *J* = 7.4 Hz, 1H), 6.92 (d, *J* = 8.4 Hz, 1H), 5.55 (s, 2H), 3.85 ppm (s, 3H);

^{13}C NMR (126 MHz, $CDCl_3$) δ = 155.5, 143.5, 135.1, 128.9, 128.8, 128.4, 127.7, 127.6, 123.0, 120.9, 119.3, 110.7, 55.3, 53.9 ppm;

MS (EI) m/z = 265.1 [M^+].

1-Benzyl-4-(4-(pentyloxy)phenyl)-*1H*-1,2,3-triazole (4i):[30]

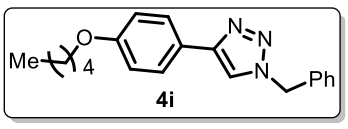

White solid; mp = 116-118 °C (reported mp = 117–119 °C);

^{1}H NMR (500MHz, $CDCl_3$) δ = 7.65 - 7.82 (m, *J* = 8.8 Hz, 2 H), 7.57 (s, 1 H), 7.35 - 7.50 (m, 3 H), 7.32 (d, *J* = 6.5 Hz, 2 H), 6.83 - 7.06 (m, *J* = 8.4 Hz, 2 H), 5.57 (s, 2 H), 3.98 (t, *J*

= 6.5 Hz, 2 H), 1.80 (quin, *J* = 6.9 Hz, 2 H), 1.32 - 1.52 (m, 4 H), 0.94 ppm (t, *J* = 7.1 Hz, 3 H);

^{13}C NMR (126MHz, $CDCl_3$) δ = 159.2, 148.2, 134.8, 129.1, 128.7, 128.0, 127.0, 123.0, 118.6, 114.8, 68.1, 54.2, 28.9, 28.2, 22.5, 14.0 ppm;

MS (EI) m/z = 265.1 [M^+].

1-Benzyl-4-(naphthalen-1-yl)-*1H*-1,2,3-triazole (4j):[31]

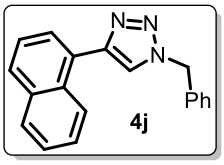

White solid; mp = 74-76 °C (reported mp = 74-75 °C);

^{1}H NMR (400MHz, $CDCl_3$) δ = 8.38 (dd, *J* = 5.8, 3.4 Hz, 1 H), 7.82 - 7.99 (m, 2 H), 7.73 (s, 1 H), 7.70 (d, *J* = 6.7 Hz, 1 H), 7.47 - 7.59 (m, 3 H), 7.31 - 7.44 (m, 4 H), 5.67 ppm (s, 2 H);

^{13}C NMR (101MHz, $CDCl_3$) δ = 147.3, 134.6, 133.8, 131.0, 129.2, 128.9, 128.8, 128.4, 128.1, 128.0, 127.2, 126.6, 125.9, 125.4, 125.3, 122.4, 54.3 ppm;

MS (EI) m/z = 285.1 [M^+].

1-(4-Methoxybenzyl)-4-phenyl-*1H*-1,2,3-triazole (4k):[32]

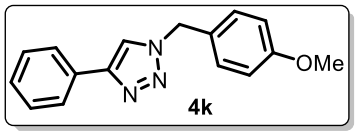

White solid; mp = 134-136 °C;

^{1}H NMR (500MHz, $CDCl_3$) δ = 7.81 - 7.77 (m, 2 H), 7.64 (s, 1 H), 7.42 - 7.36 (m, 2 H), 7.31 (d, *J* = 7.2 Hz, 1 H), 7.25 (s, 2 H), 6.91 (d, *J* = 8.8 Hz, 2 H), 5.49 (s, 2 H), 3.80 ppm (s, 3 H);

^{13}C NMR (126MHz, $CDCl_3$) δ = 159.9, 148.0, 130.5, 129.6, 128.7, 128.0, 126.6, 125.6, 119.3, 114.4, 55.3, 53.7 ppm;

MS (EI) m/z = 265.1 [M^+].

2-(1-Benzyl-*1H*-1,2,3-triazol-4-yl)pyridine (4l): [25]

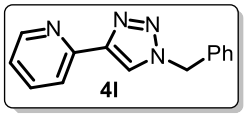

White solid; mp = 114-116 °C (reported mp 112–113 °C);

^{1}H NMR (500MHz, $CDCl_3$) δ = 8.54 (d, *J* = 4.2 Hz, 1 H), 8.18 (d, *J* = 8.0 Hz, 1 H), 8.06 (s, 1 H), 7.77 (dt, *J* = 1.7, 7.7 Hz, 1 H), 7.43 - 7.32 (m, 5 H), 7.21 (ddd, *J* = 1.0, 5.5, 6.9 Hz, 1 H), 5.59 ppm (s, 2 H);

^{13}C NMR (126MHz, $CDCl_3$) δ = 150.2, 149.3, 148.7, 136.9, 134.3, 129.2, 128.8, 128.3, 122.8, 121.9, 120.2, 54.4 ppm;

MS (EI) m/z = 236.2 [M^+].

1-Benzyl-4-heptyl-*1H*-1,2,3-triazole (4m):[33]

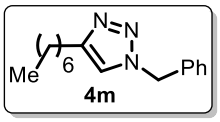

4m

White solid; mp = 66-68 °C (reported mp = 61–62 °C);

^{1}H NMR (400MHz, $CDCl_3$) δ = 7.20 - 7.09 (m, 3 H), 7.04 (d, *J* = 7.9 Hz, 2 H), 6.99 - 6.90 (m, 1 H), 5.28 (s, 2 H), 2.47 (t, *J* = 7.9 Hz, 2 H), 1.42 (quin, *J* = 7.3 Hz, 2 H), 1.13 - 0.99 (m, 10 H), 0.66 ppm (t, *J* = 6.7 Hz, 3 H);

^{13}C NMR (101MHz, $CDCl_3$) δ = 149.0, 135.0, 129.0, 128.9, 128.5, 127.9, 120.4, 53.9, 31.8, 29.4, 29.3, 29.2, 29.2, 29.0, 25.7, 22.6, 14.1 ppm;

MS (EI) m/z = 258.2 [M^+].

1-Butyl-4-phenyl-*1H*-1,2,3-triazole (4n):[34]

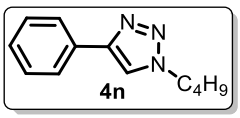

4n

Colorless thick liquid;

^{1}H NMR (400MHz, $CDCl_3$) δ = 7.83 (d, *J* = 7.3 Hz, 2 H), 7.75 (s, 1 H), 7.46 - 7.37 (m, 2 H), 7.33 (d, *J* = 7.3 Hz, 1 H), 4.39 (t, *J* = 7.3 Hz, 2 H), 1.99 - 1.88 (m, 2 H), 1.47 - 1.31 (m, 2 H), 0.97 ppm (t, *J* = 7.3 Hz, 3 H);

^{13}C NMR (101MHz, $CDCl_3$) δ = 147.6, 130.7, 128.7, 128.0, 125.6, 119.4, 50.0, 32.2, 19.6, 13.4 ppm;

MS (EI) m/z = 201.1 [M^+].

2.1.7 Selected NMR spectra:

^{1}H NMR of 4-phenyl-*1H*-1,2,3-triazole (400MHz, DMSO-d6):

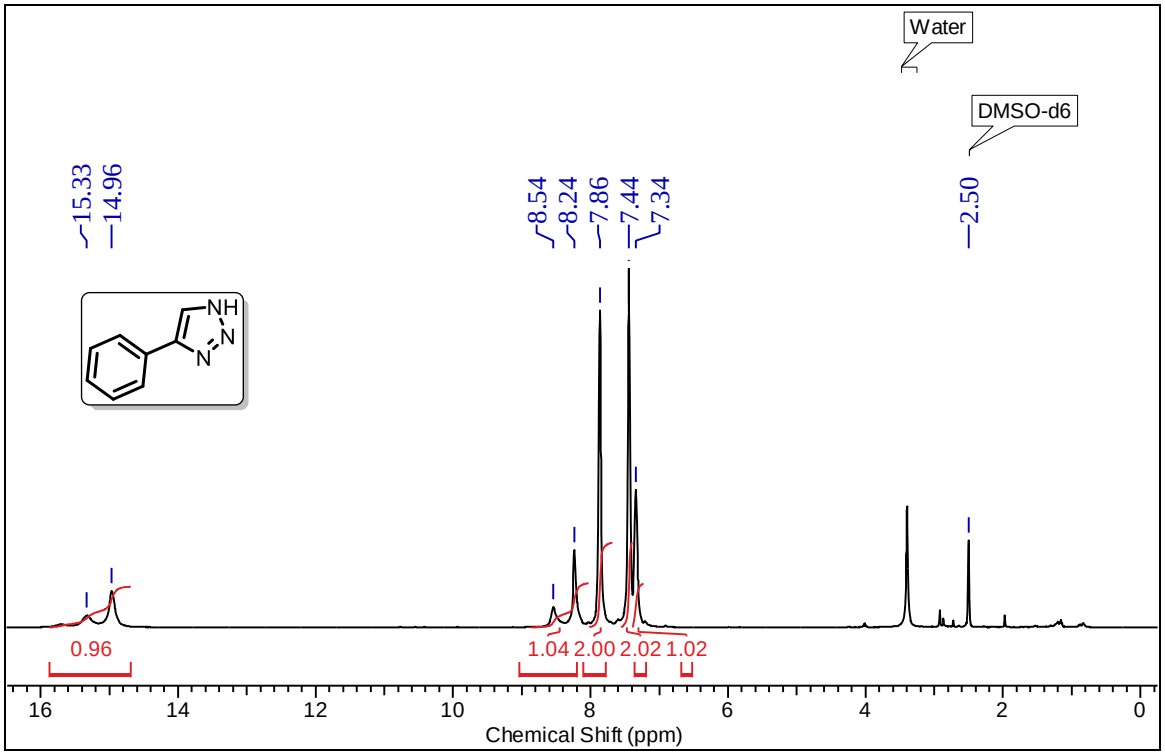

^{13}C NMR of 4-phenyl-*1H*-1,2,3-triazole (100MHz, DMSO-d6):

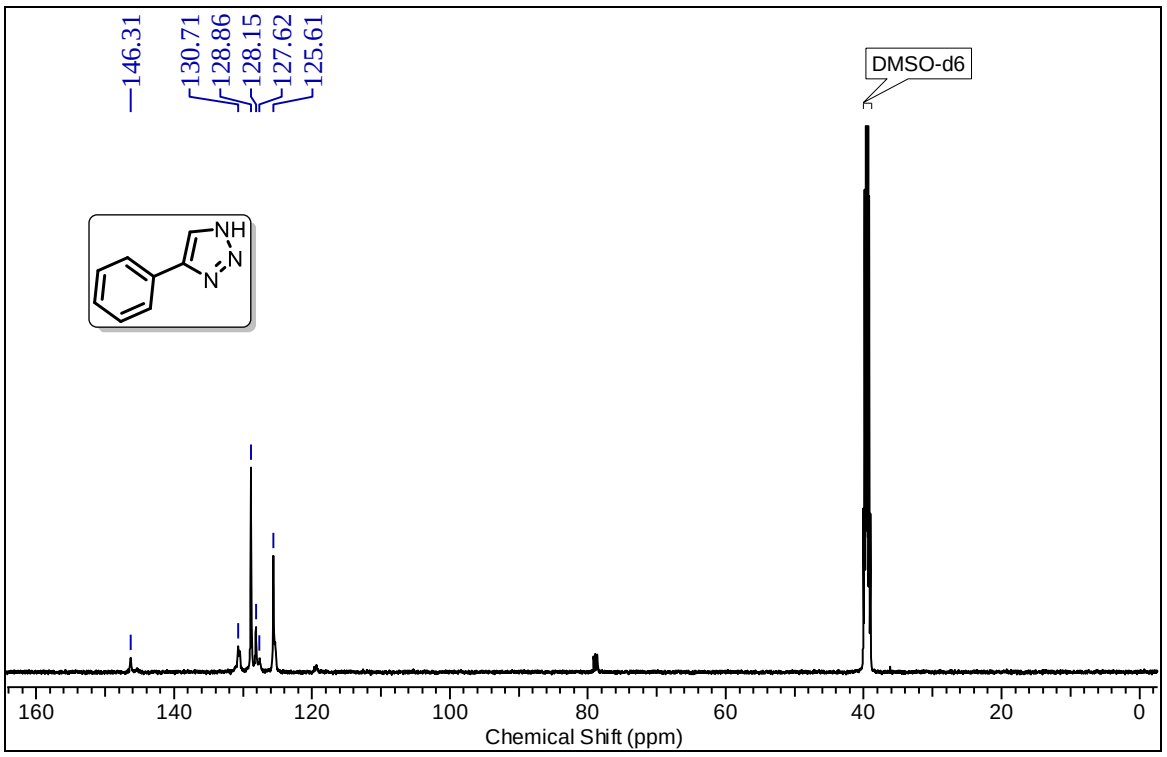

^{1}H NMR of 1-Benzyl-4-phenyl-*1H*-1,2,3-triazole (3a) (400MHz, $CDCl_3$):

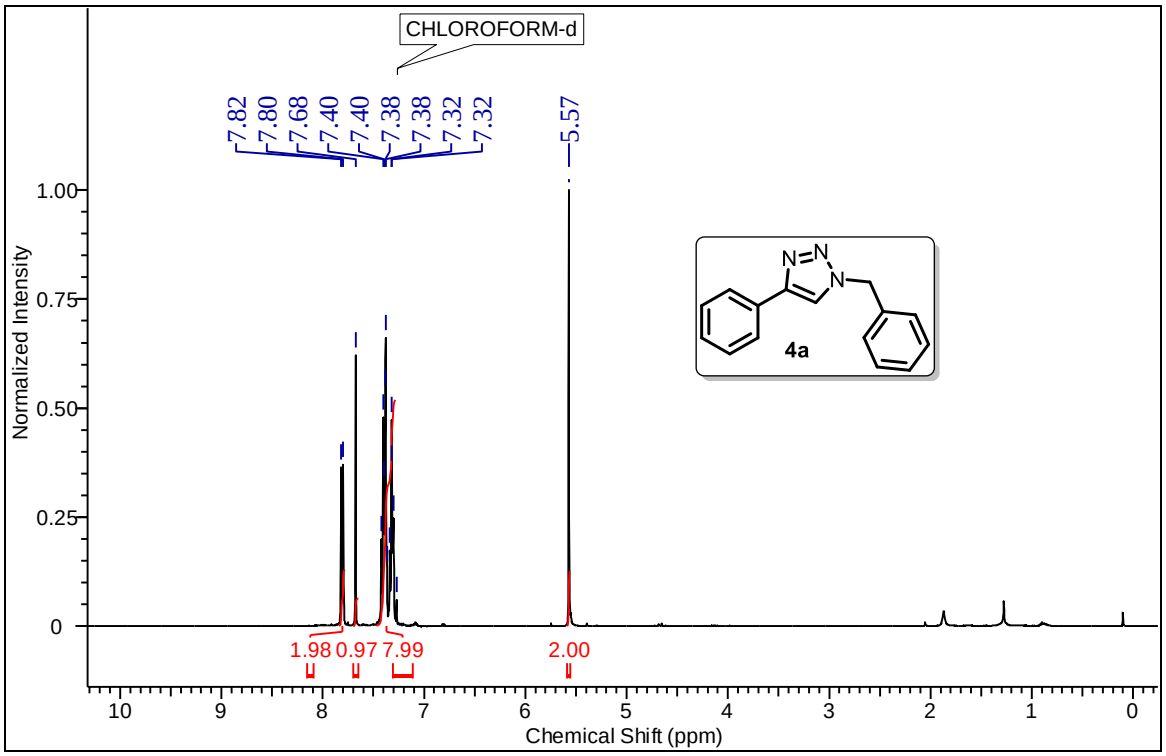

^{13}C NMR of 1-Benzyl-4-phenyl-*1H*-1,2,3-triazole (3a) (101MHz, $CDCl_3$):

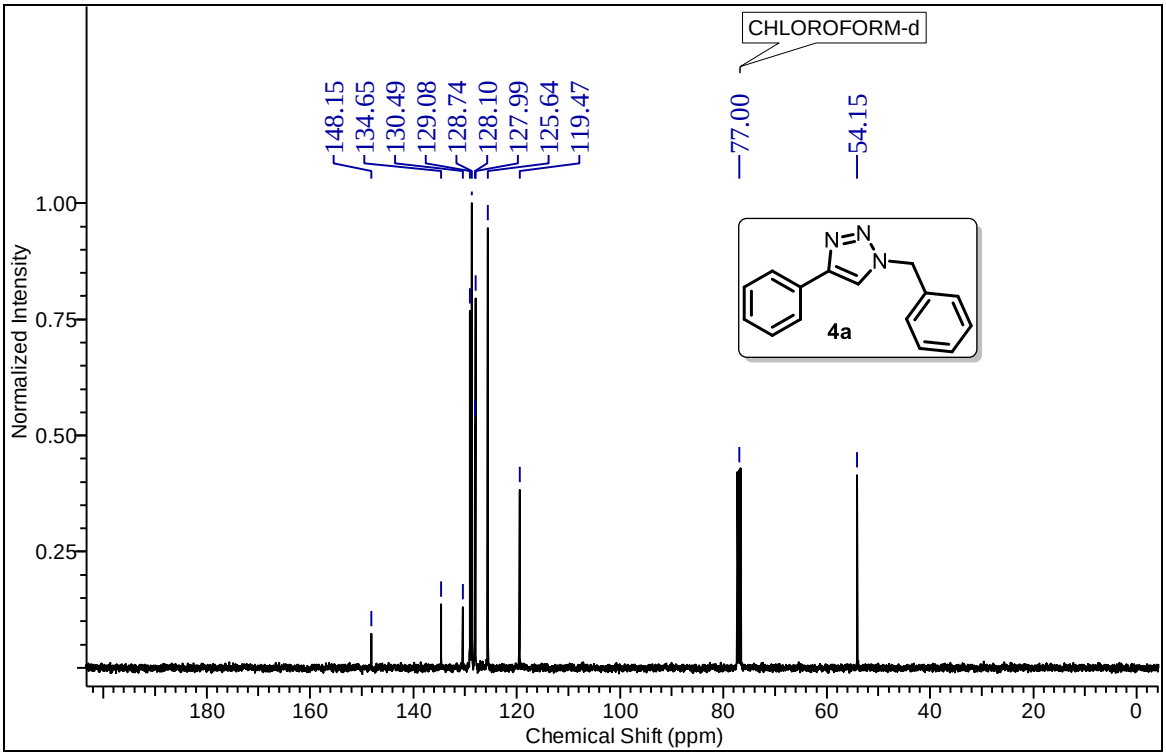

^{1}H NMR of 1-Benzyl-4-(*p*-tolyl)-*1H*-1,2,3-triazole (3b) (400MHz, $CDCl_3$):

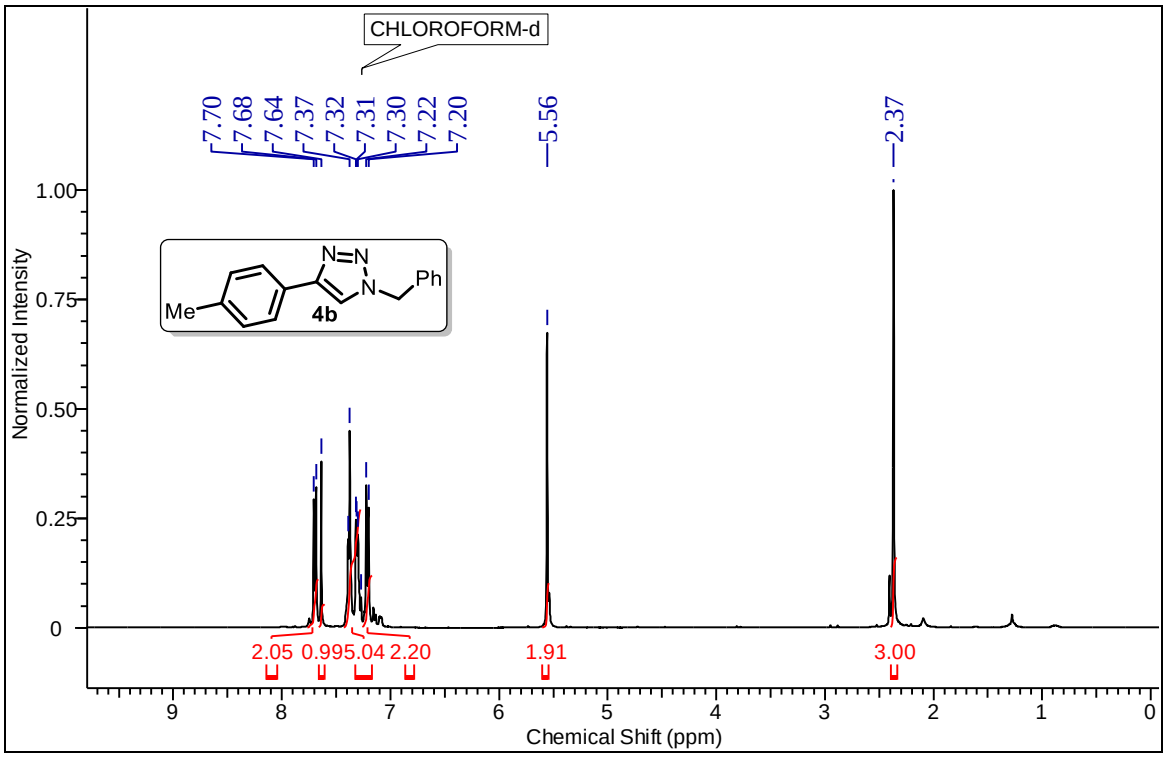

^{13}C NMR of 1-Benzyl-4-(*p*-tolyl)-*1H*-1,2,3-triazole (3b) (101MHz, $CDCl_3$):

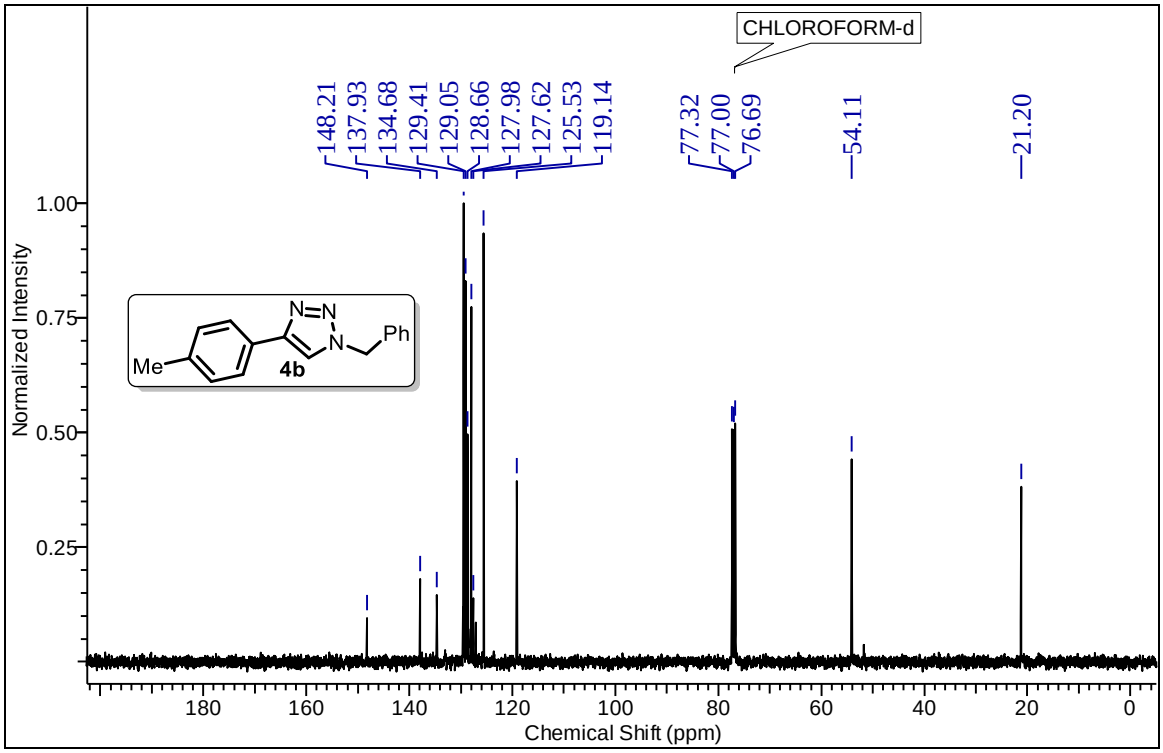

^{1}H NMR of 4-(1-Benzyl-*1H*-1,2,3-triazol-4-yl)benzonitrile (4c) (500MHz, $CDCl_3$):

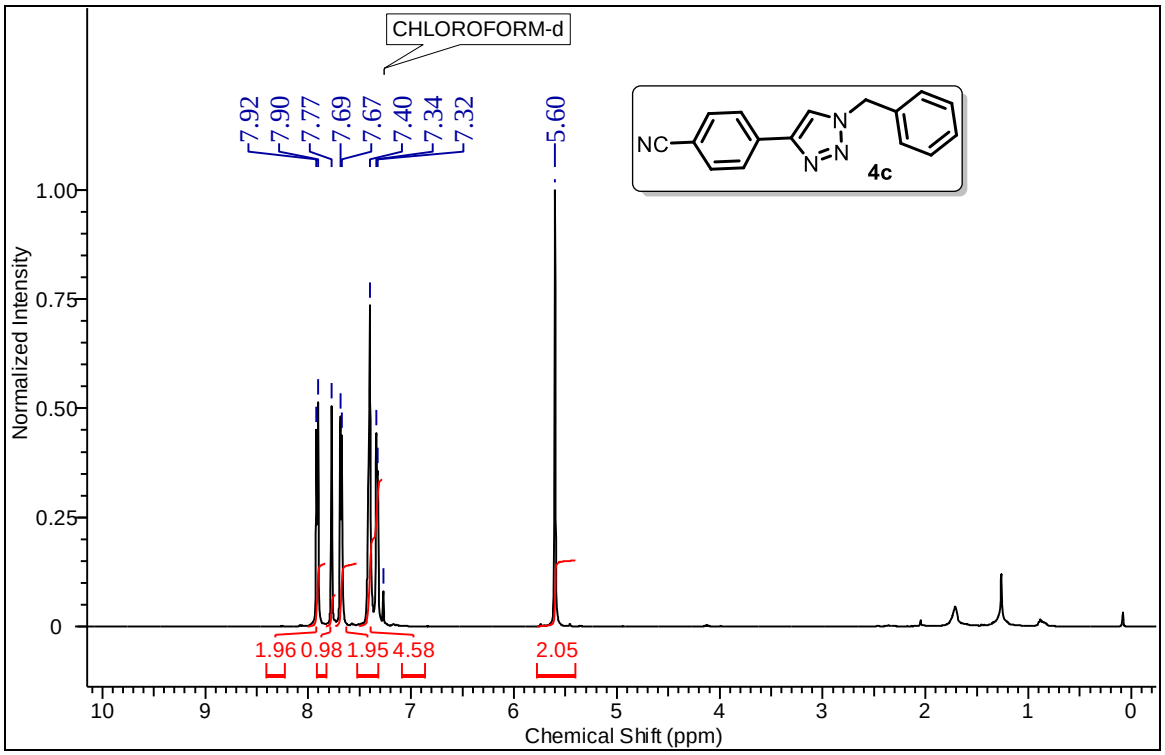

^{13}C NMR of 4-(1-Benzyl-*1H*-1,2,3-triazol-4-yl)benzonitrile (4c) (126MHz, $CDCl_3$):

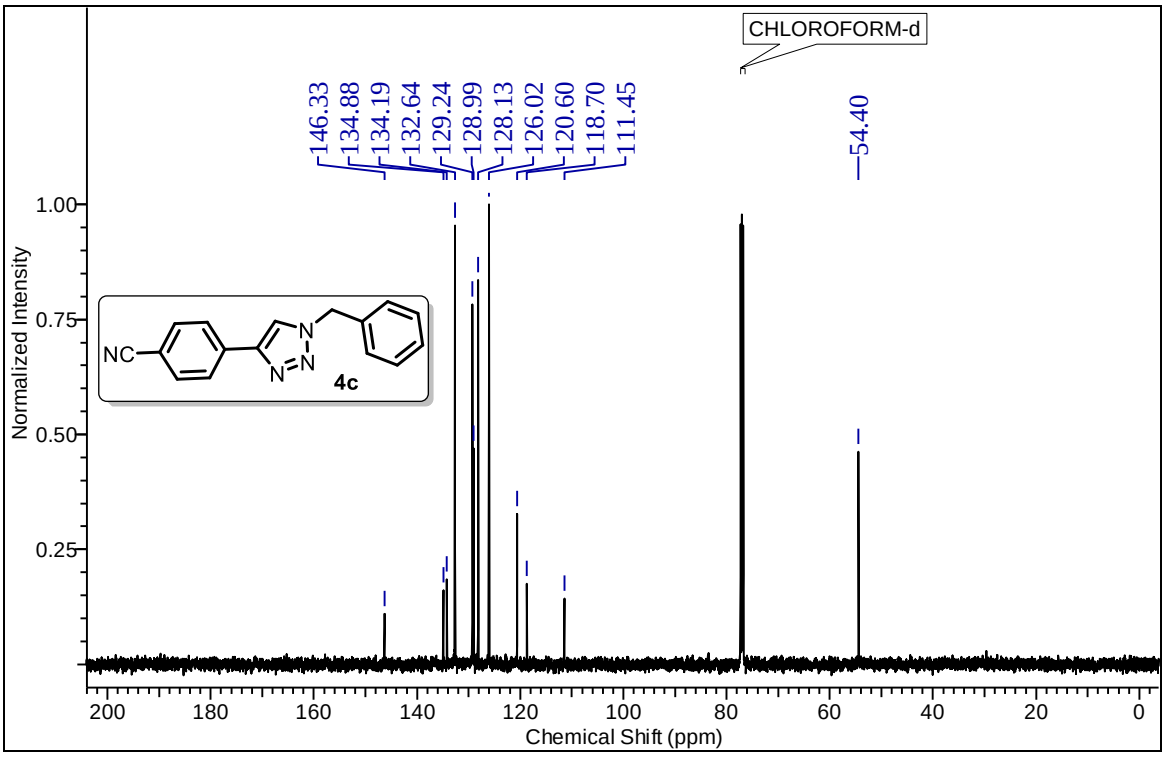

^{1}H NMR of 1-(4-(1-Benzyl-*1H*-1,2,3-triazol-4-yl)phenyl)ethan-1-one (4f) (400MHz, $CDCl_3$):

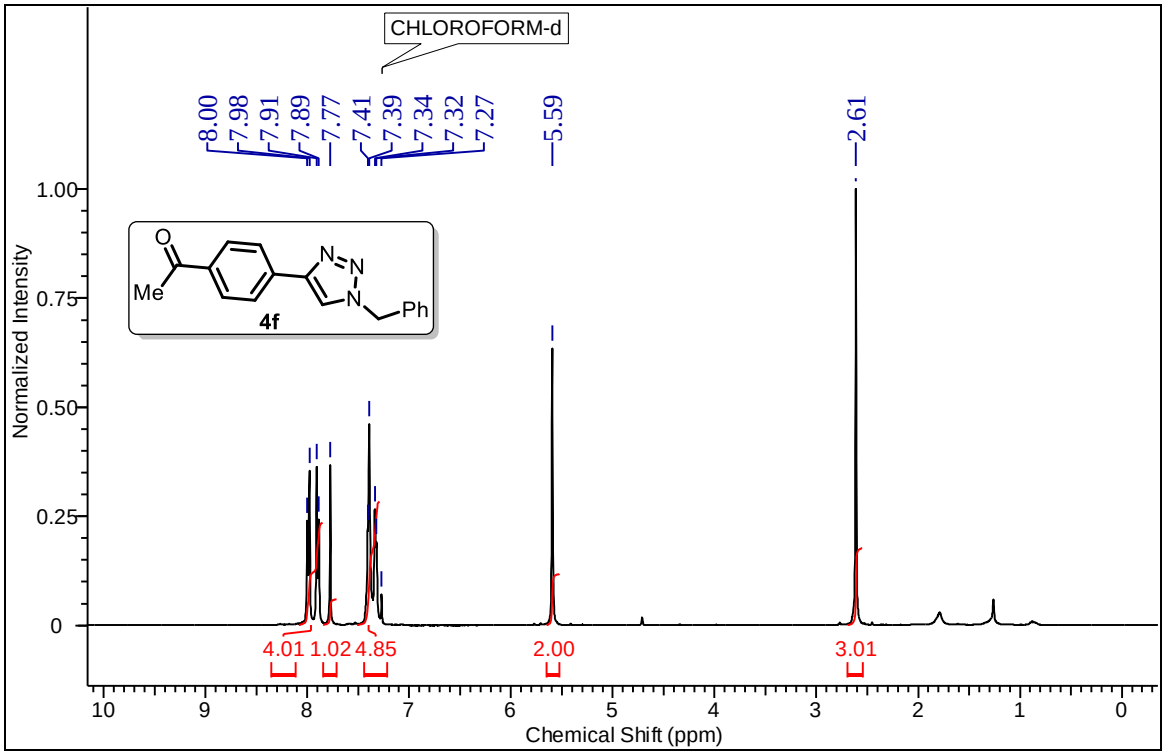

^{13}C NMR of 1-(4-(1-Benzyl-*1H*-1,2,3-triazol-4-yl)phenyl)ethan-1-one (4f) (101MHz, $CDCl_3$):

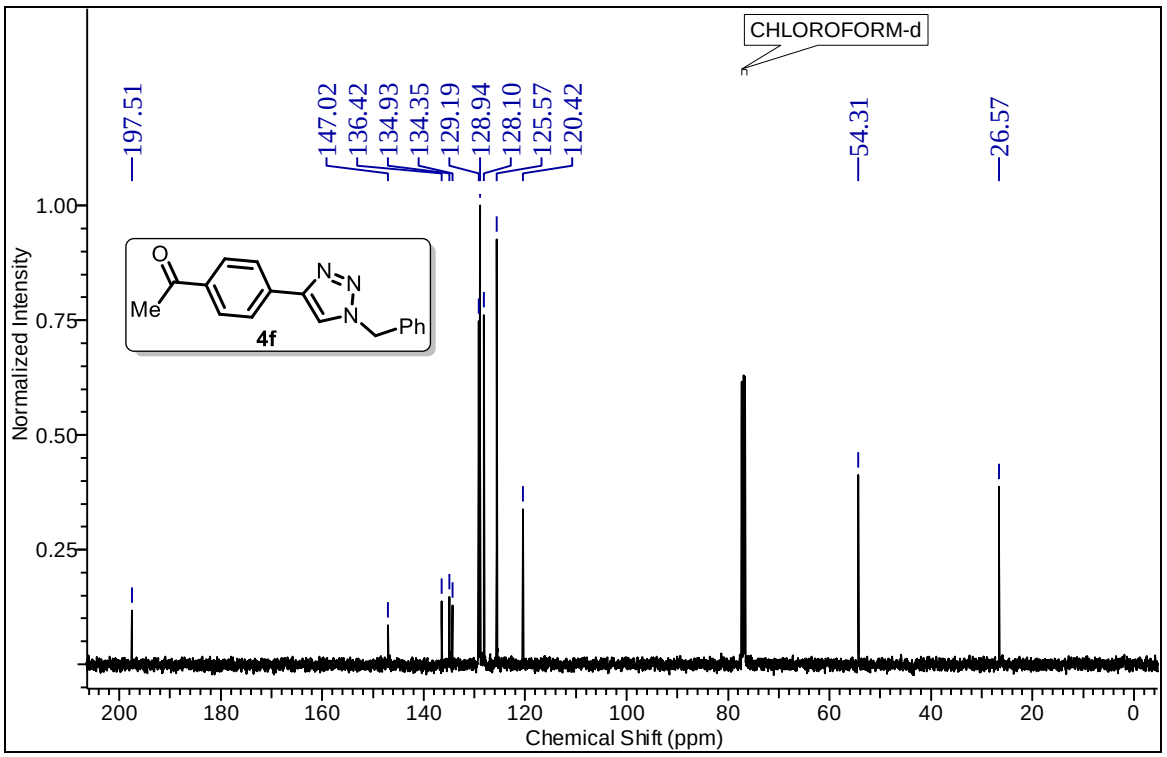

^{1}H NMR of 1-Benzyl-4-(4-methoxyphenyl)-*1H*-1,2,3-triazole (4g) (400MHz, $CDCl_3$):

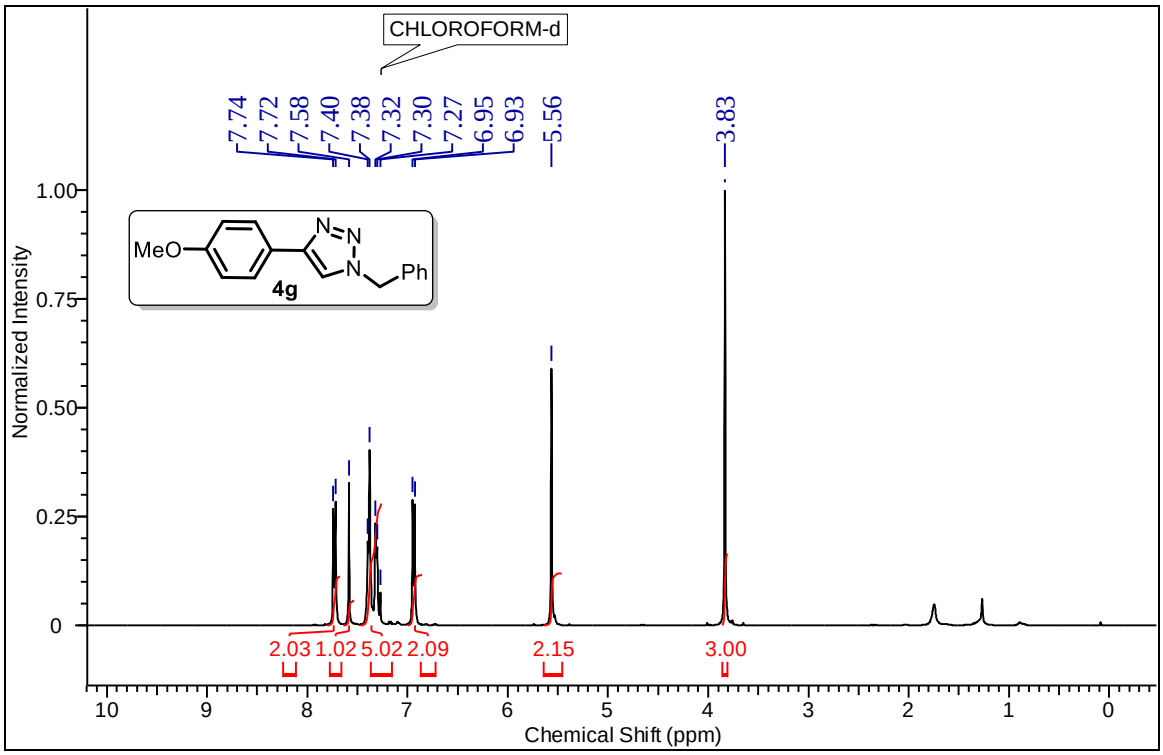

^{13}C NMR of 1-Benzyl-4-(4-methoxyphenyl)-*1H*-1,2,3-triazole (4g) (101MHz, $CDCl_3$):

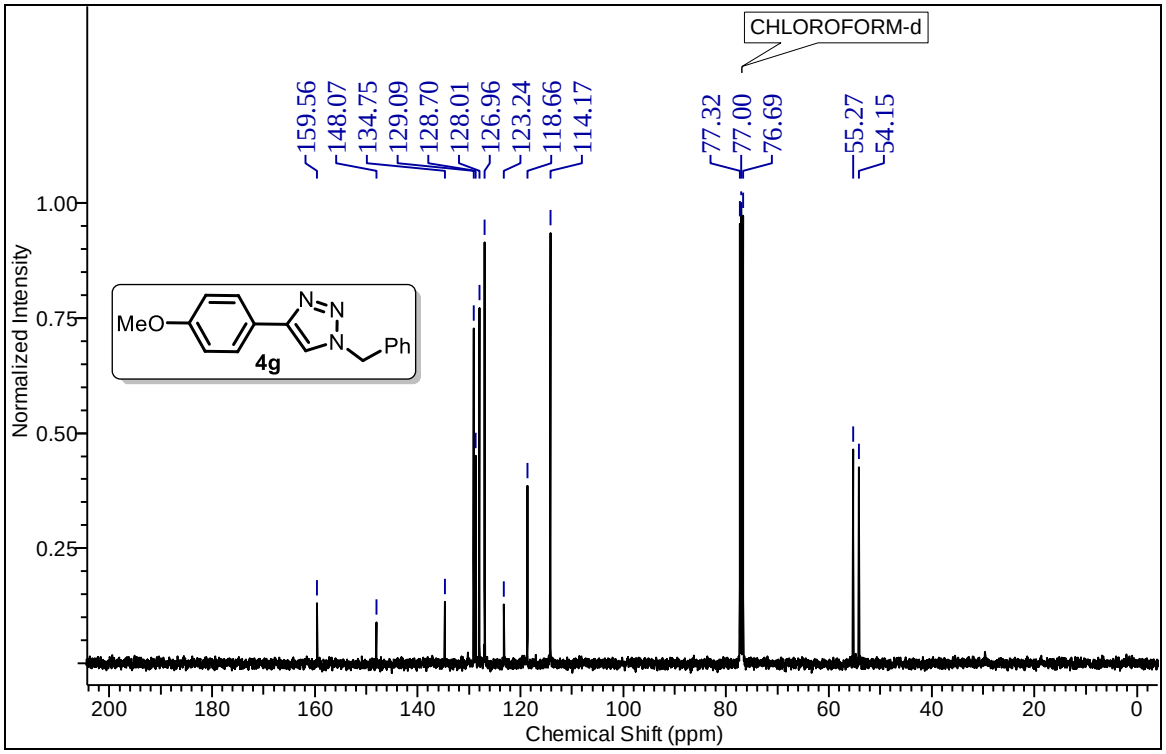

^{1}H NMR of 1-Benzyl-4-(naphthalen-1-yl)-*1H*-1,2,3-triazole (4j) (400MHz, $CDCl_3$):

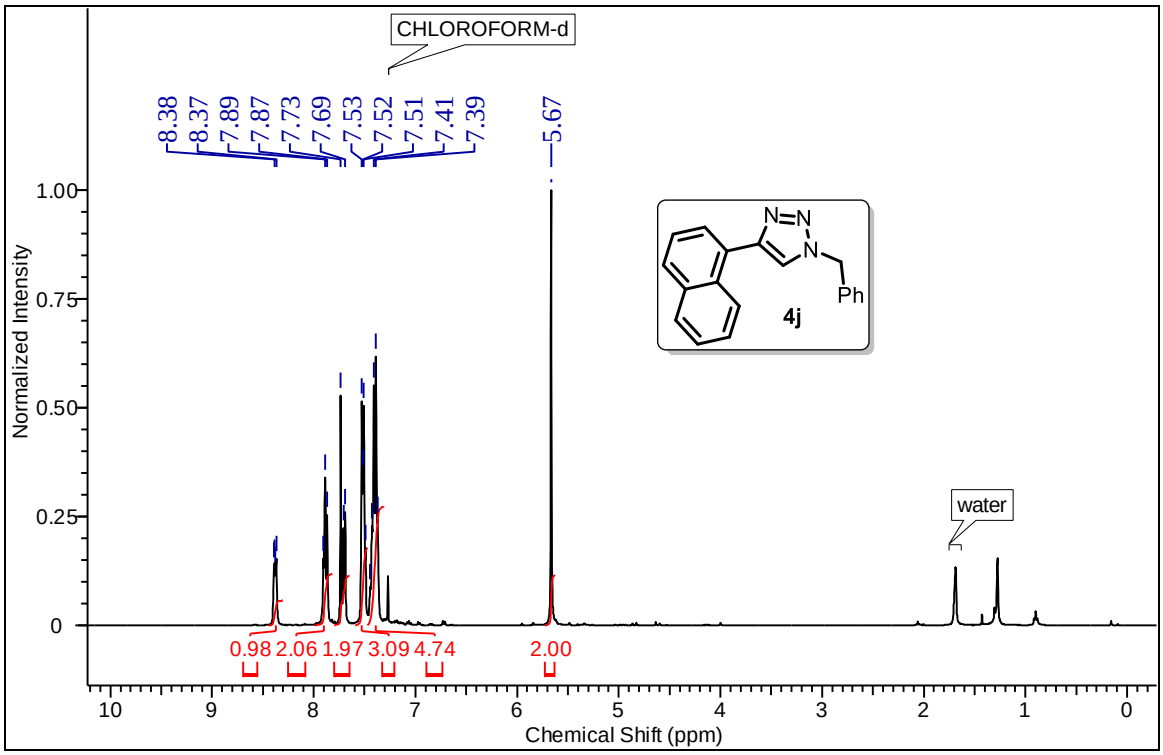

^{13}C NMR of 1-Benzyl-4-(naphthalen-1-yl)-*1H*-1,2,3-triazole (4j) (101MHz, $CDCl_3$):

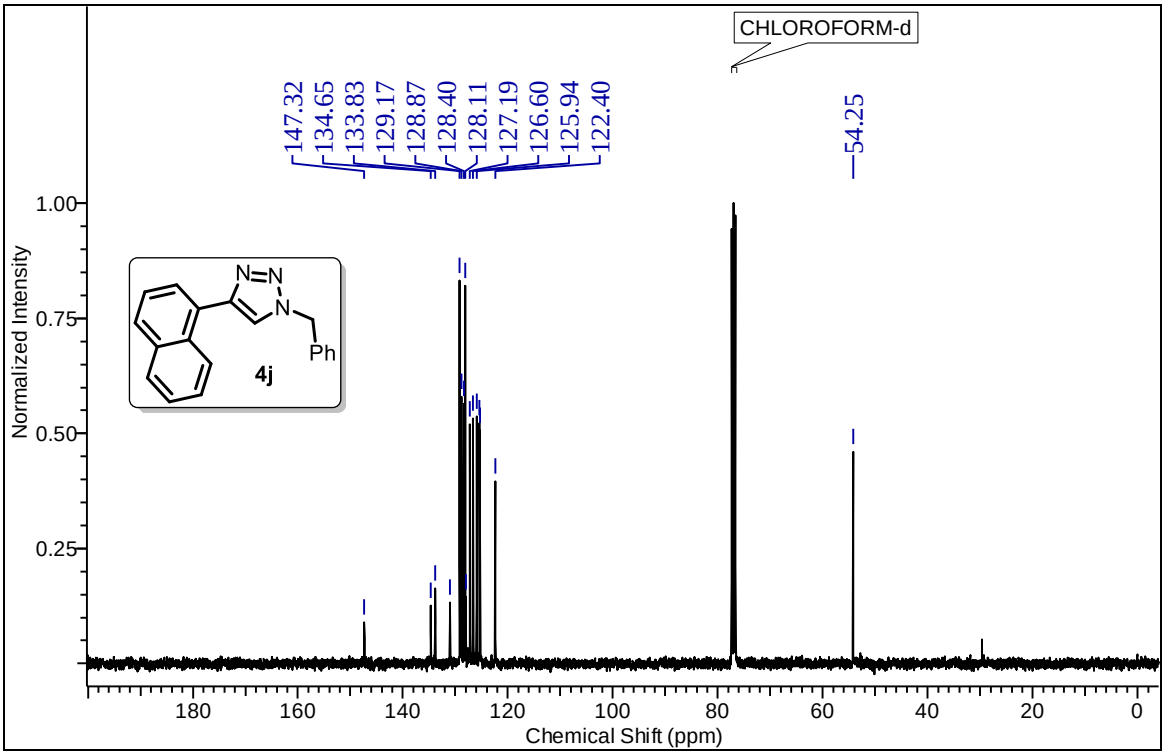

^{1}H NMR of 1-(4-Methoxybenzyl)-4-phenyl-*1H*-1,2,3-triazole (4k) (500MHz, $CDCl_3$):

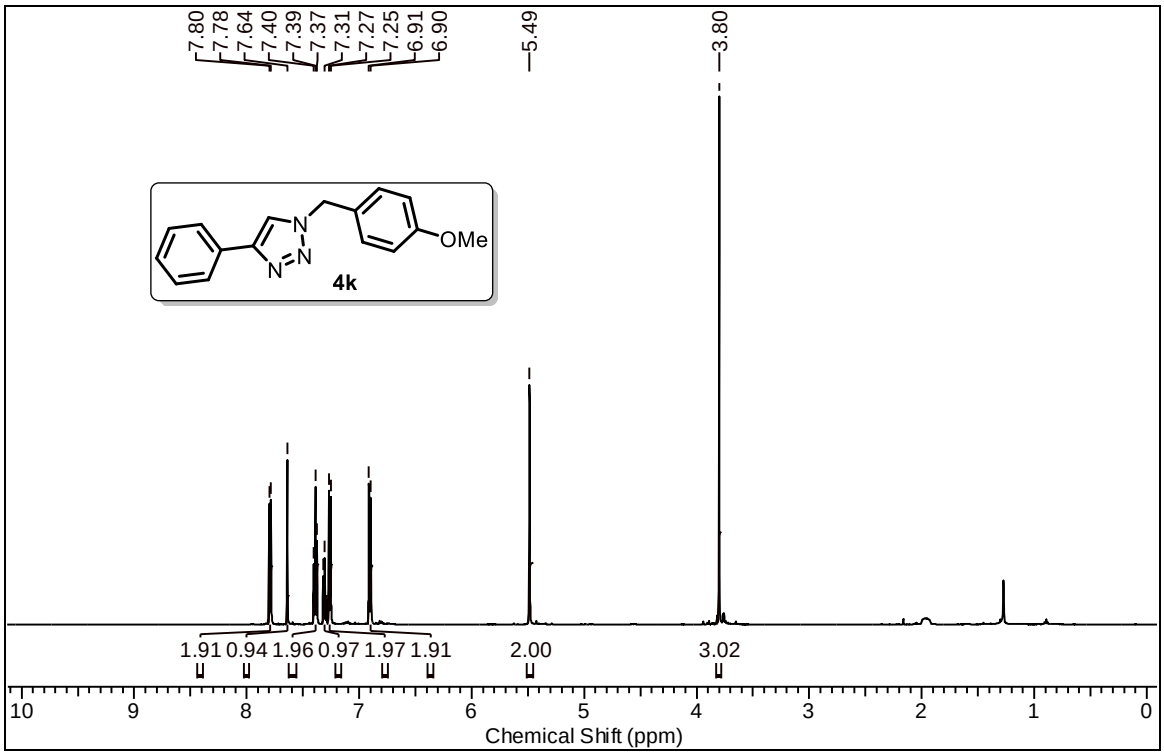

^{13}C NMR of 1-(4-Methoxybenzyl)-4-phenyl-*1H*-1,2,3-triazole (4k) (126MHz, $CDCl_3$):

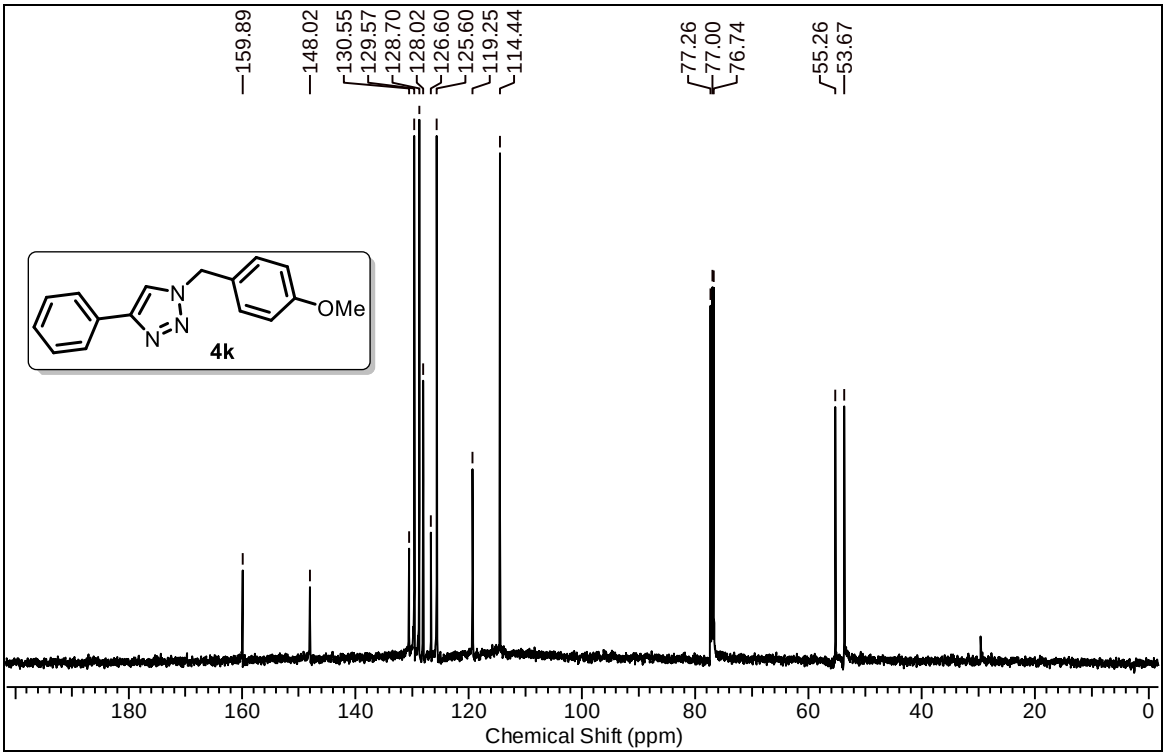

^{1}H NMR of 2-(1-Benzyl-*1H*-1,2,3-triazol-4-yl)pyridine (4l) (500MHz, $CDCl_3$):

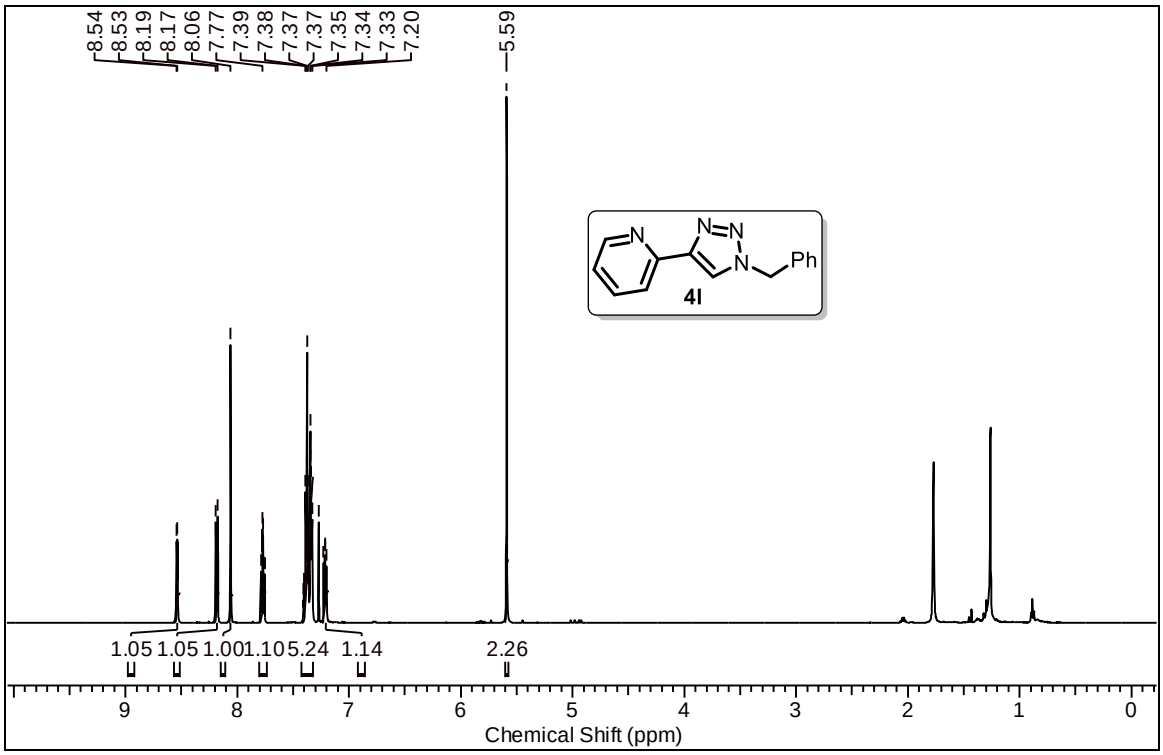

^{13}C NMR of 2-(1-Benzyl-*1H*-1,2,3-triazol-4-yl)pyridine (4l) (126MHz, $CDCl_3$):

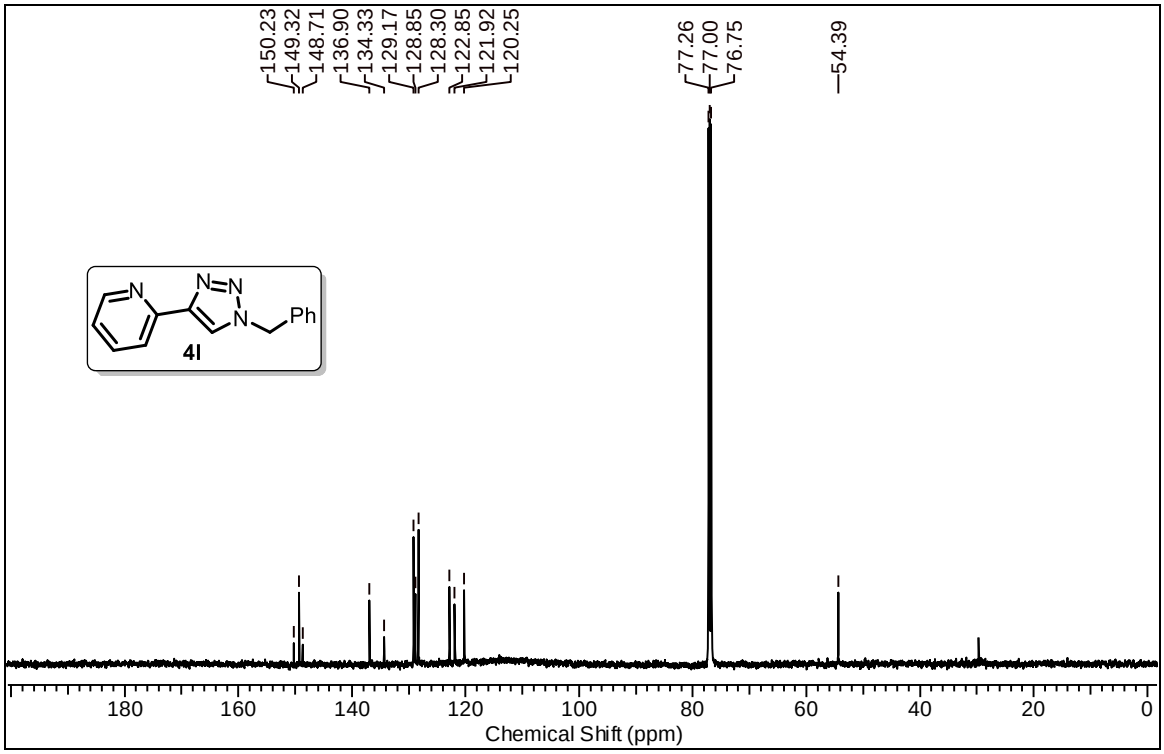

^{1}H NMR of 1-Benzyl-4-heptyl-*1H*-1,2,3-triazole (4m) (400MHz, $CDCl_3$):

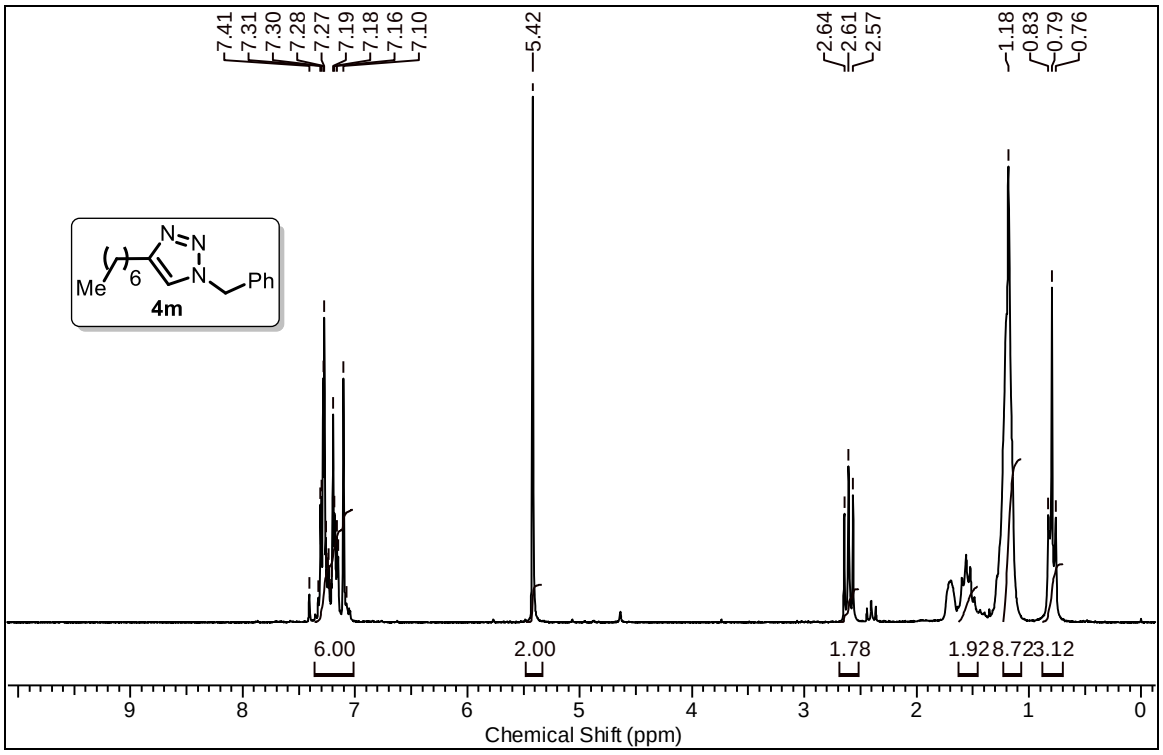

^{13}C NMR of 1-Benzyl-4-heptyl-*1H*-1,2,3-triazole (4m) (101MHz, $CDCl_3$):

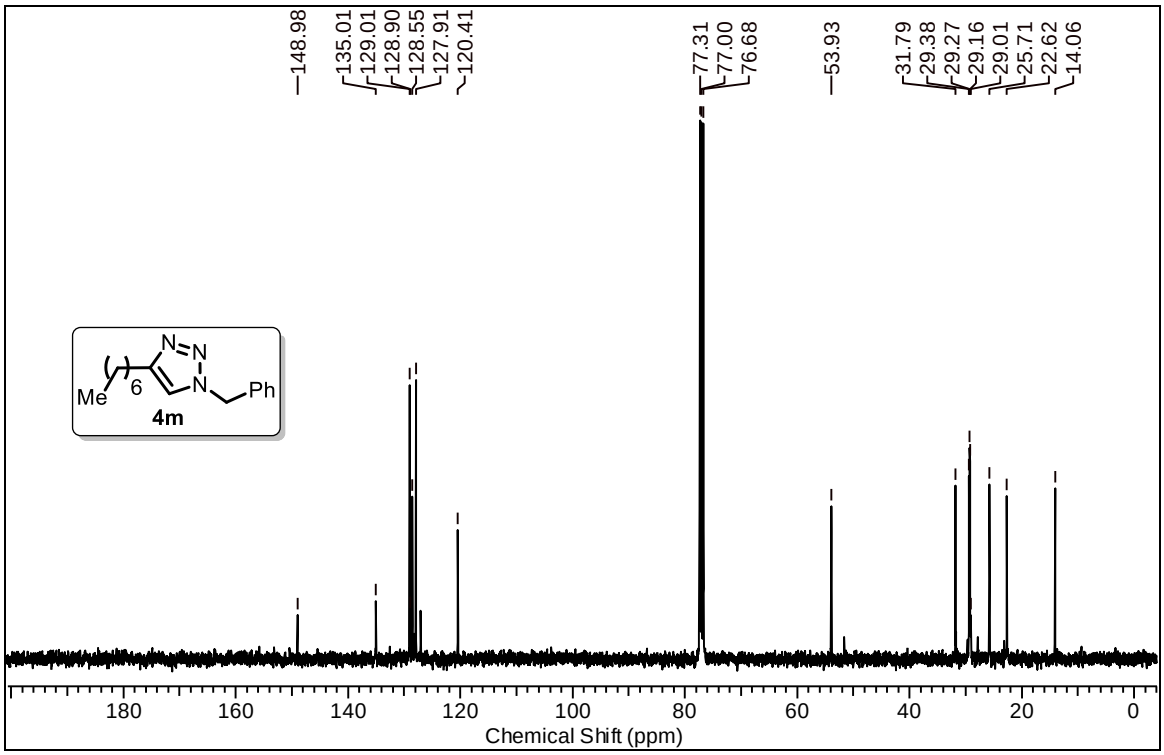

^{1}H NMR of 1-Butyl-4-phenyl-*1H*-1,2,3-triazole (4n) (400MHz, $CDCl_3$):

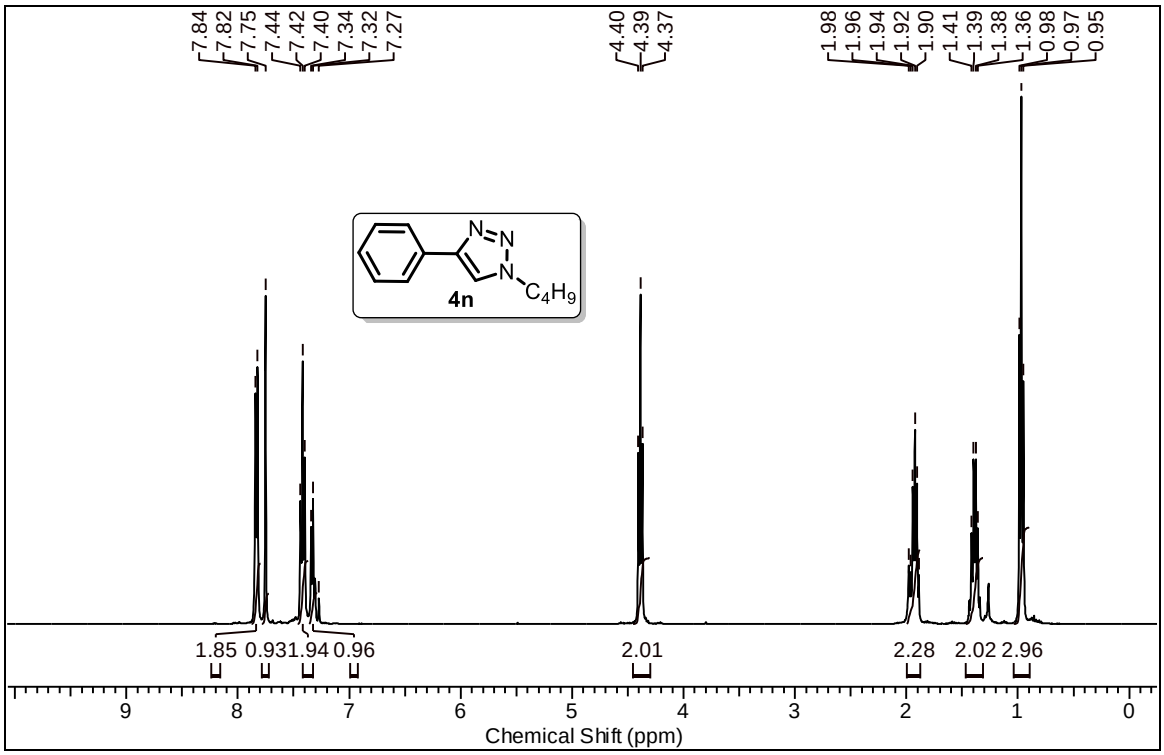

^{13}C NMR of 1-Butyl-4-phenyl-*1H*-1,2,3-triazole (4n) (101MHz, $CDCl_3$):

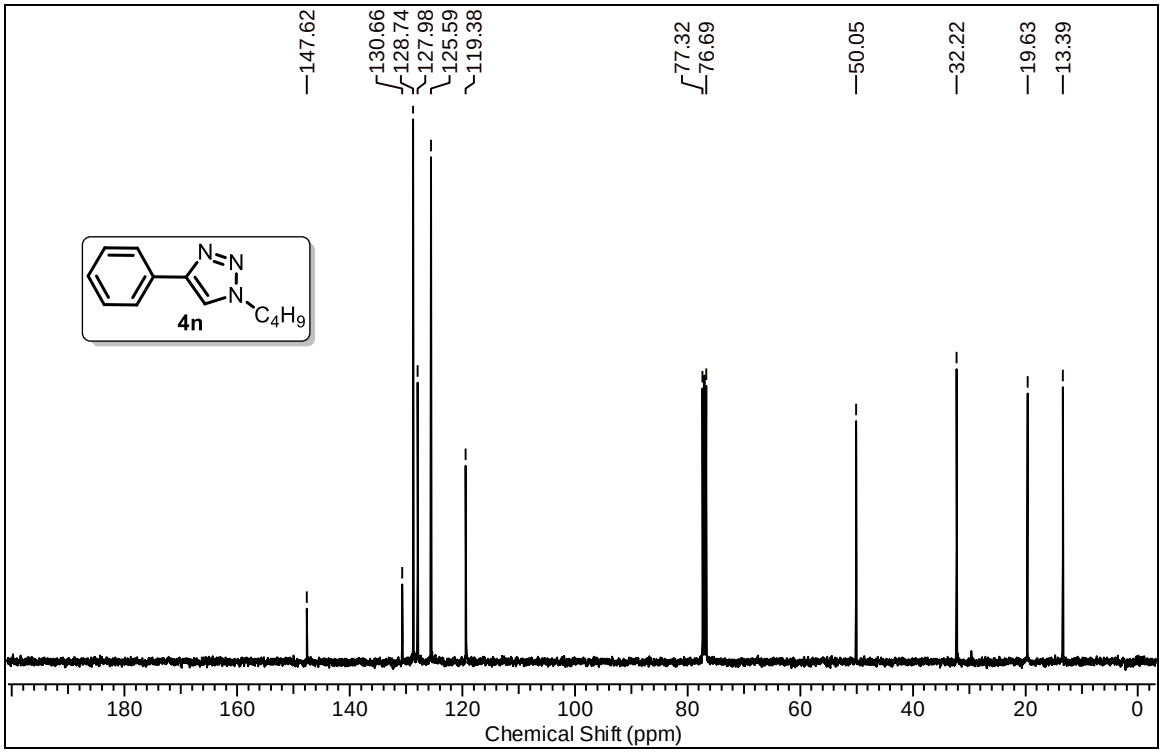

2.1.8 References:

[1] Beck, J. S.; Vartuli, J. C.; Roth, W. J.; Leonowicz, M. E.; Kresge, C. T.; Schmitt, K. D.; Chu, C. T. W.; Olson, D. H.; Sheppard, E. W.; McCullen, S. B.; Higgins, J. B.; Schlenker, J. L. *J. Am. Chem. Soc.* **1992**, *114*, 10834–10843.

[2] Zhao, D. Y.; Feng, J. L.; Huo, Q. S.; Melosh, N.; Fredrickson, G. H.; Chmelka, B. F.; Stucky, G. D. *Science* **1998,** *279*, 548–552.

[3] a) Hess, C. *Chem. Phys. Chem.* **2009,** *10*, 319–326; b) Cavalleri, M.; Hermann, K.; Knop-Gericke, A.; Hävecker, M.; Herbert, R.; Hess, C.; Oestereich, A.; Döbler, J.; Schlögl, R. *J. Catal.* **2009,** *262*, 215–223.

[4] a) Hoang, V. T.; Huang, Q.; Eic, M.; Do, T. O.; Kaliaguine, S. *Langmuir* **2005**, *21*, 2051–2057; b) Han, Y. J.; Stucky, G. D.; Butler, A. *J. Am. Chem. Soc.* **1999**, *121*, 9897–9898.

[5] a) Scott, B. J.; Wirnsberger, G.; Stucky, G. D. *Chem. Mater.* **2001**, *13*, 3140–3150; b) Yang, P.; Wirnsberger, G.; Huang, H. C.; Cordero, S. R.; McGehee, M. D.; Scott, B.; Deng, T.; Whitesides, G. M.; Chmelka, B. F.; Buratto, S. K.; Stucky, G. D. *Science* **2000**, *287*, 465–467.

[6] Randy, M.; Aerts, C. A.; Humbeeck, J. V.; Augustijns, P.; Den M.; Guy V.; Martens, J. A. *Chem. Commun.* **2007**, *13*, 1375–1377.

[7] Valenti G, Rampazzo R, Bonacchi S, Petrizza L, Marcaccio M, Montalti M, Prodi L, Paolucci F. *J. Am. Chem. Soc.* **2016**, *138*, 15935–15942.

[8] Mitran, R. -A.; Berger, D.; Munteanu, C.; Matei, C. *J. Phys. Chem. C*. **2015**, *119*, 15177–15184.

[9] Sarkar, S. M.; Rahman, Md. L.; Yusoff, M. M. *RSC Adv.* **2015**, *5*, 1295-1300.

[10] Anand, N.; Ramudu, P.; Reddy, K. H. P.; Rao, K. S. R.; Jagadeesh, B.; Babu, V. S. P.; Burri, D. R. *App. Catal. A: General* **2013,** *454*, 119-126.

[11] Feng, X.; Yan, M.; Zhang, T.; Liu Y.; Bao, M. *Green Chem.* **2010**, *12*, 1758-1766.

[12] Paul, L.; Banerjee, B.; Bhaumik, A.; Alia, M. *J. Solid State Chemistry* **2016**, 237, 105-112.

[13] Fath Vavsari, V.; Mohammadi Ziarani, G.; Badiei, A. *RSC Adv.* **2015**, *5*, 91686–91707.

[14] Wang, H.; Gao, X.; Wang, Y.; Wang, J.; Niu, X.; Deng, X. *Ceram. Int.* **2012**, *38*, 6931–6935.

[15] a) Huisgen, R.; Szeimies, G.; Möbius, L. *Chem. Ber.* **1967**, *100*, 2494-2507; b) Singh, M. S.; Chowdhury, S.; Koley, S. *Tetrahedron* **2016**, *72*, 5257-5283.

[16] Leophairatana, P.; De Silva, C. C.; Koberstein J. T. *Polymer Chem.* **2018**, *56*, 75–84.

[17] a) Kolb, H. C.; Sharpless, K. B. *Drug Discov. Today* **2003**, *8*, 1128-1137; b) Dheer, D.; Singh, V.; Shankar, R. *Bioorganic Chemistry* **2017**, *71*, 30-54

[18] a) Struthers, H.; Mindt, T. L.; Schibli, R. *Dalton Trans.* **2010**, *39*, 675-696; b) Romero, T.; Orenes, R. A.; Espinosa, A.; Tárraga, A.; Molina, P. *Inorg. Chem.* **2011**, *50*, 8214-8224; c) Byrne, J. P.; Kitchen, J. A.; Gunnlaugsson, T. *Chem. Soc. Rev.* **2014**, *43*, 5302-5325; d) Crowley, J. D.; McMorran, D. A. in *Click Triazoles* (Ed.: J. Košmrlj), Springer Berlin Heidelberg, Berlin, Heidelberg, **2012**, pp. 31-83; e) Sharma, P.; Singh, A. P. *RSC Adv.* **2014**, *4*, 43070-43079.

[19] a) Jiang, L.; Wang, Z.; Bai, S.-Q.; Hor, T. S. A. *Dalton Trans.* **2013**, *42*, 9437-9443; b) Nador, F.; Volpe, M. A.; Alonso, F.; Feldhoff, A.; Kirschning, A.; Radivoy, G. *Appl. Catal. A.* **2013**, *455*, 39-45; c) Singla, M.; Mathur, P.; Gupta, M.; Hundal, M. S. *Transition Met. Chem.* **2008**, *33*, 175-182; d) Gruenwald, K. R.; Kirillov, A. M.; Haukka, M.; Sanchiz, J.; Pombeiro, A. J. L. *Dalton Trans.* **2009**, *12*, 2109-2120

[20] a) Patil, R. D.; Sasson, Y. *Asian J. Org. Chem.* **2015**, *4*, 1258-1261; b) Bai, S.-Q.; Jiang, L.; Zuo, J.-L.; Hor, T. S. A. *Dalton Trans.* **2013**, *42*, 11319-11326; c) Gonda, Z.; Novak, Z. *Dalton Trans.* **2010**, *39*, 726-729; d) Wang, D.; Zhao, M.; Liu, X.; Chen, Y.; Li, N.; Chen, B. *Org. Biomol. Chem.* **2012**, *10*, 229-231; e) Wang, F.; Fu, H.; Jiang, Y.; Zhao, Y. *Green Chem.* **2008**, *10*, 452-456; f) Wang, C.; Ikhlef, D.; Kahlal, S.; Saillard, J.-Y.; Astruc, D. *Coordination Chemistry Reviews* **2016**, *316*, 1-20.

[21] a) Johansson, J. R.; Beke-Somfai, T.; Stålsmeden, A. S.; Kann, N. *Chem. Rev.* **2016**, *116*, 14726–14768; b) Liu, P. N.; Li, J.; Su, F. H.; Ju, K. D.; Zhang, L.; Shi, C.; Sung, H. H. Y.; Williams, I. D.; Fokin, V. V.; Lin, Z.; Jia, G. *Organometallics* **2012**, *31*, 4904-4915.

[22] Molla, R. A.; Roy, A. S.; Ghosh, K.; Salam, N.; Iqubal, M. A.; Tuhina, K.; Islam S. M. *J. Organomet. Chem.* **2015**, *776*, 170-179.

[23] Creary, X.; Anderson, A.; Brophy, C.; Crowell, F.; Funk, Z. *J. Org. Chem.* **2012**, *77* , 8756–8761.

[24] Sharma, P.; Rathod, J.; Singh, A. P.; Kumar, P.; Sasson, Y.; *Catal. Sci. Technol.* **2018**, *8*, 3246-3259.

[25] Ghodsinia, S. S. E.; Akhlaghinia, B.; Jahanshahi, R. *RSC Adv.* **2016**, *6*, 63613-63623.

[26] Jung, S. H.; Choi, K.; Pae, A. N.; Lee, J. K.; Choo, H.; Keum, G.; Cho, Y. S.; Min, S.-J.

Org. Biomol. Chem. **2014**, *12*, 9674-9682.

[27] Zhang, C.; Huang, B.; Chen, Y.; Cui, D.-M. *New J. Chem.* **2013**, *37*, 2606-2609.

[28] Liu, P. N.; Siyang, H. X.; Zhang, L.; Tse, S. K. S.; Jia, G. *J. Org. Chem.* **2012**, *77*, 5844- 5849.

[29] Silvestri, I. P.; Andemarian, F.; Khairallah, G. N.; Yap, S. W.; Quach, T.; Tsegay, S.; Williams, C. M.; O'Hair, R. A. J.; Donnellya, P. S.; Williams, S. J. *Org. Biomol. Chem*. **2011**, *9*, 6082–6088.

[30] Meng, X.; Xu, X.; Gao, T.; Chen, B. *Eur. J. Org. Chem*. **2010**, *28***,** 5409–5414.

[31] Krisztián, L.; Kele, P.; Novák, Z. *Synthesis* **2009**, *20*, 3527-3532.

[32] Asano, K.; Matsubara, S. *Org. Lett.* **2010**, *12*, 4988-4991.

[33] Doiron, J.; Soultan, A. H.; Richard, R.; Touré, M. M.; Picot, N.; Richard, R.; Čuperlović-Culf, M.; Robichaud, G. A.; Touaibia, M. *Eur. J. Med. Chem*. **2011**, *46*, 4010-4024.

[34] Gonda, Z.; Novák, Z. *Dalton Trans.* **2010**, *39*, 726-729.

Chapter 2: Section B

PMO silica supported Pd complex as heterogeneous catalyst: Recyclable tool for C-C bond forming reactions

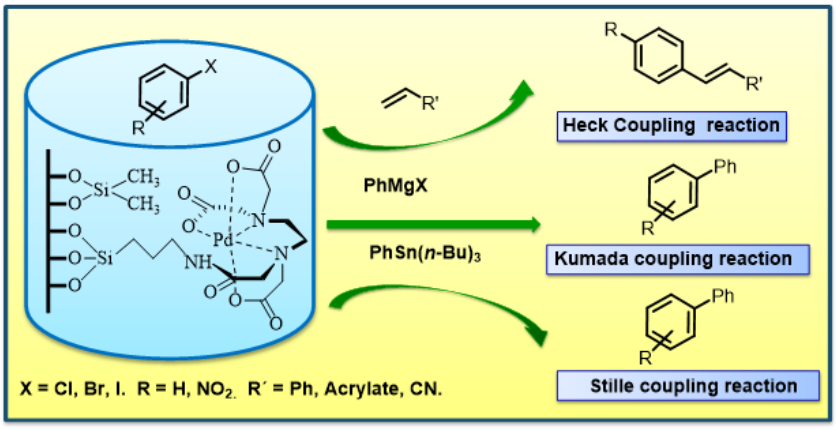

2.2.1 Introduction

Palladium-catalyzed coupling reaction has become an essential and hands-on method for making the C-C bond using aromatic halides with a variety of nucleophilic coupling partner in organic chemistry.[1] Heck, Kumada, Stille, Sonogashira and Suzuki coupling reactions have been extensively explored for the construction of various organic frame work and complex natural product by stitching new C-C bonds.[2] Pd metal plays a crucial role during the course of coupling reactions; the homogeneous Pd complex being completely consumed during the reaction and can not be recovered from the reaction medium. To overcome this limitation, the solid supported Pd catalysts were developed, such as supported over activated carbon, metal oxides, polymer/dendrimer, clay, molecular sieves, mesoporous and nanoporous silica, etc. which are heterogeneous in nature and could be easily recovered after completion of the reaction.[3]

Because of the morphology of SBA-15 like high surface area, uniform pore size and stability,[4] modified SBA-15 with the covalently grafted organic functional group could become the suitable attractive alternate for the homogeneous palladium catalyst. The covalently attached organic functional group could provide a site for the metal binding and while application, it will reduce the leaching of active moiety from the solid support.

As a part of continuous work for the exploration of SBA-15 as catalyst support, we have designed, synthesized and characterized solid supported Pd-EDTA complex SBA-15-EDTA-Pd catalyst with the help of our catalysis division collaborator Dr. A. P. Singh. The developed silica supported heterogeneous catalyst SBA-15-EDTA-Pd was screened for several carbon-carbon coupling reactions.

2.2.2 Present work and Hypothesis

After the synthesis and characterization of catalyst, we envisioned the screening of the catalyst for Suzuki, Sonogashira, Heck, Kumada, and Stille coupling reactions. The details of synthesis and characterization of SBA-15-EDTA-Pd catalyst and application for Suzuki and Sonogashira reactions could be easily accessed from the online publication.[5] This section deals with the catalytic application for the Heck, Kumada, and Stille coupling reactions.

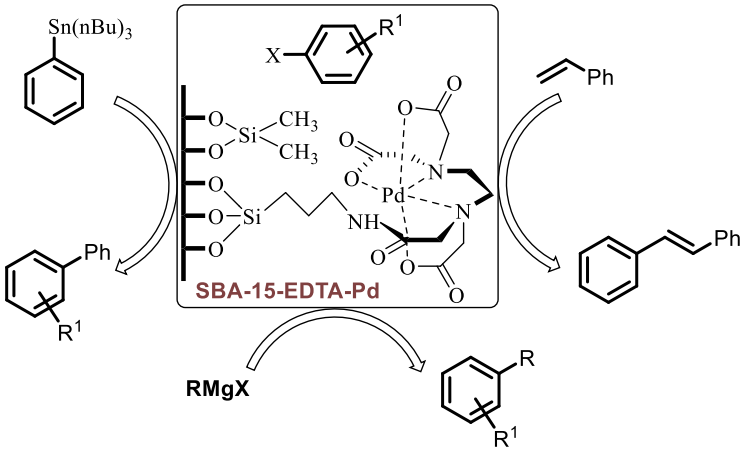

Figure 1: SBA-15-EDTA-Pd catalyst and proposed catalytic reactions

2.2.3 Results and Discussion:

The developed catalyst SBA-15-EDTA-Pd showed excellent reactivity with all the coupling reactions without requiring other additives. Heck, Stille and Kumada cross-coupling reactions work smoothly with the developed catalyst. The obtained results are illustrated in table 1, 2, 3, and 4 respectively.

2.2.3.1 Mizoroki-Heck coupling reaction

Table 1: Optimization of Heck coupling

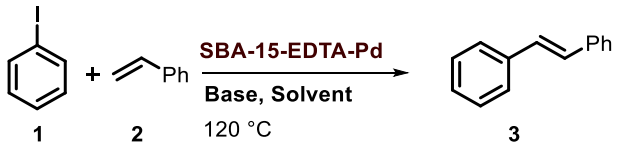

Entry	Base	Solvent	Yield (%)[b]
1	K_2CO_3	DMF	37
2	Na_2CO_3	DMF	40
3	NaOH	DMF	41
4	$NaHCO_3$	DMF	29
5	**NEt_3**	**DMF**	**99**
6	NEt_3	Xylene	8
7	NEt_3	DMSO	89
8	NEt_3	1,4-Dioxane	10
9	NEt_3	THF	39
10	NEt_3	Toluene	15
11	NEt_3	NMP	75

a) Reaction conditions: styrene (1.15 mmol), iodobenzene (1 mmol), Base (3 mmol), Solvent 3.5 mL, SBA-15-EDTA-Pd catalyst (0.87 mmol% Pd) **b)** Isolated yields, Reaction monitored by GC.

In the beginning, the heterogeneous catalyst SBA-15-EDTA-Pd was screened for the coupling of aryl halides with an olefin to make the $C(sp^2)$-$C(sp^2)$ bond (Heck reaction). Iodobenzene and simple styrene were chosen as a model substrate for the Heck reaction and screened by varying the base and solvent, as discussed in table 1. To optimize the best conditions, the coupling reaction was performed with iodobenzene and 1.15 equivalent of styrene in the presence K_2CO_3 as a base and refluxed in DMF, the desired product was obtained in 37% yield only (table 1 entry 1). Further, we have screened other inorganic bases such as Na_2CO_3, NaOH, and $NaHCO_3$, etc. but the improvement in the yield (up to 41%) was not observed (Table 1, entry 2-4). After these observations we switched over to organic base, when the reaction was performed with triethylamine (TEA), the reaction was completed within 6 hours delivering the desired coupled product **4** in excellent yield (99%) (Table 1, entry 5).

Furthermore, for the temperature optimization when the reaction was performed at 50°C, the reaction did not trigger even on prolongation for 24h. At reflux temperature the more stable *trans*-stilbene **4** was formed as a single isomer with 99 % yield in 6 h at 120 ^oC. Next, to find the scope of the solvents, we have screened the reaction under the same condition with a variety of solvents. Reaction displayed comparable reactivity with solvent DMSO and NMP the yield of desired product was 89% and 75% respectively (table 1 entry 7, 11). In other solvents such as xylene, the yield of stilbene was very poor (8% to 39%) (Table 1, entry 6, 8-10). The DMF was found to be the best solvent from the other solvent screened. After the optimized condition in hand, further we have screened the catalyst with an array of the aryl halide and olefin to generalize the reactivity of the catalyst SBA-15-EDTA-Pd, obtained results are illustrated in table 2.

The catalyst was screened with the Chloro-, Bromo- and Iodobenzene with the aromatic olefins styrene, and 4-methyl styrene, the reaction was very sluggish with the chlorobenzene and required longer time, resulted in lower yield as compared to the bromo- (Br-Ph) and iodobenzene (I-Ph) (**3a-b**). Catalyst displayed comparable reactivity with Br-/I- Ph, as the reaction with I-Ph was faster than Br-Ph. Further, methyl acrylate, ethyl acrylate, acrylonitrile, methyl methacrylate, and acrylic acid were reacted smoothly with iodobenzene delivering the respective cross-coupled product in excellent yield up to 99 %

(Table 2, **3c-g**). In the case of methacrylate (**3f**), the time required to complete the reaction was increased due to the more steric bulk on olefin. The electron deficient aryl halides like

Table 2: Substrate scope of the Heck reaction

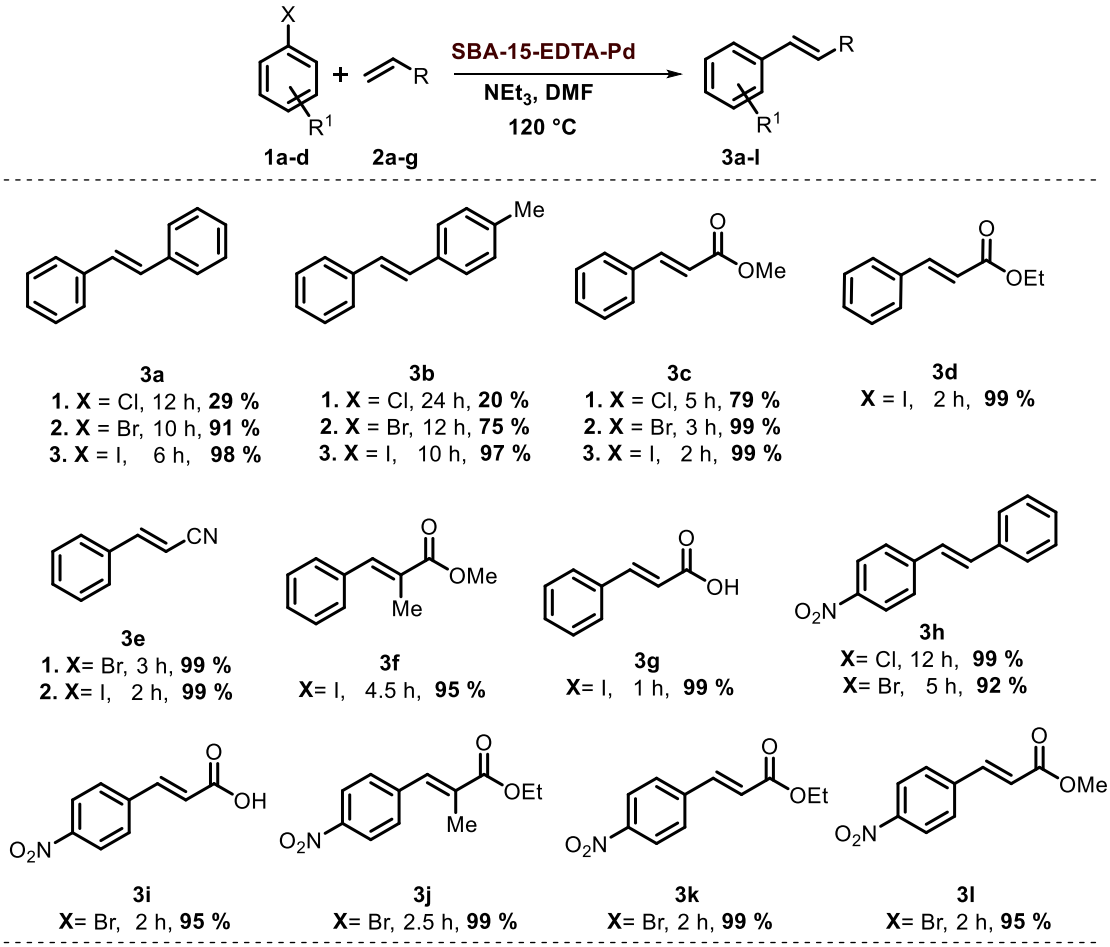

4-chloronitrobenzene; 4-bromonitrobenzene hassle-free reacted with styrene and gave the corresponding coupled product **3h** (4-nitro stilbene) in 99 % and 92 % yields respectively. Additionally, in case of aryl halides with electron-withdrawing functional groups like chloro/bromo nitrobenzene, the rate of coupling reaction increased with active olefins, acrylates *viz:* acrylic acid, ethyl methacrylate, ethyl acrylate and methyl acrylate affording the desired coupled products **3i-l** in excellent yields up to 99 %.

Moreover, the catalytic activity of solid supported SBA-15–EDTA–Pd was studied with a homogeneous EDTA-Pd complex with iodobenzene and simple styrene, the yield of product **3a** was 99 %.

After establishing the catalytic activity for the Heck reactions, further, we deliberated exploring performance of silica supported SBA-15-EDTA-Pd catalyst for Stille (Table 3) and Kumada coupling reactions (Table 4).

2.2.3.2 Stille Coupling Reactions

Generally, the coupling reaction of aryl halides and phenyl stannane reagent requires the dry and inert condition with long reaction time with Pd/phosphine catalyst system. The solid supported catalyst SBA-15-EDTA-Pd was studied for Stille coupling reaction, thus iodobenzene and phenyltributyltin was refluxed in the presence of base CsF (cesium fluoride) in DMSO. The reaction proceeded smoothly with an excellent yield of coupled product biphenyl **5a** (94 %) without phosphine.

Table 3: Substrate scope of the Stille coupling reaction

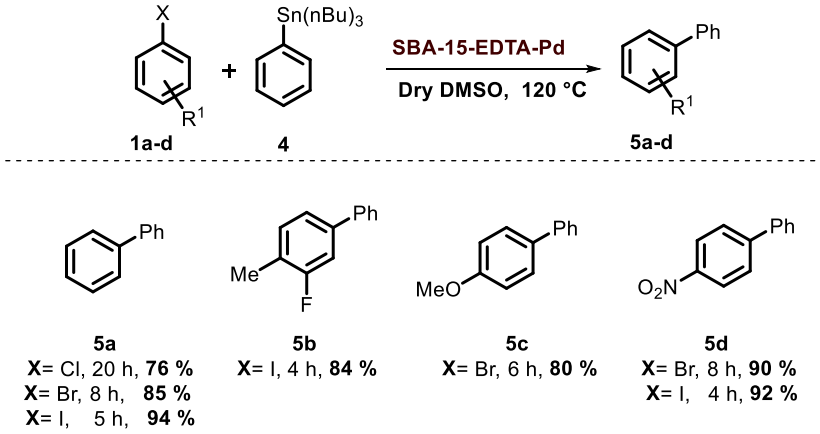

5a
X= Cl, 20 h, **76 %**
X= Br, 8 h, **85 %**
X= I, 5 h, **94 %**

5b
X= I, 4 h, **84 %**

5c
X= Br, 6 h, **80 %**

5d
X= Br, 8 h, **90 %**
X= I, 4 h, **92 %**

Stille coupling reaction was screened with the various aryl halides like chloro-, bromo-, iodobenzene including electron deficient and electron-rich functional groups. The reaction of phenyltributyltin in the presence of the catalytic amount of SBA-15-EDTA-Pd (0.87 mmol % Pd) smoothly afforded the corresponding desired products **5a-d** in good to excellent yields (76– 94 %).

2.2.3.3 Tamao-Kumada coupling reaction

Further, to extend the efficacy of the catalyst SBA-15-EDTA-Pd, we have examined Tamao-Kumada coupling reaction. Thus, the reaction was performed between iodobenzene and Grignard reagent RMgBr in THF at room temperature (Table 4). Various aryl halides treated with the nucleophile PhMgBr (Phenyl magnesium bromide) in the presence of SBA-15-EDTA-Pd in THF to afford the corresponding coupled products **7a-d** in moderate to good yields (60-78 %).

Table 4: Substrate scope of the Tamao-Kumada coupling reaction

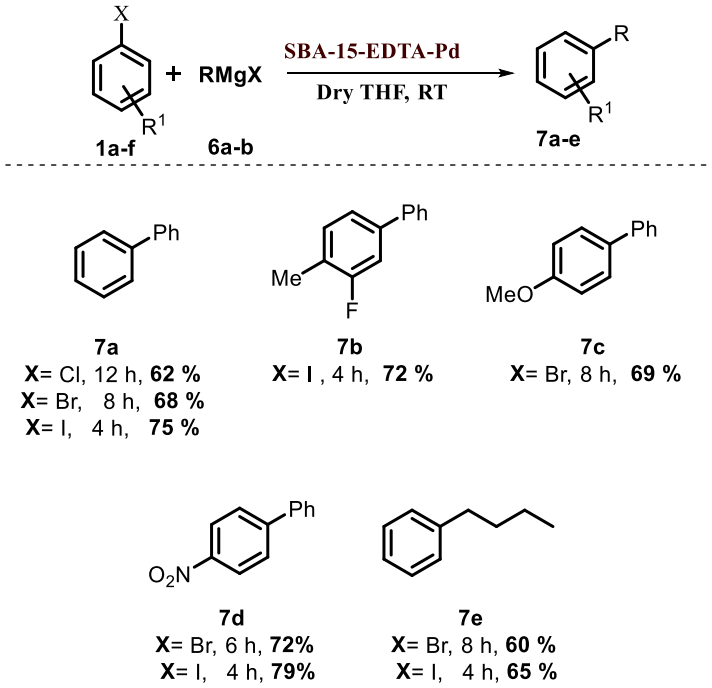

7a
X= Cl, 12 h, **62 %**
X= Br, 8 h, **68 %**
X= I, 4 h, **75 %**

7b
X= **I** , 4 h, **72 %**

7c
X= Br, 8 h, **69 %**

7d
X= Br, 6 h, **72%**
X= I, 4 h, **79%**

7e
X= Br, 8 h, **60 %**
X= I, 4 h, **65 %**

Alkyl Grignard reagent butylmagnesium bromide also coupled easily with iodo- and bromobenzene under the reaction conditions and delivered the corresponding product **7e** in reasonable yields.

2.2.3.4 Heterogeneity and Recycling studies of Catalyst SBA-15-EDTA-Pd

To establish the heterogeneity and recyclability of the synthesized catalyst, the hot filtration test was performed for the detection of Pd metal leaching from the solid surface. During the Heck reaction after 1 hour in between the reaction the catalyst was removed by filtration, the conversion of iodobenzene was 58%. Further supernatant liquid was stirred under reflux condition for an additional 5 hours. There was no progress of reaction observed with the supernatant liquid used, which revealed that during the reaction the Pd metal remains on the solid support even at the higher temperature.

After the hot filtration analysis, the catalyst was subjected for recyclability study; after the completion of the Heck reaction, the reaction mixture was filtered off using sintered glass funnel. The catalyst was washed with the organic solvents like DMF (3-5 mL), DCM (5 mL) and followed by acetone (2-5 mL). The catalyst was overnight dried in the oven and reused for the next catalytic cycle. The yield of the products was more or less comparable with fresh SBA-15-EDTA-Pd catalyst and recycled catalyst. After the five recycle, the catalyst was subjected for the ICP analysis for the Pd metal content, it showed that the loss of Pd metal was less than 1.0 weight % of total Pd in SBA-15-EDTA-Pd.

2.2.4 Conclusions

In conclusions, we have reported the synthesis of highly stable and recyclable solid supported SBA-15-EDTA-Pd (0.87 mmol % Pd) and its application for the various C-C bond formation reactions. The developed catalyst proved to be an efficient tool for the Heck, Stille, and Kumada coupling reactions. The catalyst was heterogeneous and enabled easy separation from the reaction mixture and recycled up to five times without loss of catalytic activity. The catalyst exhibits the superior activity regarding reaction time, isolation, Pd metal loading, and yields of products than the earlier reports.

2.2.5 Experimental procedure:

2.2.5.1 Catalyst SBA-15–Pd–EDTA synthesis

The synthesis and characterization of SBA-15-EDTA-Pd catalyst was carried out following the method described by Singh, and Sharma.[5]

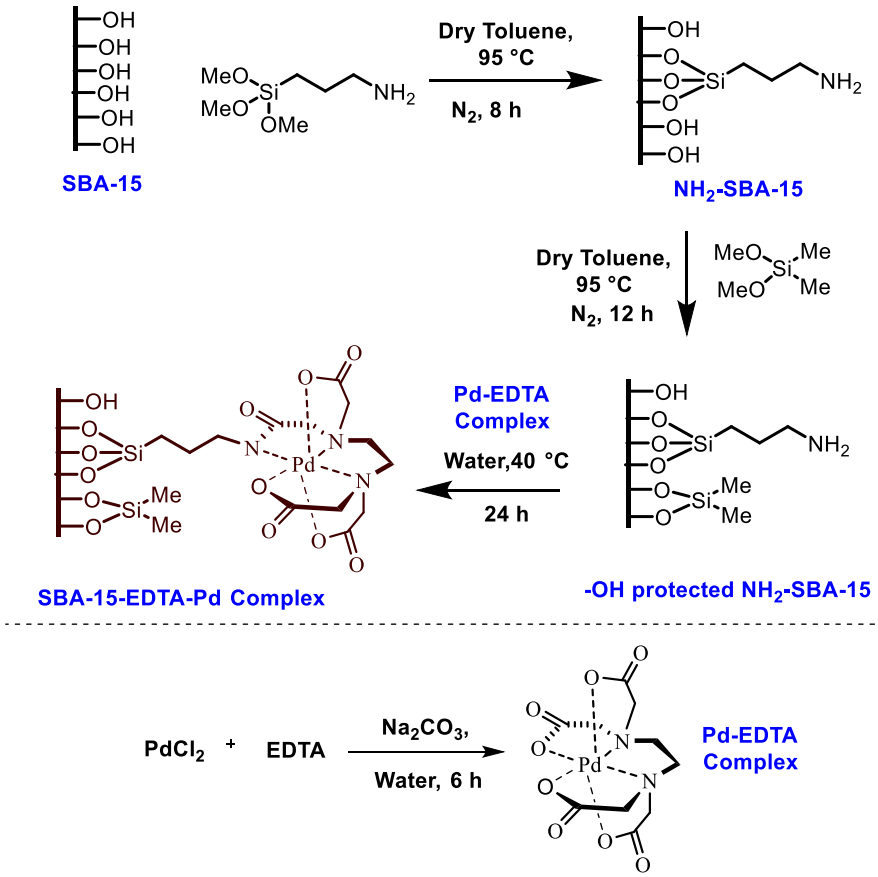

Scheme 1: Synthesis of SBA-15-EDTA-Pd catalyst

SBA-15 was prepared as per the reported procedure using tri-block P_{123} as a template under acidic conditions.[12] Surface modification of SBA-15 was done by a post-synthesis grafting method under N_2 atmosphere.[6] Pd-EDTA complex was synthesized by the earlier reported procedure.[7] To the resultant solution, the calculated amount (1.0 g) of organo-modified SBA-15 was added, along with the slow addition of 25 ml of Millipore water.[5] The resultant material was named SBA-15–EDTA–Pd. The procedure involves stirring a mixture of the calculated amount of EDTA-Pd complex and amino-functionalized SBA-15 with slow addition of Millipore water at 75 °C for 24 h. Later obtained material was washed with distilled water and soxhlet extracted to remove the unanchored materials from SBA-15 surface. The resultant material was named SBA-15–EDTA–Pd.

The surface properties of the functionalized catalyst were analyzed by a series of characterization techniques like elemental analysis, XRD, N_2 sorption measurement isotherm, FT-IR, XPS, and DRS UV–Visible, SEM and TEM. Furthermore; the catalyst was well characterized for its texture, the structure of organo-functionalization and mesoporous along with other physicochemical properties were characterized by using analytical techniques such as solid state ^{13}C, ^{29}Si NMR, CP-OES, TGA & DTA, DRS UV–Visible, SEM and TEM.[5]

2.2.5.2 General procedure for Heck coupling reactions

Screening of the catalyst SBA-15-EDTA-Pd for Mizoroki -Heck reaction was done in 25 mL two neck round bottom flask. In a typical run aryl halide (1 mmol), (1.15 mmol) olefin, (3 mmol) triethylamine, (3.5 mL) solvent N, N´-dimethylformamide (DMF) and SBA-15-EDTA-Pd (15 mg, 0.87 mmol % Pd) were stirred at 120 °C. The reaction mixture was analyzed by GC at measured time intervals. After separating by column chromatography, the products were analyzed by GC, ^{1}H, and ^{13}C NMR.

2.2.5.3 General procedure for the Kumada coupling reaction

Aryl halide (1 mmol), catalyst SBA-15-EDTA-Pd (15 mg, 0.87 mmol % Pd) and 5 ml freshly distilled dry THF were taken in the two-necked 50 ml round bottom flask under the argon atmosphere then after 1.8 equivalent Grignard reagent was added in the reaction mixture through the rubber septum. The reaction mixture was stirred at room temperature for the given time. Completion of the reaction was monitored by thin layer chromatography (pet ether 100 %) and reaction mass quenched with saturated ammonium chloride solution and extracted with ethyl acetate (20 mL x 3), the organic layer dried over anhydrous sodium sulfate and evaporated under reduced pressure. The crude product was subjected to column chromatography to obtain the pure compound.

2.2.5.4 General procedure for the Stille coupling reaction

In the oven dried 2 neck RBF, Aryl halide (1 mmol), Catalyst SBA-15-EDTA-Pd (15 mg, 0.87 mmol % Pd), CsF (2 equivalent), phenyl tributyl tin (1.5 equivalent) and 3 ml dry DMSO were taken. The reaction mixture heated at 120 °C for a given time under argon atmosphere. Completion of the reaction was monitored by thin layer chromatography (pet ether 100 %). After the completion of reaction 20 mL ethyl acetate was added, and the reaction mixture was filtered through Whatman filter paper to recover the catalyst. Filtrate was washed 2 times with brine solution and dried over anhydrous sodium sulfate and

concentrated under reduced pressure. The crude product was subjected to column chromatography to obtain the pure compound.

2.2.5.5 Analytical data

(*E*)-Stilbene (3a):[8]

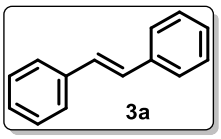

Crystalline white Solid; mp = 120-122 °C (Reported mp = 122-124 °C);

^{1}H NMR (200 MHz, $CDCl_3$) δ = 7.57-7.50 (m, 4 H), 7.43 - 7.33 (m, 4 H), 7.33-7.28 (m, 2 H), 7.13 ppm (s, 2 H);

^{13}C NMR (50 MHz, $CDCl_3$) δ = 137.4, 128.7, 127.6, 126.5 ppm;

GC-MS (m/z) = 180 $[M]^+$.

(*E*)-1-Methyl-4-styrylbenzene (3b):[9]

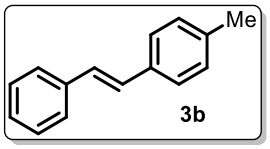

White Solid; mp = 118-120 °C (reported mp = 118-119 °C);

^{1}H NMR (300 MHz, $CDCl_3$) δ = 7.49 (d, J = 7.6 Hz, 2H), 7.41–7.31 (m, 4H), 7.26–7.21 (m, 1H), 7.16 (d, J = 8.3 Hz, 2H); 7.06 (s, 2H), 2.35 ppm (s, 3H);

^{13}C NMR (75 MHz, $CDCl_3$) δ = 137.6, 134.6, 129.5; 129.3, 128.7, 127.8, 127.6, 127.5, 126.8, 126.5, 21.3 ppm;

GC-MS (m/z) = 194 $[M]^+$.

(*E*)-Methyl Cinnamate (3c): [9]

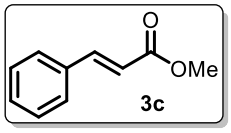

Colorless liquid.

^{1}H NMR (200 MHz, $CDCl_3$) δ = 7.71 (d, J = 16 Hz, 1 H), 7.62 - 7.30 (m, 5 H), 6.45 (d, J = 15.9 Hz, 1 H), 3.80 ppm (s, 3 H);

^{13}C NMR (50MHz, $CDCl_3$) δ = 167.4, 144.8, 134.3, 130.2, 128.8, 128.0, 117.7, 51.6 ppm;

GC-MS (m/z) = 162 $[M]^+$.

(*E*)-Ethyl cinnamate (3d):[10]

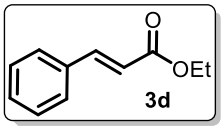

Colorless liquid.

^{1}H NMR (200MHz, $CDCl_3$) δ = 7.62 (d, *J* = 16 Hz, 1 H), 7.51 - 7.37 (m, 2 H), 7.29 (d, *J* = 3.3 Hz, 3 H), 6.37 (d, *J* = 16 Hz, 1H), 4.19 (q, *J* = 7.1 Hz, 2 H), 1.26 ppm (t, *J* = 7.1 Hz, 3 H);

^{13}C NMR (50MHz, $CDCl_3$) δ = 166.6, 144.3, 134.2, 129.9, 128.6, 127.8, 118.0, 60.2, 14.1, ppm;

GC-MS (m/z) = 176 $[M]^+$.

(*E*)-Cinnamonitrile (3e):[11]

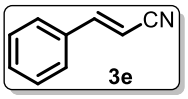

Colorless liquid.

^{1}H NMR (500 MHz, $CDCl_3$) δ = 7.71-7.66 (m, 3H), 7.55-7.50 (m, 2H,), 7.41 (d, *J* = 16.8 Hz, 1H), 6.18 ppm (d, *J* = 16.8 Hz, 1H);

^{13}C NMR (100 MHz, $CDCl_3$) δ = 151.5, 134.4, 132.1, 130.0, 128.3, 119.1, 97.2 ppm;

GC-MS (m/z) = 129 $[M]^+$.

(*E*)-Methyl 2-methyl-3-phenylacrylate (3f):[12]

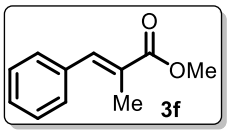

Colorless liquid.

^{1}H NMR (400 MHz, $CDCl_3$): δ = 7.92 (d, *J* = 16.0 Hz, 1H), 7.21–7.41 (m, 5H), 3.83 (s, 3H), 2.15 ppm (s, 3H);

^{13}C NMR (100 MHz, $CDCl_3$): δ = 14.1, 52.0, 127.9, 129.6, 135.8, 138.9, 169.1 ppm;

GC-MS (m/z) 176 $[M]^+$.

Cinnamic acid (3g):[9]

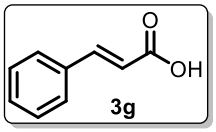

White solid; mp = 132-134°C (reported mp = 132-133°C);

^{1}H NMR (200MHz, $CDCl_3$) δ = 7.82 (d, J = 16.0 Hz, 1 H), 7.66 - 7.51 (m, 2 H), 7.48 - 7.37 (m, 3 H), 6.52 ppm (d, J = 16.0 Hz, 1 H);

^{13}C NMR (50MHz, $CDCl_3$) δ = 172.6, 147.1, 134.0, 130.7, 128.9, 128.4, 117.3 ppm;

GC-MS (m/z) = 148 $[M]^+$.

(*E*)-1-Nitro-4-styrylbenzene (3h):[13]

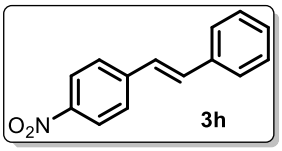

Yellow solid; mp = 160-162°C (reported mp = 159-160 °C);

^{1}H NMR (200 MHz, $CDCl_3$) δ = 8.40 (d, J = 8.8 Hz, 2 H), 7.81 (d, J = 8.7 Hz, 2 H), 7.77 - 7.67 (m, 2 H), 7.64 - 7.48 (m, 3 H), 7.46 - 7.31 ppm (m, 2 H);

^{13}C NMR (50MHz, $CDCl_3$) δ = 146.7, 143.8, 136.1, 133.3, 128.9, 127.0, 126.8, 126.2, 124.1 ppm;

GC-MS (m/z) = 225.2$[M]^+$.

(*E*)-3-(4-Nitrophenyl)acrylic acid (3i):[14]

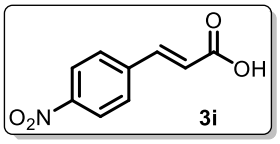

Light yellow solid; mp = compound decomposed at 285-290°C;

^{1}H NMR (200 MHz, $CDCl_3$) δ = 10.24 (br. s., 1 H), 7.82 (d, J = 16 Hz, 1 H), 7.67-7.33 (m, 5 H), 6.48 ppm (d, J = 16 Hz, 1 H);

^{13}C NMR (50 MHz, $CDCl_3$) δ = 172.6, 147.1, 134.0, 130.7, 128.9, 128.4, 117.3 ppm;

GC-MS (m/z) = 193 $[M]^+$.

(*E*)-Ethyl 2-methyl-3-(4-nitrophenyl) acrylate (3j):[15]

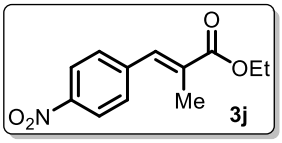

Yellow solid; mp = 66-68°C (reported mp = 67-69°C);

^{1}H NMR (200 MHz, $CDCl_3$) δ = 8.26 (d, J = 10 Hz, 2 H), 7.70 (s, 1 H), 7.54 (d, J = 8 Hz, 2 H), 4.31 (q, J = 7.2 Hz, 2 H), 2.13 (d, J = 1.4 Hz, 3 H), 1.37 ppm (t, J =7.1 Hz, 3 H);

^{13}C NMR (50 MHz, $CDCl_3$) δ = 167.8, 147.2, 142.5, 136.0, 132.3, 130.2, 123.6, 61.3, 14.25, 14.18 ppm;

GC-MS (m/z) = 235 $[M]^+$.

(*E*)-Ethyl 3-(4-nitrophenyl) acrylate (3k):[16]

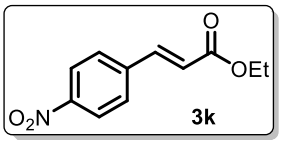

Yellow solid; mp = 136-138°C (reported mp = 138-139°C);

^{1}H NMR (200 MHz, $CDCl_3$) δ = 8.25 (d, J = 8.7 Hz, 2 H), 7.83 - 7.59 (m, 3 H), 6.56 (d, J = 16.0 Hz, 1 H), 4.41- 4.19 (m, 2 H), 1.36 ppm (t, J = 7.1 Hz, 3 H);

^{13}C NMR (50 MHz, $CDCl_3$) δ = 166.0. 148.4, 141.5, 140.5, 128.6, 124.1, 122.5, 77.6, 76.4, 61.0, 14.2 ppm;

GC-MS (m/z) = 221 $[M]^+$.

(*E*)-Methyl 3-(4-nitrophenyl)acrylate (3l):[17]

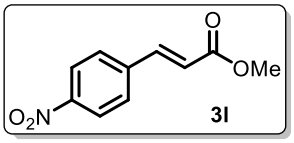

Pale yellow solid; mp = 138-140°C (reported mp = 138°C);

^{1}H NMR (200 MHz, $CDCl_3$) δ = 8.24 (d, J = 8.8 Hz, 2 H), 7.78 - 7.60 (m, 3 H), 6.55 (d, J = 16.0 Hz, 1 H), 3.83 ppm (s, 3 H);

^{13}C NMR (50 MHz, $CDCl_3$) δ = 166.4, 148.4, 141.8, 140.4, 128.6, 124.1, 122.0, 52.0 ppm;

GC-MS (m/z) = 207 $[M]^+$.

1'-Biphenyl (5a, 7a):[18]

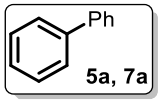

White solid; mp = 68-70°C (reported mp = 69-70°C);

^{1}H NMR (200 MHz, $CDCl_3$) δ = 7.73 - 7.55 (m, 4 H), 7.49 - 7.33 ppm (m, 6 H);

^{13}C NMR (50 MHz, $CDCl_3$) δ = 127.20, 128.79 ppm;

GC-MS (m/z) = 154 $[M]^+$.

3-Fluoro-4-methyl-1,1'-biphenyl (5b, 7b):[19]

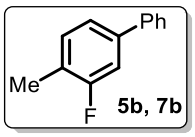

White solid; mp = 36-38°C (reported mp = 38-39 °C);

^{1}H NMR (400 MHz, DMSO-d6) δ = 7.67 (dd, *J* = 1.4, 7.3 Hz, 2 H), 7.52 - 7.30 (m, 6 H), 2.27 - 2.25 ppm (m, 3 H);

^{13}C NMR (101 MHz, DMSO-d6) δ = 162.3, 159.9, 140.0, 139.9, 138.7, 138.4, 132.1, 132.0, 129.0, 127.7, 127.4, 126.7, 126.5, 123.7, 123.5, 123.3, 123.1, 122.3, 122.1, 113.0, 112.9, 112.8, 112.7, 13.9, 13.8 ppm;

GC-MS (m/z) = 186$[M]^+$.

4-Methoxy-1,1'-biphenyl (5c, 7c):[20]

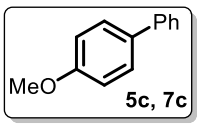

White Solid; mp = 84-86°C (reported mp = 86-88°C);

^{1}H NMR (400 MHz, DMSO-d6) δ = 7.55 - 7.67 (m, 4 H), 7.42 (t, *J* = 7.6 Hz, 2 H), 7.25 - 7.35 (m, 1 H), 7.02 (d, *J* = 8.6 Hz, 2 H), 3.79 ppm (s, 3 H);

^{13}C NMR (101 MHz, DMSO-d6) δ =158.9, 139.8, 132.5, 128.9, 127.8, 126.7, 126.2, 114.4, 55.2 ppm;

GC-MS (m/z) = 184 $[M]^+$.

4-Nitro-1,1'-biphenyl (5d, 7d):[20]

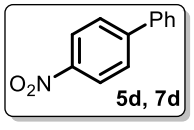

Yellow Solid; mp = 112-114°C (reported mp = 114-115°C);

^{1}H NMR (400 MHz, $CDCl_3$) δ = 8.31 (d, J = 8.3 Hz, 2 H), 7.75 (d, J = 8.6 Hz, 2 H), 7.64 (d, J = 7.3 Hz, 2 H), 7.56 - 7.42 ppm (m, 3 H);

^{13}C NMR (101 MHz, $CDCl_3$) δ = 147.6, 147.1, 138.8, 129.1, 128.9, 127.8, 127.4, 124.1 ppm;

GC-MS (m/z) = 199 $[M]^+$.

***n*-Butylbenzene (7e)**:[12a]

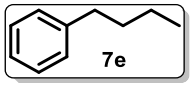

Colourless liquid.

^{1}H NMR (300 MHz, $CDCl_3$) δ = 7.27 (t, J = 6.7 Hz, 2H), 7.21–7.18 (m, 3H), 2.59 (t, J = 7.6 Hz, 2H), 1.66–1.50 S12 (m, 2H), 1.38–1.21 (m, 2H), 0.86 ppm (t, J = 6.5 Hz, 3H);

^{13}C NMR (75 MHz, $CDCl_3$) δ = 142.7, 128.2, 127.9, 125.8, 35.1, 31.2, 22.4, 14.0 ppm;

GC-MS (m/z) = 134 $[M]^+$.

2.2.6 Selected NMR Spectra:

^{1}H NMR of (*E*)-Methyl Cinnamate (3c) (200 MHz, $CDCl_3$):

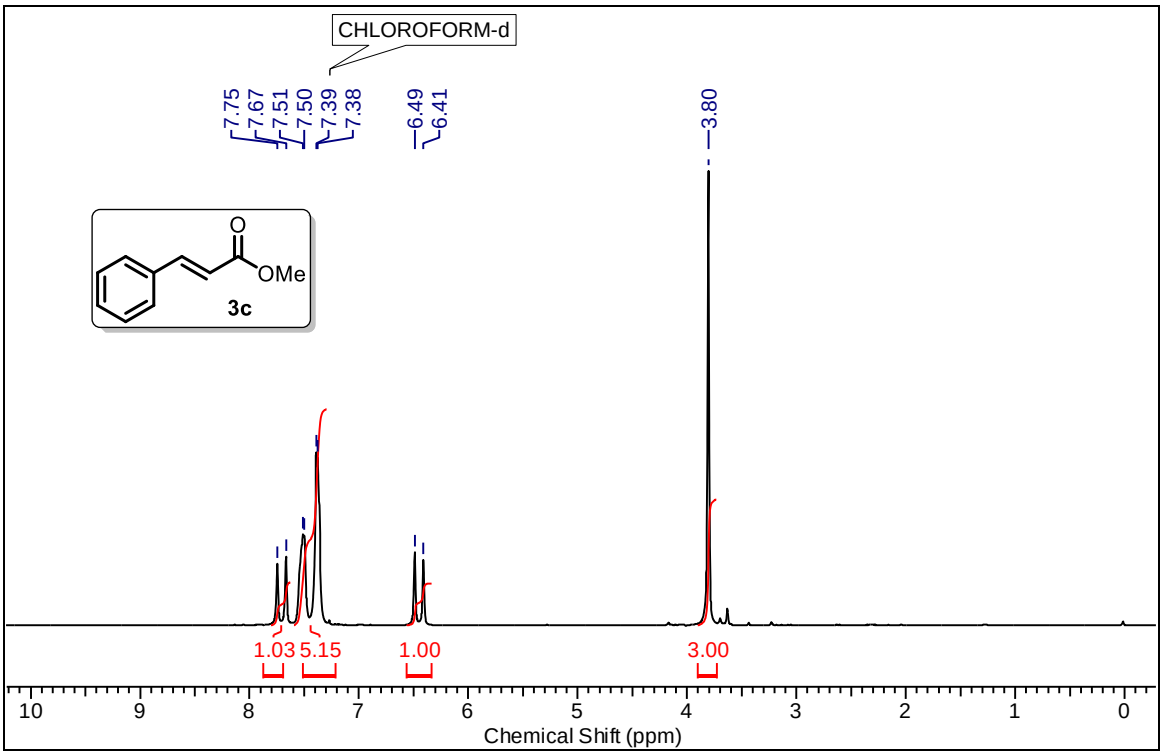

^{13}C NMR of (*E*)-Methyl Cinnamate (3c) (50MHz, $CDCl_3$):

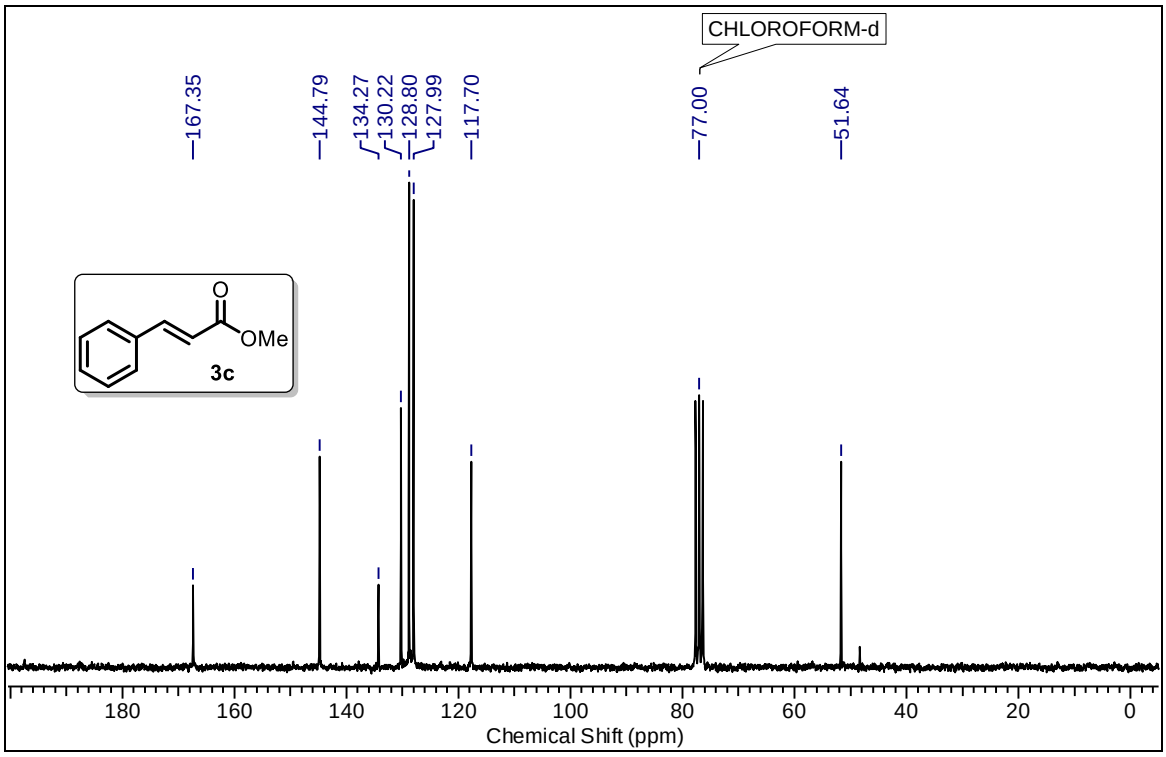

^{1}H NMR of (*E*)-Ethyl cinnamate (3d) (200MHz, $CDCl_3$):

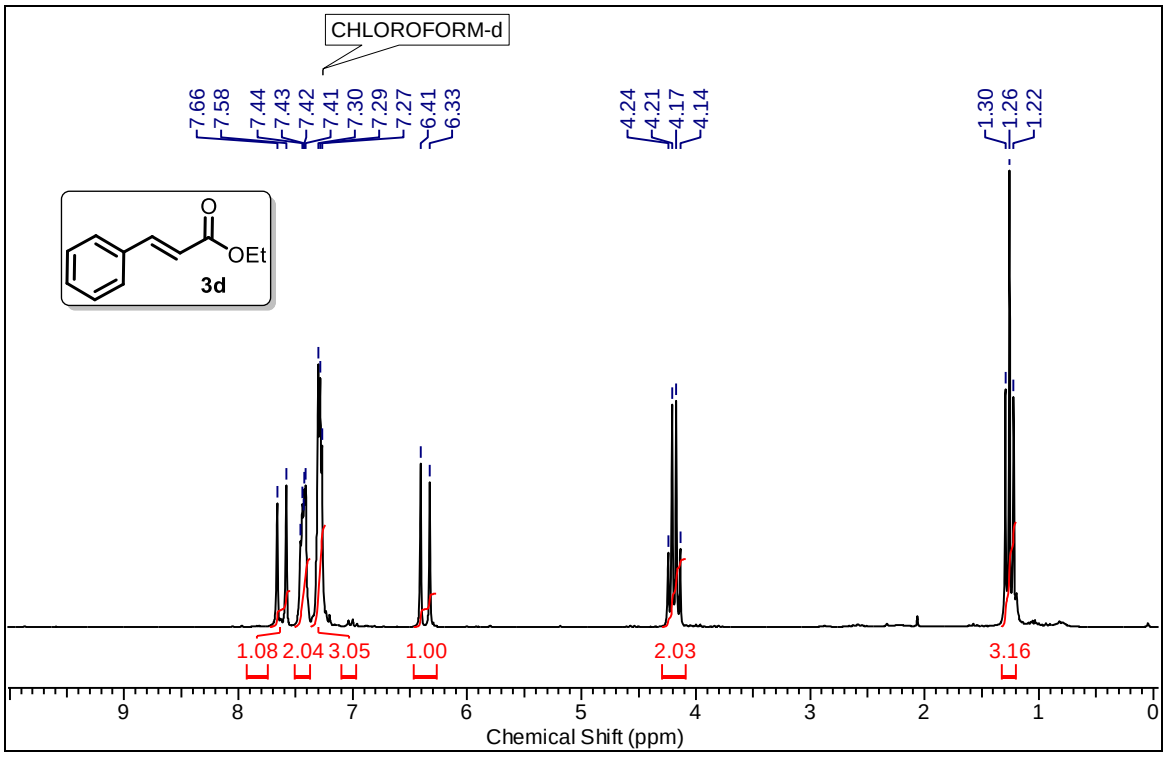

^{13}C NMR of (*E*)-Ethyl cinnamate (3d) (50MHz, $CDCl_3$):

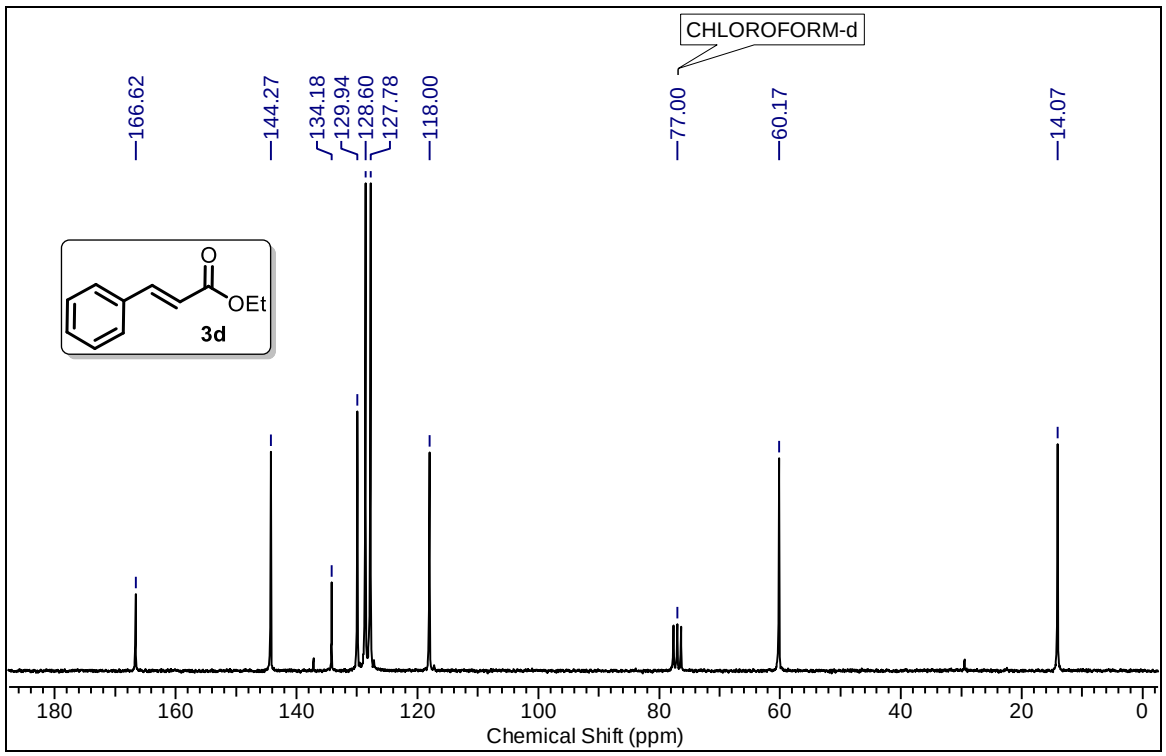

^{1}H NMR of Cinnamic acid (3g) (200MHz, $CDCl_3$):

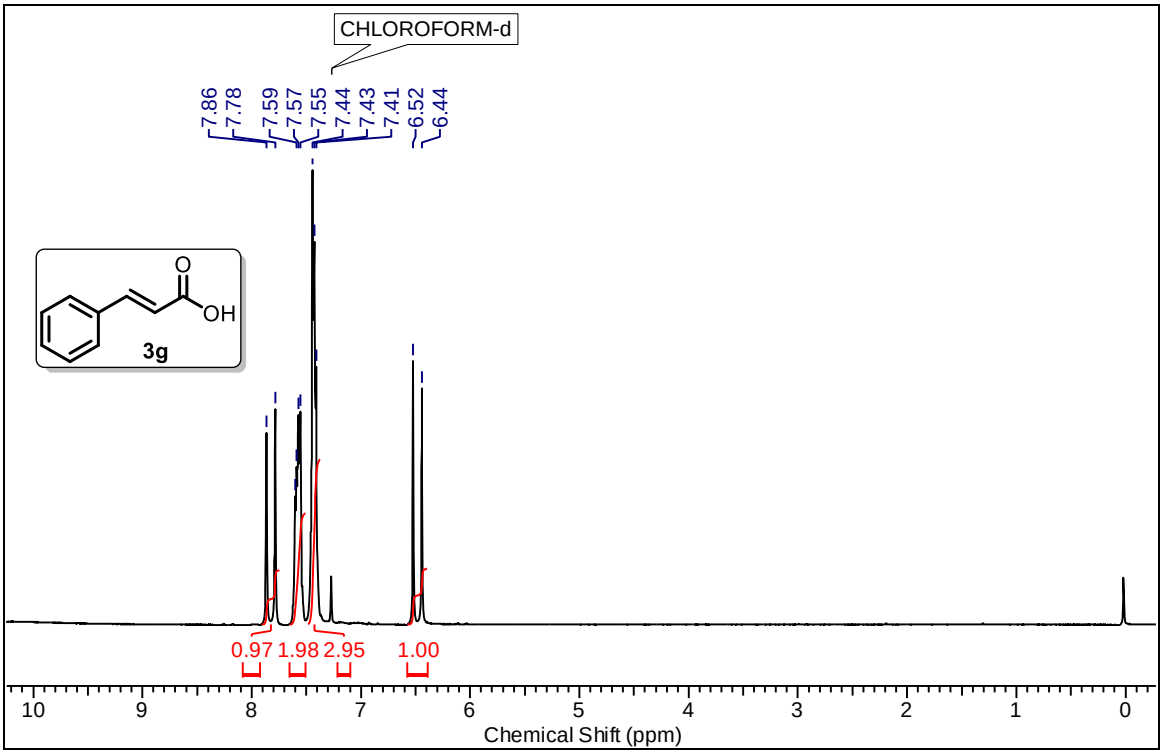

^{13}C NMR of Cinnamic acid (3g) (50MHz, $CDCl_3$):

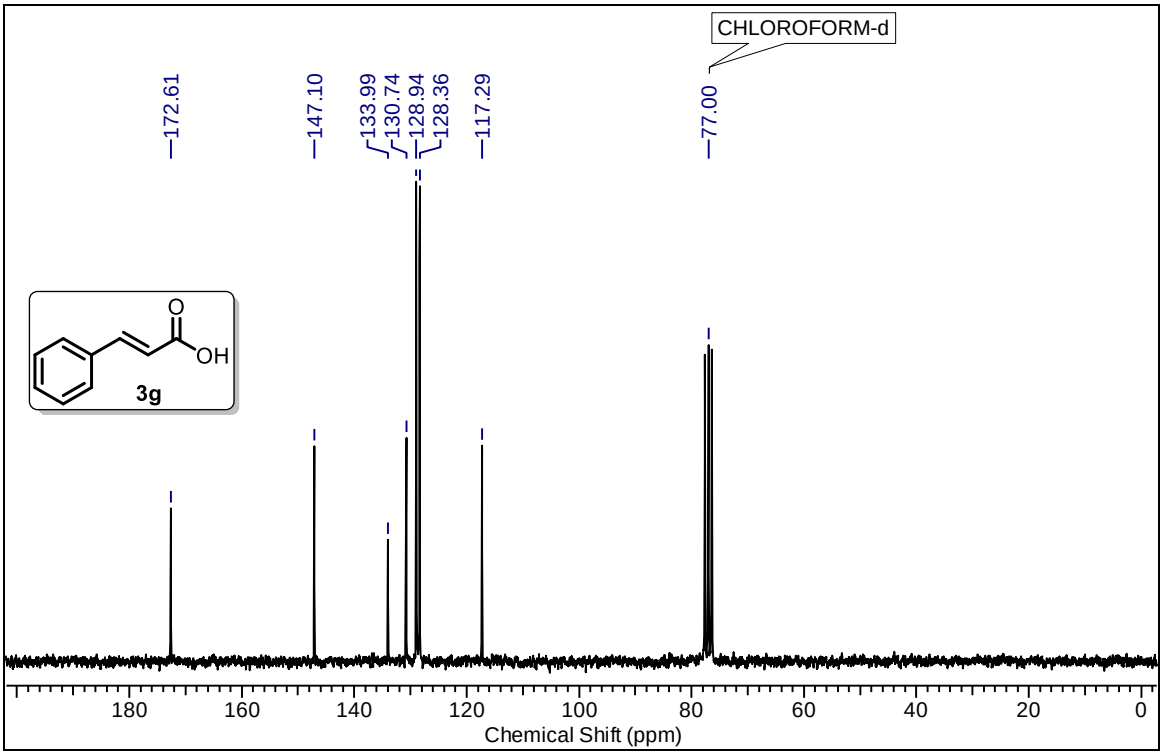

^{1}H NMR of (*E*)-1-Nitro-4-styrylbenzene (3h) (200 MHz, $CDCl_3$):

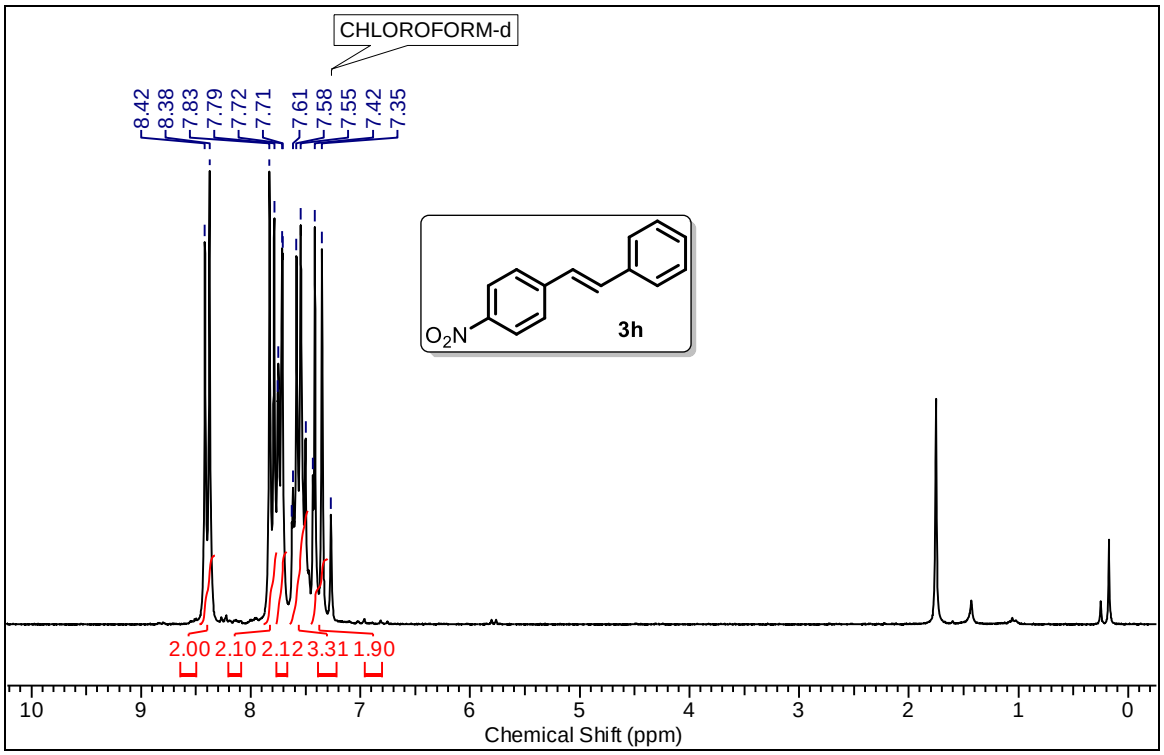

^{13}C NMR of (*E*)-1-Nitro-4-styrylbenzene (3h) (50MHz, $CDCl_3$):

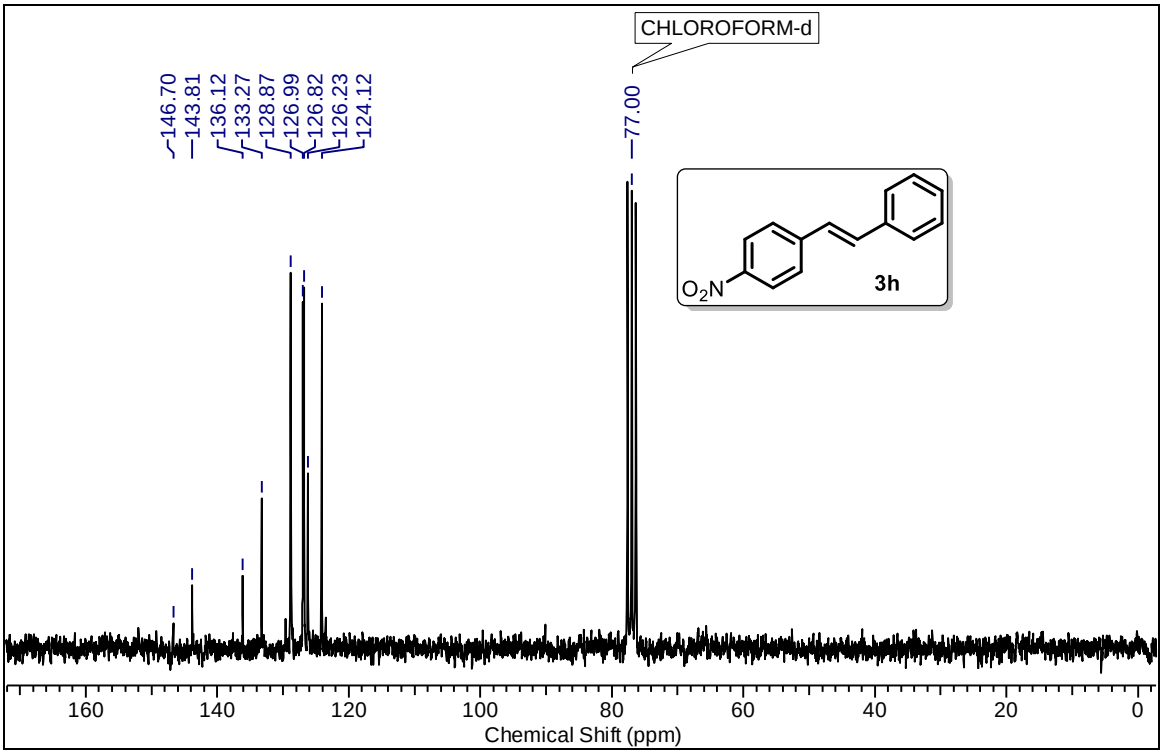

^{1}H NMR of (*E*)-3-(4-Nitrophenyl)acrylic acid (3i) (200 MHz, $CDCl_3$):

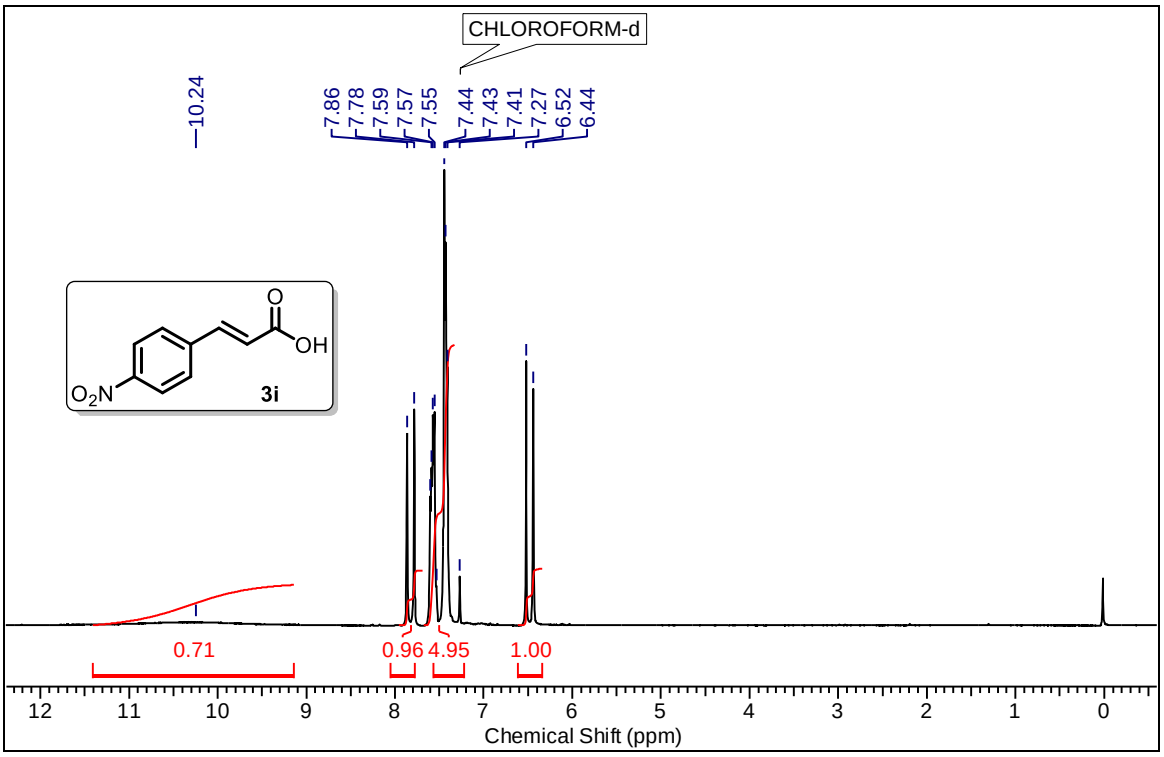

^{13}C NMR of (*E*)-3-(4-Nitrophenyl)acrylic acid (3i) (50 MHz, $CDCl_3$):

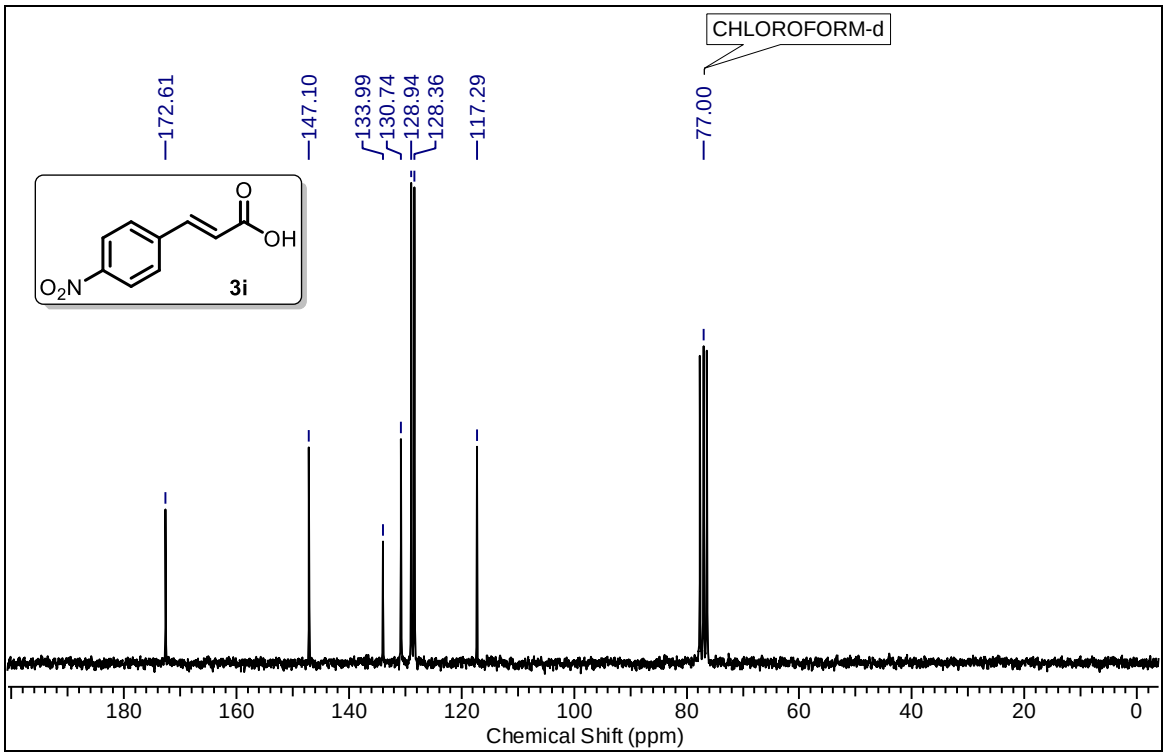

^{1}H NMR of (*E*)-Ethyl 2-methyl-3-(4-nitrophenyl) acrylate (3j) (200 MHz, $CDCl_3$):

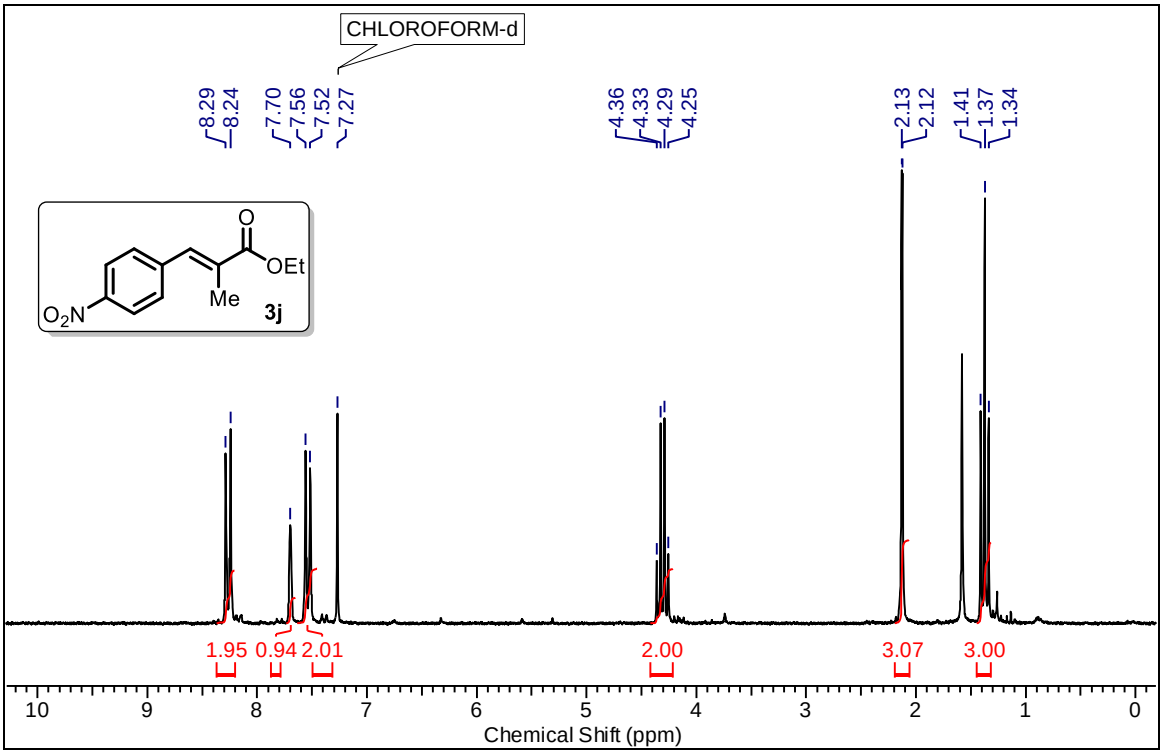

^{13}C NMR of (*E*)-Ethyl 2-methyl-3-(4-nitrophenyl) acrylate (3j) (50 MHz, $CDCl_3$):

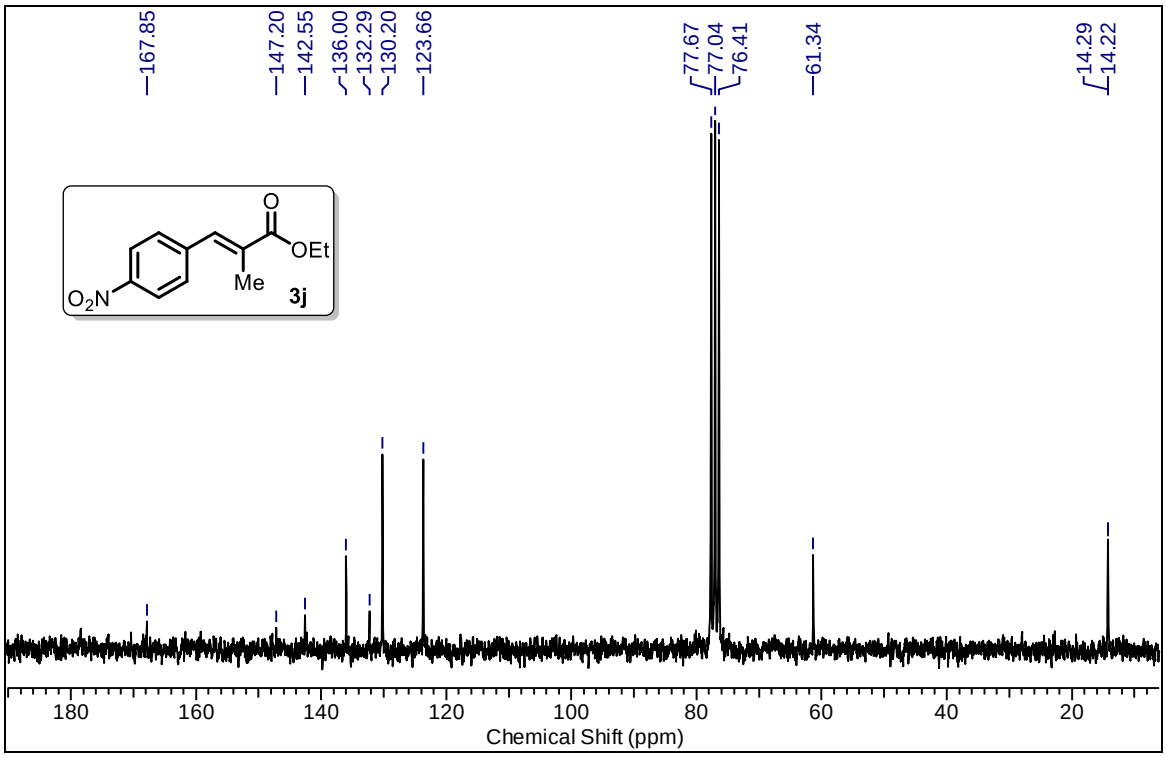

^{1}H NMR of (*E*)-Ethyl 3-(4-nitrophenyl) acrylate (3k) (200 MHz, $CDCl_3$):

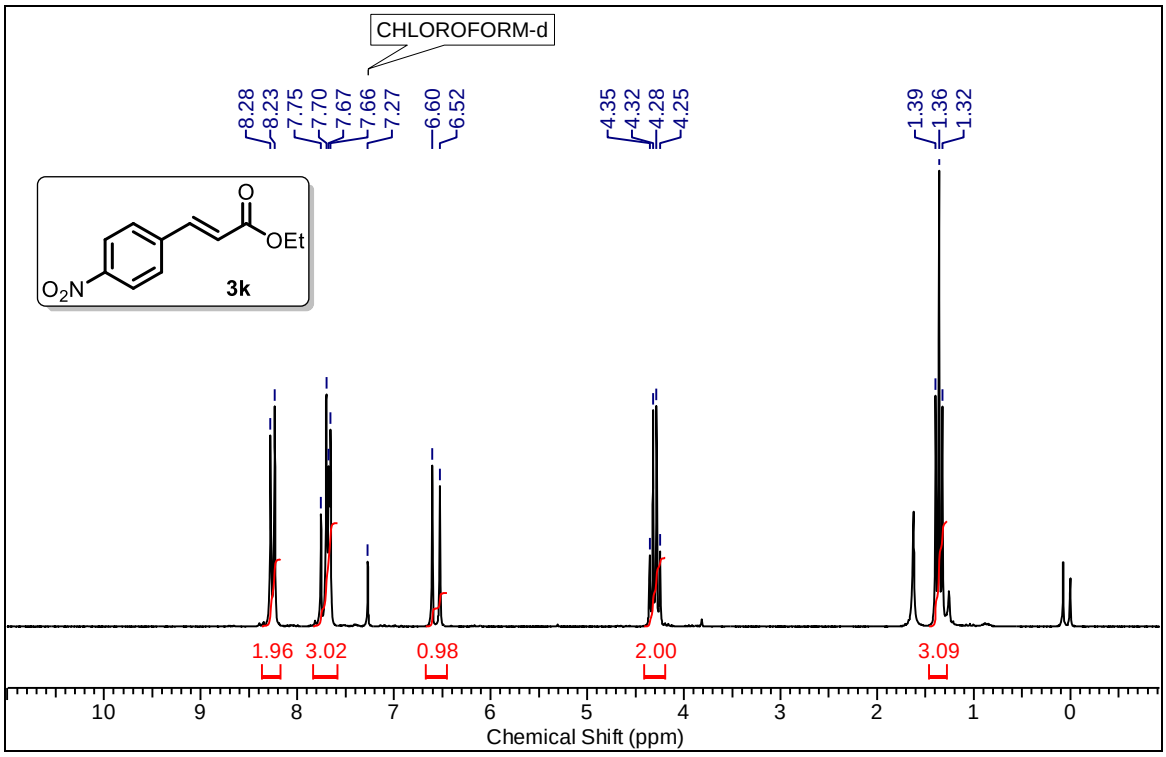

^{13}C NMR of (*E*)-Ethyl 3-(4-nitrophenyl) acrylate (3k) (50 MHz, $CDCl_3$):

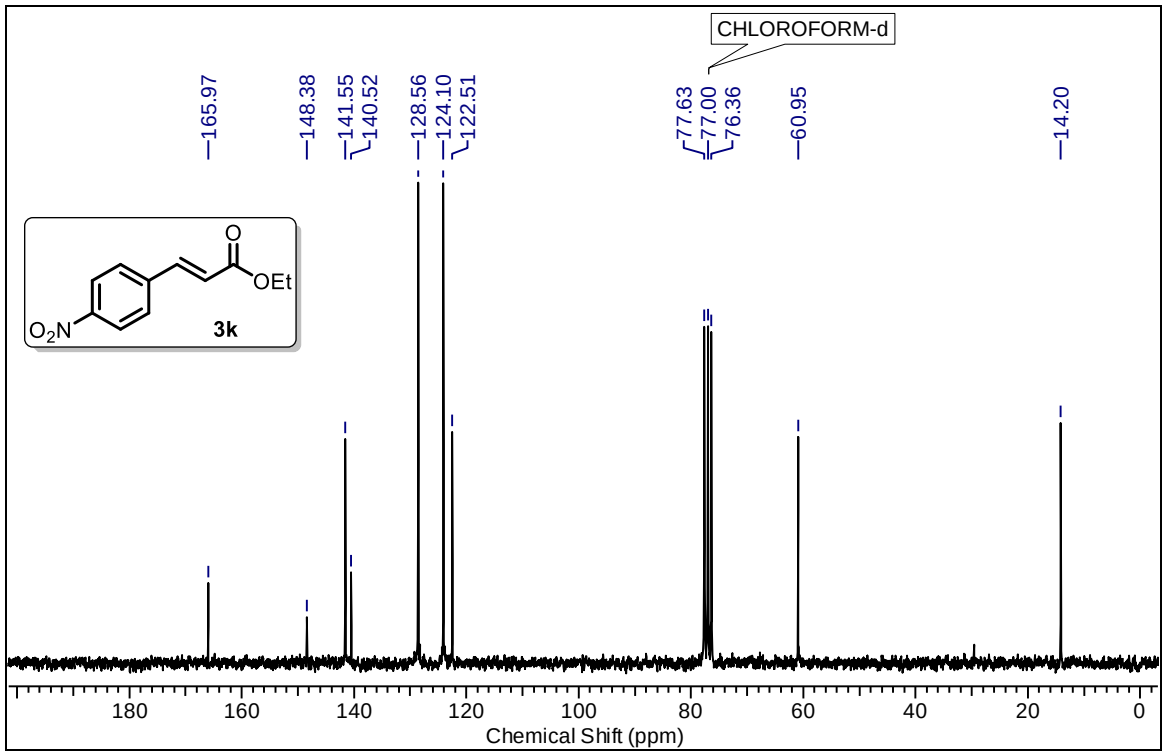

^{1}H NMR of 3-Fluoro-4-methyl-1,1'-biphenyl (5b, 7b) (400 MHz, DMSO-d6):

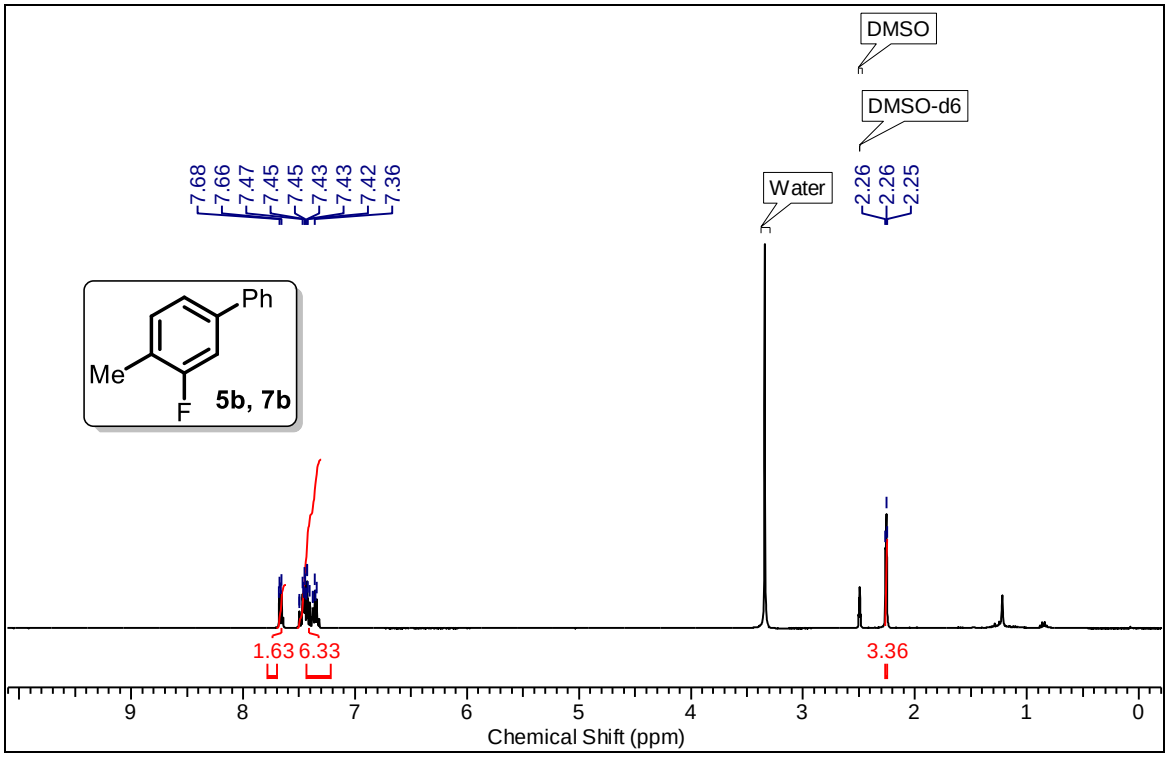

^{13}C NMR of 3-Fluoro-4-methyl-1,1'-biphenyl (5b, 7b) (101 MHz, DMSO-d6):

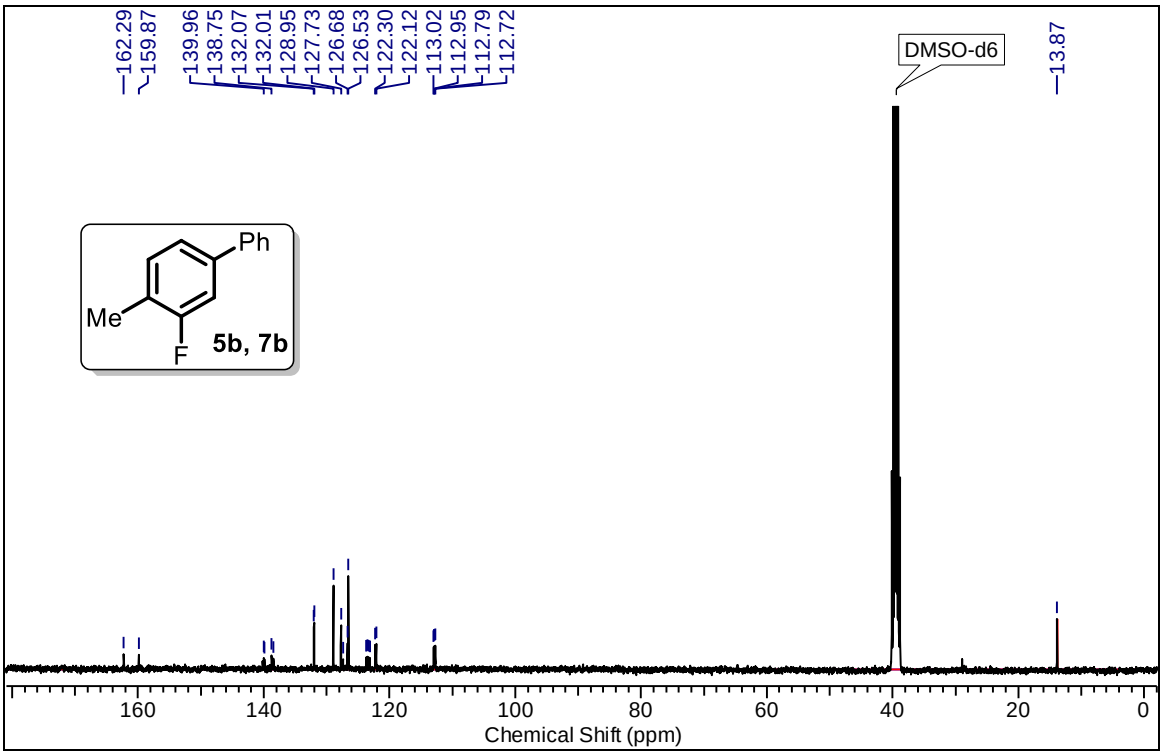

^{1}H NMR of 4-Methoxy-1,1'-biphenyl (5c, 7c) (400 MHz, DMSO-d6):

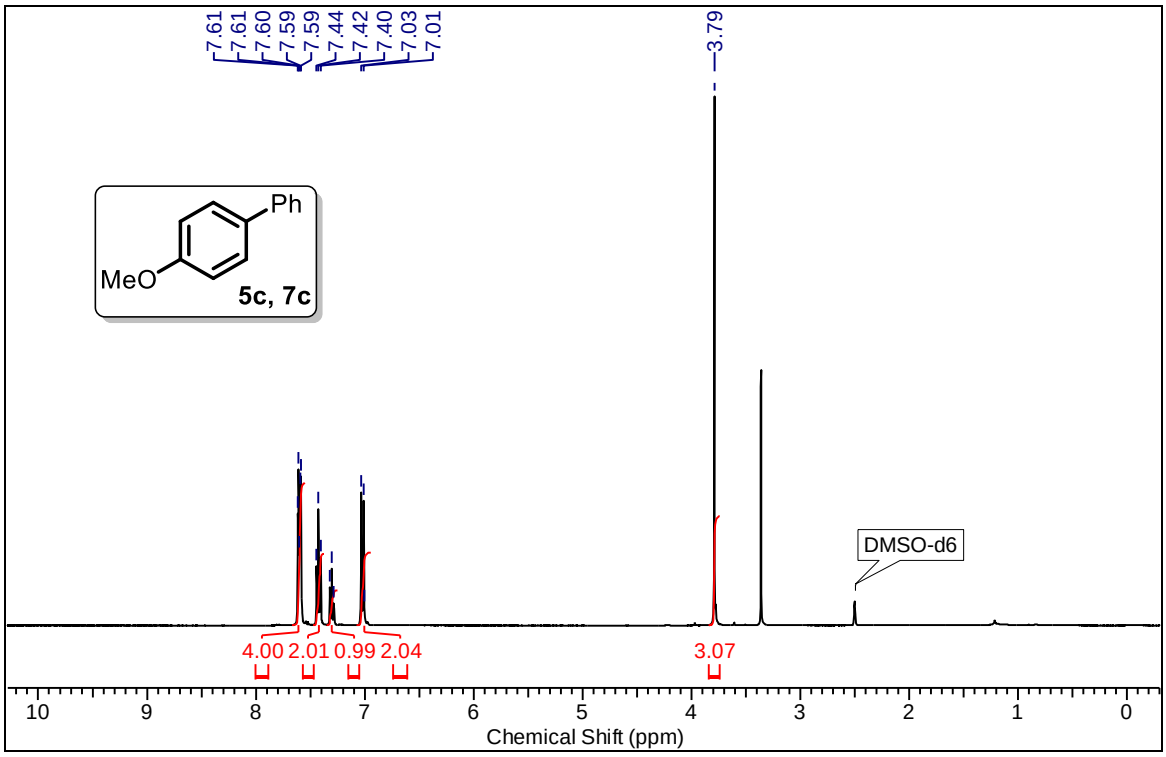

^{13}C NMR of 4-Methoxy-1,1'-biphenyl (101 MHz, DMSO-d6):

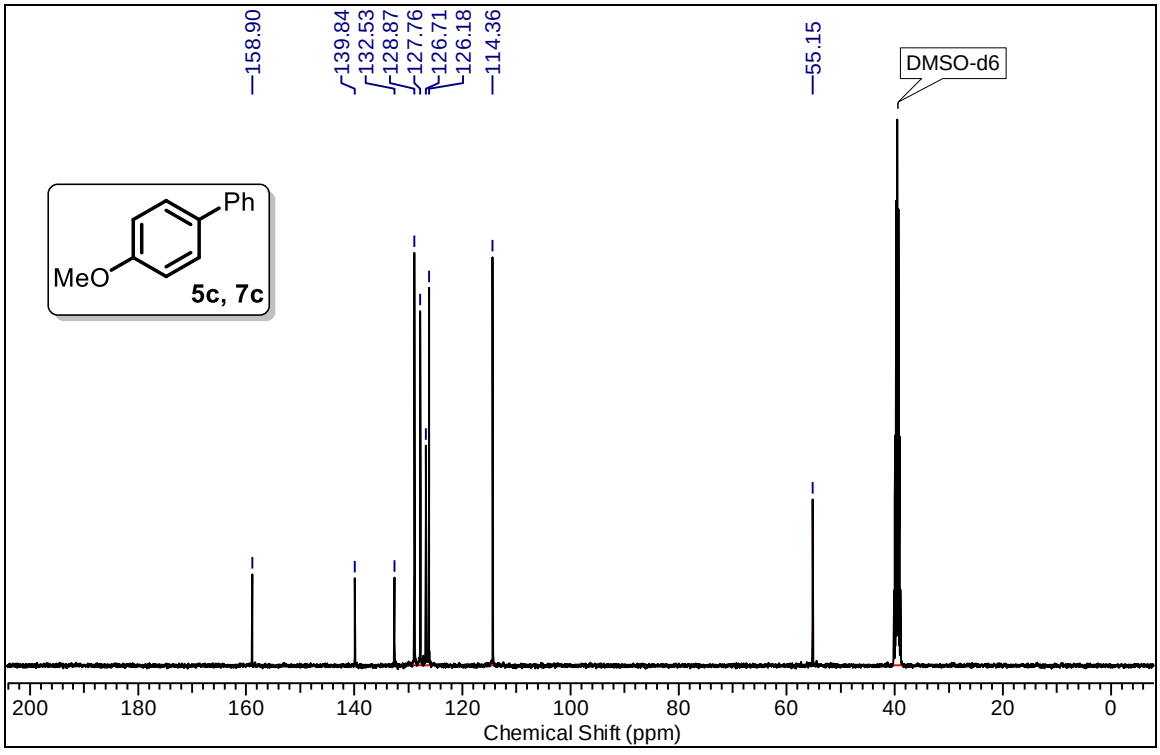

^{1}H NMR of 4-Nitro-1,1'-biphenyl (5d, 7d) (400 MHz, $CDCl_3$):

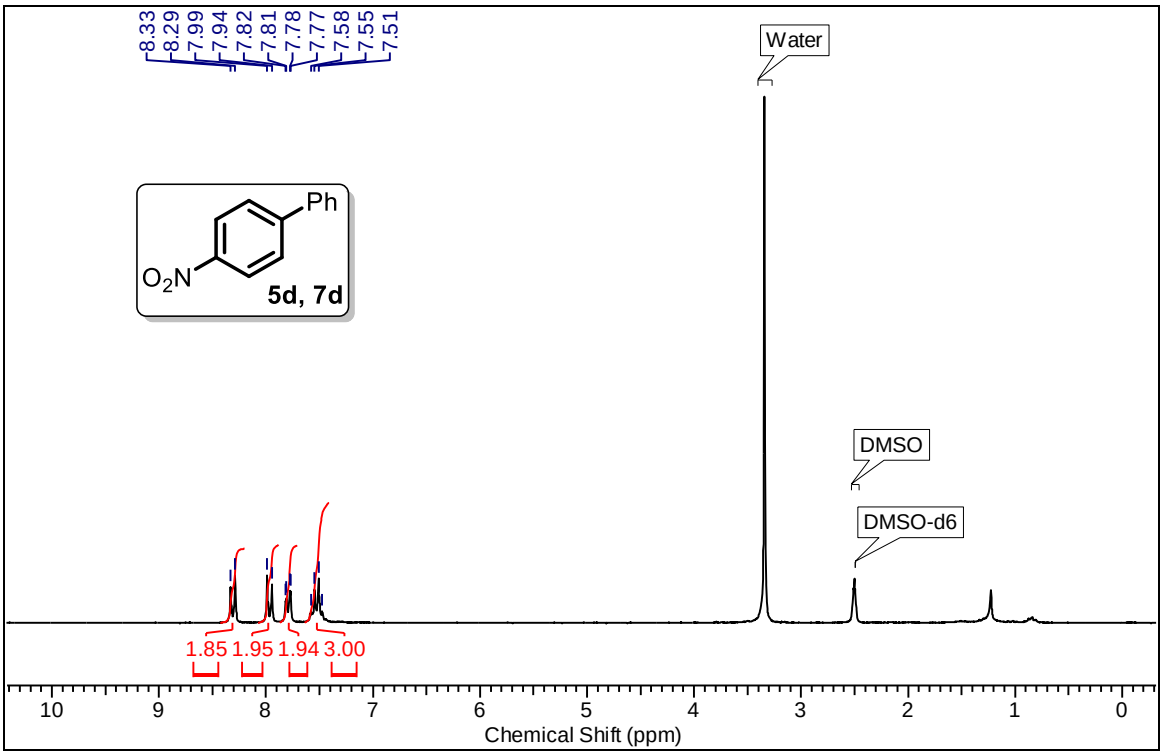

^{13}C NMR of 4-Nitro-1,1'-biphenyl (5d, 7d) (101 MHz, $CDCl_3$):

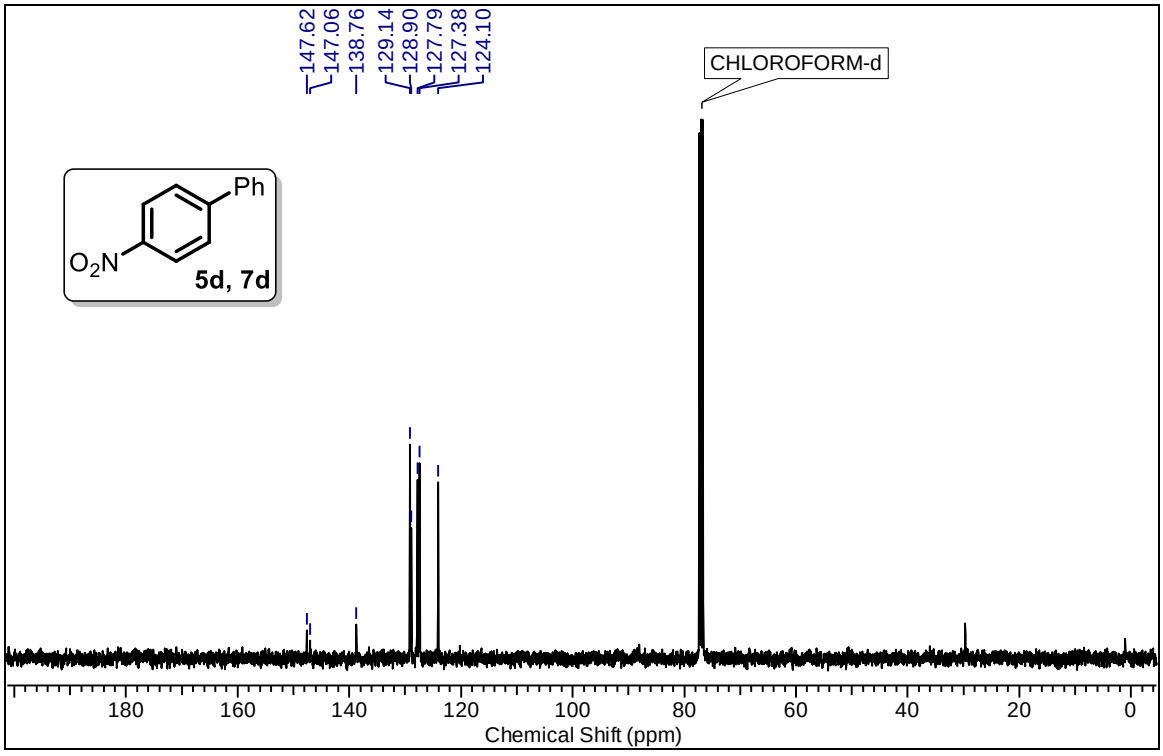

2.2.7 References:

[1] a) Lamblin, M.; Hardy, L. N.; Hierso, J. C.; Fouquet, E.; Felpinb, F. X. *Adv. Synth. Catal*. **2010**, *352*, 33-79. b) Pal, A.; Gosh, R.; Adarsh, A. A.; Sarkar, A. *Tetrahedron* **2010**, *66*, 5451-5458. c) Frisch, A. C.; Rataboul, F.; Zapf, A.; Beller, M.; *J. Organometal. Chem.* **2003**, *687*, 403-409.

[2] a) Beletskaya, I. P.; Andrei, V.; Cheprakov, A. V. *Chem. Rev.* **2000**, *100*, 3009-3066; b) Dounay, A. B.; Overman L. E. *Chem. Rev.* **2003**, *103*, 2945–2964; c) Wang, D.; Gao, S. *Org. Chem. Front.* **2014**, *1*, 556-566; d) Stanforth, S. P. *Tetrahedron* **1998**, *54*, 263-303.

[3] a) Dahan, A.; M. Portnoy, *Org. Lett.* **2003**, *5*, 1197-1200; b) Cwik, A.; Hell, Z.; Figueras, F. *Adv. Syn. Catal.* **2006**, *348*, 523-530; c) Choudary B. M.;, Madhi, S.; Chowdari, N. S.; Kantam, M. L.; Sreedhar, B. *J. Am. Chem. Soc.* **2002**, *124*, 14127-14136; d) Rostamnia, S.; Doustkhah, E. *RSC Adv.* **2014**, *4*, 28238-28248; e) Dandapat, A.; Jana, D.; De, G. *Appl. Catal. A: Gen.* **2011**, *396*, 34-39.

[4] a) Ying, J. Y.; Mehnert, C. P;. Wong, M. S. *Angew. Chem. Int. Ed.* **1999**, *38*, 56-77; b) Zhao, D.; Feng, J.; Huo, Q.; Melosh, N.; Fredrickson, G. H.; Chmelka, B. F.; Stucky, G. D. *Science* **1998**, *279*, 548-552; c) Kureshy, R. I.; Khan, A. H.; Pathak, K.; Jasra, V. *Tetrahedron Asymm.* **2005**, *16*, 3562-3569.

[5] Sharma, P.; Singh, A. P. *Catal. Sci. Technol.* **2014**, *4*, 2978-2989.

[6] Sharma, P.; Singh, A. P. *RSC Adv.* **2014**, *4*, 58467-58475.

[7] Dmitri, N.; Korolev, D. N.; Bumagin, N. A. *Tetrahedron Lett.* **2005**, *46*, 5751-5754.

[8] a) Modak, A.; Mondal, J.; Sasidharan, M.; Bhaumik, A. *Green Chem.* **2011**, *13*, 1317-1331: b) Sun, P.; Zhu, Y.; Yang, H.: Yan, H.; Lu, L.; Zhang, X. *J. Mao. Org. & Biomol. Chem.* **2012**, *10*, 4512-4515; c) Sobhani, S.; Falatooni, Z. M.; Asadi, S.: Honarmand, M. *Catal. Lett*. **2016**, *146*, 255-268.

[9] Shaikh, T.M.; Hong, F.-E. *Beilstein J. Org. Chem.* **2013**, *9*, 1578-1588.

[10] Shu, Z.; Zhou, Y.; Zhang, Y.; Wang, J. *Org. Chem. Front.* **2014**, *1*, 1123-1127

[11] McNulty, J.; Das, P. E. *J. Org Chem.* **2009**, 24, 4031-4035.

[12] a) Amini, M.; Bagherzadehi, M.; Moradishoeili Z.; Boghaei, D. *RSC Adv.* **2012**, *2*, 12091-12095; b) Huang, S.; Jia, A.; Jin, G. *Chem. Commun.* **2013**, *49*, 2403-2405.

[13] Tao, B.; Boykin, D. W. *J. Org. Chem.* **2004**, *69*, 4330-4335.

[14] Du, Z.; Zhou, W.; Wang, F.; Wang, J. *Tetrahedron* **2011**, *67*, 4914-4918.

[15] Lei, W.; Pin-Hua, L. *Chin. J. Chem.* **2006**, *24*, 770-774.

[16] Ackermann, L. A.; Kapdi, R.; Schulzke, C. *Org. Lett.* **2010**, *12*, 2298-2301.

[17] Yu, C.; Tian, B.; Fan, J.; Stucky, G. D.; Zhao, D. *J. Am. Chem. Soc.* **2002**, *124***,** 4556-4557.

[18] Lebel, H.; Davi, M. *Adv. Synth. Catal.* **2008**, *350*, 2352-2358

[19] Kutonova, K. V.; Trusova, M. E.; Stankevic, A. V.; Postnikov, P. S.; Filimonov V. D. *Beilstein J. Org. Chem.* **2015,** *11*, 358-362

[20] Moses, J. E.; Baldwin, J. E.; Brückner, S.; Eade, S. J.; Adlington R. M. *Org. Biomol. Chem.* **2003**, *1*, 3670-3684.

Chapter 3: Section A

Brønsted acid catalyzed C-C bond formation via Michael addition of Vinyl azide to *p*-Quinone methides

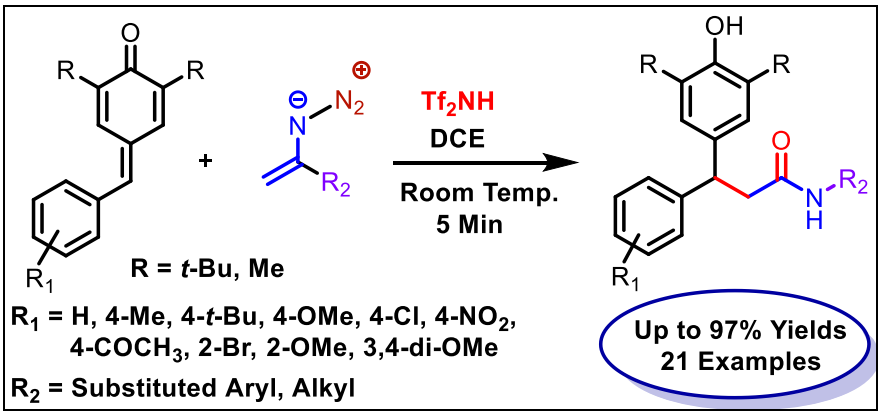

3.1.1 Introduction: *p*-Quinone Methides (*p*-QMs):

p-Quinone methides framework, containing cyclohexadiene with exocyclic methylene and a carbonyl group in extended conjugation is present in the various natural products in plant pigments and fungal metabolites (Figure 1). The diverse natural products with potent biological activities, such as a kendomycin[1] natural product with quinone core structure have anti-tumor, anti-bacterial, endothelin receptor antagonist and anti-osteoporosis agent. Celastrol[2] and Pristimerin,[3] the methyl ester of Celastrol, a triterpenoid with *p*-quinone methide core structure exhibit anti-inflammatory, antioxidant, antitumor, antiviral and contraceptive activities. Taxadone and its isomer Maytenoquinone display several important biological activities, such as anticancer,[4] antibacterial,[5] antifungal[6] and antifeedant[7] activities.

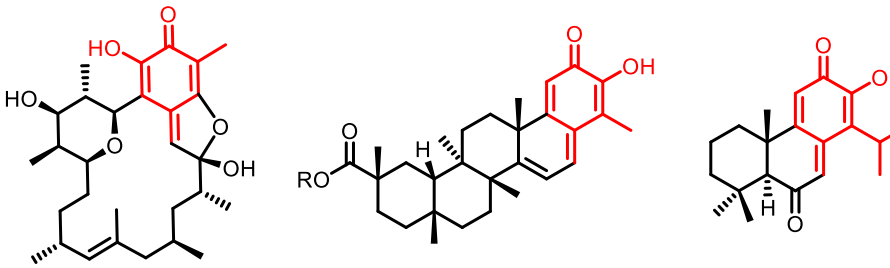

Figure 1: Representative natural products containing *p*-QMs core

Due to the presence of carbonyl group, the *p*-quinone methides structure, being polar in nature, becomes a highly reactive intermediate. Simple *p*-quinone methides are very short-lived and highly unstable so to isolate under normal circumstances is difficult, because it quickly reacts with nucleophiles and other reactants. Some structurally modified *p*-QMs have been prepared to stabilize it by inserting bulky substituents near the carbonyl group; usually when it is the *tert*-butyl group, the respective *p*-QMs become highly stable and could be used further to study the chemical property. The reactivity and thus the stability of quinone methides can be influenced by the presence of electron withdrawing or donating substituents on the ring relative to the carbonyl group.[8] Because of the additional driving force of aromatization, *p*-QMs are more reactive as compared to vinyl ketones. Hence it distinguishes all their other transformations.[9]

3.1.2 Reactivity of *p*-QMs: A literature review

Since last few years, *p*-QMs pull the attention to the organic chemist. Its unique reactivity[10] is extensively studied in the variety of organic transformations with an array of

nucleophiles.[11] *p*-Quinone methide motif serves as powerful Michael acceptors, and the 1,6-conjugate addition reactions have been profoundly explored by various group of chemists (Tortosa,[12] Lin,[13] Cui[14] , and Li[15]) using Lewis acid, organocatalytic and transition metal catalysts (Scheme 1). Fu-Sheng He and co-workers have reported the asymmetric synthesis of α-amino acid using copper-catalyzed enantioselective 1,6-addition to the *p*-QMs.[16] Anand and co-workers have thoroughly studied the addition reaction of *p*-QMs using various nucleophiles and using the variety of mode of activation such as Lewis acid, *N*-heterocyclic carbene, bis(amino) cyclopropenylidene and the transition metal as a catalyst.[17]

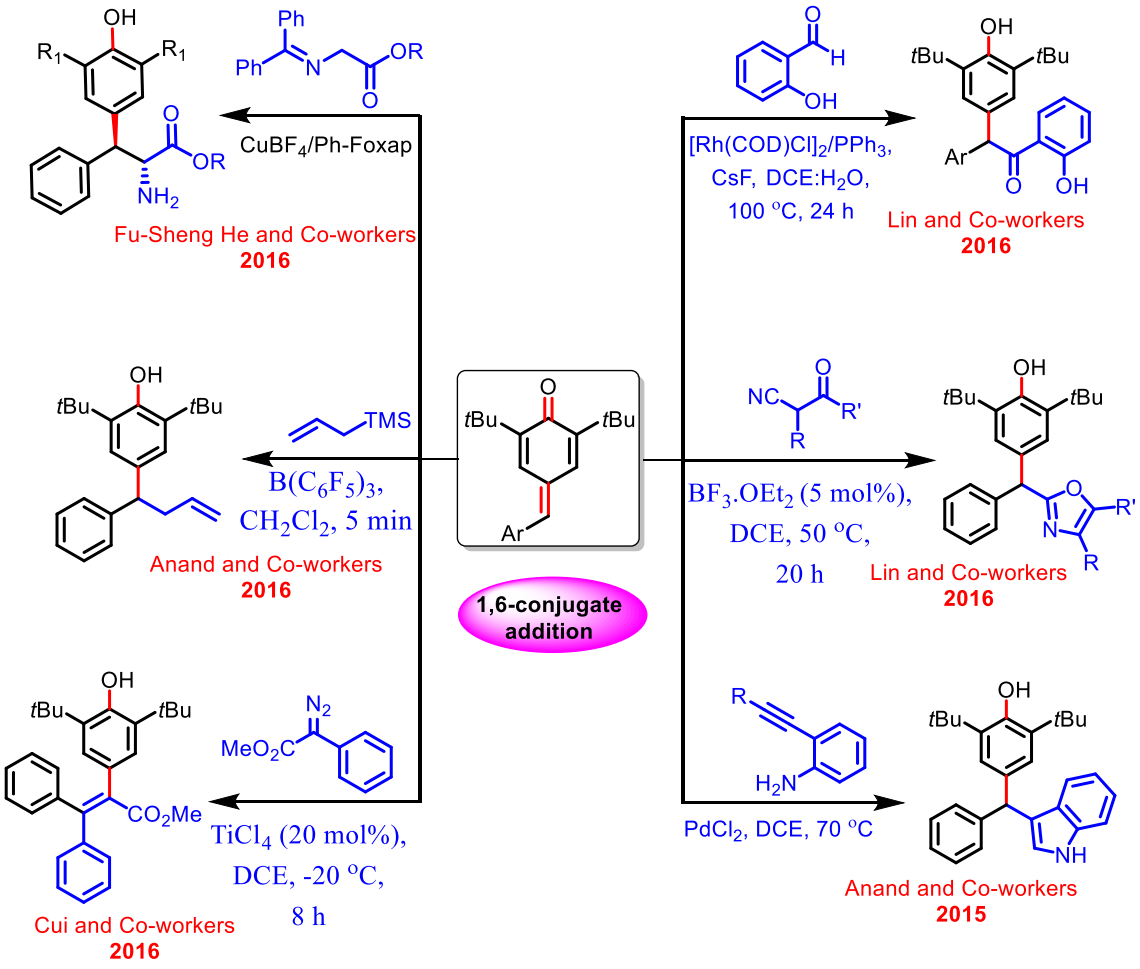

Scheme 1: Intermolecular 1,6-conjugate addition on *p*-QMs

In 2016, Lin and co-workers reported a metal-free, and Lewis acid ($BF_3.OEt_2$) catalyzed intermolecular 1,6-conjugate addition of various nucleophiles with *p*-QMs, allowing direct synthesis of unsymmetrical triarylmethanes under mild conditions. The reported protocol shows the wide range of functional-group tolerance and scalability up to gram scale (Scheme 2).[18] The same group have also studied the other series of intermolecular addition

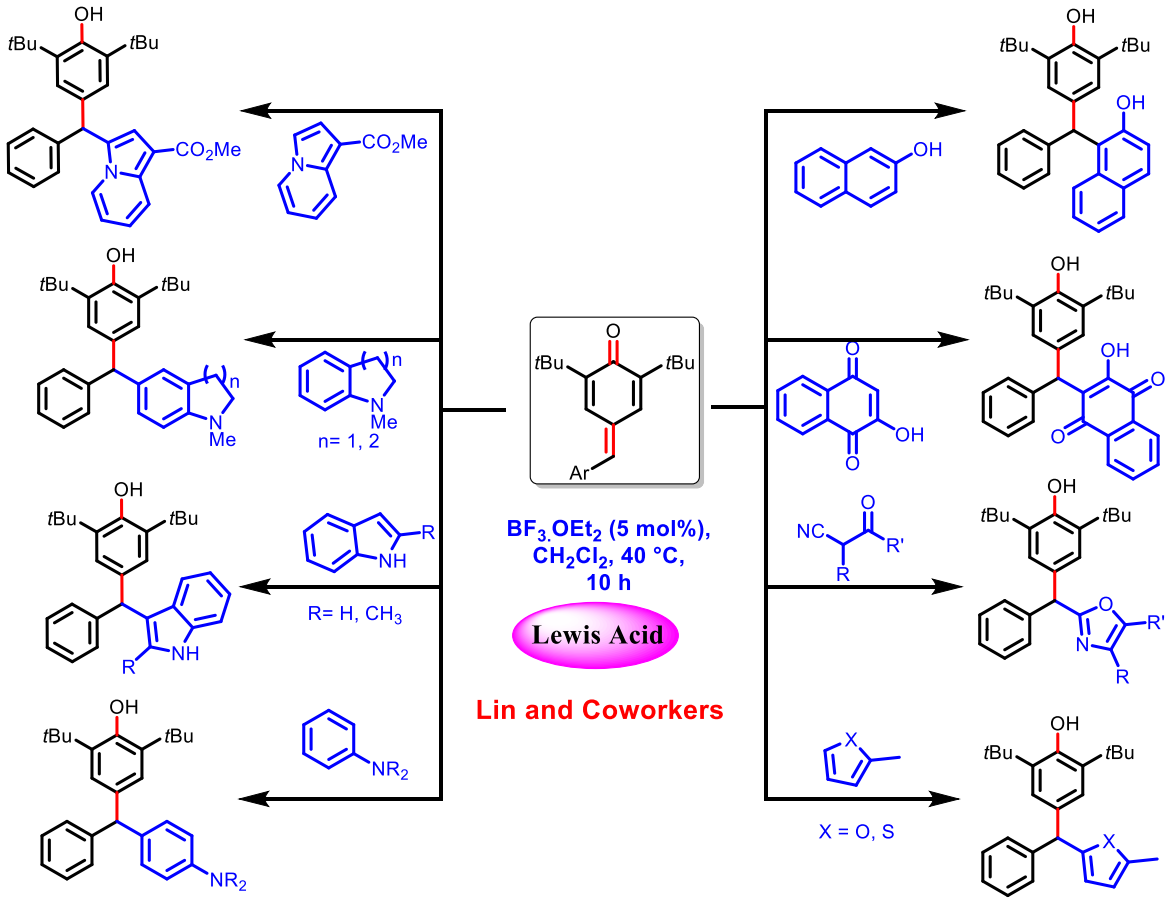

Scheme 2: $BF_3.OEt_2$ catalyzed intermolecular 1,6-nucleophilic addition

reactions and explored the significant transformations of *p*-QMs like Pd/bifunctional thiourea catalyzed [3+2] annulation of *p*-QMs and vinyl cyclopropanes to give the spiro-cycles with excellent diastereoselectivity,[19] The spiro-cycles were also constructed via

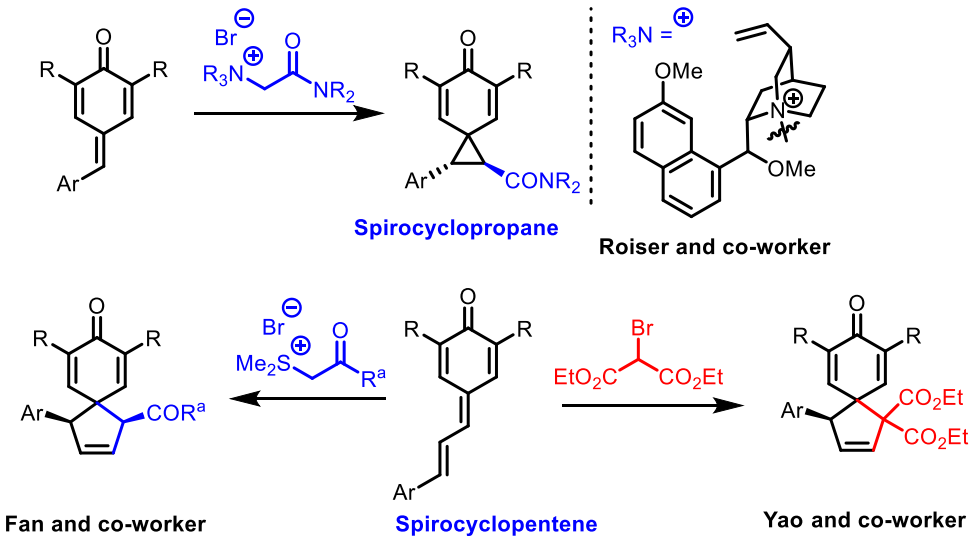

Scheme 3: [3+2] annulation of *p*-QMs to provide the spiro-cycles

tandem 1,6-addition /cyclization with *p*-QMs by Fan, Yao, and Roiser co-workers using the sulfonium salts,[20] *α*-halo diester, [21] and ammonium ylides[22] respectively (Scheme 3). Intramolecular nucleophilic addition reactions of *p*-QMs have been demonstrated by China Raju and co-worker.[23] The electron rich side chain or other heterocyclic/aromatic substituents present on the *para*-quinone methides could serve as a counter nucleophilic partner for the addition reaction as depicted in Scheme 4.

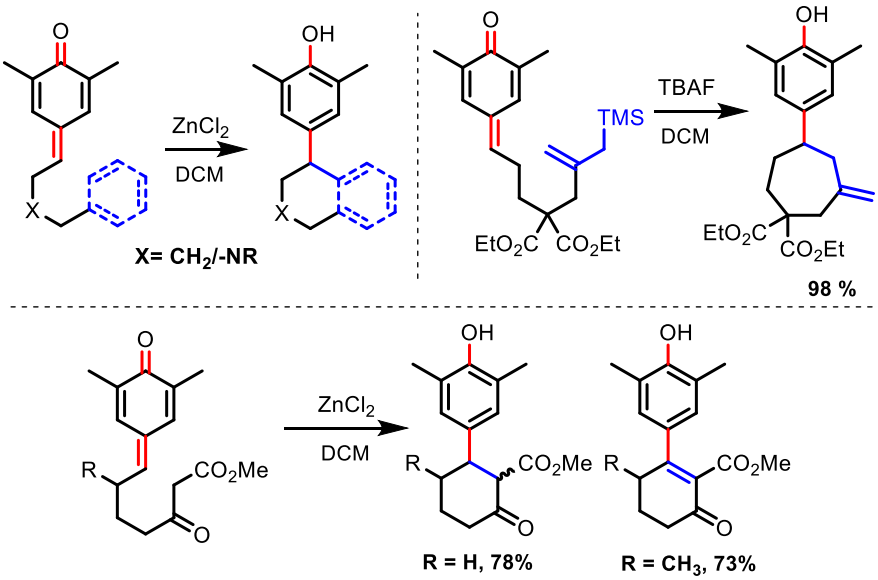

Scheme 4: Intramolecular 1,6-conjugate addition on *p*-QMs

3.1.3 Reactivity of vinyl azide: A literature review

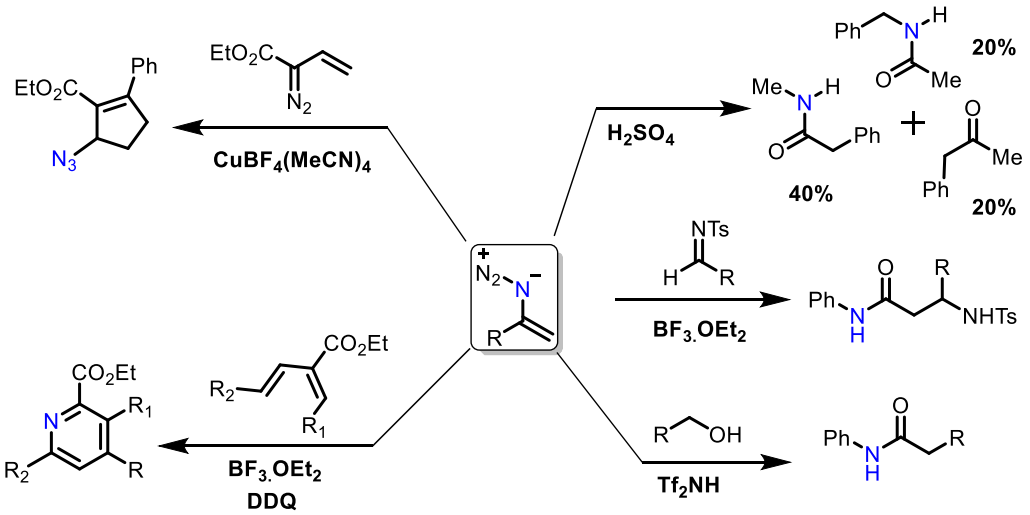

Scheme 5: Reactivity of vinyl azides

Very recently, the vinyl azide has gained the interest among synthetic chemists because of its chemical reactivity. It could serve as a good precursor for the construction of new C-C

and C-N bond for various nitrogen-containing heterocycles with metal and acid (Lewis/Brønsted) activators (Scheme 5).[24] The distinct reactivity of vinyl azide as an enamine type nucleophile[25] is known to give amide framework via Schmidt type rearrangement.[26] These reports reveal that vinyl azide could serve as an excellent nucleophilic precursor for the amide under the mild reaction conditions.

3.1.4 Present Work:

The above literature reports inspired us to explore the reactivity of *p*-QMs, and vinyl azide via acid catalyzed 1,6-conjugate addition reaction.

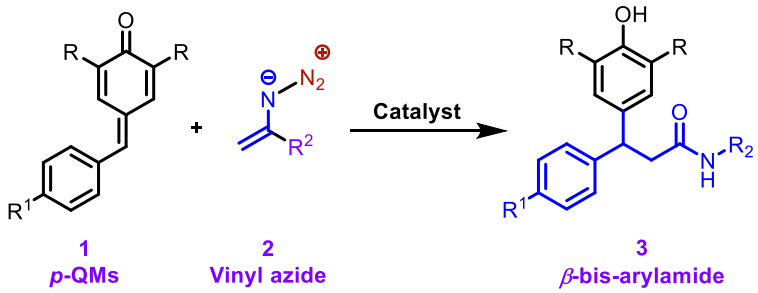

Scheme 6: Hypothesis for the 1,6-conjugate addition of vinyl azide to *p*-QMs

We envisioned that *p*-QMs could serve as good Michael acceptor for the enamine type attack of vinyl azide to deliver interesting *β*-bis-arylamide framework (Scheme 6), it is a privileged structure present in various drug molecules and natural products (Figure 2).

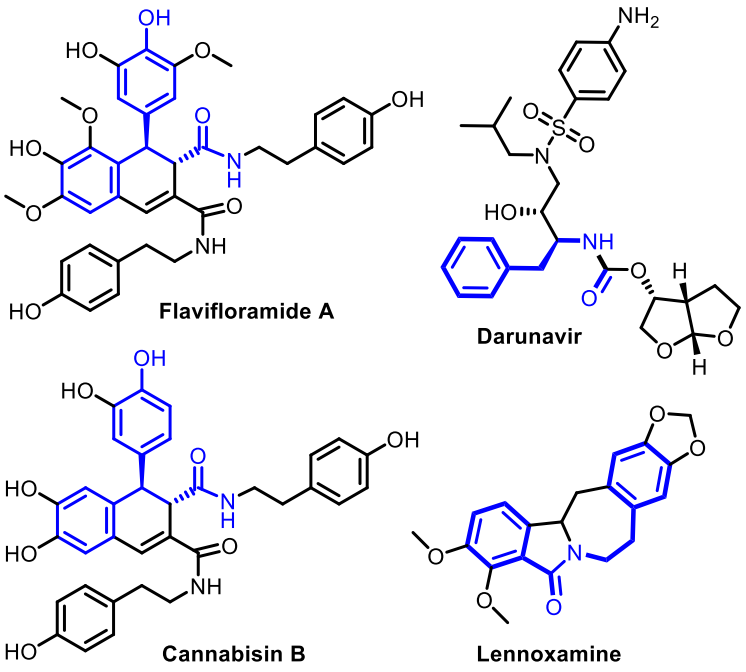

Figure 2: Privileged pharmaceutically active and naturally occurring amides

The biological importance of *β*-bis-aryl amides propelled extensive endeavor towards its synthesis and development of novel and scalable protocols. Various approaches for its synthesis have been reported in the literature;[27] nevertheless, the most of them suffer from the limitations like the application of an expensive metal catalyst, sluggish reaction progress, harsh reaction conditions, and tedious workup. Hence, the development of mild and metal-free catalytic conditions for this reaction is highly desirable.

3.1.5 Results and discussion:

3.1.5.1. Optimization of reaction conditions:

To study our hypothesis of the 1,6-addition of nucleophilic vinyl azide to the *p*-quinone methide, we began with simple *p*-QMs **1a** and phenyl vinyl azide **2a** as a model substrate and screened to find the best reaction condition. Initially, the reaction was performed with literature reported reaction conditions frequently used for the vinyl azide reactions by Chiba *et al.*[24] The 1,6-conjugate addition of phenyl vinyl azide with *p*-QMs was carried

Table 1: Optimization of 1,6-conjugate addition [a]

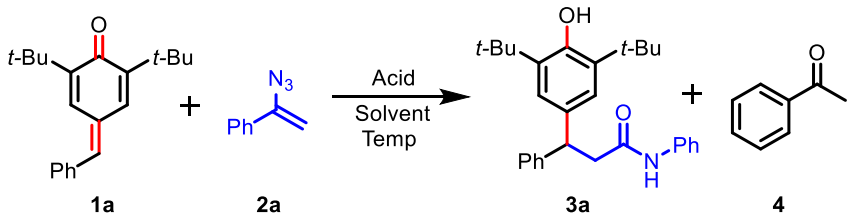

Entry	Acid	Solvent	Time	Temp °C	Yield % [b]	
					3a	**4**
1	$BF_3.OEt_2$	DCM	5h	-40	65	18
2	$BF_3.OEt_2$	DCM	5h	-30	56	25
3	$BF_3.OEt_2$	DCM	5h	0	30	63
4[c]	$BF_3.OEt_2$	DCM	2h	rt	trace	78
5[d]	$BF_3.OEt_2$	DCM	1h	rt	72	32
6[d]	Tf_2NH [e]	DCE	30 min	0	82	43
7[d]	Tf_2NH [e]	DCE	5 min	rt	89	46
8[d]	Tf_2NH [f]	DCE	5 min	rt	85	39
9[d,g]	**Tf_2NH [f]**	**DCE**	**5 min**	**rt**	**92**	**5**
10[d,g]	Tf_2NH [f]	DCE	5 min	40	66	34
11 [h]	$BF_3.OEt_2$	DCE	1h	rt	49	38

[a] Unless and otherwise stated, the reaction was performed with *p*-quinone methide (0.034 mmol, 10 mg), water (2 equiv.) $BF_3.OEt_2$ (2 equiv.) and 1 mL of DCM (dichloromethane) by slow addition of a solution of Vinyl azide **2** (2 equiv.) in DCM (2 mL). [b] Isolated yields. [c] Vinyl azide was directly added at once. [d] Addition sequence was changed, the solution of acid was added dropwise and without additive (water). [e] 2 equiv. Tf_2NH. [f] 10 mole % Tf_2NH, [g] 1.2 equiv phenyl vinyl azide was used. [h] 10 mol% $BF_3.OEt_2$, 2 equiv. H_2O and 1.2 equiv. phenyl vinyl azide was used

out in the presence of $BF_3.OEt_2$ and additive (water) in DCM at -40 °C. However, the desired product **3a** was obtained with a reasonable yield of 65% (Table-1, entry-1) with several other by-products such as acetophenone and acetanilide. The main drawback of this condition was the very slow addition (around 5h) of vinyl azide solution at the lower temperature (-40°C). Further, to optimize the conditions, the reaction was performed by varying the reaction temperature, When the temperature was increased up to -30 °C, the yield of product **3a** dropped to 56 % (Table-1, entry-2) with the increase in the formation of by-product. The yield diminished to 30 % when the temperature of the reaction was increased 0°C, and because of self-decomposition of vinyl azide in the acidic medium, the acetophenone was obtained as a major by-product (table-1 entry-3). At room temperature, the desired product **3a** was found only in trace amount and acetophenone obtained as the major product (Table-1, entry 4). From these results, we envisioned that, in the presence of excess acid in the reaction mixture, the self-hydrolysis reaction of phenyl vinyl azide is competing with the addition reaction with *p*-QMs at the higher temperature. In order to rectify these limitations, the reaction was performed by changing the addition order of $BF_3.OEt_2$ and phenyl vinyl azide **2a,** hence, *p*-quinone methide, vinyl azide, and two equivalent water were taken in DCM and the $BF_3.OEt_2$ was added dropwise at room temperature. Delightfully, the obtained results were as per expectation, affording the desired product **3a** in good yield (72 %) only in 1h, and with by-product acetophenone due to self-decomposition of vinyl azide (Table-1 entry-5). Further to improve the reaction conditions we switched over to the application of Brønsted acid triflimide (Tf_2NH) as an activator for *p*-QMs and vinyl azide. Gratifyingly, when Tf_2NH was used in place of $BF_3.OEt_2$ at 0 °C, the reaction was completed within 30 min, and smoothly delivered the desired product **3a** in excellent yield (82 %) (Table-1, entry-6). When the temperature was increased to rt, the reaction time drastically decreased to 5 min as confirmed by TLC. As per literature precedence,[28] the reaction was examined for the catalytic amount of Tf_2NH. The 10 mol % Tf_2NH was found sufficient to elicit the proposed transformation within 5 min at rt and afforded the desired product in excellent yield (89%) (Table-1, entry-7). To

reduce the formation of other by-products, next, we optimized for the amount of vinyl azide used in the reaction. The excess vinyl azide was decomposed to acetophenone. The best-optimized reaction condition was that when 10 mol% triflimide as a catalyst with a little excess of vinyl azide (1.2 equiv) has delivered the anticipated product **3a** in 92% yield with the only little amount of side product (Table-1, entry-9). The compound **3a** was obtained as a white solid with melting point 194-196 °C, and ^{1}H and ^{13}C NMR spectroscopy analysis unambiguously characterized the structure of **3a**. The proton NMR showed the characteristic signals for all the functional group present on the core structure like singlet at δ 1.39 ppm with 18 hydrogen represents the presence of the two *tert*-butyl groups in the compound. Triplet and doublet signals at δ 4.51 and 3.06 ppm represent one benzylic CH group adjacent to carbonyl CH_2 respectively. The singlet at δ 6.81 and 5.12 ppm represent the presence of –NH and –OH functional group. In proton decoupled carbon NMR, the compound **3a** shows the seventeen different signals in accordance with the proposed structure. Further, the elemental formula was confirmed by the high resolution mass spectrometric analysis; the obtained data are in accordance with the literature report.[29] Further, to investigate the effect of temperature, the reaction was performed at 40°C, the yield of **3a** was diminished to 66%, and the rate of competing reaction for the formation of acetophenone was increased (Table-1, entry-10). Another reaction was performed with catalytic $BF_3.OEt_2$ (10 mol %), the yield of the desired product **3a** was diminished to 49% with an increase in the formation of by-product in considerable amount (Table-1, entry-11).

3.1.5.2. The scope of *p*-QMs for the addition reaction

After having the best-optimized condition in hand, next to prove the generality we have scrutinized the developed condition by varying the functional group of *p*-QMs and vinyl azide, the scope of the reaction is illustrated in Table 2. First, the array of substituted *p*-quinone methides was screened for the scope of reactions. 4-Substituted *p*-QMs **1a-o** smoothly delivered the respective β-bis arylamide **3a-o** on reaction with phenyl vinyl azide **2a** regardless of the electronic nature of substituents (electron donating or withdrawing) in good to excellent yield. The optimized condition is compatible with the variety of functional groups, like electron donating such as methyl, *t*-butyl, methoxy and electron withdrawing groups chloro, bromo, nitro, ester, the respective product was obtained in excellent yields 83-93% (**3a-j**).

Table 2: Substrate scope of *p*-QMs for 1,6-conjugate addition

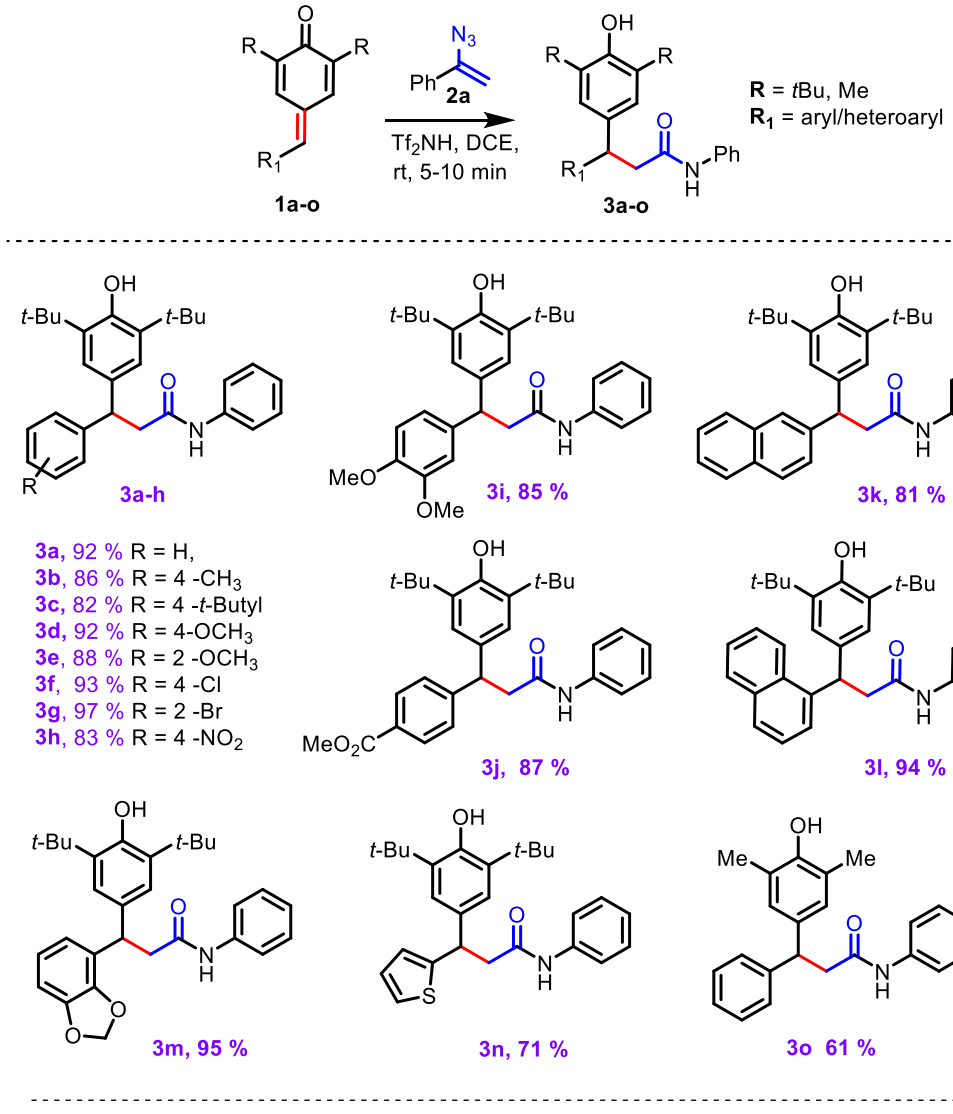

Reaction condition; **1** (0.030 – 0.055 mmol), **2** (1.2 equiv.), Tf_2NH (10 mol %), 2 mL DCE, rt, 5 min, Yields refer to isolated pure product**.**

Moreover, the *ortho*, *meta* and polysubstituted phenyl ring of *p*-QMs was found to be quite amenable under the reaction condition (**3e, 3f, and 3h**). Furthermore, the *p*-quinone methide containing the fused aromatic and heterocyclic moieties like 1- and 2-naphthyl, benzodioxole, and thiophene **3k-n** respectively were also well tolerated under the optimized reaction conditions (yields **71-97**%). *p*-QMs with R = methyl group in place of *t*-butyl group on the quinone ring, (highly unstable *p*-QMs) also smoothly reacted with phenyl vinyl azide and delivered the respective product **3o** in moderate yield (61%).

3.1.5.3. The scope of vinyl azide for the addition reaction

Besides, to study the generality of developed reaction, various phenyl vinyl azides were also screened under the reaction condition.

Table 3: Substrate scope of vinyl azide for 1,6-conjugate addition

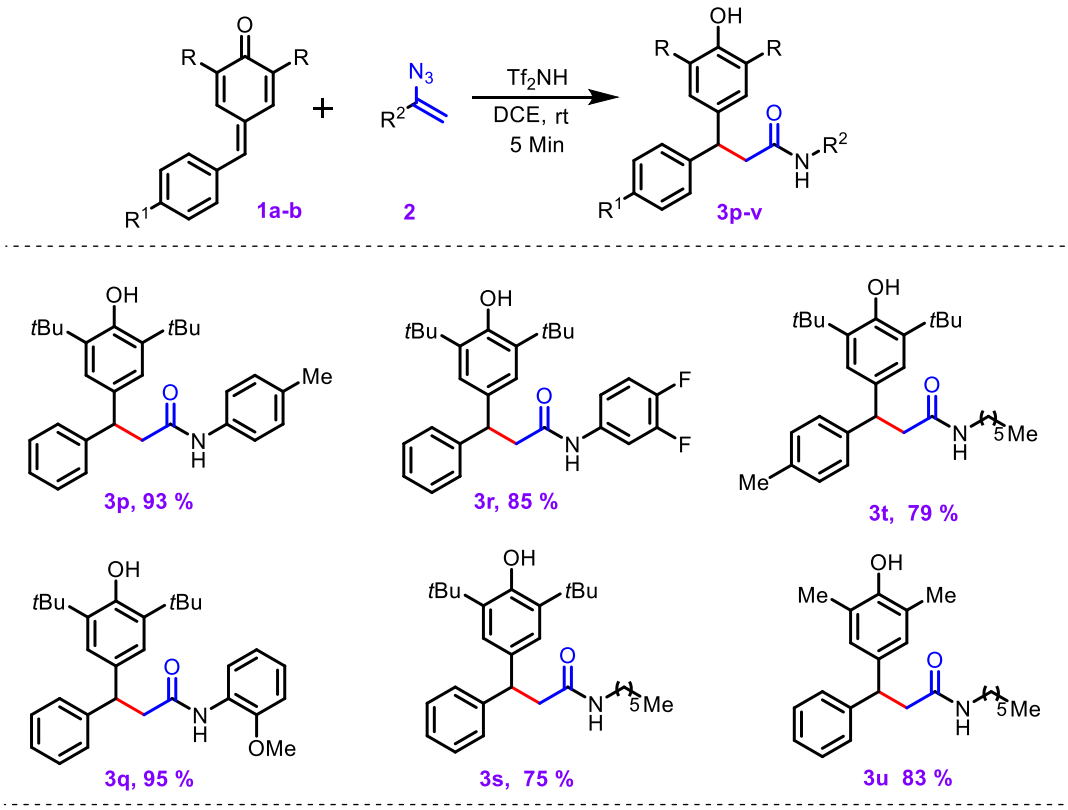

As shown in Table 3 the phenyl vinyl azides with the substitution on the phenyl ring as 4-methyl, 2-methoxy, and 3,4-difluoro group, smoothly reacted with the simple *p*-QMs and afforded the desired products **3p-r** in excellent yield (85-95%). Further to establish the generality of the method, the reaction was performed using alkyl vinyl azide with both the *p*-QMs (R= *t*-Bu or Me), to get the products **3s-u** in good to excellent yields, (75-83%).

3.1.5.4 Synthetic utility of the method: De-*tert*-butylation of *β-bis*-arylamides

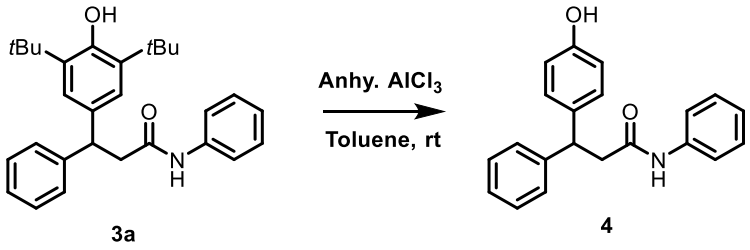

Scheme 7: De-*tert*-butylation of *β*-Bis-arylamides

To demonstrate the synthetic efficacy of this method the product *β-bis*-arylamides was subjected to the retro Friedel-Crafts de-*tert*-butylation (Scheme 6). The compound **3a** was treated with anhy. $AlCl_3$ in toluene, the two *tert*-butyl groups, were removed from the compound **3a** furnishing the desired phenol **4** in excellent yield. The phenolic compound **4** represents the core structure of a privileged pharmaceutically active and naturally occurring motif.

3.1.5.5 Plausible mechanism for the formation of *β*-bis-arylamides

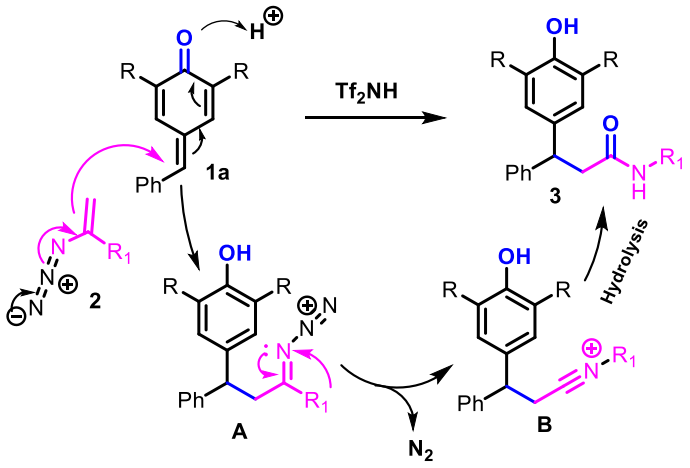

Figure 3: Plausible mechanism for the formation of *β*-bis-arylamides

The plausible reaction mechanism was illustrated from the recent literature report (Figure 3). The *p*-QMs could be activated by hydrogen ion of Tf_2NH followed by 1,6-attack of nucleophilic vinyl azide **2**, forms the intermediate A, which undergoes Schmidt rearrangement to furnish the nitrilium ion intermediate B. Subsequent hydrolysis would afford the desired product **3**.

3.1.6 Conclusions

In conclusion, we have established the efficient protocol for the Tf_2NH catalyzed 1,6-conjugate addition of vinyl azide to the Michael acceptor *p*-quinone methide to afford the *β*-bis-arylamides. The developed method is catalytic, highly efficient with regard to yields, reaction time and substrate scope. Further studies to explore the Michael acceptor property of *p*-quinone methide with other substrate are underway in our laboratory.

3.1.7 Experimentals:

3.1.7.1 Synthetic Procedure for vinyl azide [30]

To a solution of phenylacetylene (1.6 mL, 15 mmol), TMS-N_3 (3.4 mL, 30 mmol) and H_2O (0.5 mL, 30 mmol) in DMSO (25 mL) at 80 ^oC, Ag_2CO_3 (0.4 gm, 3 mmol) was added. The reaction mixture was then stirred for 1 h (until completely consumed phenyl acetylene monitored by TLC). Then the reaction mixture was extracted with dichloromethane (3 × 25 mL). The organic layer was washed with brine (3 × 60 mL), dried over anhydrous Na_2SO_4 and concentrated under reduced pressure. The crude product was purified by column chromatography (silica gel 100-200 mesh; 100 % pet ether) and concentrated in vacuo to afford vinyl azide in 75 % yield as a yellow liquid.

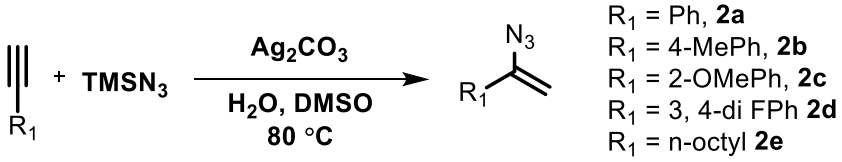

3.1.7.2 Synthesis of *p*-Quinone Methide [31]

In an oven dried Dean-Stark apparatus, phenol (25.0 mmol) and the corresponding aldehyde (25.0 mmol) were taken in toluene (100 mL), the reaction mixture was heated to reflux followed by dropwise addition of piperidine (50.0 mmol, 4.94 mL) within one hour. Then, the reaction mixture was continued to reflux for next 3 hours. After cooling just below the boiling point of the reaction mixture, acetic anhydride (50.0 mmol, 2.55 g) was added, and stirring was continued for 15 min. Then the reaction mixture was poured on ice-water (500 mL) and extracted with DCM (4 × 200 mL). The combined organic phase was dried over anhydrous Na_2SO_4, and the solvent was evaporated under reduced pressure.

Table 4: Synthesis of various *p*-QMs:

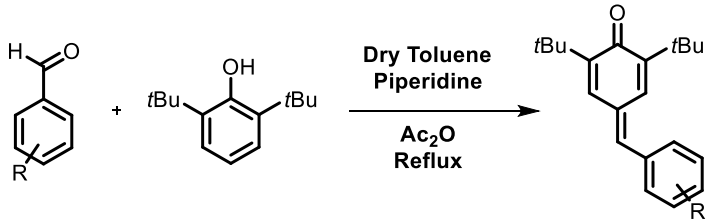

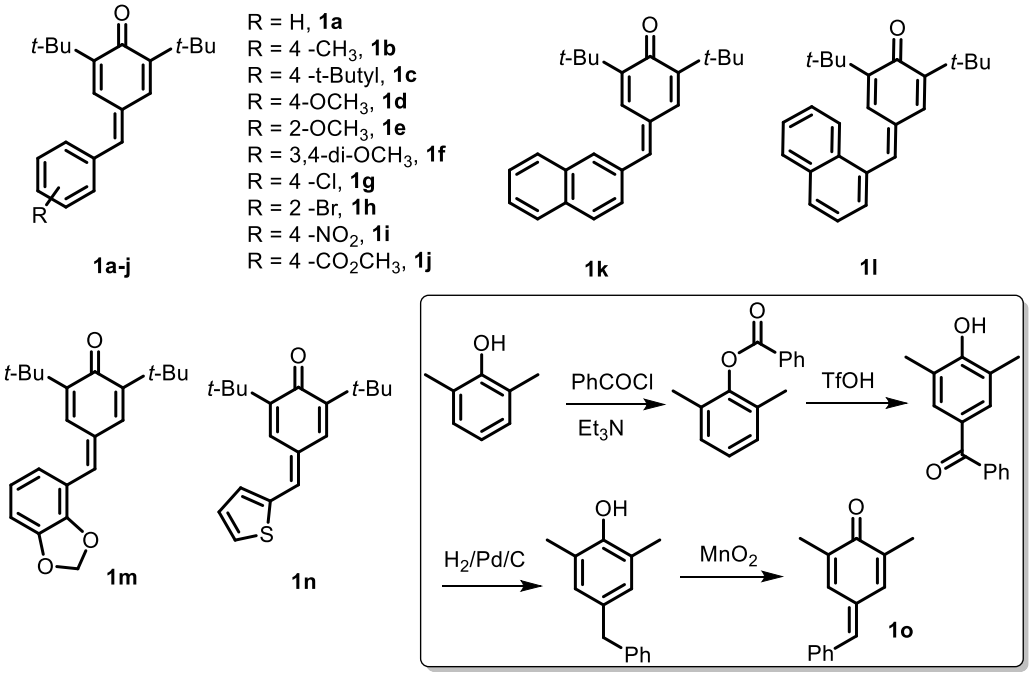

The crude products were purified by column chromatography and further recrystallized from n-hexane, affording *p*-quinone methide in good yields. Compound **1o** was prepared according to literature report.[12]

3.1.7.3 General experimental Procedure for the synthesis of amide

The *p*-quinone methide **1** (0.030 – 0.055 mmol, 15 mg), phenyl vinyl azide **2** (1.2 equiv.) in 1 ml of DCE were taken into the oven dried 5 ml reaction vials with a magnetic bar. Then, 10 mole % triflimide (Tf_2NH) dissolved in 0.5 ml of DCE was added dropwise, and the reaction mixture stirred at room temperature for 5 min. The completion of the reaction was confirmed by the thin layer chromatography using 9:1 pet ether: ethyl acetate solvent system. The starting material *p*-quinone methide was completely consumed within 5 min. After the completion of the reaction, the reaction mass was concentrated under the high vacuum, and the crude product was purified by column chromatography on silica gel 100-200 mesh to obtain the product as white solid.

3.1.7.4 Characterization data of the synthesized compounds:

3-(3,5-Di-*tert*-butyl-4-hydroxyphenyl)-*N*,3-diphenylpropanamide (3a):[29]

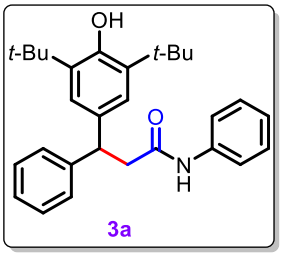

White solid; mp = 194-196 °C (reported mp = 193−195 °C); ***Rf*** = 0.32 (1:9 EtOAc : Pet ether);

^{1}H NMR (500MHz , $CDCl_3$) δ = 7.32 (app. d, J = 4.6 Hz, 4 H), 7.23 (m, 5 H), 7.08 (s, 2 H), 7.07 - 7.02 (m, 1 H), 6.81 (s, 1 H), 5.12 (s, 1 H), 4.51 (t, J = 7.6 Hz, 1 H), 3.06 (d, J = 7.6 Hz, 2 H), 1.39 ppm (s, 18 H);

^{13}C NMR (125MHz, $CDCl_3$) δ = 169.7, 152.5, 143.9, 137.6, 136.1, 133.9, 128.8, 128.7, 127.7, 126.5, 124.2, 124.2, 119.8, 47.7, 45.3, 34.4, 30.2 ppm;

HRMS (FTMS + p ESI): m/z $[M+H]^+$ calcd for $C_{29}H_{36}O_2N$; 430.2742; found: 430.2741.

3-(3,5-Di-*tert*-butyl-4-hydroxyphenyl)-*N*-phenyl-3-(*p*-tolyl)propanamide (3b):[29]

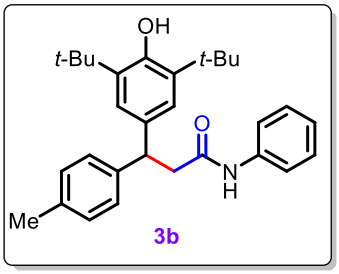

White solid; mp = 208-210 °C (reported mp = 211−213 °C); ***Rf*** = 0.30 (1:9 EtOAc: Pet ether);

^{1}H NMR (500MHz , $CDCl_3$) δ = 7.26 - 7.22 (m, 4 H), 7.21 (d, J = 8.0 Hz, 2 H), 7.13 (d, J = 7.6 Hz, 2 H), 7.08 (s, 2 H), 7.07 - 7.03 (m, 1 H), 6.79 (s, 1 H), 5.11 (s, 1 H), 4.46 (t, J = 7.6 Hz, 1 H), 3.04 (d, J = 7.6 Hz, 2 H), 2.32 (s, 3 H), 1.39 ppm (s, 18 H);

^{13}C NMR (125MHz, $CDCl_3$) δ = 169.8, 152.4, 140.9, 137.7, 136.1, 134.1, 129.4, 128.8, 127.5, 124.2, 124.1, 119.7, 47.4, 45.4, 34.4, 30.3, 21.0 ppm;

HRMS (FTMS + p ESI): m/z $[M+H]^+$ calcd for $C_{30}H_{38}O_2N$; 444.2897; found: 444.2899.

3-(4-(*Tert*-butyl)phenyl)-3-(3,5-di-*tert*-butyl-4-hydroxyphenyl)-*N*-phenylpropanamide (3c):

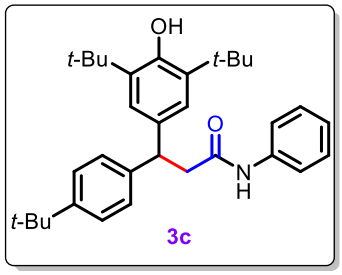

Colourless thick liquid; ***Rf*** =0.33 (1:9 EtOAc: Pet ether);

^{1}H NMR (400MHz, $CDCl_3$) δ = 7.34 (app. d, *J* = 7.9 Hz, 2 H), 7.27 - 7.20 (m, 4 H), 7.20 - 7.15 (m, 2 H), 7.11 (s, 2 H), 7.04 (t, *J* = 6.7 Hz, 1 H), 6.72 (s, 1 H), 5.12 (s, 1 H), 4.45 (t, *J* = 7.6 Hz, 1 H), 3.05 (d, *J* = 7.9 Hz, 2 H), 1.40 (s, 18 H), 1.30 ppm (s, 9 H);

^{13}C NMR (100MHz, $CDCl_3$) δ = 169.9, 152.5, 149.3, 140.8, 137.6, 136.1, 134.0, 128.8, 127.2, 125.6, 124.2, 124.1, 119.7, 47.5, 45.5, 34.4, 31.3, 30.3 ppm;

HRMS (FTMS + p ESI): m/z $[M+H]^+$ calcd for $C_{33}H_{44}O_2N$; 486.3367; found: 486.3367.

3-(3,5-Di-*tert*-butyl-4-hydroxyphenyl)-3-(4-methoxyphenyl)-*N*-phenylpropanamide (3d):[29]

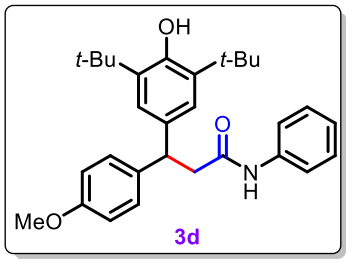

White solid; mp = 190-192 °C (reported mp = 191−192 °C); ***Rf*** = 0.46 (1: 4 EtOAc: Pet ether);

^{1}H NMR (500MHz, $CDCl_3$) δ = 7.26 - 7.18 (m, 6 H), 7.07 (s, 2 H), 7.06 - 7.03 (m, 1 H), 6.86 (d, *J* = 8.4 Hz, 2 H), 6.83 - 6.78 (m, 1 H), 5.11 (s, 1 H), 4.46 (t, *J* = 7.6 Hz, 1 H), 3.79 (s, 3 H), 3.02 (d, *J* = 7.6 Hz, 2 H), 1.39 ppm (s, 18 H);

^{13}C NMR (125MHz, $CDCl_3$) δ = 169.8, 158.2, 152.4, 137.7, 136.1, 136.0, 134.3, 128.8, 128.6, 124.1, 119.7, 114.0, 55.2, 46.9, 45.5, 34.4, 30.3 ppm;

HRMS (FTMS + p ESI): m/z $[M+H]^+$ calcd for $C_{30}H_{38}O_3N$; 460.2846; found: 460.2845.

3-(3,5-Di-*tert*-butyl-4-hydroxyphenyl)-3-(2-methoxyphenyl)-*N*-phenylpropanamide (3e):

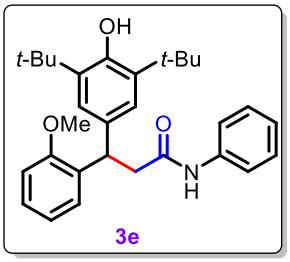

Colourless thick liquid; ***Rf*** = 0.43 (1: 4 EtOAc: Pet ether);

^{1}H NMR (400MHz, $CDCl_3$) δ = 7.26 - 7.18 (m, 5 H), 7.26 - 7.18 (m, 1 H), 7.16 (s, 2 H), 7.08 - 7.01 (m, 1 H), 6.99 (s, 1 H), 6.94 (t, *J* = 7.9 Hz, 1 H), 6.88 (d, *J* = 7.9 Hz, 1 H), 5.10 (s, 1 H), 4.86 (t, *J* = 7.6 Hz, 1 H), 3.84 (s, 3 H), 3.16 – 3.03 (m, 2 H), 1.40 ppm (s, 18 H);

^{13}C NMR (100MHz, $CDCl_3$) δ = 170.1, 156.7, 152.4, 135.9, 133.4, 132.2, 128.8, 128.0, 127.6, 124.5, 124.0, 120.8, 119.6, 110.9, 55.5, 44.0, 41.1, 34.4, 30.3 ppm;

HRMS (FTMS + p ESI): m/z $[M+H]^+$ calcd for $C_{30}H_{38}O_3N$; 460.2846; found: 460.2837.

3-(4-Chlorophenyl)-3-(3,5-di-*tert*-butyl-4-hydroxyphenyl)-*N*-phenylpropanamide (3f):[29]

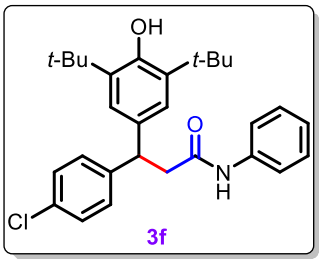

White solid; mp = 216-218 °C (reported mp = 213− 215 °C); ***Rf*** = 0.20 (1: 9 EtOAc: Pet ether);

^{1}H NMR (500MHz, $CDCl_3$) δ =7.31 - 7.21 (m, 8 H), 7.10 - 7.05 (m, 1 H), 7.03 (s, 2 H), 6.85 (s, 1 H), 5.14 (s, 1 H), 4.52 (t, *J* = 7.6 Hz, 1 H), 3.06 - 2.96 (m, 2 H), 1.39 ppm (s, 18 H);

^{13}C NMR (125MHz, $CDCl_3$) δ = 169.3, 152.6, 142.5, 137.5, 136.2, 133.5, 132.2, 129.0, 128.9, 128.7, 124.3, 124.1, 119.8, 46.9, 45.0, 34.4, 30.2 ppm;

HRMS (FTMS + p ESI): m/z $[M+H]^+$ calcd for $C_{29}H_{35}O_2NCl$; 464.2351; found: 464.2351.

3-(2-Bromophenyl)-3-(3,5-di-*tert*-butyl-4-hydroxyphenyl)-*N*-phenylpropanamide (3g):

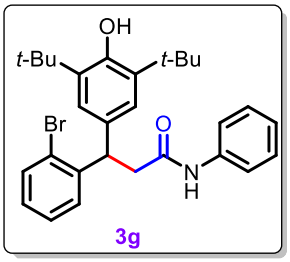

White solid; mp = 226-228 °C ; ***Rf*** = 0.26 (1: 9 EtOAc: Pet ether);

^{1}H NMR (400MHz, $CDCl_3$) δ = 7.57 (d, *J* = 7.9 Hz, 1 H), 7.38 - 7.21 (m, 6 H), 7.15 (s, 2 H), 7.09 - 7.04 (m, 2 H), 6.95 (s, 1 H), 5.13 (s, 1 H), 5.00 (t, *J* = 7.6 Hz, 1 H), 3.09 (d, *J* = 7.9 Hz, 2 H), 1.39 ppm (s, 18 H);

^{13}C NMR (100MHz, $CDCl_3$) δ = 169.1, 152.6, 142.9, 137.6, 136.1, 133.4, 132.2, 128.9, 128.1, 128.0, 127.7, 124.9, 124.5, 124.2, 119.7, 46.0, 44.2, 34.4, 30.3 ppm;

HRMS (FTMS + p ESI): m/z $[M+H]^+$ calcd for $C_{29}H_{35}O_2NBr$; 508.1846; found: 508.1847.

3-(3,5-Di-*tert*-butyl-4-hydroxyphenyl)-3-(4-nitrophenyl)-*N*-phenylpropanamide (3h):[29]

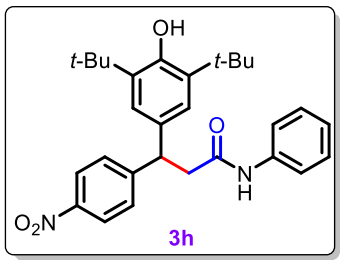

White solid; mp = 216-218 °C (reported mp = 108− 110 °C); ***Rf*** = 0.20 (1: 9 EtOAc: Pet ether);

^{1}H NMR (500MHz, $CDCl_3$) δ = 8.13 (d, *J* = 8.4 Hz, 2 H), 7.44 (d, *J* = 8.0 Hz, 2 H), 7.29 (br. s., 1 H), 7.27 - 7.17 (m, 3 H), 7.05 (t, *J* = 7.1 Hz, 1 H), 6.99 (s, 2 H), 6.94 (s, 1 H), 5.14 (s, 1 H), 4.66 (t, *J* = 7.4 Hz, 1 H), 3.04 (d, *J* = 7.2 Hz, 2 H), 1.35 ppm (s, 18 H);

^{13}C NMR (125MHz, $CDCl_3$) δ = 168.7, 152.8, 151.7, 146.5, 137.4, 136.5, 132.5, 129.0, 128.6, 124.5, 124.2, 123.8, 119.8, 47.1, 44.3, 34.4, 30.2 ppm;

HRMS (FTMS + p ESI): m/z $[M+H]^+$ calcd for $C_{29}H_{35}O_4N_2$; 475.2591; found: 475.2590.

3-(3,5-Di-*tert*-butyl-4-hydroxyphenyl)-3-(3,4-dimethoxyphenyl)-*N*-phenylpropanamide (3i):

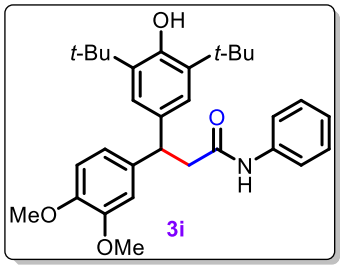

Colourless thick liquid; ***Rf*** = 0.60 (1: 1 EtOAc: Pet ether);

^{1}H NMR (500MHz, $CDCl_3$) δ = 7.25 (app. d, *J* = 4.2 Hz, 4 H), 7.09 (s, 2 H), 7.07 - 7.02 (m, 1 H), 6.88 - 6.77 (m, 4 H), 5.12 (s, 1 H), 4.46 (t, *J* = 7.4 Hz, 1 H), 3.86 (s, 3 H), 3.83 (s, 3 H), 3.02 (d, *J* = 7.6 Hz, 2 H), 1.40 ppm (s, 18 H);

^{13}C NMR (125MHz, $CDCl_3$) δ = 169.8, 152.5, 148.9, 147.7, 137.6, 136.5, 136.1, 134.0, 128.9, 124.2, 124.2, 119.7, 119.4, 111.4, 111.3, 55.9, 55.8, 47.3, 45.7, 34.4, 30.3 ppm;

HRMS (FTMS + p ESI): m/z $[M+H]^+$ calcd for $C_{31}H_{40}O_4N$; 490.2952; found: 490.2953.

Methyl 4-(1-(3,5-di-*tert*-butyl-4-hydroxyphenyl)-3-oxo-3-(phenylamino)propyl) benzoate (3j):[29]

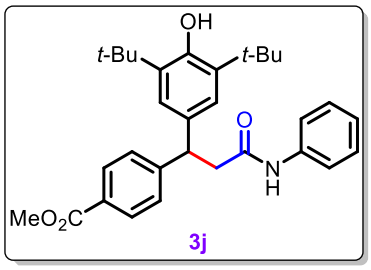

White solid; mp = 200-202 °C (reported mp=197−198 °C); ***Rf*** =0.20 (1: 9 EtOAc: Pet ether);

^{1}H NMR (400MHz, $CDCl_3$) δ = 7.99 (d, *J* = 7.9 Hz, 2 H), 7.39 (d, *J* = 7.9 Hz, 2 H), 7.30 - 7.20 (m, 6 H), 7.12 - 7.05 (m, 1 H), 7.04 (s, 2 H), 6.90 (s, 1 H), 5.14 (s, 1 H), 4.61 (t, *J* = 7.3 Hz, 1 H), 3.90 (s, 3 H), 3.06 (d, *J* = 7.9 Hz, 2 H), 1.38 ppm (s, 18 H);

^{13}C NMR (100MHz, $CDCl_3$) δ = 169.2, 167.0, 152.6, 149.3, 137.5, 136.2, 133.2, 129.9, 128.9, 128.3, 127.8, 124.3, 124.2, 119.8, 52.0, 47.5, 44.7, 34.4, 30.2 ppm;

HRMS (FTMS + p ESI): m/z $[M+H]^+$ calcd for $C_{31}H_{38}O_4N$; 488.2795; found: 488.2796.

3-(3,5-Di-*tert*-butyl-4-hydroxyphenyl)-3-(naphthalen-2-yl)-*N*-phenylpropanamide (3k):

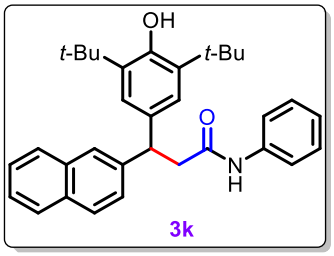

White solid; mp = 228-230 °C (reported mp = 230− 231 °C); ***Rf*** = 0.30 (1: 9 EtOAc: Pet ether);

^{1}H NMR (500MHz, $CDCl_3$) δ = 7.84 - 7.73 (m, 4 H), 7.51 - 7.40 (m, 3 H), 7.21 (app. s., 4 H), 7.13 (s, 2 H), 7.08 - 7.00 (m, 1 H), 6.83 (s, 1 H), 5.13 (s, 1 H), 4.69 (t, *J* = 7.6 Hz, 1 H), 3.21 - 3.09 (m, 2 H), 1.39 ppm (s, 18 H);

^{13}C NMR (125MHz, $CDCl_3$) δ = 169.7, 152.5, 141.4, 137.6, 136.2, 133.8, 133.5, 132.3, 128.8, 128.3, 127.8, 127.6, 126.4, 126.0, 125.8, 125.6, 124.3, 124.2, 119.8, 47.7, 45.1, 34.4, 30.3 ppm;

HRMS (FTMS + p ESI): m/z $[M+H]^+$ calcd for $C_{33}H_{38}O_2N$; 480.2897; found: 480.2897.

3-(3,5-Di-*tert*-butyl-4-hydroxyphenyl)-3-(naphthalen-1-yl)-*N*-phenylpropanamide (3l):

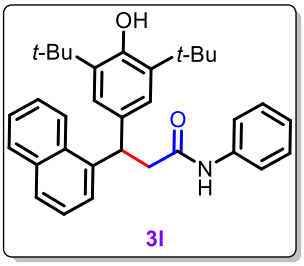

Thick colourless liquid; ***Rf*** = 0.30 (1: 9 EtOAc: Pet ether);

^{1}H NMR (500MHz, $CDCl_3$) δ = 8.25 (d, *J* = 8.4 Hz, 1 H), 7.86 (d, *J* = 7.6 Hz, 1 H), 7.76 (d, *J* = 7.6 Hz, 1 H), 7.51 - 7.43 (m, 4 H), 7.23 (app. d, *J* = 4.2 Hz, 3 H), 7.15 (s, 2 H), 7.09 - 7.01 (m, 1 H), 6.84 (s, 1 H), 5.41 - 5.30 (m, 1 H), 5.09 (s, 1 H), 3.26 - 3.08 (m, 2 H), 1.35 ppm (s, 18 H);

^{13}C NMR (125MHz, $CDCl_3$) δ = 169.9, 152.4, 139.7, 137.6, 136.1, 134.1, 133.5, 131.5, 128.8, 128.8, 127.3, 126.2, 125.5, 125.3, 124.4, 124.1, 123.9, 123.9, 119.7, 45.5, 43.0, 34.3, 30.2 ppm;

HRMS (FTMS + p ESI): m/z $[M+H]^+$ calcd for $C_{33}H_{38}O_2N$; 480.2897; found: 480.2899.

3-(Benzo[d][1,3]dioxol-4-yl)-3-(3,5-di-*tert*-butyl-4-hydroxyphenyl)-*N*-phenylpropanamide (3m):

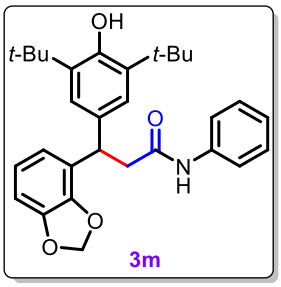

Thick colourless liquid; ***Rf*** =0.42 (1: 4 EtOAc: Pet ether);

^{1}H NMR (500MHz, $CDCl_3$) δ = 7.29 - 7.23 (m, 4 H), 7.06 (s, 3 H), 6.85 (s, 1 H), 6.82 - 6.72 (m, 3 H), 5.92 (app. d, J = 2.7 Hz, 2 H), 5.12 (s, 1 H), 4.44 (t, J = 7.6 Hz, 1 H), 3.00 (d, J = 8.0 Hz, 2 H), 1.40 ppm (s, 18 H);

^{13}C NMR (125MHz, $CDCl_3$) δ = 169.6, 152.5, 147.8, 146.1, 137.9, 137.6, 136.1, 134.1, 128.9, 124.2, 124.0, 120.5, 119.8, 108.3, 108.2, 100.9, 47.3, 45.3, 34.4, 30.3 ppm;

HRMS (FTMS + p ESI): m/z $[M+H]^+$ calcd for $C_{30}H_{36}O_4N$; 474.2637; found: 474.2637.

3-(3,5-Di-*tert*-butyl-4-hydroxyphenyl)-*N*-phenyl-3-(thiophen-2-yl)propanamide (3n):[29]

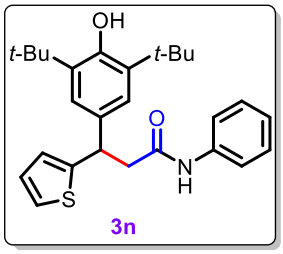

White solid; mp = 170-172 °C (reported mp = 172−175 °C); ***Rf*** = 0.20 (1: 9 EtOAc: Pet ether);

^{1}H NMR (400MHz, $CDCl_3$) δ = 7.26 (app. s., 4 H), 7.18 (app. d, J = 4.3 Hz, 1 H), 7.15 (s, 2 H), 7.07 (br. s., 1 H), 6.99 - 6.88 (m, 2 H), 6.82 (s, 1 H), 5.15 (s, 1 H), 4.76 (t, J = 7.3 Hz, 1 H), 3.13 - 2.95 (m, 2 H), 1.41 ppm (s, 18 H);

^{13}C NMR (100MHz, $CDCl_3$) δ = 169.1, 152.8, 148.0, 137.6, 136.2, 133.6, 128.9, 126.8, 124.6, 124.3, 124.1, 123.9, 119.8, 47.1, 43.6, 34.4, 30.3 ppm;

HRMS (FTMS + p ESI): m/z $[M+H]^+$ calcd for $C_{27}H_{34}O_2NS$; 436.2305; found: 436.2304.

3-(4-Hydroxy-3,5-dimethylphenyl)-*N*,3-diphenylpropanamide(3o):

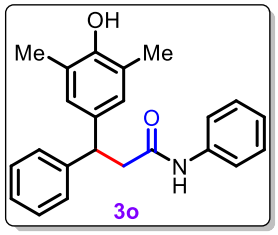

Colourless thick liquid; ***Rf*** = 0.38 (1:2 EtOAc: Pet ether);

^{1}H NMR (400MHz, $CDCl_3$) δ = 7.35 - 7.26 (m, 6 H), 7.23 (app. d, J = 7.9 Hz, 3 H), 7.07 (br. s., 1 H), 6.92 (br. s., 1 H), 6.89 (s, 2 H), 4.63 (br. s., 1 H), 4.50 (t, J = 7.6 Hz, 1 H), 3.04 (d, J = 7.3 Hz, 2 H), 2.20 ppm (s, 6 H);

^{13}C NMR (125MHz, $CDCl_3$) δ = 169.6, 150.9, 144.1, 137.5, 135.0, 128.8, 128.7, 127.8, 127.6, 126.5, 124.3, 123.3, 120.0, 46.8, 44.6, 16.0 ppm;

HRMS (FTMS + p ESI): m/z $[M+H]^+$ calcd for $C_{23}H_{24}NO_2$; 346.1802; found: 346.1798.

3-(3,5-Di-*tert*-butyl-4-hydroxyphenyl)-3-phenyl-*N*-(*p*-tolyl)propanamide (3p):

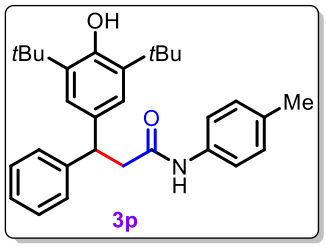

Colourless thick liquid; ***Rf*** = 0.50 (1: 4 EtOAc: Pet ether);

^{1}H NMR (500MHz, $CDCl_3$) δ = 7.32 (app. d, J = 4.2 Hz, 4 H), 7.24 - 7.19 (m, 1 H), 7.10 (d, J = 8.4 Hz, 2 H), 7.08 (s, 2H), 7.04 (d, J = 8.4 Hz, 2 H), 6.72 (s, 1 H), 5.11 (s, 1 H), 4.51 (t, J = 7.6 Hz, 1 H), 3.04 (d, J = 7.6 Hz, 2 H), 2.28 (s, 3 H), 1.39 ppm (s, 18 H);

^{13}C NMR (125MHz, $CDCl_3$) δ = 169.6, 152.5, 144.0, 136.1, 135.1, 134.0, 133.8, 129.3, 128.7, 127.7, 126.5, 124.2, 119.9, 47.7, 45.2, 34.4, 30.3, 20.8 ppm;

HRMS (FTMS + p ESI): m/z $[M+H]^+$ calcd for $C_{30}H_{38}O_2N$; 444.2897; found: 444.2898.

3-(3,5-Di-*tert*-butyl-4-hydroxyphenyl)-*N*-(2-methoxyphenyl)-3-phenylpropanamide (3q):

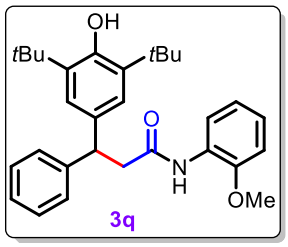

Colourless liquid; ***Rf*** = 0.50 (1: 4 EtOAc: Pet ether);

^{1}H NMR (500MHz, $CDCl_3$) δ = 8.32 (d, *J* = 8.0 Hz, 1 H), 7.57 (s, 1 H), 7.36 - 7.28 (m, 4 H), 7.22 - 7.19 (m, 1 H), 7.06 (s, 2 H), 6.99 (t, *J* = 7.2 Hz, 1 H), 6.92 (t, *J* = 7.4 Hz, 1 H), 6.80 (d, *J* = 8.0 Hz, 1 H), 5.06 (s, 1 H), 4.56 (t, *J* = 7.6 Hz, 1 H), 3.76 (s, 3 H), 3.16 - 3.01 (m, 2 H), 1.38 ppm (s, 18 H);

^{13}C NMR (125MHz, $CDCl_3$) δ = 169.5, 152.3, 147.6, 144.1, 135.8, 134.2, 128.5, 127.8, 127.6, 126.3, 124.2, 123.4, 121.0, 119.7, 109.8, 55.6, 47.5, 45.4, 34.3, 30.2 ppm;

HRMS (FTMS + p ESI): m/z $[M+H]^+$ calcd for $C_{30}H_{38}O_2N$; 460.2846; found: 460.2838.

3-(3,5-Di-*tert*-butyl-4-hydroxyphenyl)-*N*-(3,4-difluorophenyl)-3-phenylpropanamide (3r):

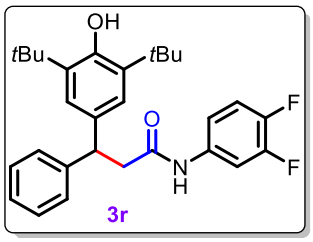

Colourless thick liquid; ***Rf*** =0.30 (1: 9 EtOAc: Pet ether);

^{1}H NMR (500MHz, $CDCl_3$) δ = 7.39 - 7.28 (m, 5 H), 7.26 - 7.20 (m, 1 H), 7.07 (s, 2 H), 7.00 (q, *J* = 8.9 Hz, 1 H), 6.76 - 6.66 (m, 2 H), 5.13 (s, 1 H), 4.48 (t, *J* = 7.8 Hz, 1 H), 3.04 (d, *J* = 7.6 Hz, 2 H), 1.39 ppm (s, 18 H);

^{13}C NMR (125MHz, $CDCl_3$) δ = 170.0, 152.8, 151.2, 143.9, 136.5, 134.3, 134.0, 129.0, 127.9, 126.9, 125.6, 124.4, 117.3 (d, $J_{C\text{-}F}$ = 19.1 Hz), 115.5, 109.8 (d, $J_{C\text{-}F}$ = 21.9 Hz), 48.0, 45.4, 34.7, 30.5 ppm;

HRMS (FTMS+p ESI): m/z $[M+H]^+$ calcd for $C_{29}H_{34}O_2NF_2$; 466.2552; found: 466.2556.

3-(3,5-Di-*tert*-butyl-4-hydroxyphenyl)-*N*-hexyl-3-phenylpropanamide (3s):

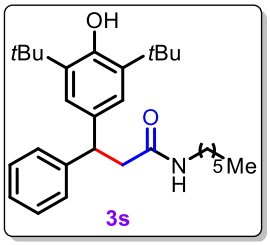

Colourless thick liquid; ***Rf*** =0.34 (1: 5 EtOAc: Pet ether);

^{1}H NMR (500MHz , $CDCl_3$) δ = 7.35 - 7.27 (m, 4 H), 7.22 - 7.18 (m, 1 H), 7.05 (s, 2 H), 5.16 (br. s., 1 H), 5.09 (s, 1 H), 4.44 (t, *J* = 7.8 Hz, 1 H), 3.17 - 3.00 (m, 2 H), 2.92 - 2.81

(m, 2 H), 1.41 (s, 18 H), 1.27 - 1.14 (m, 6 H), 1.13 - 1.06 (m, 2 H), 0.87 ppm (t, *J* = 7.1 Hz, 3 H)

^{13}C NMR (125MHz, $CDCl_3$) δ = 171.3, 152.3, 144.1, 135.8, 134.2, 128.5, 127.7, 126.3, 124.2, 47.7, 44.3, 39.4, 34.4, 31.4, 30.3, 29.3, 26.3, 22.5, 14.0 ppm;

HRMS (FTMS + p ESI): m/z $[M+H]^+$ calcd for $C_{29}H_{44}NO_2$; 438.3367; found: 438.3363.

3-(3,5-Di-*tert*-butyl-4-hydroxyphenyl)-*N*-hexyl-3-(*p*-tolyl)propanamide (3t):

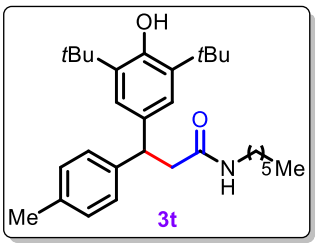

Colourless thick liquid; ***Rf*** = 0.40 (1: 5 EtOAc: Pet ether);

^{1}H NMR (500MHz, $CDCl_3$) δ = 7.21 - 7.13 (m, 2 H), 7.13 - 7.07 (m, 2 H), 7.04 (s, 2 H), 5.17 (br. s., 1 H), 5.07 (s, 1 H), 4.38 (t, *J* = 7.8 Hz, 1 H), 3.16 - 3.00 (m, 2 H), 2.91 - 2.78 (m, 2 H), 2.31 (s, 3 H), 1.40 (s, 18 H), 1.26 - 1.15 (m, 6 H), 1.12 - 1.05 (m, 2 H), 0.86 ppm (t, *J* = 7.1 Hz, 3 H)

^{13}C NMR (100MHz, $CDCl_3$) δ = 171.4, 152.2, 141.1, 135.8, 135.8, 134.4, 129.2, 127.5, 124.1, 47.4, 44.3, 39.4, 34.3, 31.4, 30.3, 29.3, 26.3, 22.4, 20.9, 14.0

HRMS (FTMS + p ESI): m/z $[M+H]^+$ calcd for $C_{30}H_{46}NO_2$; 452.3523; found: 452.3522.

***N*-Hexyl-3-(4-hydroxy-3,5-dimethylphenyl)-3-phenylpropanamide (3u):**

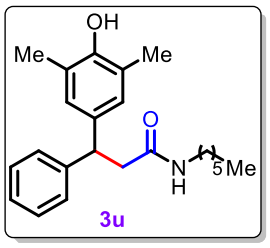

Colourless thick liquid; ***Rf*** =0.45 (1: 2 EtOAc: Pet ether);

^{1}H NMR (500MHz, $CDCl_3$) δ = 7.27 (app. d, *J* = 7.2 Hz, 2 H), 7.25 - 7.21 (m, 2 H), 7.20 - 7.15 (m, 1 H), 6.84 (s, 2 H), 5.18 (br. s., 1 H), 4.60 (br. s., 1 H), 4.40 (t, *J* = 7.8 Hz, 1 H), 3.17 - 3.02 (m, 2 H), 2.83 (d, *J* = 8.0 Hz, 2 H), 2.20 (s, 6 H), 1.29 - 1.13 (m, 8 H), 1.11 - 1.04 (m, 2 H), 0.87 ppm (t, *J* = 7.2 Hz, 3 H);

^{13}C NMR (125MHz, $CDCl_3$) δ = 171.2, 150.8, 144.3, 135.2, 128.5, 127.8, 127.6, 126.3, 123.0, 46.8, 43.8, 39.4, 31.4, 29.4, 26.3, 22.5, 16.0, 14.0 ppm;

HRMS (FTMS + p ESI): m/z $[M+H]^+$ calcd for $C_{23}H_{32}NO_2$; 354.2428; found: 354.2428.

General experimental Procedure for the de-*tert*-butylation of β-Bis-arylamides

In the oven dried 50 ml RBF, the compound **3a** was taken in 10 ml of dried toluene followed by addition of anhy. $AlCl_3$ at once, under the Argon atmosphere. The reaction mixture was stirred at room temperature until the completion of reaction. The reaction mixture was cooled to 0^oC and the ice water was added to quench the $AlCl_3$, extracted with ethyl acetate (15 ml X 3), combined organic layer was dried with anhy, Na_2SO_4 and concentrated under reduced pressure followed by column chromatography purification to give the desired productc.

3-(4-Hydroxyphenyl)-*N*,3-diphenylpropanamide (4a):

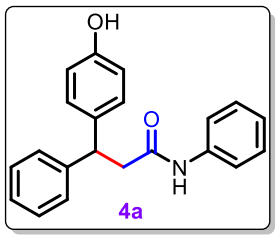

Colourless thick liquid; ***Rf*** = 0.20 (1: 2 EtOAc: Pet ether);

^{1}H NMR (500MHz, DMSO-d_6) δ = 9.95 (s, 1 H), 9.28 (br. s., 1 H), 7.52 - 7.42 (m, J = 8.0 Hz, 2 H), 7.32 - 7.18 (m, 6 H), 7.18 - 7.03 (m, 3 H), 6.99 (app. t, *J* = 7.2 Hz, 1 H),

6.71 - 6.60 (m, *J* = 8.0 Hz, 2 H), 4.45 (t, *J* = 8.0 Hz, 1 H), 3.01 ppm (d, *J* = 8.0 Hz, 2 H);

^{13}C NMR (125MHz, DMSO-d6) δ = 169.5, 155.7, 145.0, 139.2, 134.6, 128.8, 128.6, 128.5, 127.6, 126.2, 123.3, 119.2, 115.3, 46.1, 42.6 ppm;

HRMS (FTMS + p ESI): m/z $[M+Na]^+$ calcd for $C_{21}H_{19}NO_2Na$; 340.1308; found: 340.1301.

3.1.8 Selected NMR Spectra:

^{1}H NMR of 3-(3,5-Di-*tert*-butyl-4-hydroxyphenyl)-*N*,3-diphenylpropanamide (3a) ($CDCl_3$, 500MHz):

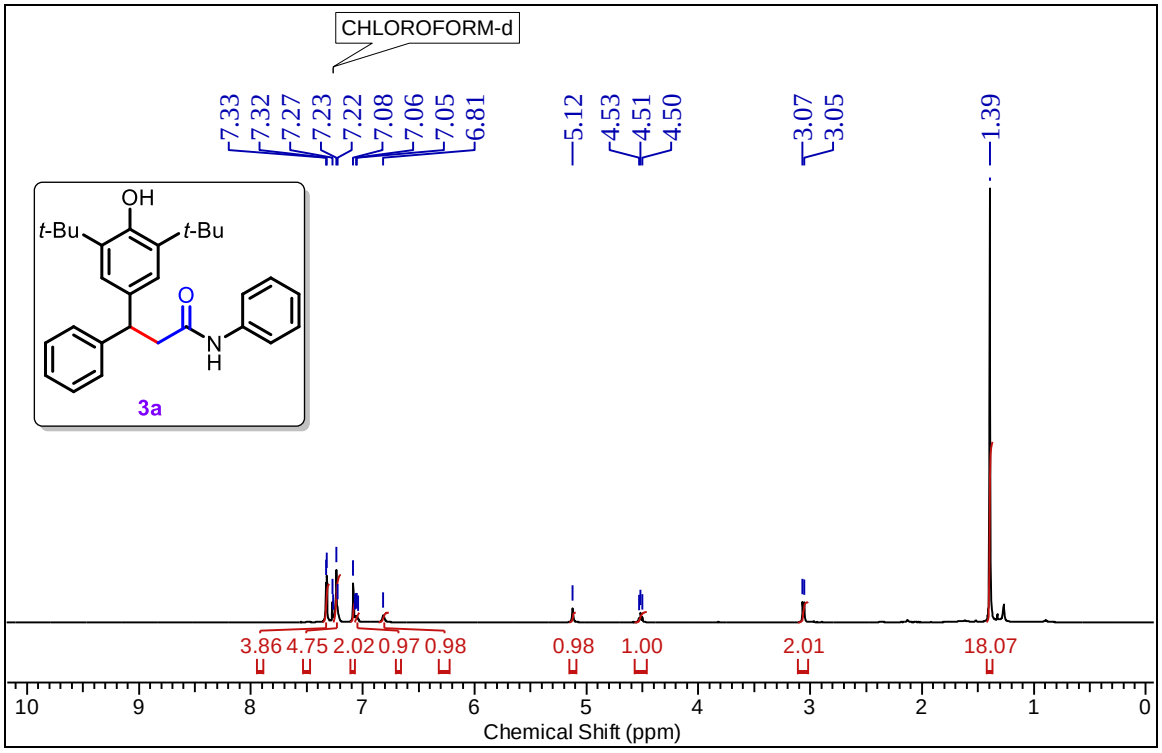

^{13}C NMR of 3-(3,5-Di-*tert*-butyl-4-hydroxyphenyl)-*N*,3-diphenylpropanamide (3a) ($CDCl_3$, 125MHz)

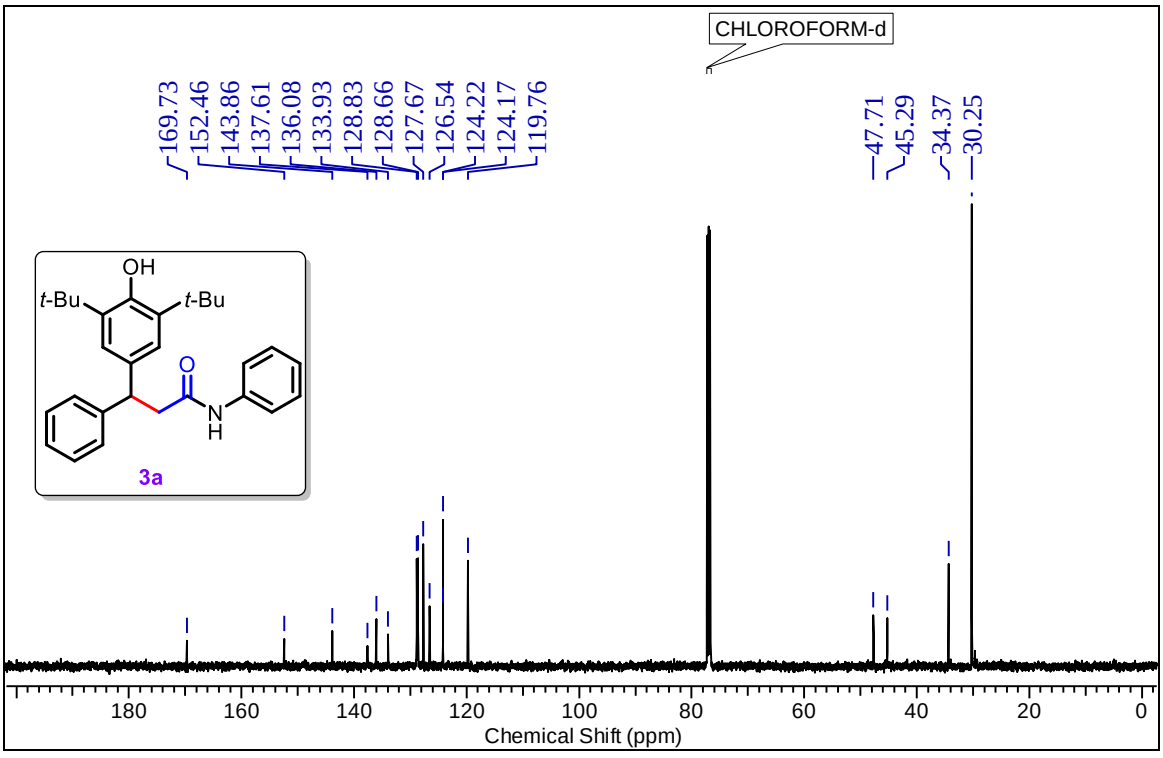

^{1}H NMR of 3-(3,5-Di-*tert*-butyl-4-hydroxyphenyl)-*N*-phenyl-3-(*p*-tolyl)propanamide (3b) (500MHz , $CDCl_3$):

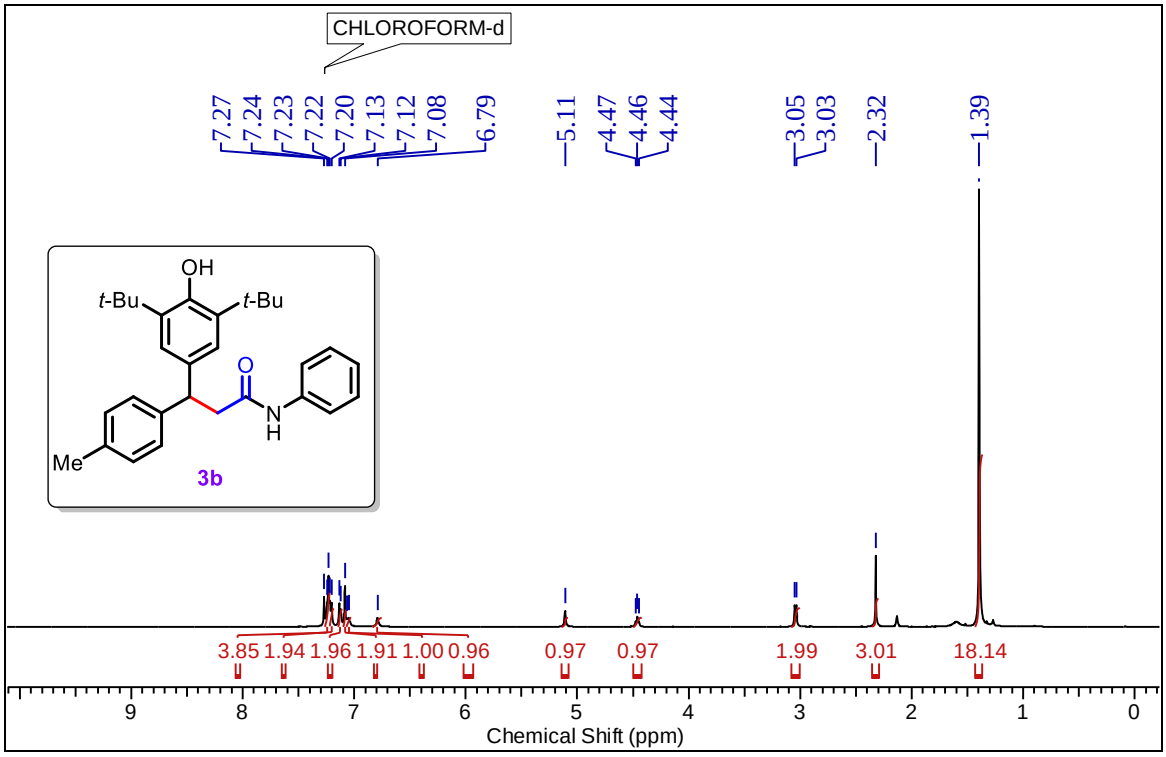

^{13}C NMR of 3-(3,5-Di-*tert*-butyl-4-hydroxyphenyl)-*N*-phenyl-3-(*p*-tolyl)propanamide (3b) (125MHz, $CDCl_3$):

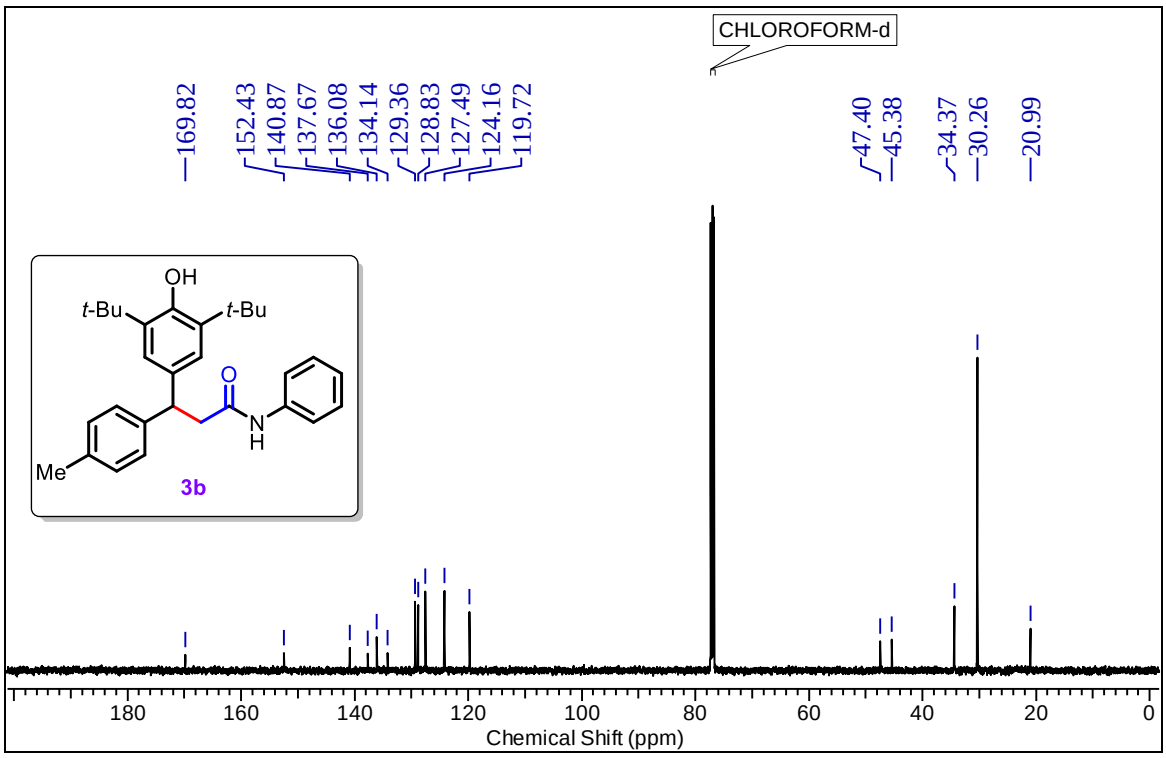

^{1}H NMR of 3-(3,5-Di-*tert*-butyl-4-hydroxyphenyl)-3-(4-methoxyphenyl)-*N*-phenyl propanamide (3d) (500MHz, $CDCl_3$):

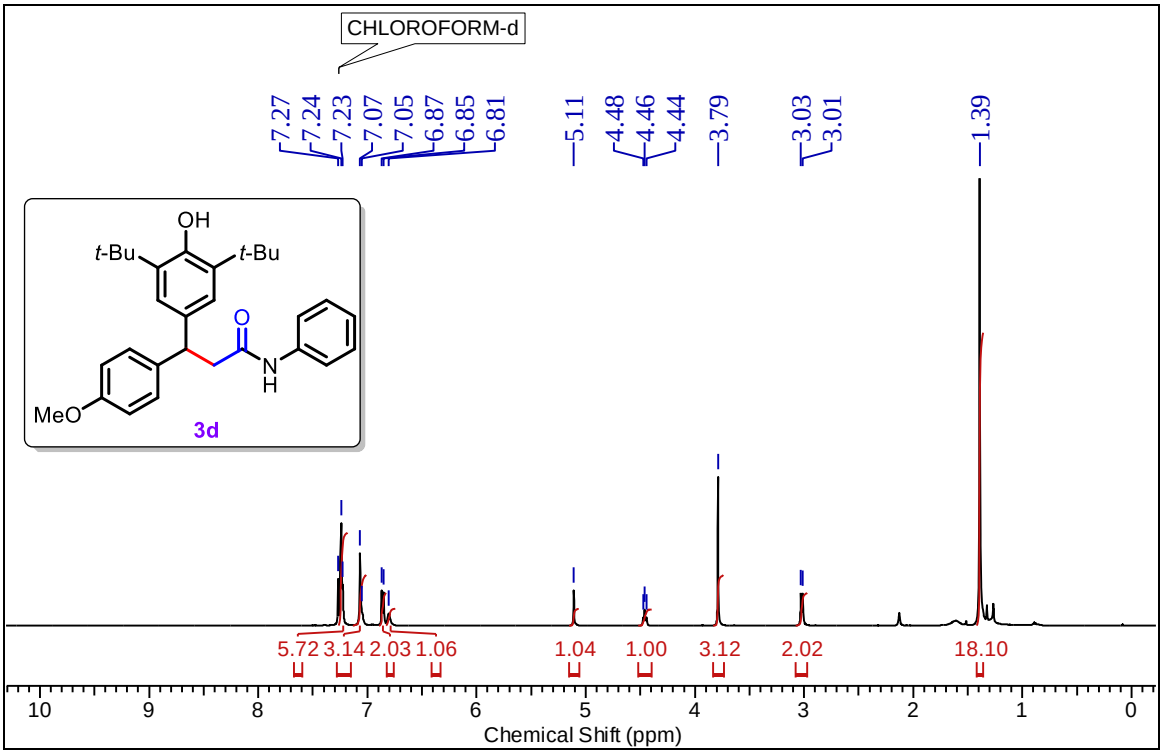

^{13}C NMR of 3-(3,5-Di-*tert*-butyl-4-hydroxyphenyl)-3-(4-methoxyphenyl)-*N*-phenyl propanamide (3d) (125MHz, $CDCl_3$):

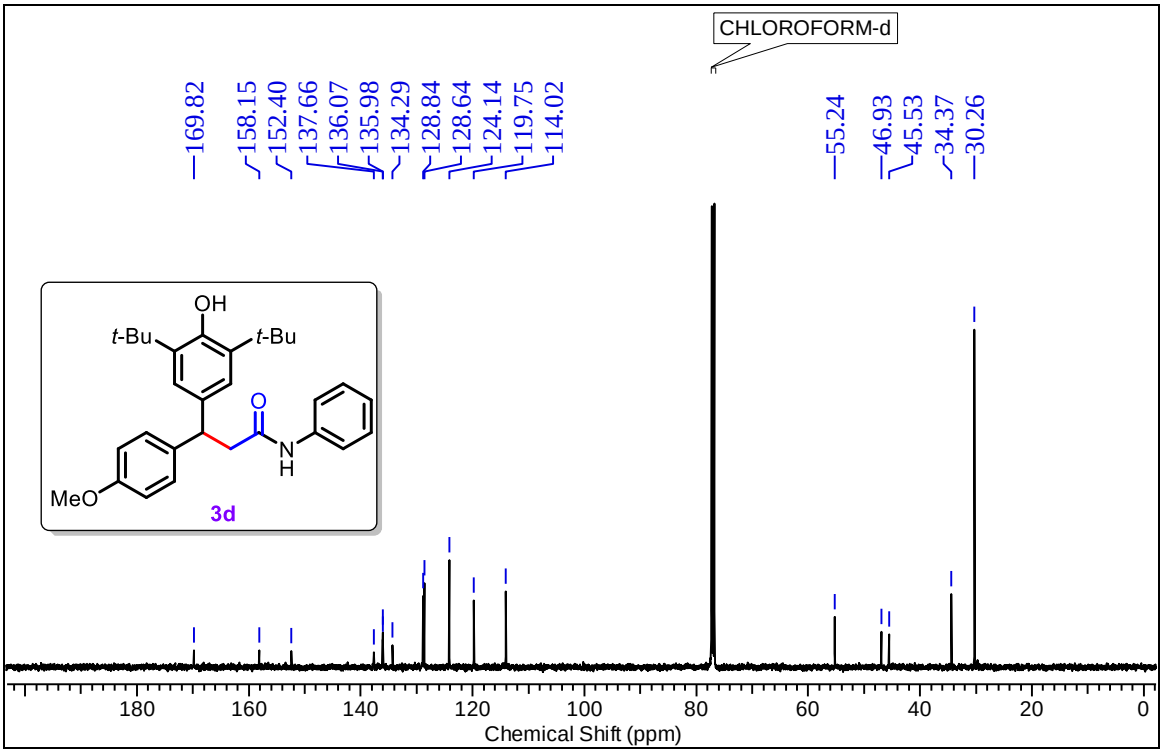

^{1}H NMR of 3-(3,5-Di-*tert*-butyl-4-hydroxyphenyl)-3-(3,4-dimethoxyphenyl)-*N*-phenyl propanamide (3i) (500MHz, $CDCl_3$):

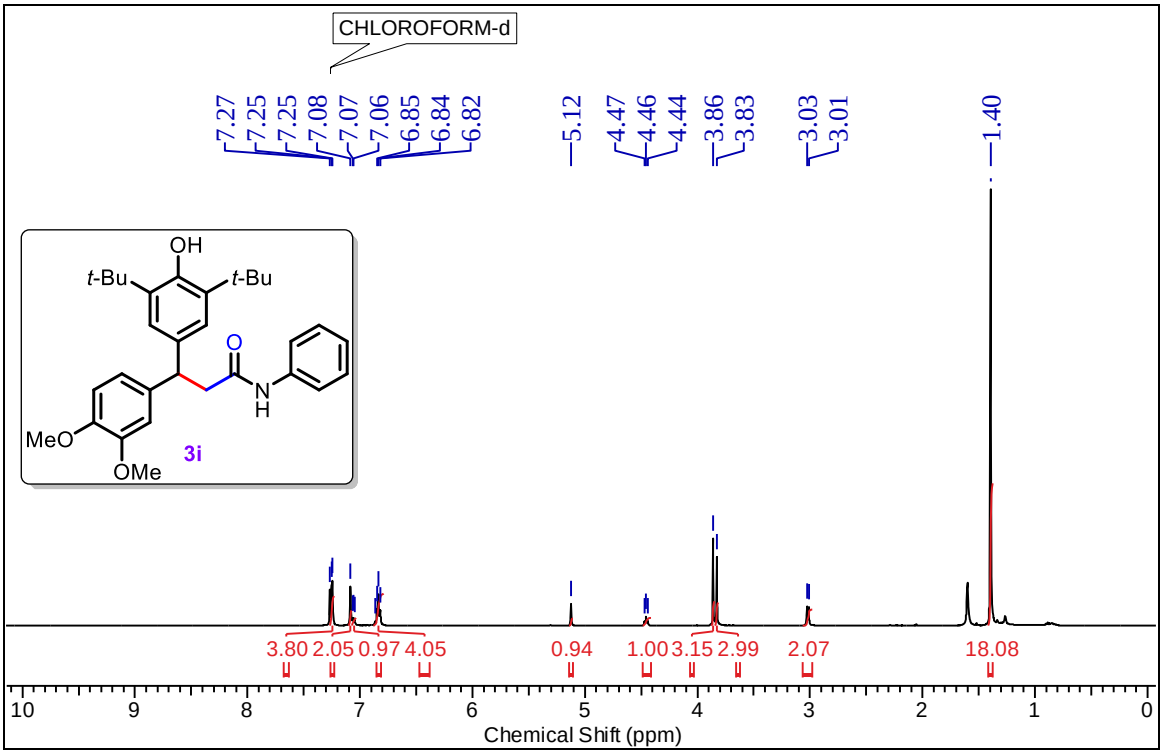

^{13}C NMR of 3-(3,5-Di-*tert*-butyl-4-hydroxyphenyl)-3-(3,4-dimethoxyphenyl)-*N*-phenyl propanamide (3i) (125MHz, $CDCl_3$):

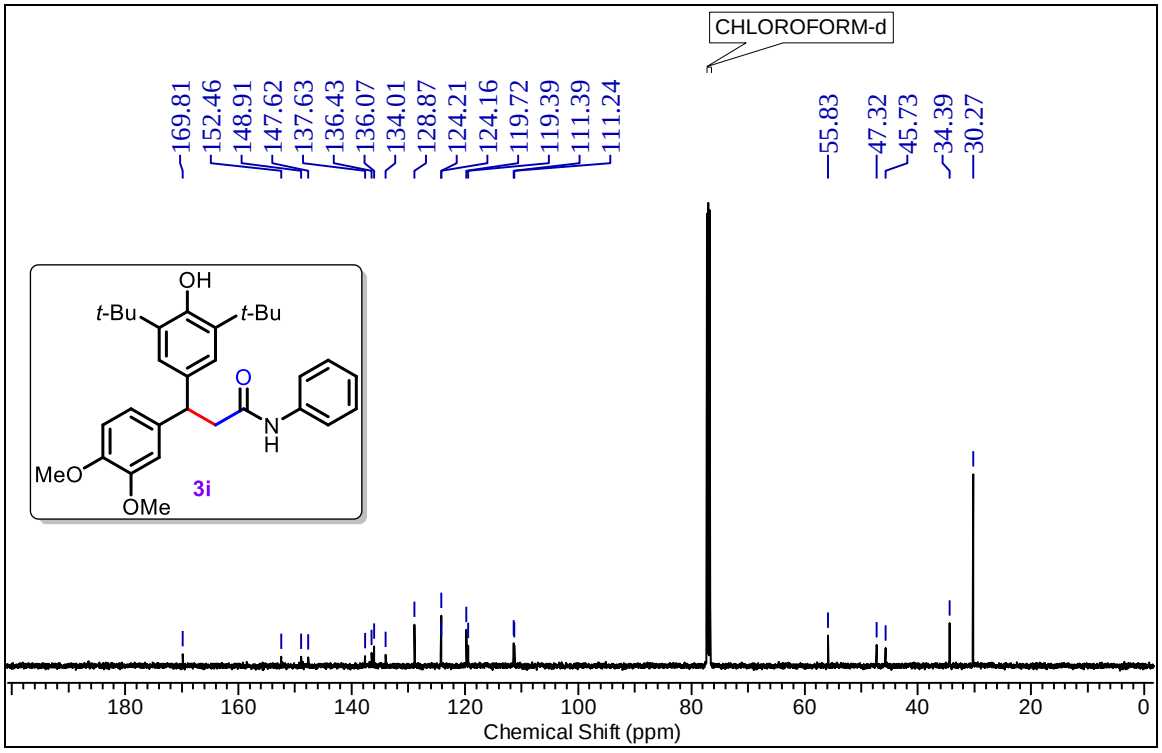

^{1}H NMR of 3-(4-Chlorophenyl)-3-(3,5-di-*tert*-butyl-4-hydroxyphenyl)-*N*-phenyl propanamide (3f) (500MHz, $CDCl_3$):

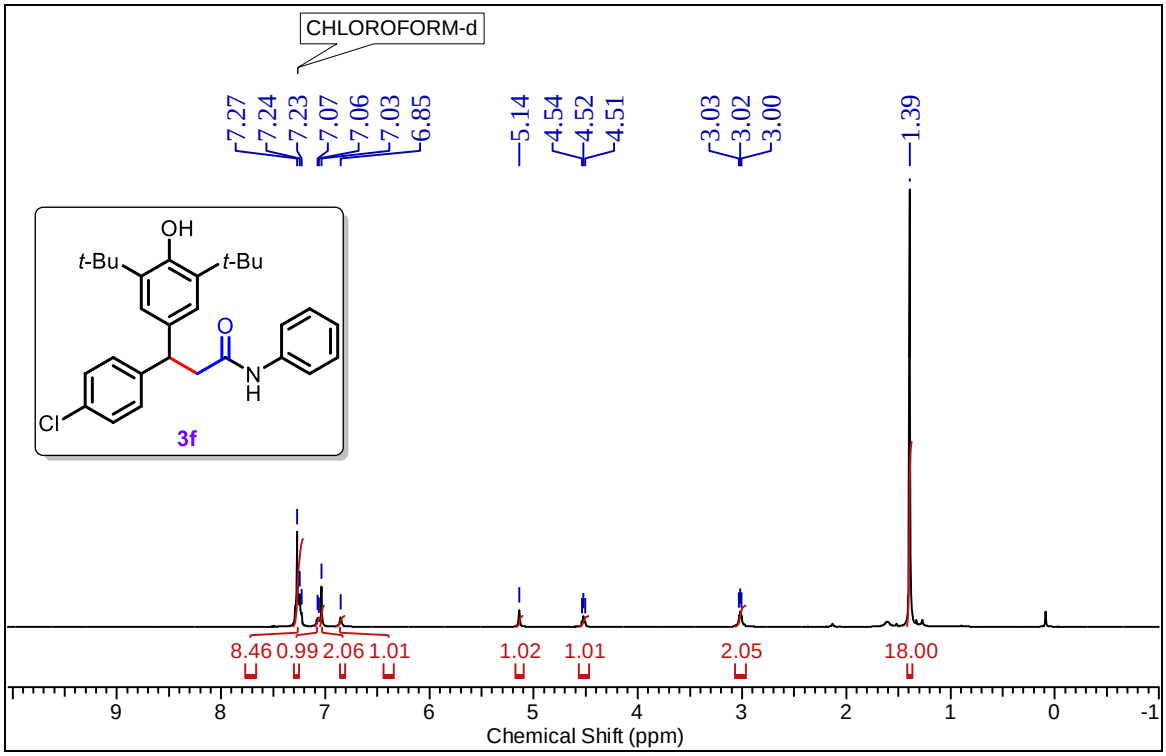

^{13}C NMR of 3-(4-Chlorophenyl)-3-(3,5-di-*tert*-butyl-4-hydroxyphenyl)-*N*-phenyl propanamide (3f) (125MHz, $CDCl_3$):

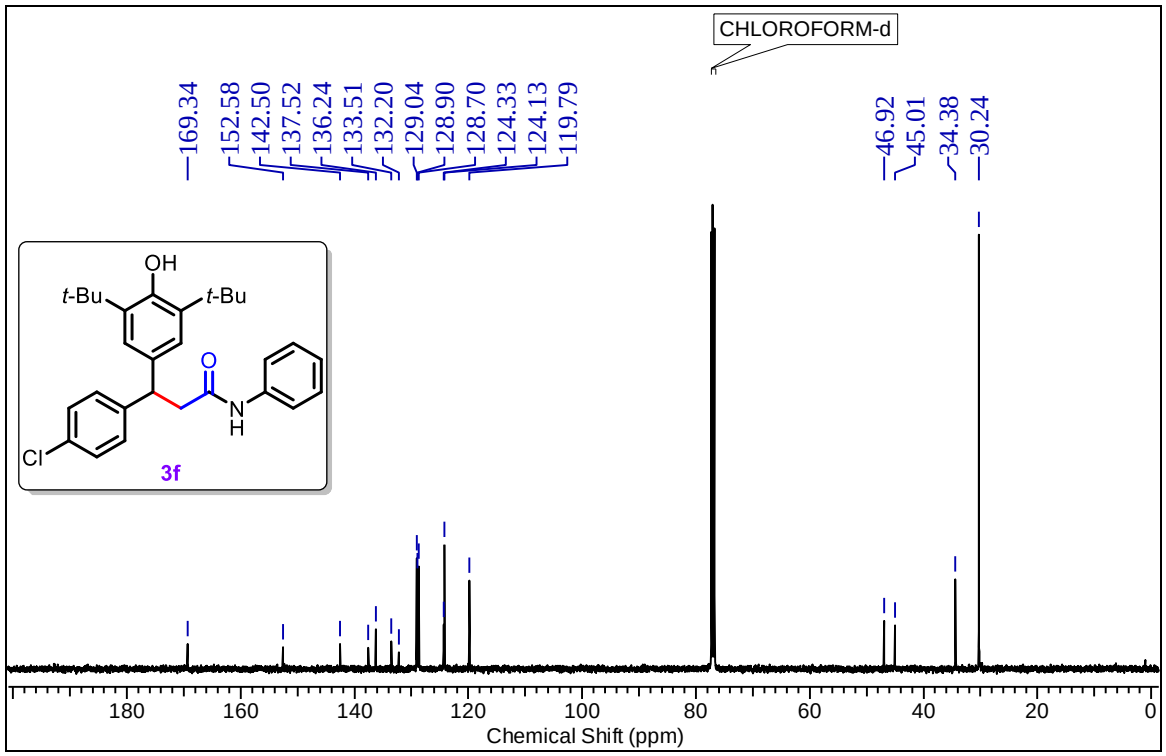

^{1}H NMR of 3-(2-Bromophenyl)-3-(3,5-di-*tert*-butyl-4-hydroxyphenyl)-*N*-phenyl propanamide (3g) (400MHz, $CDCl_3$):

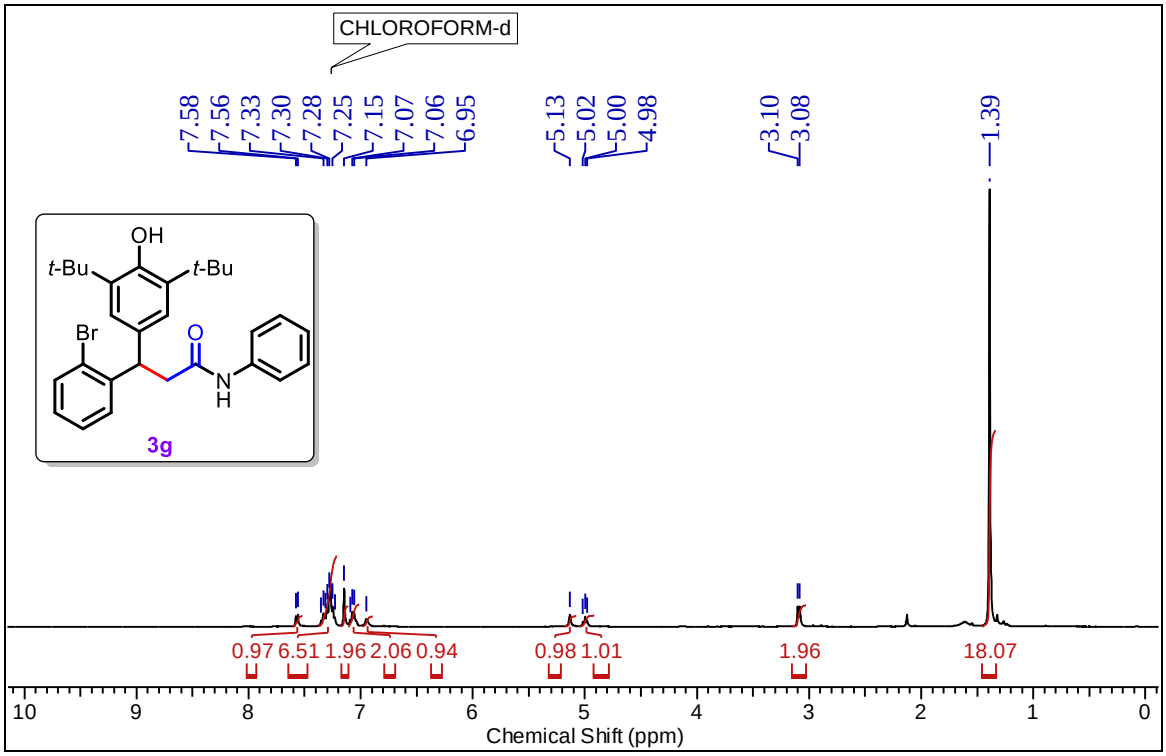

^{13}C NMR of 3-(2-Bromophenyl)-3-(3,5-di-*tert*-butyl-4-hydroxyphenyl)-*N*-phenyl propanamide (3g) (100MHz, $CDCl_3$)

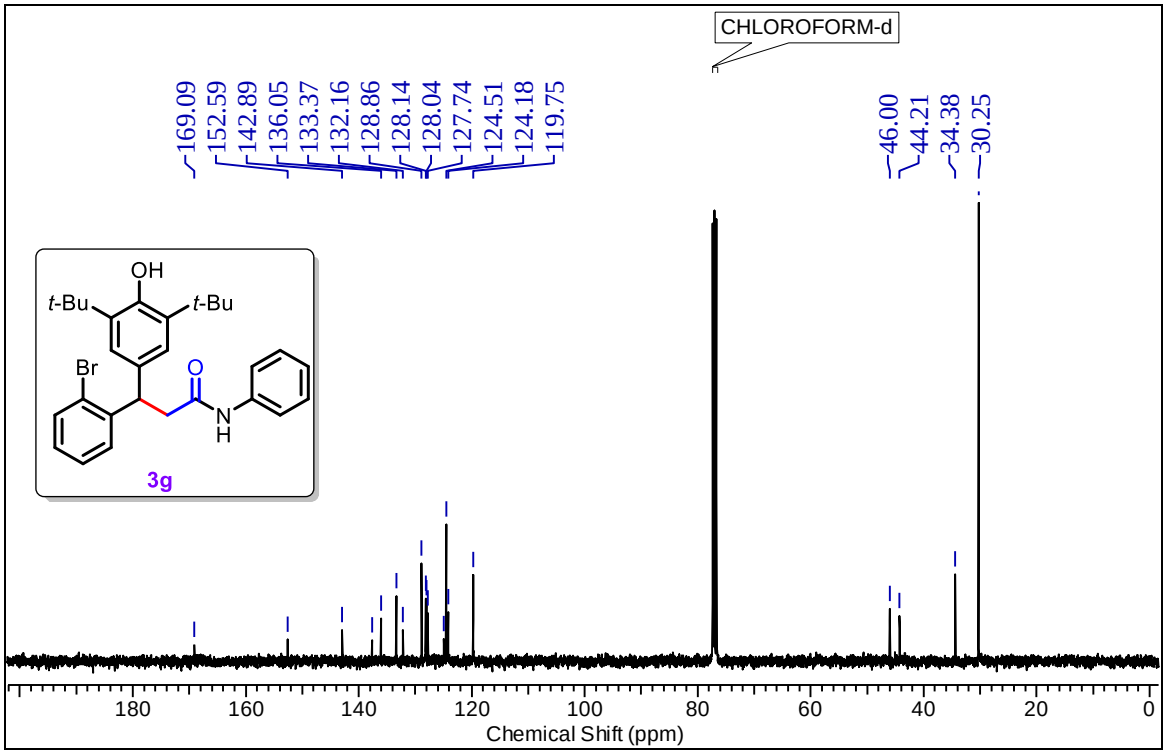

^{1}H NMR of 3-(3,5-Di-*tert*-butyl-4-hydroxyphenyl)-3-(4-nitrophenyl)-*N*-phenylpropan amide (3h) (500MHz, $CDCl_3$):

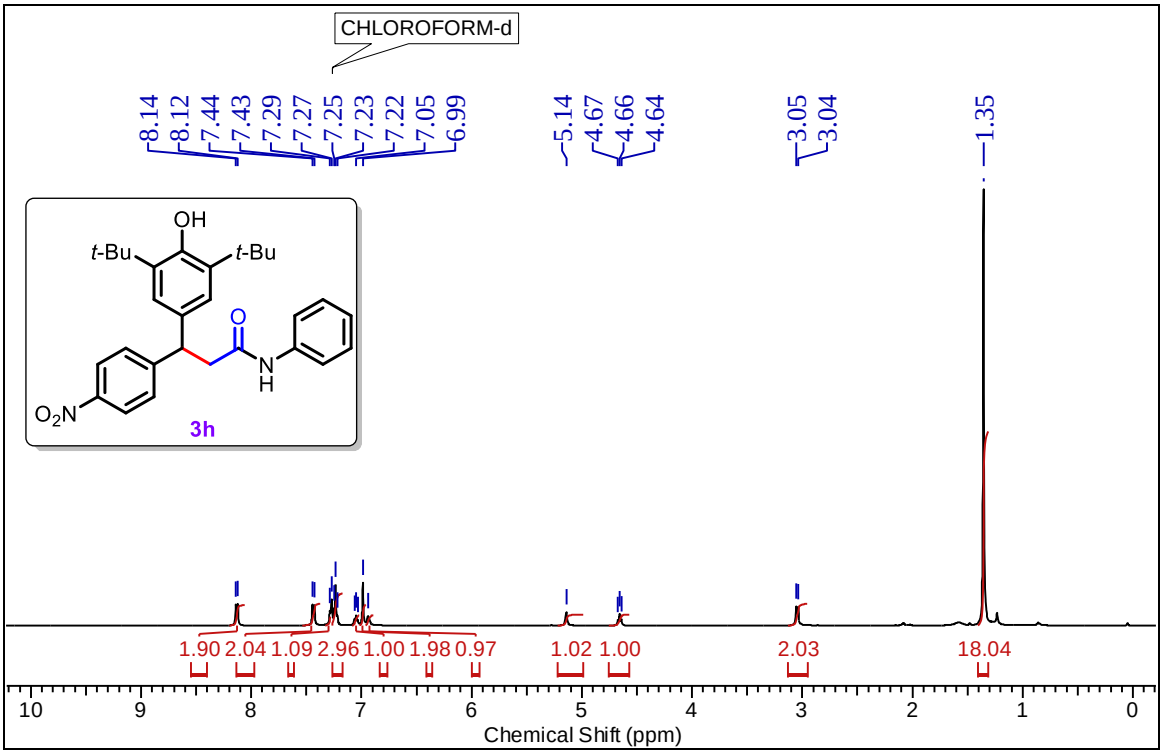

^{13}C NMR of 3-(3,5-Di-*tert*-butyl-4-hydroxyphenyl)-3-(4-nitrophenyl)-*N*-phenylpropan amide (3h) (125MHz, $CDCl_3$):

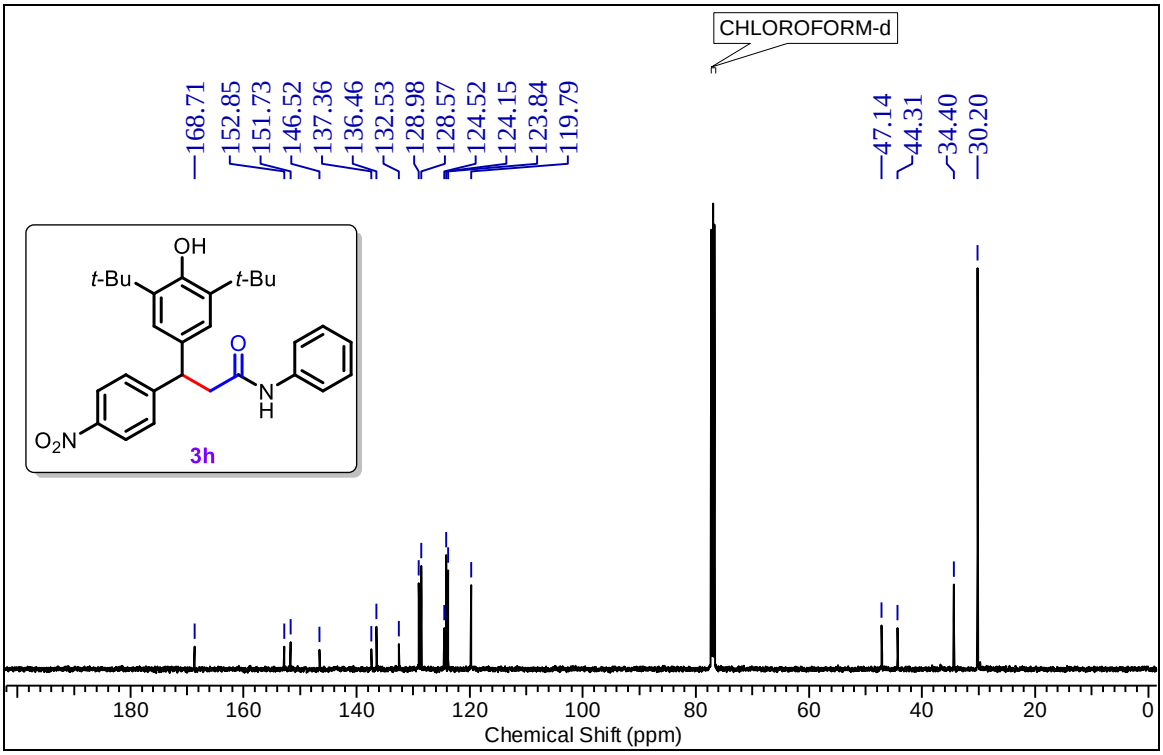

^{1}H NMR of Methyl 4-(1-(3,5-di-*tert*-butyl-4-hydroxyphenyl)-3-oxo-3-(phenylamino) propyl)benzoate (3j) (400MHz, $CDCl_3$):

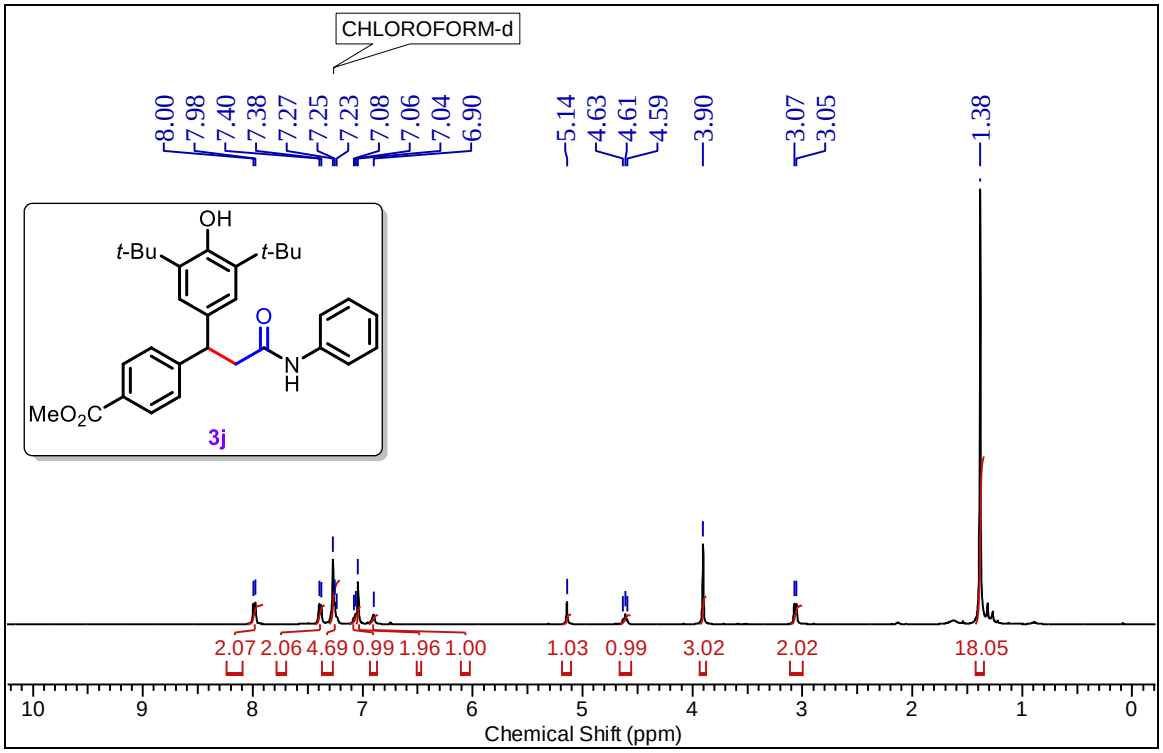

^{13}C NMR of Methyl 4-(1-(3,5-di-*tert*-butyl-4-hydroxyphenyl)-3-oxo-3-(phenylamino) propyl)benzoate (3j) (100MHz, $CDCl_3$):

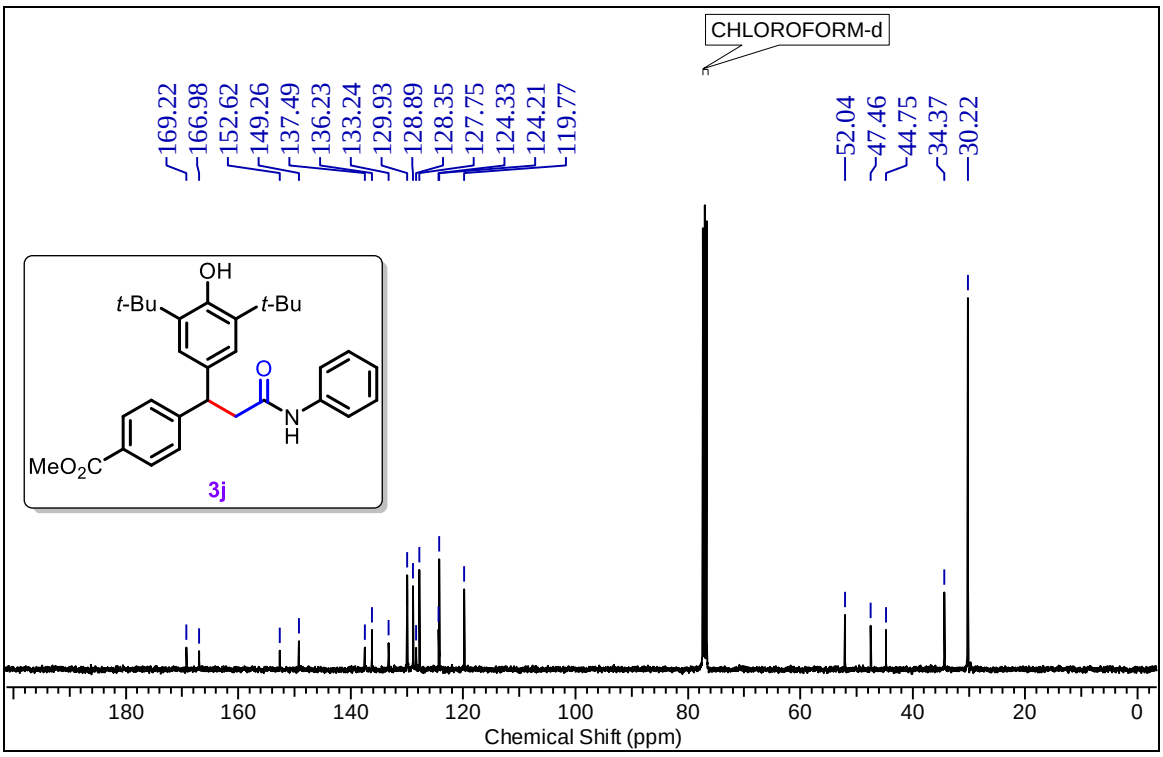

^{1}H NMR of 3-(3,5-Di-*tert*-butyl-4-hydroxyphenyl)-3-(naphthalen-1-yl)-*N*-phenyl propanamide (3l) (500MHz, $CDCl_3$):

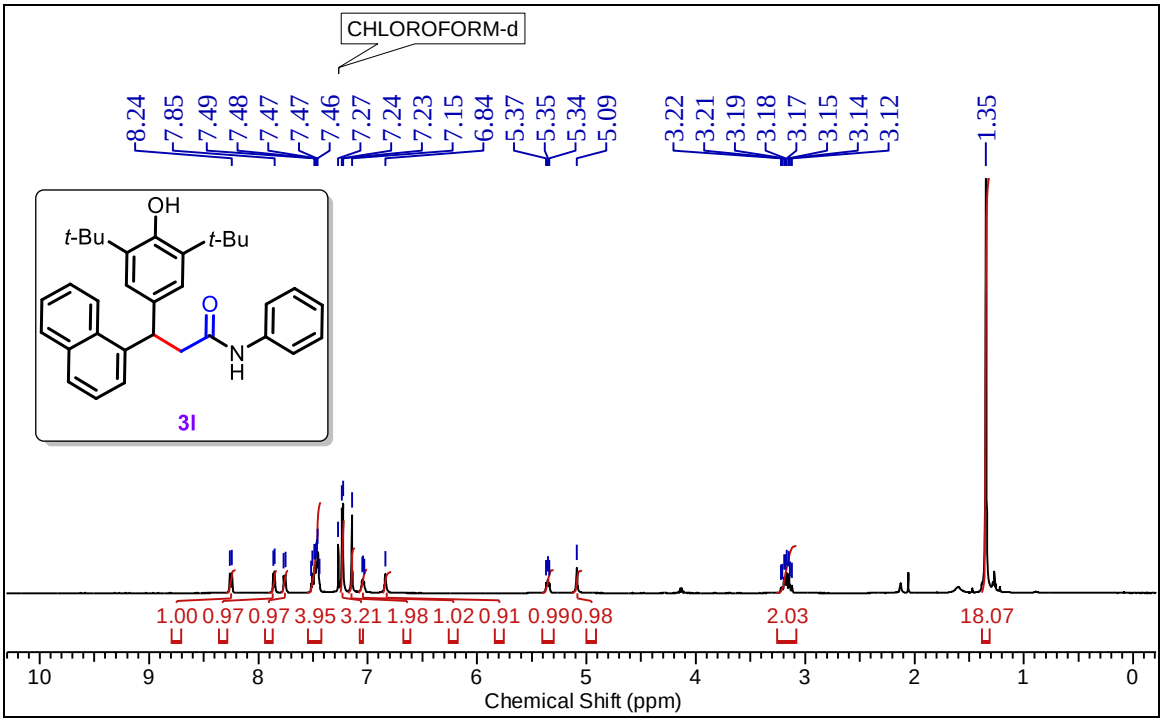

^{13}C NMR of 3-(3,5-Di-*tert*-butyl-4-hydroxyphenyl)-3-(naphthalen-1-yl)-*N*-phenyl propanamide (3l) (125MHz, $CDCl_3$):

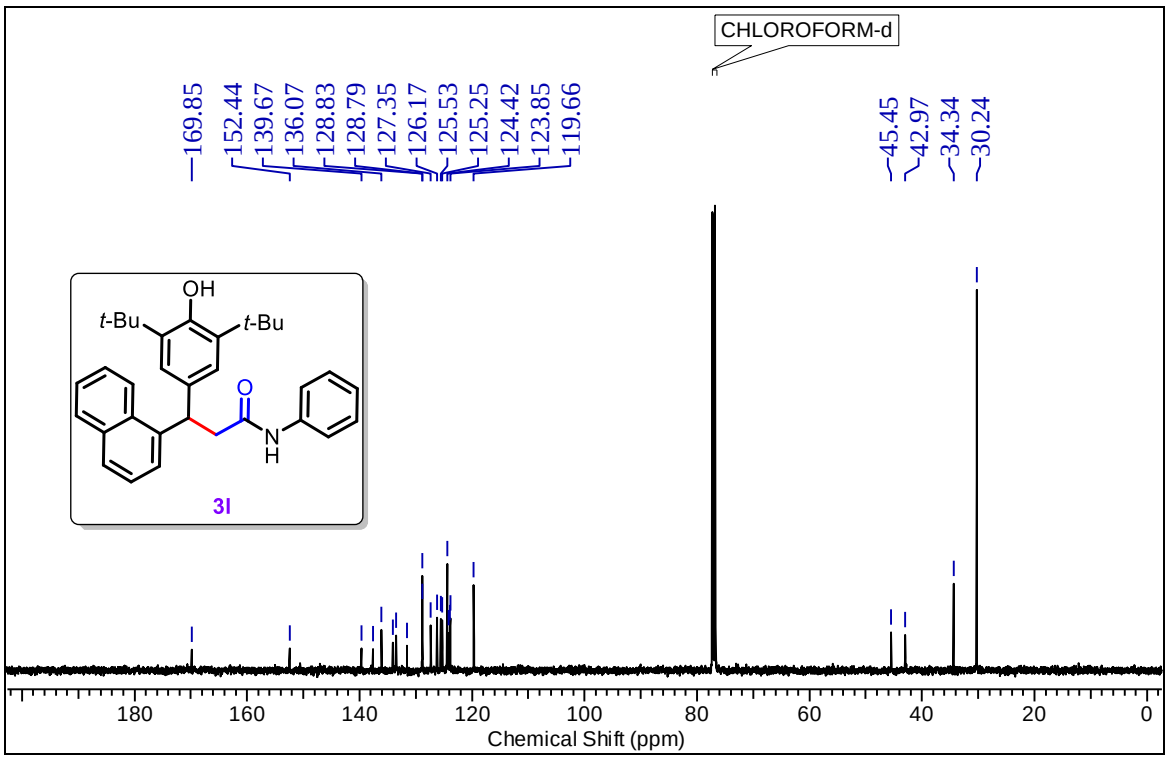

^{1}H NMR of 3-(Benzo[d][1,3]dioxol-4-yl)-3-(3,5-di-*tert*-butyl-4-hydroxyphenyl)-*N*-phenylpropanamide (3m) (500MHz, $CDCl_3$):

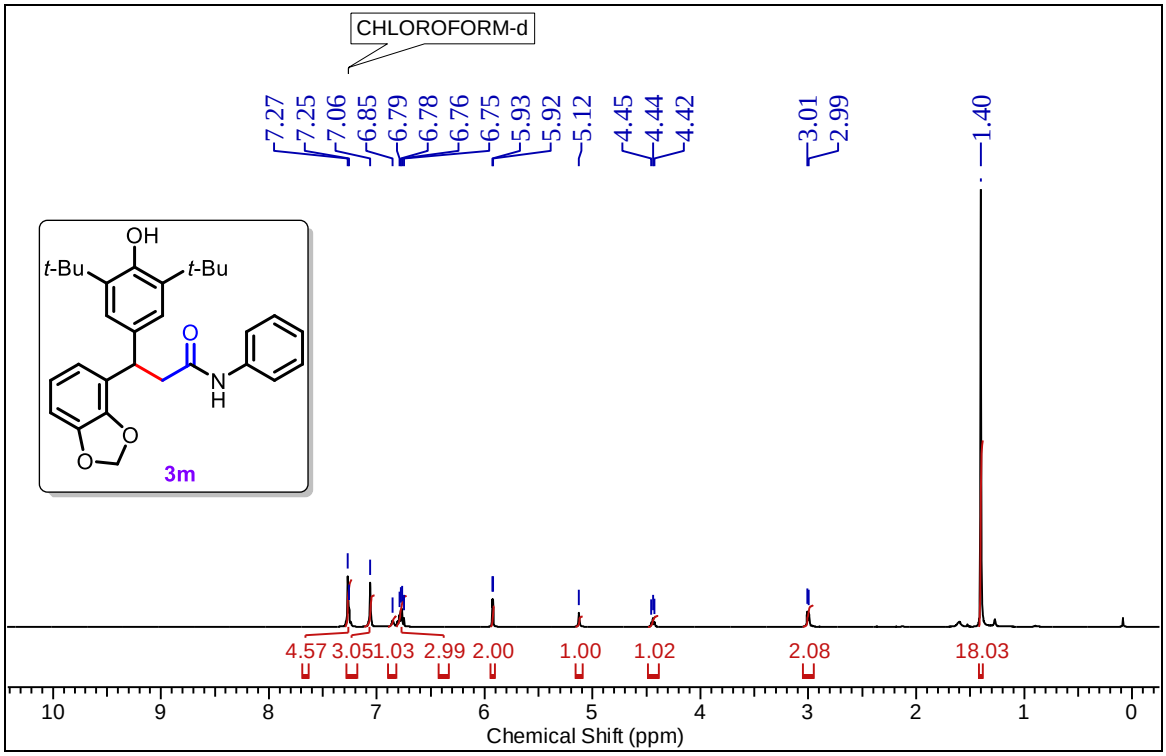

^{13}C NMR of 3-(Benzo[d][1,3]dioxol-4-yl)-3-(3,5-di-*tert*-butyl-4-hydroxyphenyl)-*N*-phenylpropanamide (3m) (125MHz, $CDCl_3$):

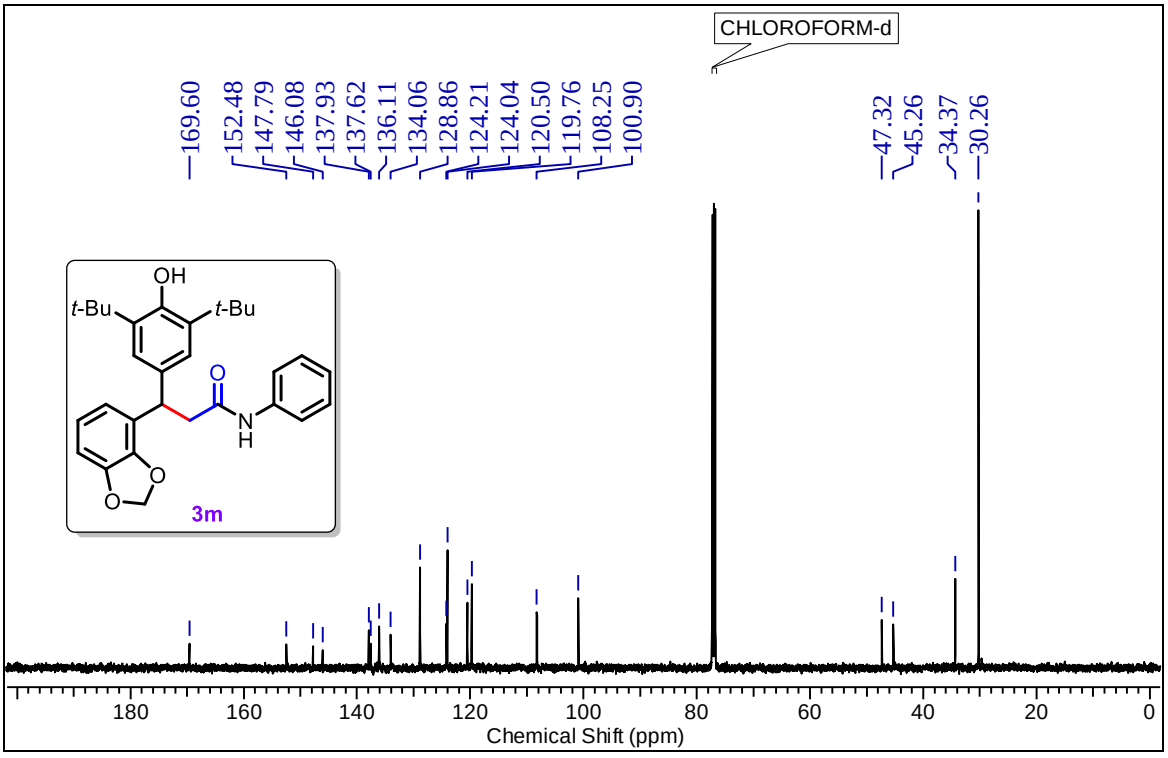

^{1}H NMR of 3-(4-Hydroxy-3,5-dimethylphenyl)-*N*,3-diphenylpropanamide (3o) (400MHz, $CDCl_3$):

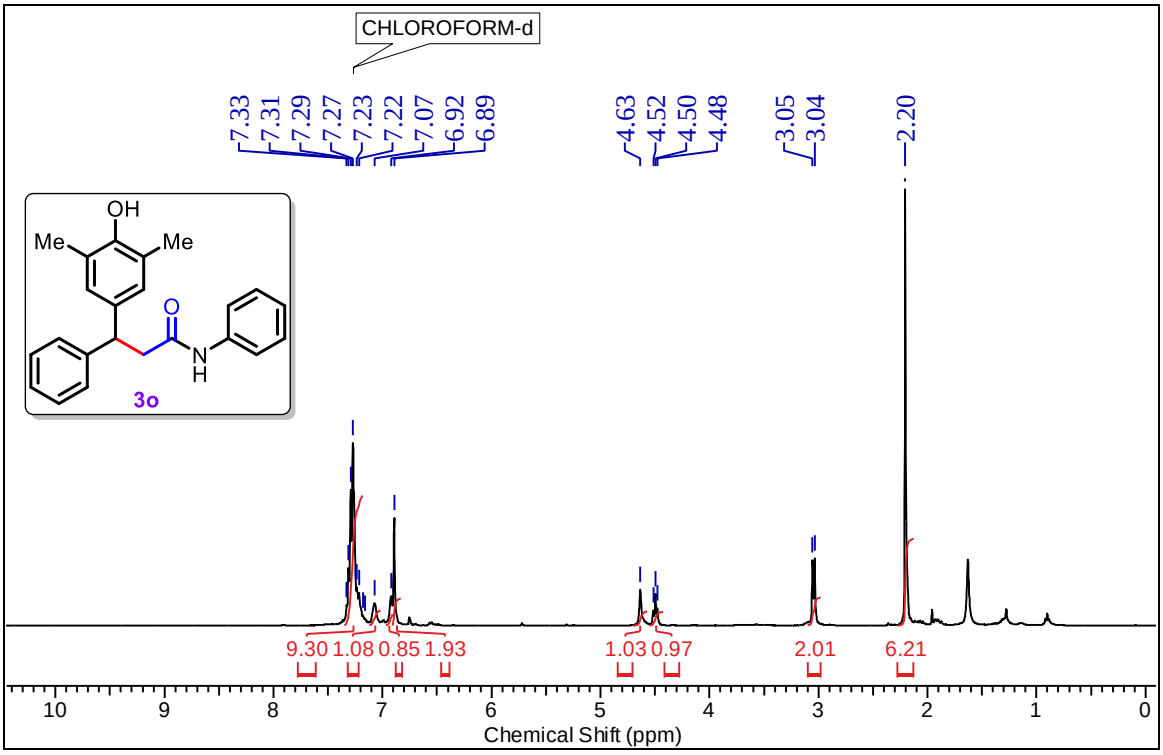

^{13}C NMR of 3-(4-Hydroxy-3,5-dimethylphenyl)-*N*,3-diphenylpropanamide (3o) (100MHz, $CDCl_3$):

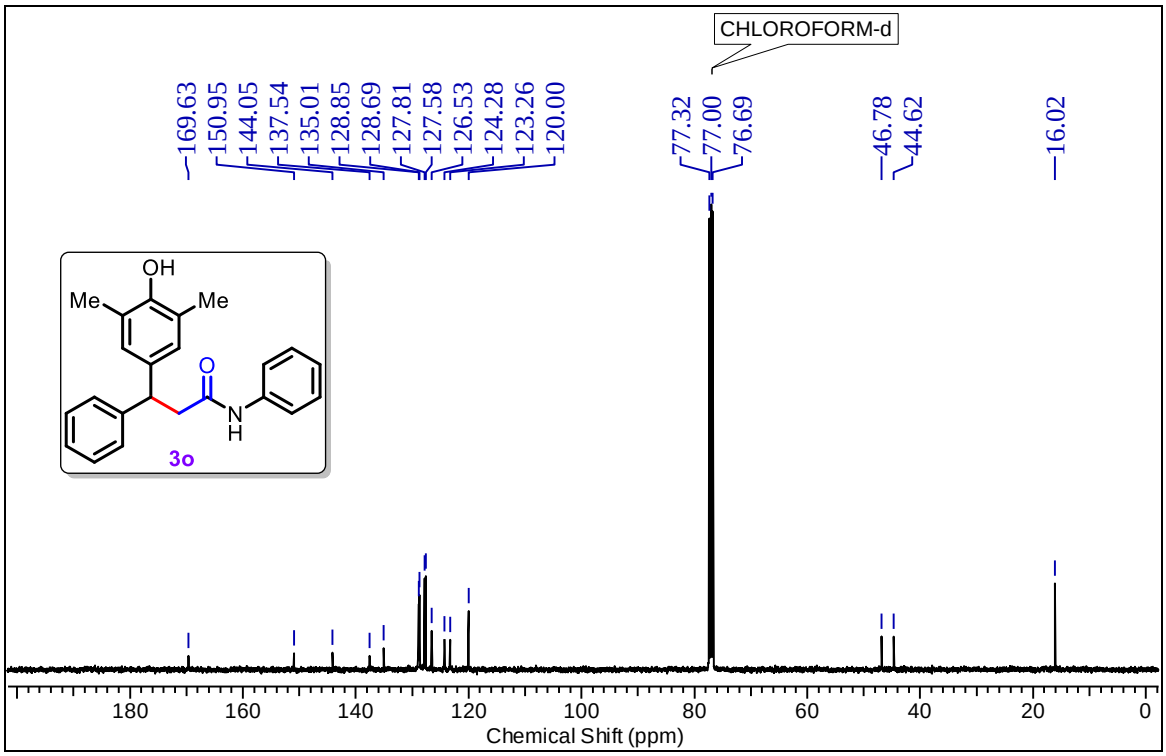

^{1}H NMR of 3-(3,5-Di-*tert*-butyl-4-hydroxyphenyl)-3-phenyl-*N*-(*p*-tolyl)propanamide (3p) (500MHz, $CDCl_3$):

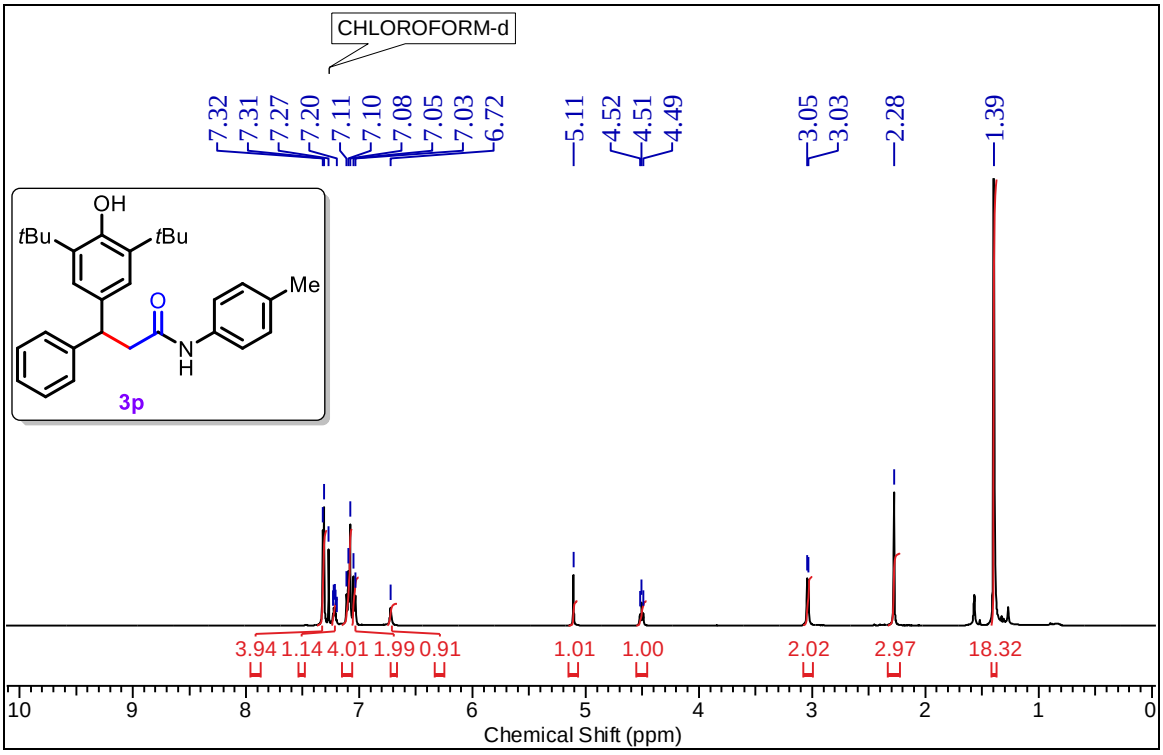

^{13}C NMR of 3-(3,5-Di-*tert*-butyl-4-hydroxyphenyl)-3-phenyl-*N*-(*p*-tolyl)propanamide (3p) (125MHz, $CDCl_3$):

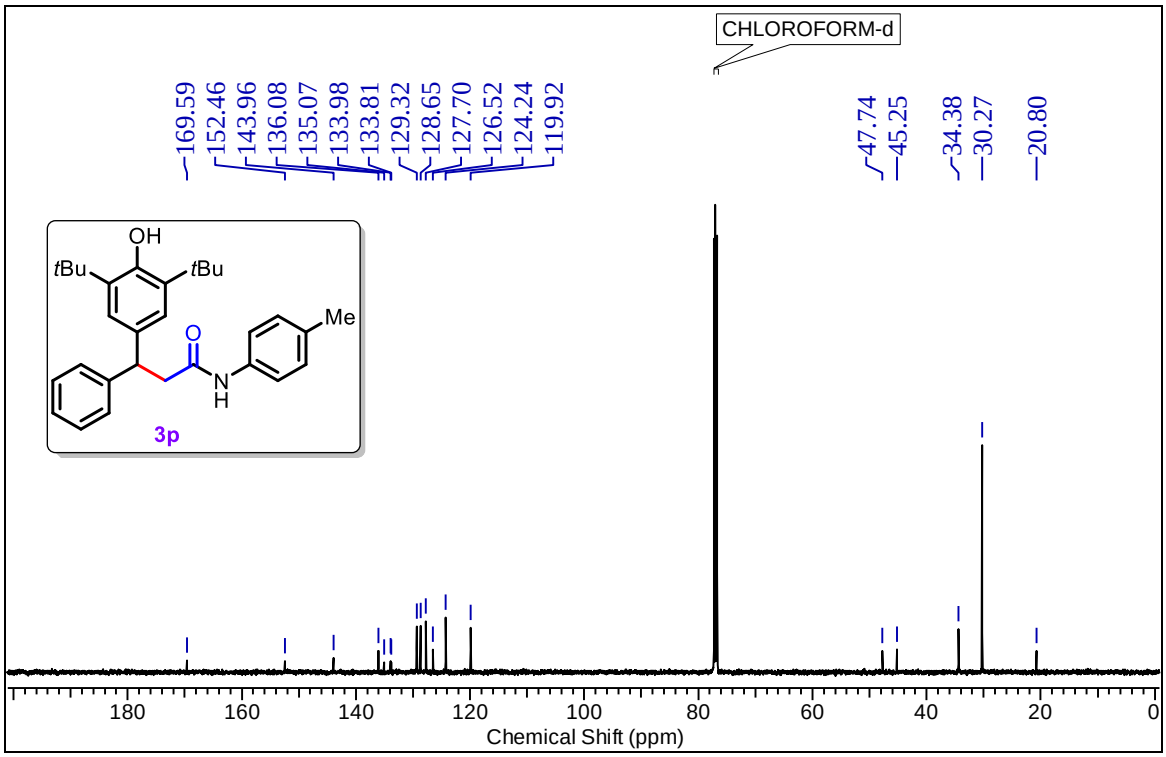

^{1}H NMR of 3-(3,5-Di-*tert*-butyl-4-hydroxyphenyl)-*N*-(3,4-difluorophenyl)-3-phenyl propanamide (3r) (500MHz, $CDCl_3$):

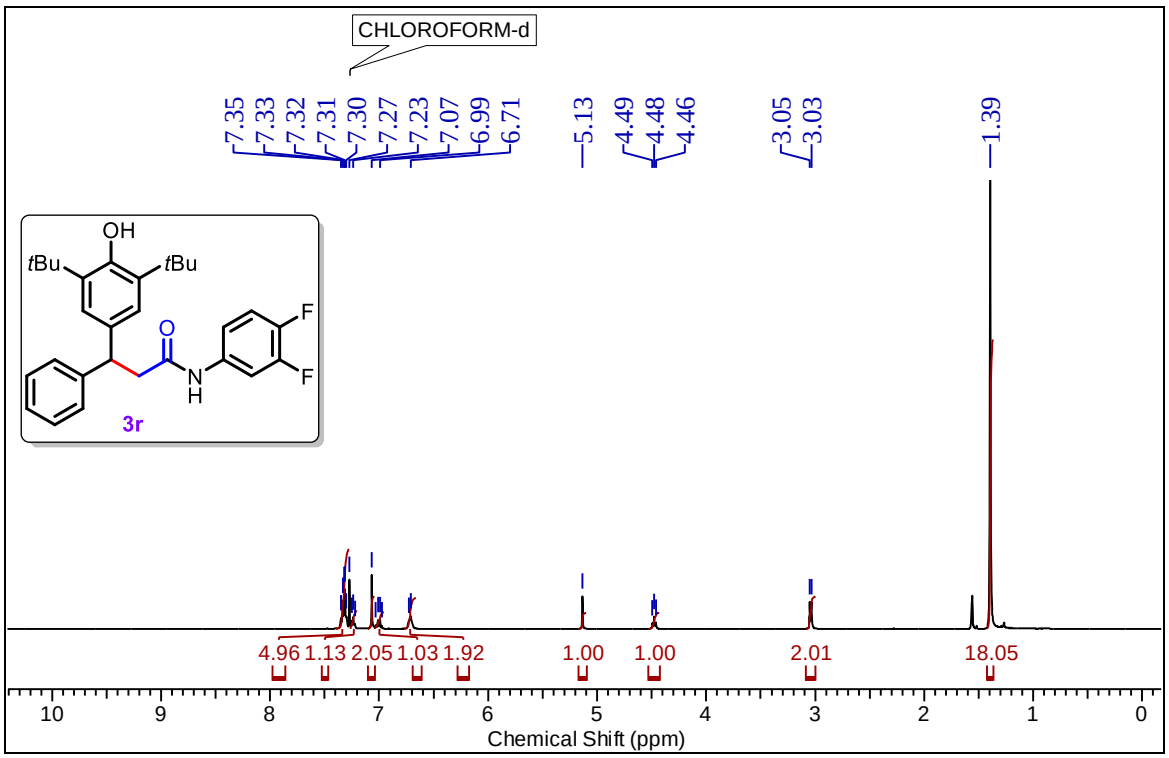

^{13}C NMR of 3-(3,5-Di-*tert*-butyl-4-hydroxyphenyl)-*N*-(3,4-difluorophenyl)-3-phenyl propanamide (3r) (125MHz, $CDCl_3$):

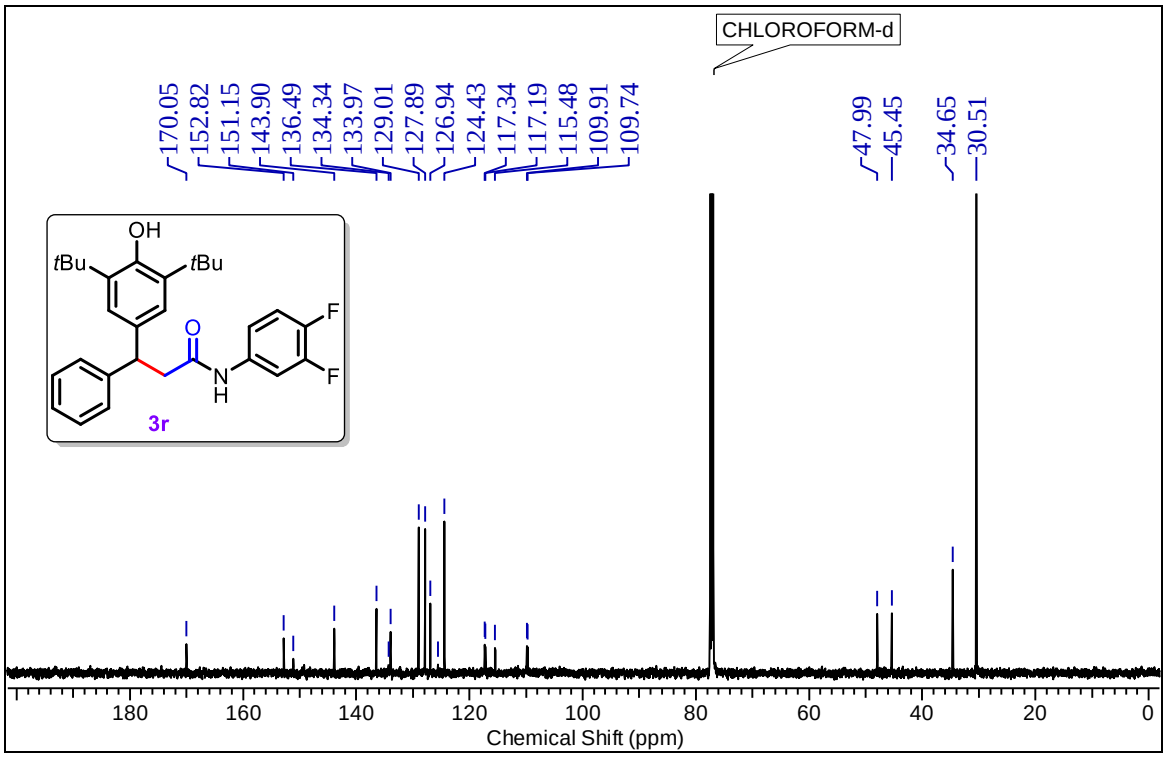

^{1}H NMR of 3-(3,5-Di-*tert*-butyl-4-hydroxyphenyl)-*N*-hexyl-3-phenylpropan amide (3s) (500MHz , $CDCl_3$):

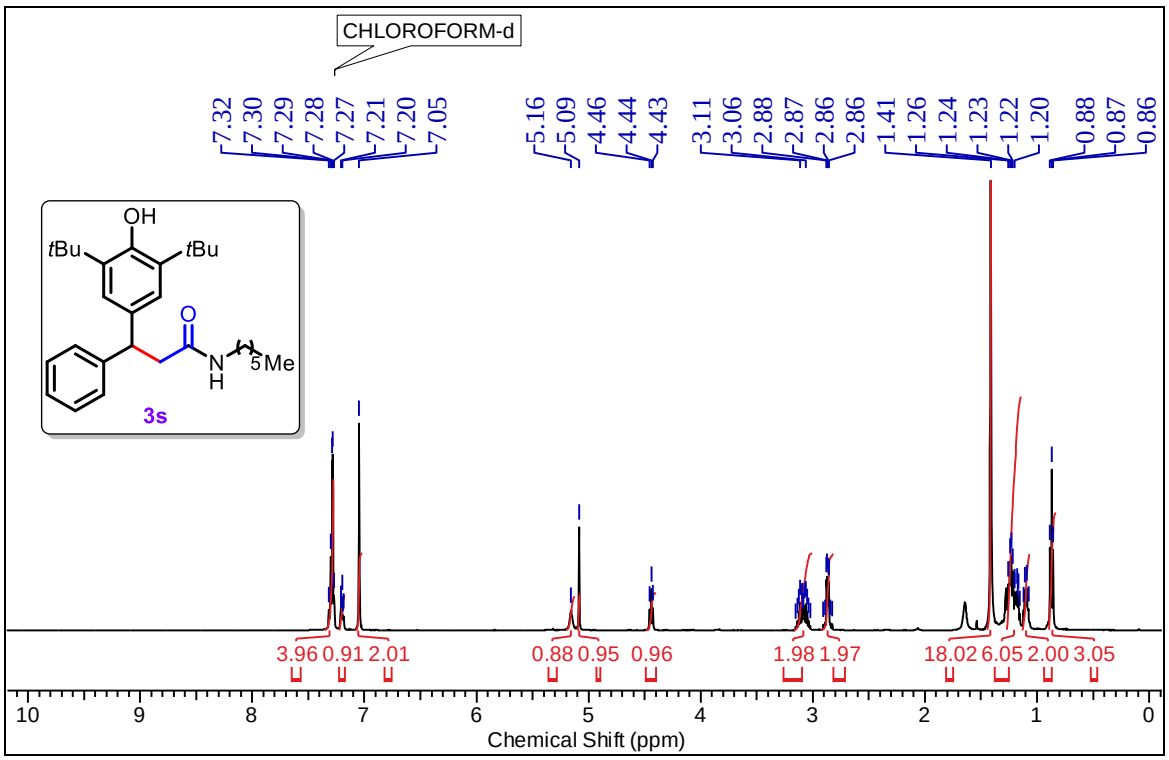

^{13}C NMR of 3-(3,5-Di-*tert*-butyl-4-hydroxyphenyl)-*N*-hexyl-3-phenylpropan amide (3s) (125MHz, $CDCl_3$):

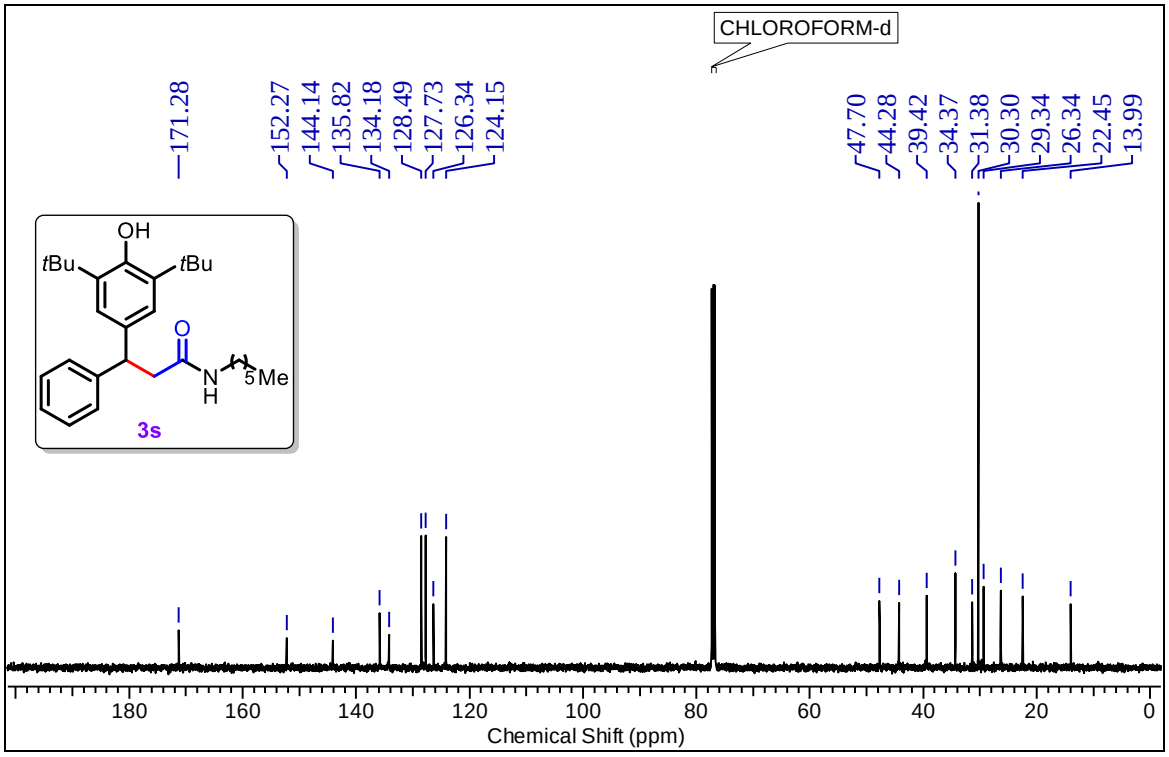

^{1}H NMR of *N*-Hexyl-3-(4-hydroxy-3,5-dimethylphenyl)-3-phenylpropanamide (3u) (500MHz, $CDCl_3$):

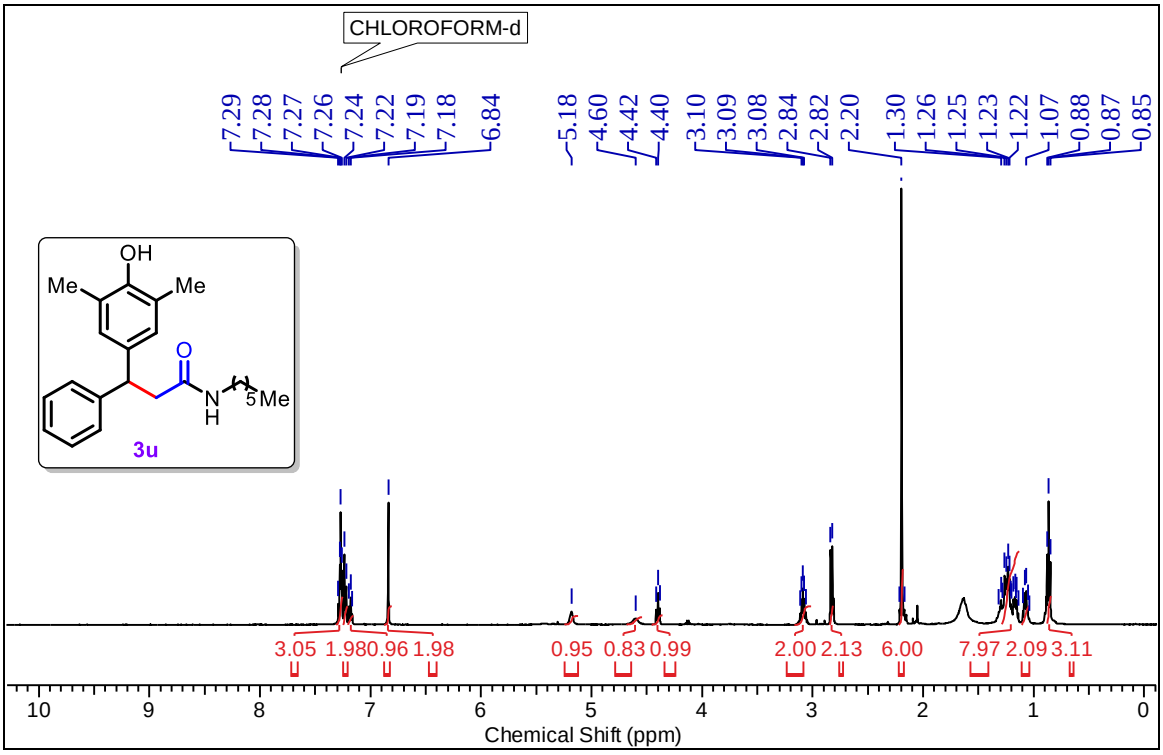

^{13}C NMR of *N*-Hexyl-3-(4-hydroxy-3,5-dimethylphenyl)-3-phenylpropanamide (3u) (125MHz, $CDCl_3$):

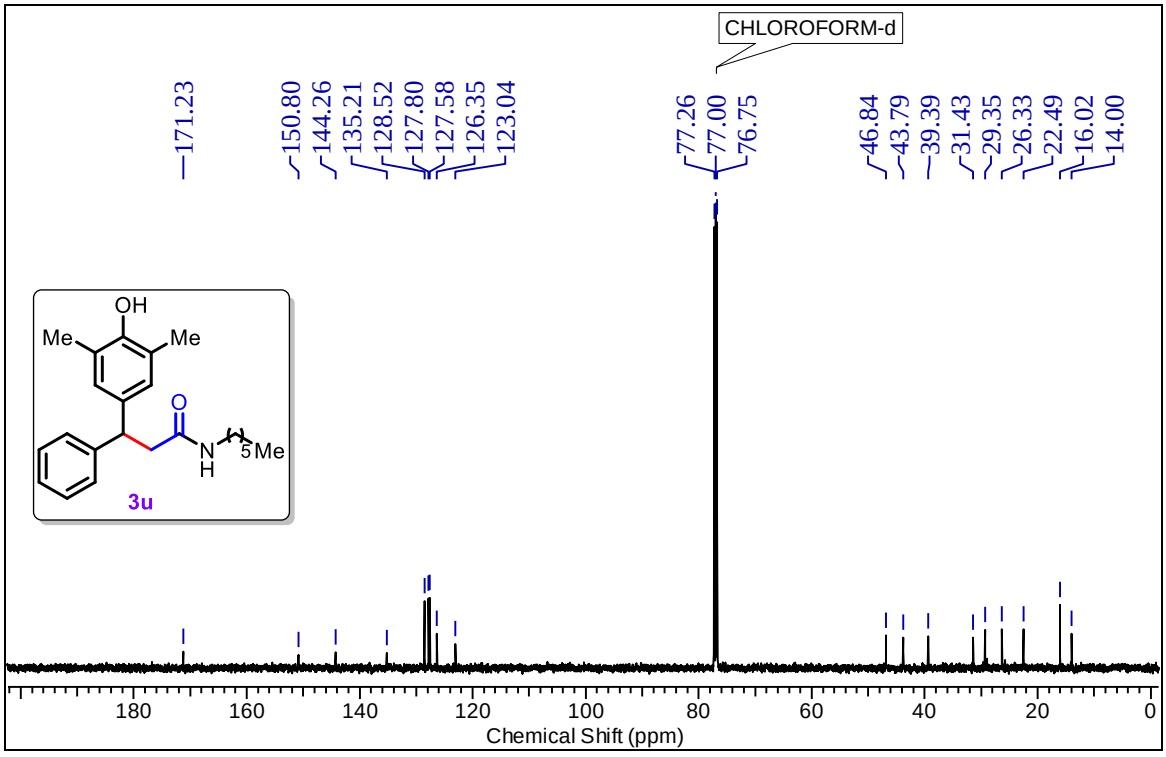

^{1}H NMR of 3-(4-Hydroxyphenyl)-*N*,3-diphenylpropanamide(4a) (400MHz, DMSO-d^{6}):

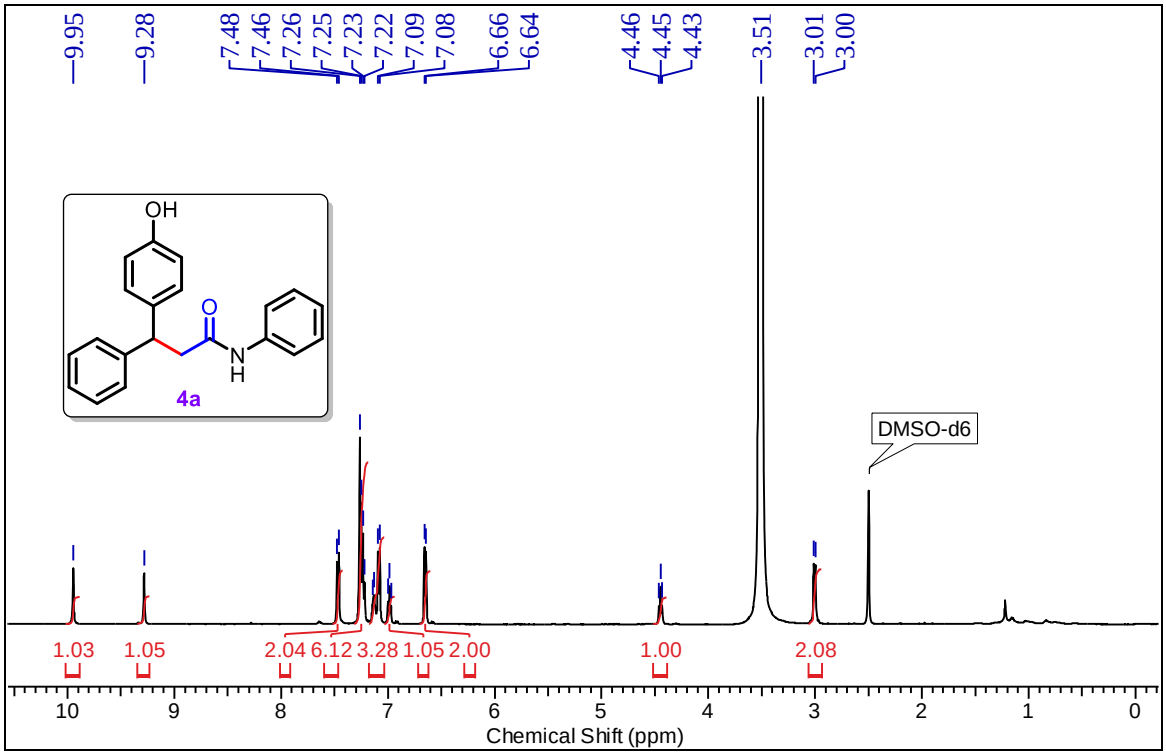

^{13}C NMR of 3-(4-Hydroxyphenyl)-*N*,3-diphenylpropanamide(4a) (101MHz, DMSO-d^{6}):

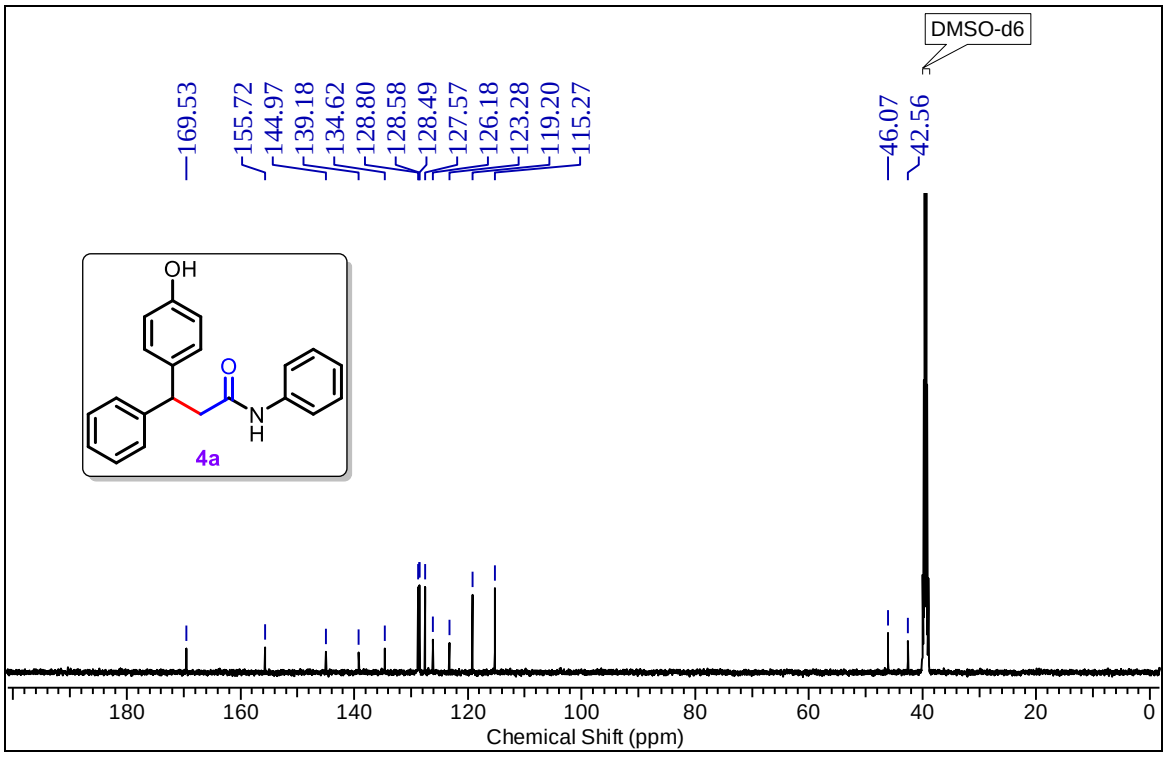

3.1.9 References:

[1] Helge B. Bode, Axel Zeeck *J. Chem. Soc. Perkin Trans. 1* **2000**, *0*, 323-328.

[2] a) Allison, A. C.; Cacabelos, R.; Lombardi, V. R. M.; Alvarez, X. A.; Vigo, C. *Prog. Neuro-Psychopharmacol. Biol. Psychiatry* **2001**, *25*, 1341-1357; b) Kim, D. H.; Shin, E. K.; Kim, Y. H.; Lee, B. W.; Jun, J. G.; Park, J. H. Y.; Kim, J. K. *Eur. J. Clin. Invest.* **2009**, *39*, 819-827.

[3] Murayama, T.; Eizuru, Y.; Yamada, R.; Sadanari, H.; Matsubara, K.; Rukung, G.; Tolo F. M.; Mungai, G. M.; Kofi-Tsekpo, M. *Antivir. Chem. Chemother*. **2007**, *18***,** 133–139.

[4] Kupchan, S. M.; Karim, A.; Marcks, C. *J. Am. Chem. Soc.* **1968**, *90*, 5923-5924.

[5] Tada, M.; Kurabe, J.; Yoshida, T.; Ohkanda, T.; Matsumoto, Y. *Chem. Pharm. Bull*. **2010**, *58*, 818–824.

[6] Norihisa, K.; Tatsuya, A.; Tetsuya, M.; Koichi, O.; Koetsu, T. *J. Chem. Ecol.* **2010**, *36*, 1381–1386.

[7] Ballesta-Acosta, M. C.; Pascual-Villalobos, M. J.; Rodríguez, B. *Spanish J. Agri. Res*. **2008**, *6*, 85–91.

[8] Thompson, D. C.; Thompson, J. A.; Sugumaran, M.; Moldeus, P. *Chem.-Biol. Interact.* **1992**, *86*, 129-162.

[9] Turner, A. B. *Q. Rev. Chem. Soc.* **1964**, *18*, 347-360.

[10] a) Peter, M. G. *Angew. Chem., Int. Ed.* **1989**, *28*, 555-570; b) Angle, S. R.; Turnbull, K. D. *J. Am. Chem. Soc.* **1989**, *111*, 1136-1138; c) Angle, S. R.; Louie, M. S.; Mattson, H. L.; Yang, W. *Tetrahedron Lett.* **1989**, *30*, 1193-1196.

[11] a) Takao, K.-i.; Sasaki, T.; Kozaki, T.; Yanagisawa, Y.; Tadano, K.-i.; Kawashima, A.; Shinonaga, H. *Org. Lett.* **2001**, *3*, 4291-4294; b) Groszek, G.; Błażej, S.; Brud, A.; Świerczyński, D.; Lemek, T. *Tetrahedron* **2006**, *62*, 2622-2630.

[12] Jarava-Barrera, C.; Parra, A.; Lopez, A.; Cruz-Acosta, F.; Collado-Sanz, D.; Cardenas, D. J.; Tortosa, M. *ACS Catal.* **2016**, *6*, 442-446.

[13] Yang, C.; Gao, S.; Yao, H.; Lin, A. *J. Org. Chem.* **2016**, *81*, 11956-11964.

[14] Huang, B.; Shen, Y.; Mao, Z.; Liu, Y.; Cui, S. *Org. Lett.* **2016**, *18*, 4888-4891.

[15] Xie, K.-X.; Zhang, Z.-P.; Li, X. *Org. Lett.* **2017**, *19*, 6708–6711.

[16] He, F.-S.; Jin, J.-H. Yang, Z.-T.; Yu, X.; Fossey, J. S.; Deng, W.-P**.** *ACS Catal.* **2016**, *6*, 652–656.

[17] a) Mahesh, S.; Kant, G.; Anand, R. V. *RSC Adv.* **2016**, *6*, 80718-80722; b) Reddy, V.; Vijaya Anand, R. *Org. Lett.* **2015**, *17*, 3390-3393; c) Jadhav, A. S.; Anand, R. V. *Org.*

Biomol. Chem. **2017**, *15*, 56-60; d) Goswami, P.; Anand, R. V. *Chem. Select* **2016**, *1*, 2556-2559; e) Arde, P.; Anand, R. V. *RSC Adv.* **2016**, *6*, 77111-77115; f) Arde, P.; Anand, R. V. *Org. Biomol. Chem.* **2016**, *14*, 5550-5554; g) Ramanjaneyulu, B. T.; Mahesh, S.; Anand, R. V. *Org. Lett.* **2015**, *17*, 3952-3955.

[18] Gao, S.; Xu, X.; Yuan, Z.; Zhou, H.; Yao, H.; Lin, A. *Eur. J. Org. Chem.* **2016**, 3006-3012.

[19] a) Yuan, Z.; Wei, W.; Lin, A.; Yao, H. *Org. Lett.* **2016**, *18*, 3370-3373; b) Li, X.; Xu, X.; Wei, W.; Lin, A.; Yao, H. *Org. Lett.* **2016**, *18*, 428-431; c) Yang, C.; Gao, S.; Yao, H.; Lin, A. *J. Org. Chem*. **2016**, *81*, 11956-11964; d) Yuan, Z.; Fang, X.; Li, X.; Wu, J.; Yao, H.; Lin, A. *J. Org. Chem.* **2015**, *80*, 11123-11130; e) Gai, K.; Fang, X.; Li, X.; Xu, J.; Wu, X.; Lin, A.; Yao, H. *Chem. Commun.* **2015**, *51*, 15831-15834.

[20] Zhang, X.-Z.; Deng, Y.-H.; Gan, K.-J.; Yan, X.; Yu, K.-Y.; Wang, F.-X.; Fan, C.-A. *Org. Lett.* **2017**, *19*, 1752-1755.

[21] Yuan, Z.; Gai, K.; Wu, Y.; Wu, J.; Lin, A.; Yao, H. *Chem. Commun.* **2017**, *53*, 3485-3488.

[22] Roiser, L.; Waser M. *Org. Lett.* **2017**, *19*, 2338-2341.

[23] China Raju, B.; Neelakantan, P.; Bhalerao, U. T. *Tetrahedron Lett.* **2004**, *45*, 7487-7489.

[24] a) Jung, N.; Bräse, S. *Angew. Chem., Int. Ed.* **2012**, *51*, 12169-12171; b) Chiba, S. *Synlett.* **2012**, 2012, 21-44; c) Stokes, B. J.; Driver, T. G. *Eur. J. Org. Chem.* **2011**, *2011*, 4071-4088; d) Driver, T. G. *Org. Biomol. Chem.* **2010**, *8*, 3831-3846; e) Liu, Z.; Liu, J.; Zhang, L.; Liao, P.; Song, J.; Bi, X. *Angew. Chem. Int. Ed.* **2014**, *53*, 5305-5309; f) Hu, B.; DiMagno, S. G. *Org. Biomol. Chem.* **2015**, *13*, 3844-3855.

[25] a) Hassner, A.; Ferdinandi, E. S.; Isbister, R. J. *J. Am. Chem. Soc.* **1970**, *92*, 1672-1675; b) Moore, H. W.; Shelden, H. R.; Weyler, W., Jr. *Tetrahedron Lett.* **1969**, *10*, 1243-1246.

[26] a) Zhang, F.; Wang, Y.; Lonca, G. H.; Zhu X.; Chiba, S.; *Angew. Chem. Int. Ed.* **2014**, *53*, 4390-4394; b) Zhu, X.; Wang, Y.-F.; Zhang, F.-L.; Chiba, S. *Chem. Asian J.* **2014**, *9*, 2458-2462; c) Stork, G.; Brizzolara, A.; Landesman, H.; Szmuszkovicz, J.; Terrell, R. *J. Am. Chem. Soc.* **1963**, *85*, 207-222; d) Zhang, Z.; Kumar, R. K.; Li, G.; Wu, D.; Bi, X. *Org. Lett.* **2015**, *17*, 6190-6193.

[27] a) Parella, R.; Gopalakrishnan, B.; Arulananda Babu, S. *J. Org. Chem.* **2013**, *78*, 11911-11934; b) Mu, D.; Gao, F.; Chen, G.; He, G. *ACS Catal.* **2017**, *7*, 1880-1885; c)

Kerdphon, S.; Quan, X.; Parihar, V. S.; Andersson, P. G. *J. Org. Chem.* **2015**, *80*, 1529-11537; d) Wasa, M.; Yu, J.-Q. *Tetrahedron* **2010**, *66*, 4811-4815.

[28] Zhang, F.-L.; Zhu, X.; Chiba, S. *Org. Lett.* **2015**, *17*, 3138-3141.

[29] Lin, C.; Shen, Y.; Huang, B.; Liu, Y.; Cui, S. *J. Org. Chem.* **2017**, *82*, 3950-3956.

[30] Liu, Z.; Liao, P.; Bi, X. *Org. Lett.* **2014**, *16*, 3668-3671.

[31] Chu, W. D.; Zhang, L. F.; Bao, X.; Zhao, X.-H.; Zeng, C.; Du, J. Y.; Zhang, G. B.; Wang, F. X.; Ma, X. Y.; Fan, C. A. *Angew. Chem. Int. Ed.* **2013**, *52*, 9229-9233.

Chapter 3: Section B

Gold-catalyzed C-C bond formation via 1,6-conjugate addition of *in situ* generated allenol acetate to *p*-Quinone methides

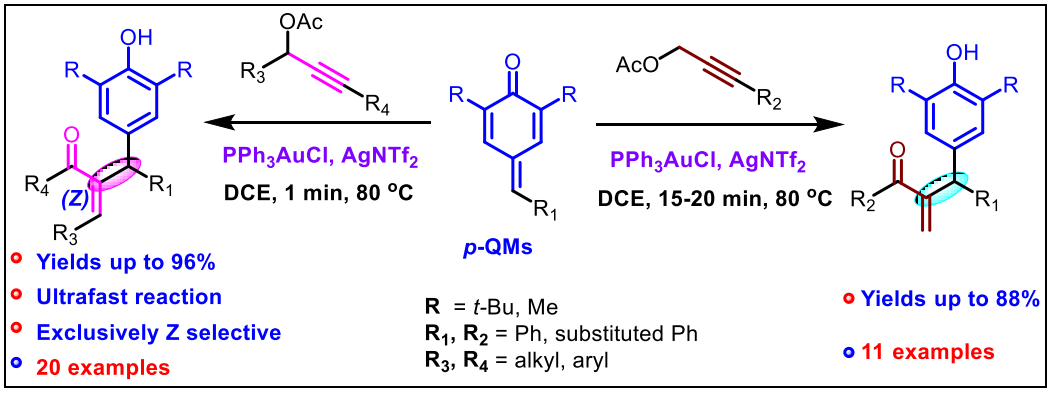

3.2.1. Introduction

Recently, the organic transformations using the soft Lewis acid (gold) catalyzed activation of C-C triple bond and allene has gained the considerable interest for the synthetic application for the construction of the organic framework of natural product analog and complex compounds.[1] Propargylic esters could undergo the [3,3]-sigmatropic rearrangement under the influence of homogeneous gold catalysis, leads to the in situ generations of gold carbene of allenol ester intermediate followed by trapping with intermolecular[2] and intramolecular [3] nucleophiles (Figure 1, Path I)

Nevertheless, to the best of our knowledge, there are only a very few reports documented in the literature to study the inherent nucleophilicity of the allenol ester,[4] which could be generated during the course of reaction via gold catalyzed [3,3]-sigmatropic rearrangement (Figure 1, Path II).

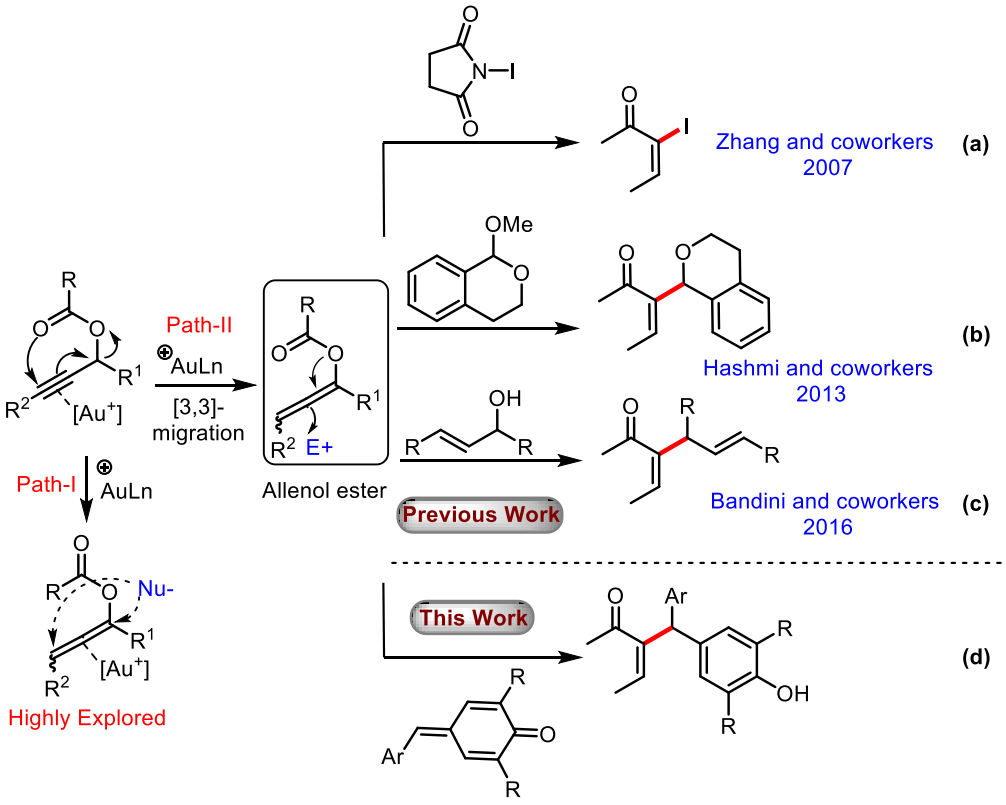

Figure 1: Intermolecular nucleophilic trapping of allenol ester generated *in situ* via gold catalyzed [3,3]-sigmatropic rearrangement

3.2.2 Literature review

In this direction, in 2007, Zhang and co-workers first developed the methods for the intermolecular trapping of the nucleophilic allenol ester with electrophilic halogens (NIS, NBS) to construct the C-X (X = Br and I) bond and synthesized the α-haloenones

(Figure 1a).[5]

In 2013, Hashmi and co-workers pioneered the application of the inherent nucleophilicity of the allenol ester for the construction of the $C(sp^3)–C(sp^2)$ bond. They have reported the gold triggered activation of alkynol ester for sigmatropic rearrangement which in situ generates the allenol ester. Simultaneously gold catalyst also acts as Lewis acid and activates acetal derivatives to generate the electrophilic oxocarbenium ions, which reacts with the nucleophilic allenol ester and produces the interesting substituted enones (Figure 1b).[6]

In this line, lastly in 2017, Bandini and co-workers have developed the *α*-functionalization of enones with allyl alcohol via gold catalyzed generation of nucleophilic allenol carboxylate through [3,3]-sigmatropic rearrangements (Figure 1c).[7] They have proposed that the Brønsted acid (pivalic acid) plays the role for the activation of allylic alcohol and assisting the formation of carbocation which could be trapped by allenol carboxylate and forms the *α*-functionalization of enones.

3.2.3 Present work

With the above literature background, the nucleophilic property of the allenol ester is less explored. On the continuation of the on-going research project in our lab for the exploration of the electrophilicity of the *p*-QMs,[8] we envisioned that the *in situ* generated nucleophilic intermediate could serve as an efficient counter partner for the intermolecular 1,6-conjugate addition with the electrophilic *p*-QMs. This method could be complementing the MBH reaction and delivers the variety of the unsymmetrical diarylmethine substituted enones as depicted in Figure 1d.

3.2.4 Results and discussion

3.2.4.1 Optimization of reaction conditions

To validate our hypothesis for gold catalyzed intermolecular nucleophilic 1,6-addition of allenol ester, *p*-QMs **1a,** and the propargylic ester **2a** were selected as a model substrate for the optimization of reaction conditions. The various parameters like catalyst, solvent, and temperature were scrutinized to establish the optimum reaction condition, and the obtained results are as illustrated in Table 1.

In the beginning, when the reaction was performed with gold(I)chloride as a catalyst in the toluene and the reaction mass was heated up to the 60 °C the expected product was not obtained and one of the reagent propargylic acetate was utterly consumed within the 5 minutes (Table 1, entry 1). Excitingly, when DCM was used as a solvent in place of

toluene, the desired compound **3a** was obtained in moderate yield (56%) with exclusive *Z*-selectivity (Table 1, entry 2). When the temperature was decreased to rt, the reaction becomes sluggish and its took up to 24 h for the complete consumption of starting material as monitored by TLC, there was no any improvement in the yield (Table 1, entry 3). In further endeavors to optimize the condition, we switched over to the harder catalyst $AuCl_3$ in CH_2Cl_2, the reaction was completed at rt and resulted in 51% yield of compound **3a** (Table 1, entry 4).

Table 1: Optimization of reaction conditions [a]

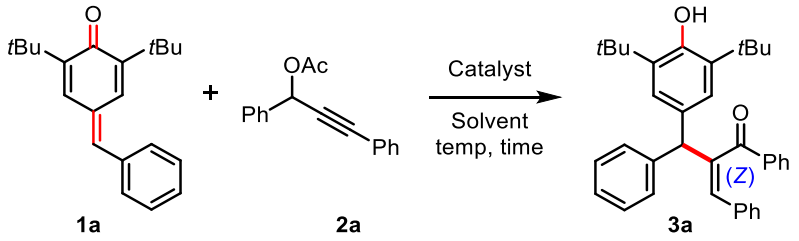

Entry	Catalyst	Solvent	Time Min/h	Yield %[b] 3a	*Z*: *E*
1	AuCl	toluene	5	N.R	--
2	AuCl	CH_2Cl_2	5	56	*Z*
3[c]	AuCl	CH_2Cl_2	24 h	48	*Z*
4[c]	$AuCl_3$	CH_2Cl_2	5	51	*Z*
5	$Ph_3PAuCl/AgNTf_2$	CH_2Cl_2	5	50	*Z*
6[c]	$Ph_3PAuCl/AgNTf_2$	DCE	60	59	1.5:1
7[e]	**$Ph_3PAuCl/AgNTf_2$**	**DCE**	**1**	**95**	***Z***
8[d]	$SPhosAuCl/AgNTf_2$	DCE	1	88	*Z*
9[d]	Dichloro(2-pyridine carboxylato)Au	DCE	3 h	24	*Z*
10[d,e]	$Ph_3PAuCl/AgNTf_2$	DCE	1	97	4:1
11[d]	$Ph_3PAuCl/AgNTf_2$	toluene	1	42	*Z*
12[d]	$Ph_3PAuCl/AgNTf_2$	CH_3CN	3 h	N.R	--
13[d]	$Ph_3PAuCl/AgNTf_2$	1,4-Dioxane	1	24	*Z*
14[d]	$AgNTf_2$	DCE	3 h	42	*Z*
15[d,f]	$Ph_3PAuNTf_2$	DCE	30	74	*Z*

[a] Reaction conditions:, 0.1 mmol **1a**, 1 equiv. **2a**, 5 mol % catalyst, 5 mol % $AgNTf_2$, 1 mL solvent, unless otherwise stated and heated at 60 °C. [b] yields, *Z*:*E* selectivity determined using ^{1}H-NMR, [c] Reaction carried out at rt, [d] Reaction carried out at 80 °C, [e] Pivaloyl ester **2h** was used, [f] Precipitate of AgCl filtered off, [g] N.R = No reaction.

Both catalysts were found inefficient to obtain the desired product. For the yield optimization, we screened the reaction with gold complex in combinations of Ag (I) salts. We began with the $Ph_3PAuCl/AgNTf_2$ combination in DCM; the reaction was completed within 5 minutes but could not lead to improvement in the outcome (Table 1, entry 5). Surprisingly, when the same catalyst $PPh_3AuCl/AgNTf_2$ combination was used in DCE, first at r.t *Z*/*E* mixture (1.5:1 as confirmed by ^{1}H-NMR analysis) of product **3a** was obtained with a slight increase in the yield (59%) (Table 1, entry 6). Gratifyingly, when the reaction was heated at 80 °C under the similar condition, the yield of the desired compound **3a** was drastically increased to 95% with exclusive Z-selectivity, and the reaction was also completed within 1 minute (Table 1, entry 7). From the above results, it could be seen that when the reaction was carried out at a higher temperature, it leads to the formation of *Z*-selective product exclusively.

After having these observations, further we have screened other gold/silver combination catalyst like $SPhosAuCl/AgNTf_2$ to get almost comparable yield of **3a** with *Z*-selectivity (Table 1, entry 8), when dichloro(2-pyridinecarboxylato)gold was used, the reaction becomes slower, and resulted in poor yield of **3a** (24%) (Table 1, entry 9).

Additionally, when propargylic pivolate was used in place of acetate, it significantly diminished the selectivity (with *Z*/*E* ratio 4:1) of the desired enone **3a** (Table 1, entry 10). Moreover, to find the best solvent for the reaction we have screened the reaction condition (entry 7) with different solvents like toluene, acetonitrile, and 1,4-dioxane but there was no significant improvement in the yields (Table 1, entry 11-13). To study the role of silver in the reaction, we have performed the control experiments. When the reaction was performed without gold complex and using the only $AgNTf_2$, the desired product was obtained in only 42% yield with complete *Z*-selectivity (Table 1, entry 12) but it becomes sluggish and completed in 3h. Next, to exclude the plausible involvement of silver during the reaction, the precipitates of AgCl was filtered off before the addition of other reagents **1a** and **2a** in the reaction vessel, the reaction was completed within 30 minutes, and the desired product **3a** was obtained in 74% yield (Table 1, entry 15). From these results, we concluded that silver might have a minimal role in enhancing the rate of reaction. But the gold(I)-complex *in situ* generated by the exchange of ligands with the Ag(I)salt plays an important role either for the activation of alkynes by Meyer–Schuster type [3,3]-sigmatropic rearrangement or *p*-QMs activation by acting as Lewis acid for the facile 1,6-conjugated addition.

3.2.4.2 Substrate scope for the formation of internal enones

Having optimized the reaction conditions (Table 1, entry 7), we proceeded further to examine the generality and the substrate scope of gold-catalyzed nucleophilic 1,6-conjugate addition. We screened the wide range of substituted *p*-QMs (**1a–1j**) and secondary propargylic acetates (**2a–2f**) containing neutral, electron-donating and -withdrawing functional groups (Table 2). The scope of the developed protocol was studied by first changing *p*-QMs (**1a**–**1j**), with 1,3-diphenyl-propargylic acetate **2a,** which undergo nucleophilic addition under the optimized condition and smoothly delivered the corresponding α-substituted enones (**3a–3j**) in good to excellent yields (**71**–**96**%) with exclusive *Z*-selectivity.

Table 2: Substrate scope for the formation of internal enones

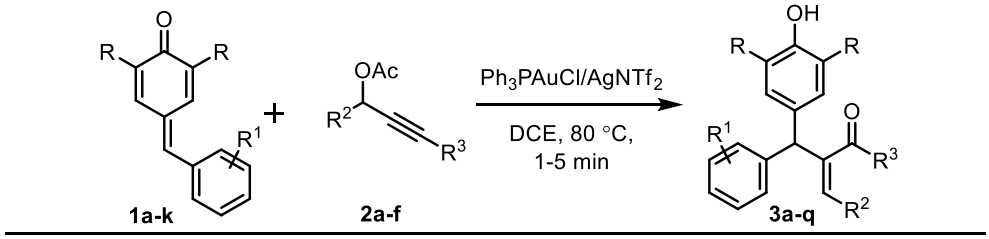

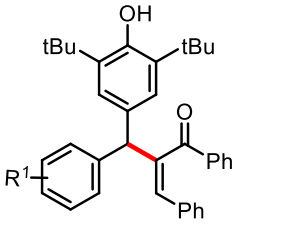

3a, R^1 = H, 95%
3b, R^1 = 4-Me, 96%
3c, R^1 = 4-OMe, 91%
3d, R^1 = 3,4-$(OMe)_2$, 71%
3e, R^1 = 3,4,5-$(OMe)_3$, 75%
3f, R^1 = 3,5-$(OMe)_2$, 73%
3g, R^1 = 1-naphthyl, 93%
3h, R^1 = 4-CO_2Me, 74%
3i, R^1 = 4-Cl, 87%

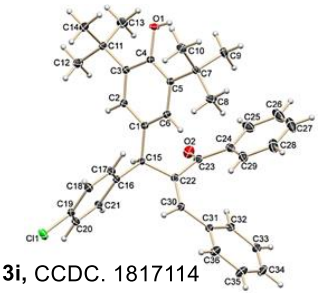

3i, CCDC. 1817114

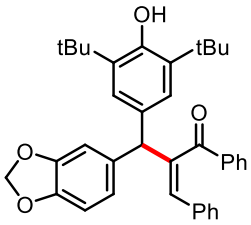

3j, 82%

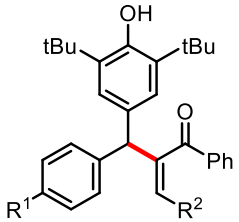

3k, R^1= -Cl, R^2= Me, 73%
3l, R^1= -CO_2Me, R^2= Me, 89%
3m, R^1= -H, R^2= *i*-Pr, 84%

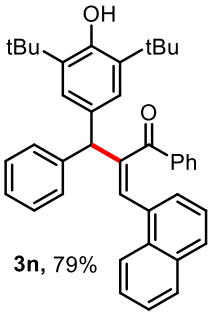

3n, 79%

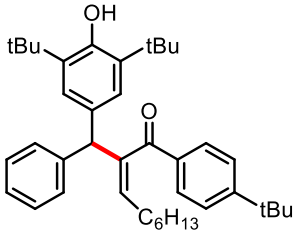

3o, 74%

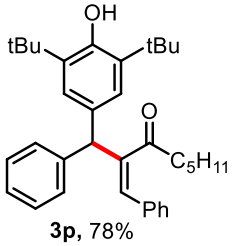

3p, 78%

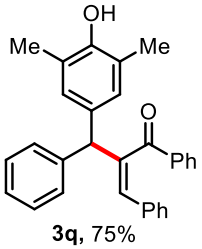

3q, 75%

Additionally, *p*-QMs synthesized from aromatic aldehydes containing a variety of functional group with electron-donating and electron-withdrawing property and present at various positions of the aromatic ring were compatible with the optimized condition, without much influence on the yields of the corresponding products. The proton NMR displayed the characteristic signals for all the functional group present on the core structure, such as singlet at δ 1.37 ppm with 18H represents two *tert*-butyl groups of *p*-QMs. Two singlet signals at δ 5.09 and 5.31 ppm represents the benzylic CH group and -OH respectively. The singlet at δ 6.57 ppm represents the presence of alkene hydrogen. In proton decoupled carbon NMR, the compound **3i** shows the twenty one different signals which are in good accordance with the proposed structure. Further, the elemental formula was confirmed by the HRMS analysis. The stereochemistry of the enone double bond was determined by the single crystal XRD analysis of compound **3i** and the geometry of double bond unambiguously found to be Z.

Subsequently, we explored the scope of propargylic acetate under the developed conditions. Interestingly, various electronically different symmetrical and unsymmetrical secondary propargylic acetates with linear and branched alkyl substitution like methyl, isopropyl, and long-chain alkane smoothly undergo 1,6-conjugate addition with *p*-quinone methides to deliver the corresponding products (**3k**–**3p**) in good yields (**73**–**89**%). A relatively less stable derivative which contains 2,6-dimethyl in place of *t*-butyl group, *p*-quinone methide **1k** readily reacted with the propargylic acetate **2a** and delivered the desired addition product **3q** in good yield (75%).

3.2.4.3 Substrate scope for the formation of terminal enones

To demonstrate the adaptability of the proposed methodology, various derivative of *p*-QMs successfully reacted with a series of primary propargylic acetates (**4a–4e**) under the optimized reaction condition to get the enones with *an exo*-double bond (Table 3).

Satisfyingly, primary propargylic ester **4a** reacted with *p*-QMs containing functional group like alkyl, aryl, ester, methoxy, and chloro substitution at the C4-position, irrespective of the electronic nature of the substituents readily affording respective α-substituted terminal enones (**5a**–**5h**) in good yields (**75**–**88**%). Next, we screened the various derivative of primary propargylic esters (**4a**–**4d**) containing different alkyl, methoxy and bromo substitutions which smoothly undergo 1,6-conjugate addition with *p*-QMs resulting in the formation of product (**5i**–**5k**) in excellent yields (**74**–**81**%).

Table 3: Substrate scope for the formation of terminal enones

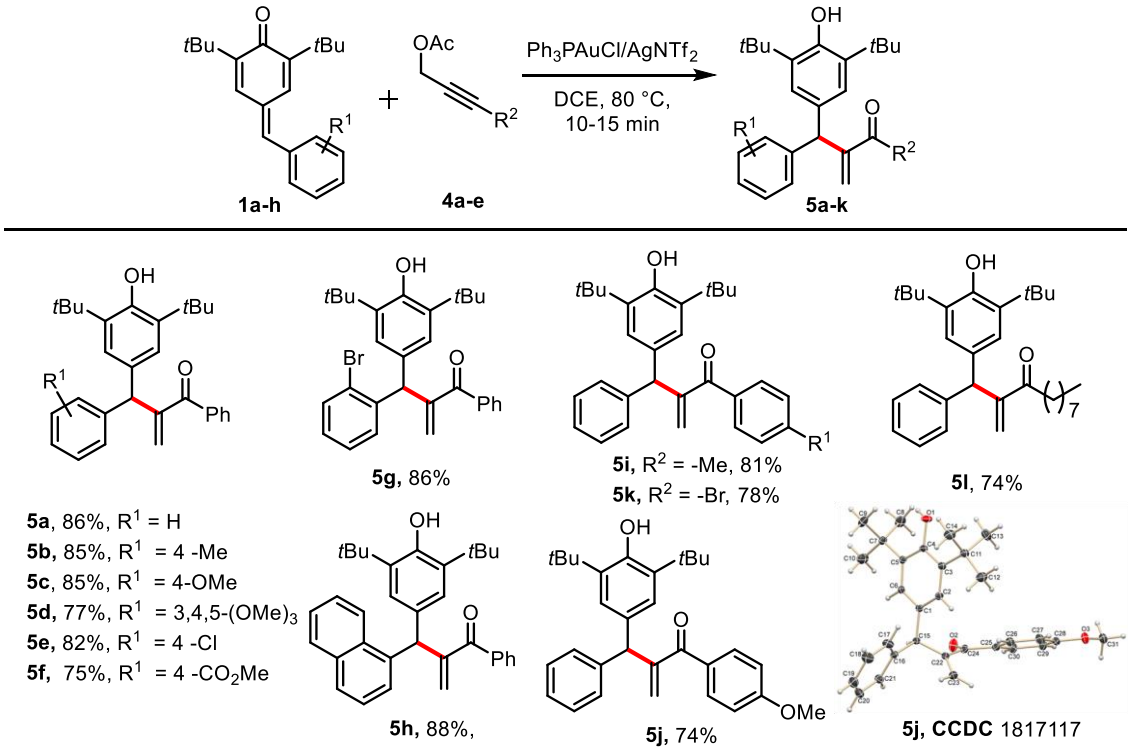

The long chain aliphatic propargylic ester **4e** also easily reacted with *p*-QMs **2a,** and the desired product **5l** was obtained in **74%** yield. The structure of terminal enones was unambiguously proven by a single-crystal XRD analysis of compound **5h** and **5j**.

3.2.4.4 The plausible reaction mechanism

Based on the literature report the plausible mechanism has been proposed.

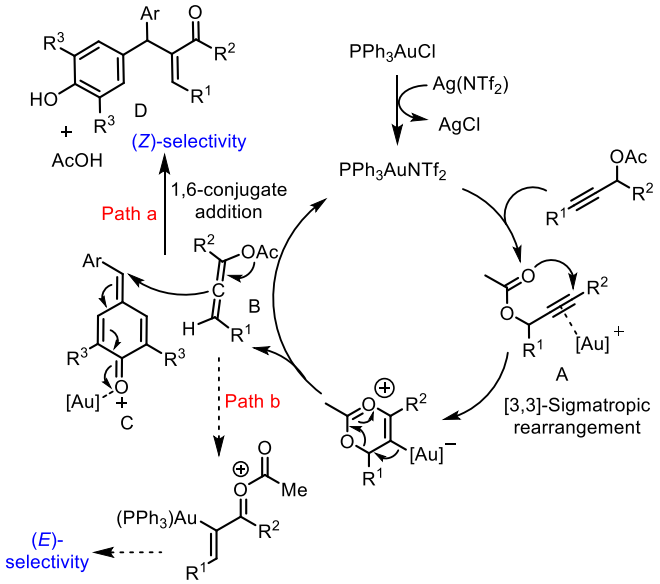

Figure 2: The plausible reaction mechanism

The reaction proceeds by gold catalyzed activation of triple bond of propargylic ester to give π-complex intermediate **A,** which undergoes [3,3]-sigmatropic rearrangement and generates nucleophilic allenol ester **B**, which is further reacted with Au-complex activated *p*-QMs **C**, furnished the desired MBH product **D** (Scheme 2). The stereoselectivity of the reaction is based on the literature report by Zhang *et al*. which shows that, if reaction proceeds *via* formation of carboxy allene **B** (**path a**) it leads to the formation of *Z*-selective product.[5]

3.2.4.6 Synthetic utility of enones

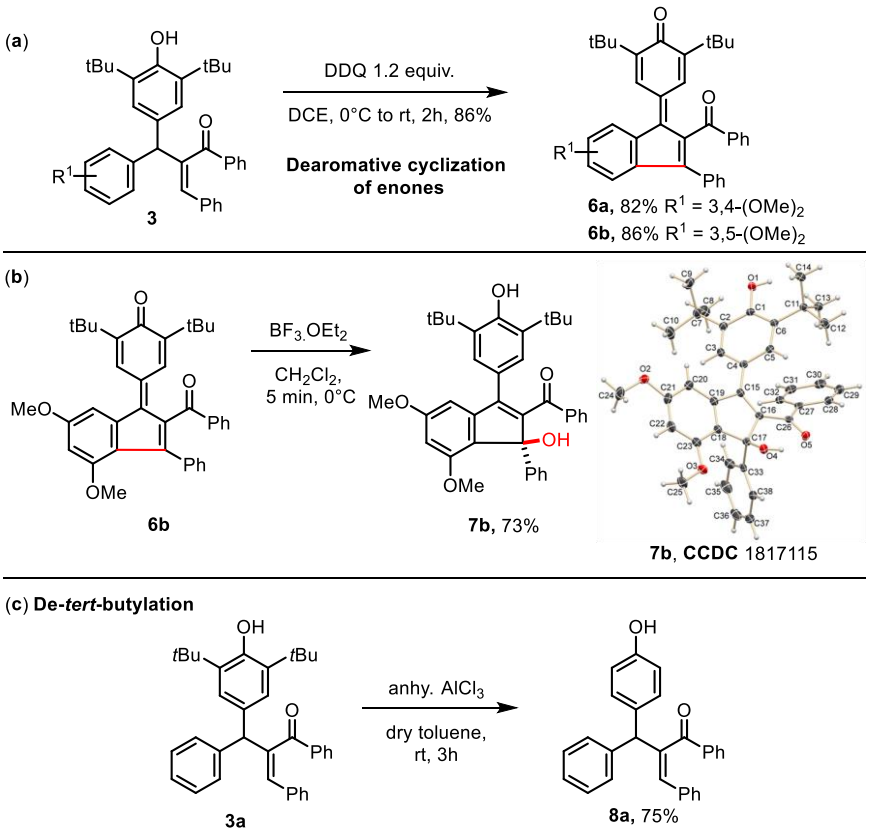

Scheme 1: Synthetic utility of enones

Finally, product modification was performed to demonstrate the synthetic utility of the proposed methodology. The compound **3d** and **3f** were treated with DDQ for oxidative dearomative cyclization to afford cyclic *p*-quinone 6a and 6b with extended conjugation (Scheme 1a) in excellent yields (82-86%). Further on treatment with $BF_3.OEt_2$ in moist CH_2Cl_2 at 0 °C compound **6b** underwent the aromatization followed by the attack of water molecules to give the interesting highly substituted indene core **7b,** the structure of the compound **7b** was unambiguously determined by a single crystal XRD analysis (Scheme 4b). Further, we demonstrated the product modification by performing removal of the *tert*-

butyl group of compound **3a** on treatment with anhydrous $AlCl_3$. The reaction smoothly delivered the product **8a** in 75% yield (Scheme 1c).

3.2.5 Conclusions

We have reported a gold (I) catalyzed [3,3]-sigmatropic rearrangement of propargylic acetate followed by trapping of incipient nucleophilic allenol ester with *p*-QMs. The developed protocol demonstrates a wide substrate scope with an array of *p*-QMs & propargylic acetates leading to the formation of MBH product, with excellent selectivity in favor of sole *Z*-isomer. The product diarylmethine-substituted enones further served as an important building block to synthesize highly functionalized indene derivatives *via* DDQ mediated oxidative dearomative cyclization.

3.2.6 Experimental:

3.2.6.1 General method for preparation of Secondary Propargylic Acetate: [9]

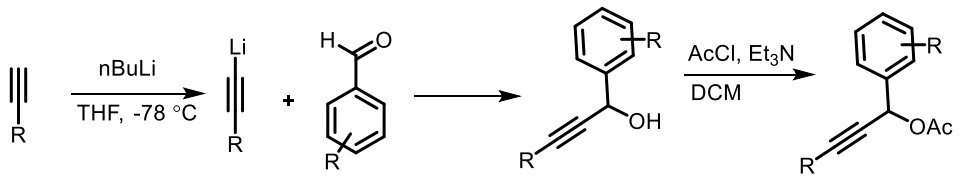

To a stirred solution of alkyne (15 mmol) in freshly dried THF (20 ml) at -78 ^{o}C was slowly added *n*-BuLi (1.6 M solution in hexane, 7.6 mL, 12.2 mmol) under argon atmosphere. The reaction mixture was stirred at -78 °C for 30 min and at room temperature for an additional 15 min. After addition of aldehyde (10 mmol) in 10 mL of THF at -78 ^{o}C, the reaction mixture was allowed to warm up to room temperature gradually, and was stirred for an additional 1h. The mixture was quenched by the saturated solution of NH_4Cl and then extracted with ethyl acetate (3 × 20 mL). The combined organic layer was washed with brine, dried over anhydrous Na_2SO_4 and concentrated under the reduced pressure to give secondary propargylic alcohol as a colorless liquid in excellent yields, which was used in subsequent steps without any further purification.

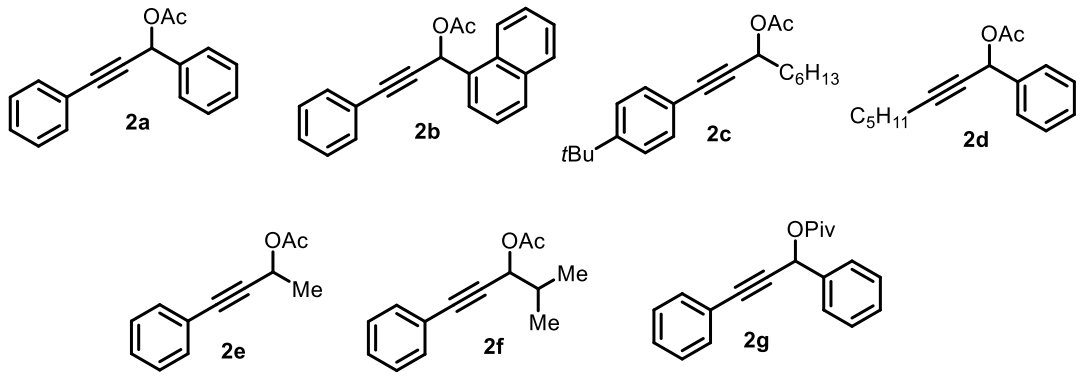

Figure 3: Synthesised Secondary Propargylic Acetate

To a solution of propargyl alcohol (10 mmol) in anhydrous CH_2Cl_2 (20 ml) was added Et_3N (20 mmol, 2.8 ml, 2 equiv) and a catalytic amount of DMAP (0.05 equiv) followed by addition of acetyl chloride/pivaloyl chloride (1.2 equiv) at 0 °C. The reaction mixture was stirred at room temperature for 2 h. After completion of the reaction (TLC), the reaction was quenched with ice cold water and mixture was diluted with CH_2Cl_2 (25 ml) and washed with 1.0 M aqueous HCl solution (25 mL × 2). Further, the organic layer was sequentially washed with sat. $NaHCO_3$ solution (20 mL × 2), water (20 ml) and sat. Na_2SO_4 solution. The combined organic layer was dried over anhydrous Na_2SO_4 and concentrated under reduced pressure. The product was purified by flash silica gel column

chromatography using pet ether /ethyl acetate as eluent to afford propargylic acetates **2a**–**2h**.

3.2.6.2 General Procedure for Preparation of Primary Propargylic acetate: [10]

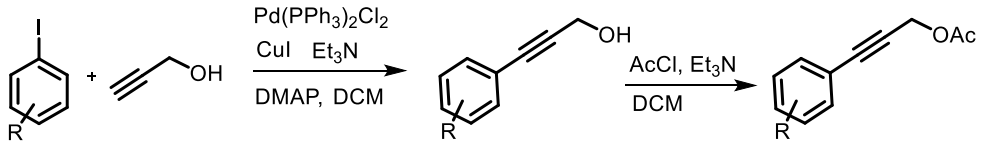

To a solution of $Pd(PPh_3)_2Cl_2$ (0.1 mmol, 70.2 mg, 1.0 mol%), CuI (0.2 mmol, 38 mg, 2.0 mol%) and iodobenzene (2.04 g, 10 mmol) in dry degassed Et_3N (40 mL) was added propargyl alcohol (0.62 g, 11 mmol, 1.1 equiv) under argon atmosphere. The reaction mixture was stirred at room temperature until the iodobenzene was consumed, as indicated by TLC. The reaction mixture was filtered through celite, washed with EtOAc, and the combined organic layer was evaporated under the reduced pressure. The residue was purified by flash silica gel column chromatography using petroleum ether: EtOAc (5:1 to 2:1) as an eluent to give the corresponding coupled aryl propargylic alcohol in good to excellent yields.

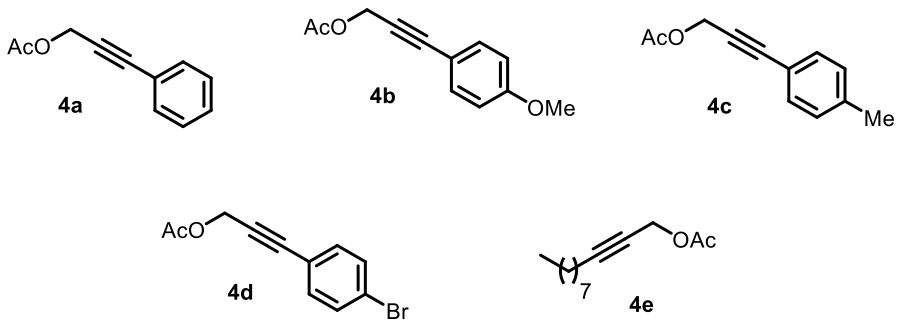

Figure 4: Preparation of Primary Propargylic acetate

To a stirred solution of aryl propargylic alcohol (1.32 g, 10.0 mmol), Et_3N (7.0 mL, 50.0 mmol) and 4-(dimethylamino)pyridine (DMAP) (127.5 mg, 1.05 mmol) in CH_2Cl_2 (50 mL) at 0 °C was slowly added acetyl chloride (1.1 equiv.) under argon atmosphere and the mixture was warmed to room temperature. After stirring for 2 h, the reaction mixture was quenched with water and extracted with CH_2Cl_2. The combined organic layer was washed with 1.0 M aqueous solution of HCl and sat. solution of $NaHCO_3$, dried over Na_2SO_4 and concentrated under reduced pressure. The obtained residue was purified by silica gel column chromatography (pet. ether /EtOAc) to afford the pure desired product **4a–4d** as a

colorless oil. Compound **4e** was prepared according to general procedure I as a colorless liquid in 65% yield.

Undec-2-yn-1-yl acetate (4e):

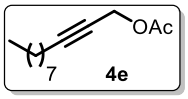

Colourless liquid; ***Rf*** = 0.72 (pet. ether: ethyl acetate = 9:1);

^{1}H NMR (200MHz, $CDCl_3$) δ = 4.66 (t, *J* = 2.0 Hz, 2 H), 2.27 - 2.15 (m, 2 H), 2.09 (s, 3 H), 1.60 - 1.43 (m, 2 H), 1.42 - 1.24 (m, 10 H), 0.87 ppm (t, *J* = 6.7 Hz, 3 H);

^{13}C NMR (50MHz, $CDCl_3$) δ = 170.3, 87.7, 73.8, 52.8, 31.8, 29.1, 29.0, 28.8, 28.4, 22.6, 20.8, 18.7, 14.0 ppm;

HRMS (ESI-TOF) m/z: $[M+Na]^+$ calcd for $C_{13}H_{22}O_2Na$ 233.1512; found 233.1510.

3.2.6.3 General Procedure for Synthesis of *p*-Quinone Methide:[11]

In an oven dried Dean-Stark apparatus, phenol (25.0 mmol) and the corresponding aldehyde (25.0 mmol, 1 equiv.) were taken in toluene (100 mL), reaction mixture was heated to reflux followed by drop wise addition of piperidine (50.0 mmol, 5ml, 2 equiv.) within 1h. Then, the reaction mixture was continued to reflux for 6 h. After cooling just below the boiling point of the reaction mixture, acetic anhydride (50.0 mmol, 4.7ml 2 equiv.) was added and stirring was continued for 30 min. Then the reaction mixture was poured on ice-water (500 mL) with continuous stirring and extracted with CH_2Cl_2 (4 × 200 mL). The combined organic phase was dried over anhydrous Na_2SO_4 and the solvent was evaporated under reduced pressure. The crude products were purified by column chromatography and further recrystallized from *n*-hexane, affording *p*-quinone methide (**1a-1j**) in good yields. Compound **1k** was prepared according to literature report.[12]

3.2.6.4 General Procedure for the gold catalyzed reaction:

To an oven dried screw cap vial (3 ml), Ph_3PAuCl (0.005 mmol, 2.5 mg, 5 mol %) and $AgNTf_2$ (0.005 mmol, 2 mg, 5 mol %) were dissolved in 1 ml of moist DCE. The reaction mixture was allowed to stir at room temperature for 5-10 min during which solution became turbid (as AgCl was precipitated out) followed by subsequent addition of *p*-QMs **1** (0.1 mmol, 1 equiv.) and propargylic acetate **2** (1 equiv.). The reaction mixture was stirred in the preheated oil bath at 80 °C and the completion of the reaction was monitored by TLC. After the completion of reaction, mixture was cooled to the room temperature, and

diluted with ethyl acetate and concentrated under reduced pressure. The crude product was purified by flash column chromatography using (pet. ether /EtOAc) ether as eluent to afford the desired product diarylmethine-substituted enones.

(*Z*)-2-((3,5-Di-*tert*-butyl-4-hydroxyphenyl)(phenyl)methyl)-1,3-diphenylprop-2-en-1-one (3a):

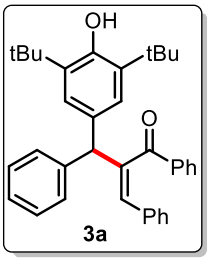

3a

White solid; mp = 73-75 ºC; *Rf* = 0.65 (pet. ether: ethyl acetate = 9:1);

^{1}H NMR (400MHz, $CDCl_3$) δ = 7.71 (d, *J* = 7.9 Hz, 2 H), 7.38 (d, *J* = 7.3 Hz, 2 H), 7.31 (t, *J* = 7.3 Hz, 3 H), 7.22 (d, *J* = 6.7 Hz, 1 H), 7.19 - 7.15 (m, 2 H), 7.09 (s, 2 H), 7.09 – 7.01 (m, 5 H), 6.57 (s, 1 H), 5.35 (s, 1 H), 5.06 (s, 1 H), 1.37 ppm (s, 18 H);

^{13}C NMR (100MHz, $CDCl_3$) δ = 200.0, 152.4, 144.5, 141.9, 136.1, 136.0, 135.5, 133.3, 132.6, 130.9, 129.5, 128.7, 128.2, 128.0, 127.9, 127.5, 126.5, 126.2, 56.4, 34.3, 30.3 ppm;

HRMS (ESI-TOF) m/z: $[M+Na]^+$ calcd for $C_{36}H_{38}O_2Na$ 525.2764; found 525.2758;

(*Z*)-2-((3,5-Di-*tert*-butyl-4-hydroxyphenyl)(*p*-tolyl)methyl)-1,3-diphenylprop-2-en-1-one (3b):

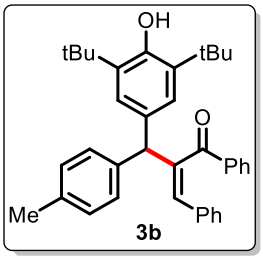

3b

Colourless thick liquid; ***Rf*** = 0.61 (pet. ether: ethyl acetate = 9:1);

^{1}H NMR (400MHz, $CDCl_3$) δ = 7.75 - 7.70 (m, 2 H), 7.34 - 7.29 (m, 1 H), 7.28 - 7.25 (m, 2 H), 7.18 (t, *J* = 7.8 Hz, 2 H), 7.13 (d, *J* = 7.8 Hz, 2 H), 7.10 (s, 2 H), 7.09 - 7.02 (m, 5 H), 6.58 (s, 1 H), 5.32 (s, 1 H), 5.05 (s, 1 H), 2. 33 (s, 3 H), 1.38 ppm (s, 18 H);

^{13}C NMR (100MHz, $CDCl_3$) δ = 200.0, 152.3, 144.7, 138.9, 136.2, 136.0, 135.9, 135.4, 133.1, 132.6, 131.0, 129.5, 129.3, 129.0, 128.7, 128.0, 127.9, 127.4, 126.1, 56.1, 34.3, 30.3, 21.0 ppm;

HRMS (ESI-TOF) m/z: $[M+Na]^+$ calcd for $C_{37}H_{40}O_2Na$ 539.2921; found 539.2916.

(*Z*)-2-((3,5-Di-*tert*-butyl-4-hydroxyphenyl)(4-methoxyphenyl)methyl)-1,3-diphenyl prop-2-en-1-one (3c):

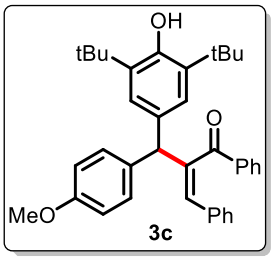

Colourless thick liquid; ***Rf*** = 0.42 (pet. ether: ethyl acetate = 95:5);

^{1}H NMR (400MHz, $CDCl_3$) δ = 7.71 (s, 1 H), 7.69 (app. d, *J* = 1.4 Hz, 1 H), 7.32 - 7.25 (m, 3 H), 7.19 - 7.13 (m, 2 H), 7.09 - 7.01 (m, 7 H), 6.84 (d, *J* = 8.7 Hz, 2 H), 6.54 (s, 1 H), 5.28 (s, 1 H), 5.04 (s, 1 H), 3.78 (s, 3 H), 1.36 ppm (s, 18 H);

^{13}C NMR (100MHz, $CDCl_3$) δ = 200.1, 158.1, 152.3, 144.8, 136.1, 136.0, 135.5, 134.0, 133.0, 132.6, 131.2, 130.5, 129.5, 128.7, 128.0, 127.9, 127.5, 126.1, 113.6, 55.7, 55.2, 34.3, 30.3 ppm;

HRMS (ESI-TOF) m/z: $[M+H]^+$ calcd for $C_{37}H_{41}O_3$ 533.3050; found 533.3047.

(*Z*)-2-((3,5-Di-*tert*-butyl-4-hydroxyphenyl)(3,4-dimethoxyphenyl)methyl)-1,3-diphenyl prop-2-en-1-one(3d):

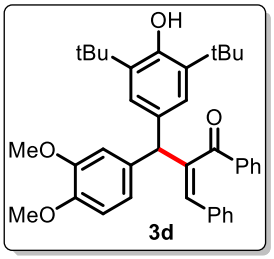

White solid: mp = 73-76 ºC; ***Rf*** = 0.48 (pet. ether: ethyl acetate = 9:1);

^{1}H NMR (400MHz, $CDCl_3$) δ = 7.74 (d, *J* = 1.4 Hz, 1 H), 7.72 (d, *J* = 1.4 Hz, 1 H), 7.32 - 7.29 (m, 1 H), 7.18 (t, *J* = 1.4 Hz, 2 H), 7.12 (s, 2 H), 7.10 - 7.03 (m, 5 H), 6.94 - 6.90 (m, 2 H), 6.83 (d, *J* = 8.2 Hz, 1 H), 6.58 (app. d, *J* = 1.4 Hz, 1 H), 5.31 (app. d, *J* = 0.9 Hz, 1 H), 5.08 (s, 1 H), 3.86 (s, 3 H), 3.83 (s, 3 H), 1.39 ppm (s, 18 H);

^{13}C NMR (100MHz, $CDCl_3$) δ = 200.0, 152.4, 148.6, 147.5, 144.7, 136.0, 135.9, 135.5, 134.3, 133.0, 132.6, 131.0, 129.5, 128.7, 128.0, 127.9, 127.5, 126.0, 121.6, 112.8, 110.8, 56.1, 55.8, 55.7, 34.3, 30.3 ppm;

HRMS (ESI-TOF) m/z: $[M+H]^+$ calcd for $C_{38}H_{43}O_4$ 563.3156; found 563.3150.

(*Z*)-2-((3,5-Di-*tert*-butyl-4-hydroxyphenyl)(3,4,5-trimethoxyphenyl)methyl)-1,3-diphenylprop-2-en-1-one (3e):

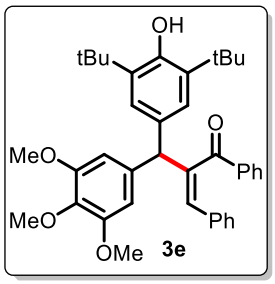

Pale yellow solid; mp = 139-141 ºC; ***Rf*** = 0.32 (pet. ether: ethyl acetate = 95:5);

^{1}H NMR (400MHz, $CDCl_3$) δ = 7.72 - 7.69 (m, 2 H), 7.34 - 7.28 (m, 1 H), 7.19 - 7.15 (m, 2 H), 7.13 (s, 2 H), 7.10 - 7.03 (m, 5 H), 6.60 (s, 2 H), 6.59 (app. d, *J* = 1.4 Hz, 1 H), 5.29 (app. d, *J* = 0.9 Hz, 1 H), 5.09 (s, 1 H), 3.82 (s, 3 H), 3.79 (s, 6 H), 1.39 ppm (s, 18 H);

^{13}C NMR (100MHz, $CDCl_3$) δ = 200.0, 152.9, 152.5, 144.4, 137.4, 136.4, 136.1, 135.9, 135.6, 133.1, 132.7, 130.6, 129.5, 128.7, 128.0, 127.9, 127.6, 126.1, 106.7, 60.8, 56.7, 56.0, 34.3, 30.3 ppm;

HRMS (ESI-TOF) m/z: $[M+Na]^+$ calcd for $C_{39}H_{44}O_5Na$ 615.3081; found 615.3073.

(*Z*)-2-((3,5-Di-*tert*-butyl-4-hydroxyphenyl)(3,5-dimethoxyphenyl)methyl)-1,3-diphenylprop-2-en-1-one (3f):

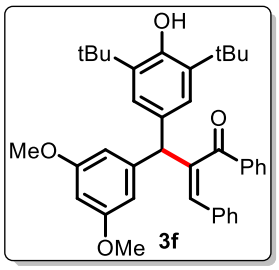

Pale yellow solid; mp = 74-76 ºC; ***Rf*** = 0.28 (pet. ether: ethyl acetate = 9:1);

^{1}H NMR (500MHz, $CDCl_3$) δ = 7.73 – 7.69 (m, 2 H), 7.32 - 7.28 (m, 1 H), 7.16 (t, *J* = 7.6 Hz, 2 H), 7.11 (s, 2 H), 7.09 - 7.02 (m, 5 H), 6.61 (d, *J* = 1.1 Hz, 1 H), 6.54 (d like, *J* = 2.3 Hz, 2 H), 6.32 (t, *J* = 2.1 Hz, 1 H), 5.29 (s, 1 H), 5.05 (s, 1 H), 3.75 (s, 6 H), 1.37 ppm (s, 18 H);

^{13}C NMR (100MHz, $CDCl_3$) δ = 199.9, 160.6, 152.5, 144.5, 144.1, 136.1, 136.0, 135.5, 133.5, 132.6, 130.5, 129.6, 128.8, 128.0, 127.9, 127.5, 126.1, 107.8, 98.5, 56.6, 55.2, 34.3, 30.3 ppm;

HRMS (ESI-TOF) m/z: $[M+H]^+$ calcd for $C_{38}H_{43}O_4$ 563.3156; found 563.3151.

(*Z*)-2-((3,5-Di-*tert*-butyl-4-hydroxyphenyl)(naphthalen-1-yl)methyl)-1,3-diphenylprop-2-en-1-one (3g):

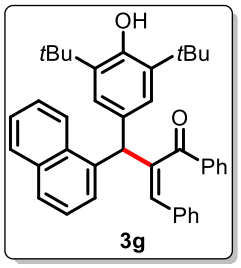

White solid; mp = 144-146 ºC; ***Rf*** = 0.52 (pet. ether: ethyl acetate = 95:5);

^{1}H NMR (400MHz, $CDCl_3$) δ = 8.58 (d, *J* = 8.2 Hz, 1 H), 7.85 (dd, *J* = 1.4, 8.2 Hz, 1 H), 7.77 - 7.72 (m, 3 H), 7.60 - 7.56 (m, 1 H), 7.50 - 7.46 (m, 1 H), 7.45 - 7.40 (m, 1 H), 7.30 (d, *J* = 7.8 Hz, 1 H), 7.25 (s, 2 H), 7.13 (t, *J* = 7.8 Hz, 2 H), 7.01 - 6.94 (m, 6 H), 6.51 (app. d, *J* = 1.4 Hz, 1 H), 6.23 (s, 1 H), 5.09 (s, 1 H), 1.41 ppm (s, 18 H);

^{13}C NMR (100MHz, $CDCl_3$) δ = 200.1, 152.6, 143.9, 138.8, 136.2, 135.6, 134.6, 134.0, 132.5, 131.9, 129.7, 129.7, 128.7, 128.5, 127.9, 127.7, 127.4, 126.7, 126.3, 125.5, 125.1, 124.6, 52.5, 34.4, 30.3 ppm;

HRMS (ESI-TOF) m/z: $[M+Na]^+$ calcd for $C_{40}H_{40}O_2Na$ 575.2921; found 575.2919.

Methyl (*Z*)-4-(2-benzoyl-1-(3,5-di-*tert*-butyl-4-hydroxyphenyl)-3-phenylallyl) benzoate (3h):

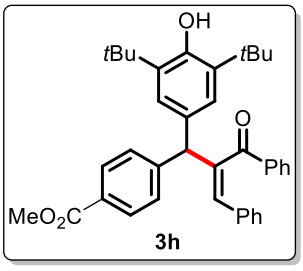

Colourless thick liquid; ***Rf*** = 0.26 (pet. ether: ethyl acetate = 95:5);

^{1}H NMR (400MHz , $CDCl_3$) δ = 7.99 (d, *J* = 8.2 Hz, 2 H), 7.70 (dd, *J* = 1.4, 8.2 Hz, 2 H), 7.46 (d, *J* = 8.2 Hz, 2 H), 7.35 - 7.30 (m, 1 H), 7.20 - 7.15 (m, 2 H), 7.09 - 7.07 (m, 4 H), 7.06 (s, 2 H), 7.05 - 7.04 (m, 1 H), 6.57 (app. d, *J* = 1.4 Hz, 1 H), 5.39 (s, 1 H), 5.09 (s, 1 H), 3.90 (s, 3 H), 1.36 ppm (s, 18 H);

^{13}C NMR (100MHz, $CDCl_3$) δ = 199.7, 167.1, 152.6, 147.5, 143.6, 136.0, 135.7, 135.7, 133.9, 132.8, 130.2, 129.6, 129.5, 129.5, 128.7, 128.4, 128.1, 128.0, 127.7, 126.1, 56.4,

52.0, 34.3, 30.2 ppm;

HRMS (ESI-TOF) m/z: $[M+H]^+$ calcd for $C_{37}H_{39}O_4$ 547.2843; found 547.2839.

(*Z*)-2-((4-Chlorophenyl)(3,5-di-*tert*-butyl-4-hydroxyphenyl)methyl)-1,3-diphenyl prop-2-en-1-one (3i):

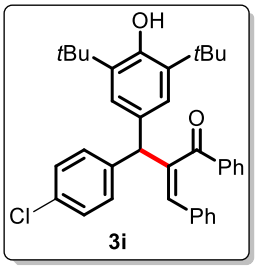

3i

White solid; mp = 143-145 ºC; ***Rf*** = 0.48 (pet. ether: ethyl acetate = 95:5);

^{1}H NMR (400MHz, $CDCl_3$) δ = 7.70 (dd, *J* = 1.4, 8.2 Hz, 2 H), 7.35 - 7.27 (m, 6 H), 7.21 - 7.16 (m, 2 H), 7.10 - 7.07 (m, 4 H), 7.06 (s, 2 H), 6.57 (aap. d, *J* = 1.4 Hz, 1 H), 5.31 (s, 1 H), 5.09 (s, 1 H), 1.37 ppm (s, 18 H);

^{13}C NMR (100MHz, $CDCl_3$) δ = 199.8, 152.6, 143.9, 140.6, 136.0, 135.7, 133.6, 132.8, 132.2, 130.8, 130.4, 129.5, 128.7, 128.4, 128.1, 128.0, 127.7, 126.0, 55.9, 34.3, 30.2 ppm;

HRMS (ESI-TOF) m/z: $[M+Na]^+$ calcd for $C_{36}H_{37}ClO_2Na$ 559.2374; found 559.2373.

(*Z*)-2-(Benzo[d][1,3]dioxol-5-yl(3,5-di-*tert*-butyl-4-hydroxyphenyl)methyl)-1,3-diphenyl prop-2-en-1-one (3j):

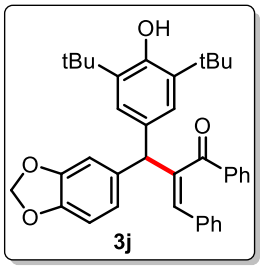

3j

Thick liquid; ***Rf*** = 0.40 (pet ether: ethyl acetate = 95:5);

^{1}H NMR (400MHz , $CDCl_3$) δ = 7.74 - 7.70 (m, 2 H), 7.35 - 7.30 (m, 1 H), 7.19 (t, *J* = 7.8 Hz, 2 H), 7.10 - 7.03 (m, 7 H), 6.88 - 6.82 (m, 2 H), 6.76 (d, *J* = 8.2 Hz, 1 H), 6.59 (app. d, *J* = 0.9 Hz, 1 H), 5.94 (s, 2 H), 5.27 (s, 1 H), 5.07 (s, 1 H), 1.38 ppm (s, 18 H);

^{13}C NMR (100MHz , $CDCl_3$) δ = 199.9, 152.4, 147.5, 146.1, 144.5, 136.1, 136.0, 135.9, 135.6, 133.3, 132.6, 130.9, 129.5, 128.7, 128.0, 127.9, 127.5, 126.0, 122.6, 110.0, 108.0, 100.9, 56.1, 34.3, 30.3 ppm;

HRMS (ESI-TOF) m/z: $[M+H]^+$ calcd for $C_{37}H_{37}O_4$ 547.2843; found 547.2839.

(*Z*)-2-((4-Chlorophenyl)(3,5-di-*tert*-butyl-4-hydroxyphenyl)methyl)-1-phenylbut-2-en-1-one (3k):

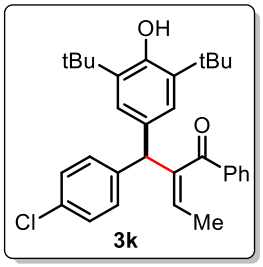

White Solid; mp = 96-99 ºC; ***Rf*** = 0.45 (pet. ether/ethyl acetate = 95:5);

^{1}H NMR (400MHz, $CDCl_3$) δ = 7.81 - 7.78 (m, 2 H), 7.53 - 7.48 (m, 1 H), 7.42 - 7.37 (m, 2 H), 7.27 - 7.21 (m, 4 H), 6.97 (s, 2 H), 5.58 (dq, *J* = 1.4, 7.2 Hz, 1 H), 5.15 (s, 1 H), 5.06 (s, 1 H), 1.56 (dd, *J* = 1.4, 7.3 Hz, 3 H), 1.37 ppm (s, 18 H)**;**

^{13}C NMR (100MHz, $CDCl_3$) δ = 199.5, 152.5, 143.7, 141.0, 137.6, 135.7, 133.0, 132.1, 131.2, 130.8, 130.1, 129.3, 128.5, 128.4, 126.0, 55.0, 34.4, 30.4, 16.1 ppm;

HRMS (ESI-TOF) m/z: $[M+Na]^+$ calcd for $C_{31}H_{35}ClO_2Na$ 497.2218; found 497.2214.

Methyl (*Z*)-4-(2-benzoyl-1-(3,5-di-*tert*-butyl-4-hydroxyphenyl)but-2-en-1-yl)benzoate (3l):

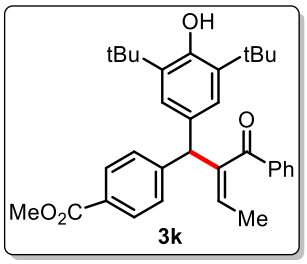

Colourless thick liquid; ***Rf*** = 0.42 (pet ether: ethyl acetate = 95:5);

^{1}H NMR (400MHz, $CDCl_3$) δ = 7.97 (d, *J* = 8.2 Hz, 2 H), 7.82 - 7.78 (m, 2 H), 7.51 (t, *J* = 7.3 Hz, 1 H), 7.42 - 7.36 (m, 4 H), 6.98 (s, 2 H), 5.61 - 5.56 (m, 1 H), 5.24 (s, 1 H), 5.07 (s, 1 H), 3.90 (s, 3 H), 1.57 (dd, *J* = 0.9, 7.3 Hz, 3 H), 1.36 ppm (s, 18 H)**;**

^{13}C NMR (100MHz, $CDCl_3$) δ = 199.3, 167.1, 152.4, 147.8, 143.4, 137.5, 135.6, 132.9, 130.8, 130.4, 129.5, 129.4, 129.2, 128.4, 128.2, 126.0, 55.5, 52.0, 34.3, 30.2, 16.1 ppm;

HRMS (ESI-TOF) m/z: $[M+H]^+$ calcd for $C_{33}H_{39}O_4$ 499.2843; found 499.2836.

(*Z*)-2-((3,5-Di-*tert*-butyl-4-hydroxyphenyl)(phenyl)methyl)-4-methyl-1-phenylpent-2-en-1-one (3m):

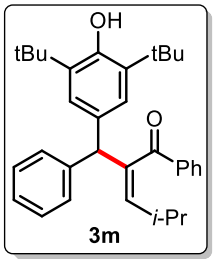

White solid; mp = 120-122 ºC; ***Rf*** = 0.48 (pet. ether: ethyl acetate = 95:5);

^{1}H NMR (400MHz, $CDCl_3$) δ = 7.78 - 7.74 (m, 2 H), 7.50 - 7.45 (m, 1 H), 7.38 - 7.33 (m, 2 H), 7.29 - 7.26 (m, 1 H), 7.26 - 7.22 (m, 3 H), 7.20 - 7.15 (m, 1 H), 6.99 (s, 2 H), 5.26 (dd, *J* = 1.4, 10.5 Hz, 1 H), 5.08 (s, 1 H), 5.03 (s, 1 H), 2.30 - 2.20 (m, 1 H), 1.35 (s, 18 H), 0.87 (d, *J* = 6.4 Hz, 3 H), 0.83 ppm (d, *J* = 6.4 Hz, 3 H);

^{13}C NMR (100MHz, $CDCl_3$) δ = 199.7, 152.2, 142.4, 141.6, 140.8, 137.7, 135.3, 132.7, 131.3, 129.4, 129.1, 128.2, 128.1, 126.2, 126.1, 55.0, 34.3, 30.3, 29.0, 22.6, 22.5 ppm;

HRMS (ESI-TOF) m/z: $[M+Na]^+$ calcd for $C_{33}H_{40}O_2Na$ 491.2921; found 491.2915.

(*Z*)-2-((3,5-Di-*tert*-butyl-4-hydroxyphenyl)(phenyl)methyl)-3-(naphthalen-1-yl)-1-phenylprop-2-en-1-one (3n):

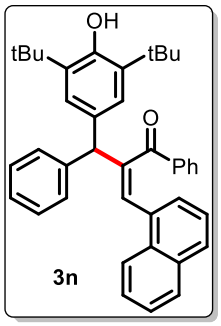

Thick liquid; ***Rf*** = 0.52 (pet. ether: ethyl acetate = 95:5);

^{1}H NMR (400MHz, $CDCl_3$) δ = 7.89 (d, *J* = 8.2 Hz, 1 H), 7.71 (d, *J* = 7.8 Hz, 1 H), 7.58 - 7.55 (m, 2 H), 7.54 - 7.51 (m, 1 H), 7.50 - 7.45 (m, 4 H), 7.38 - 7.34 (m, 2 H), 7.26 (s, 2 H), 7.24 - 7.21 (m, 1 H), 7.18 - 7.13 (m, 2 H), 7.11 - 7.05 (m, 2 H), 6.93 - 6.87 (m, 2 H), 5.58 (s, 1 H), 5.11 (s, 1 H), 1.43 ppm (s, 18 H);

^{13}C NMR (100MHz, $CDCl_3$) δ = 199.4, 152.5, 146.7, 142.2, 136.8, 135.7, 133.7, 133.0, 132.9, 132.1, 131.2, 131.1, 129.4, 128.8, 128.5, 128.4, 128.2, 127.5, 127.5, 126.5, 126.2, 126.1, 125.7, 125.0, 124.2, 55.8, 34.4, 30.3 ppm;

HRMS (ESI-TOF) m/z: $[M+H]^+$ calcd for $C_{40}H_{41}O_2$ 553.3101; found 553.3098.

(*Z*)-1-(4-(*Tert*-Butyl)phenyl)-2-((3,5-di-*tert*-butyl-4-hydroxyphenyl)(phenyl)methyl) non-2-en-1-one (3o):

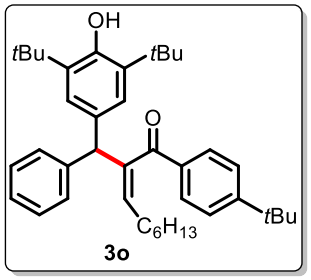

Thick liquid: ***Rf*** = 0.67 (pet. ether: ethyl acetate = 95:5);

^{1}H NMR (400MHz, $CDCl_3$) δ = 7.74 (d, *J* = 8.2 Hz, 2 H), 7.39 (d, *J* = 8.7 Hz, 2 H), 7.30 (d, *J* = 4.6 Hz, 4 H), 7.23 - 7.17 (m, 1 H), 7.00 (s, 2 H), 5.47 - 5.41 (m, 1 H), 5.17 (s, 1 H), 5.03 (s, 1 H), 1.94 - 1.87 (m, 2 H), 1.37 (s, 18 H), 1.33 (s, 9 H), 1.27 - 1.11 (m, 8 H), 0.83 ppm (t, *J* = 7.1 Hz, 3 H)**;**

^{13}C NMR (100MHz, $CDCl_3$) δ = 199.4, 156.4, 152.3, 143.3, 142.6, 135.4, 135.1, 135.0, 131.7, 130.4, 129.5, 129.3, 128.9, 128.2, 126.3, 126.2, 125.3, 55.5, 35.1, 34.4, 31.6, 31.2, 30.4, 30.0, 29.7, 29.6, 29.4, 28.8, 22.6, 14.1 ppm;

HRMS (ESI-TOF) m/z: $[M+Na]^+$ calcd for $C_{40}H_{54}O_2Na$ 589.4016; found 589.4014.

(*Z*)-2-((3,5-Di-*tert*-butyl-4-hydroxyphenyl)(phenyl)methyl)-1-phenyloct-1-en-3-one (3p):

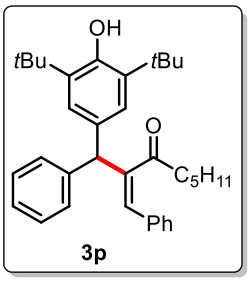

White solid; mp = 85-87 ºC; ***Rf*** = 0.57 (pet ether: ethyl acetate = 95:5);

^{1}H NMR (400MHz, $CDCl_3$) δ = 7.34 - 7.28 (m, 6 H), 7.26 - 7.20 (m, 2 H), 7.17 - 7.14 (m, 2 H), 7.08 (s, 2 H), 6.29 (s, 1 H), 5.27 (s, 1 H), 5.12 (s, 1 H), 2.07 - 1.91 (m, 2 H), 1.41 (s, 18 H), 1.23 - 1.19 (m, 2 H), 1.04 - 0.99 (m, 2 H), 0.87 - 0.84 (m, 2 H), 0.71 ppm (t, *J* = 7.3 Hz, 3 H)**;**

^{13}C NMR (100MHz, $CDCl_3$) δ = 210.6, 152.5, 149.0, 141.7, 136.7, 135.6, 131.6, 130.6, 129.5, 129.0, 128.9, 128.3, 128.2, 127.9, 127.8, 126.5, 126.1, 55.5, 43.8, 34.4, 30.9, 30.3, 23.3, 22.2, 13.8 ppm;

HRMS (ESI-TOF) m/z: $[M+H]^+$ calcd for $C_{35}H_{45}O_2$ 497.3414; found 497.3407.

(*Z*)-2-((4-Hydroxy-3,5-dimethylphenyl)(phenyl)methyl)-1,3-diphenylprop-2-en-1-one (3q):

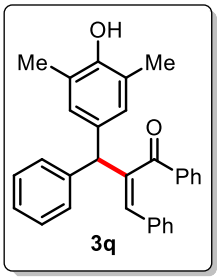

Colourless liquid; ***Rf*** = 0.52 (pet. ether: ethyl acetate = 9:1);

^{1}H NMR (500MHz, $CDCl_3$) δ = 7.78 (d, *J* = 7.6 Hz, 2 H), 7.36 - 7.29 (m, 5 H), 7.25 - 7.21 (m, 3 H), 7.11 - 7.03 (m, 5 H), 6.93 (s, 2 H), 6.54 (s, 1 H), 5.32 (s, 1 H), 4.58 (br. s., 1 H), 2.19 ppm (s, 6 H):

^{13}C NMR (126MHz, $CDCl_3$) δ = 199.8, 151.0, 144.1, 141.5, 136.0, 135.8, 133.9, 132.7, 132.2, 129.7, 129.5, 129.5, 128.8, 128.4, 128.1, 128.0, 127.6, 126.6, 122.9, 55.5, 16.0 ppm;

HRMS (ESI-TOF) m/z: $[M+Na]^+$ calcd for $C_{30}H_{26}O_2Na$ 441.1825; found 441.1818.

2-((3,5-Di-*tert*-butyl-4-hydroxyphenyl)(phenyl)methyl)-1-phenylprop-2-en-1-one (5a):

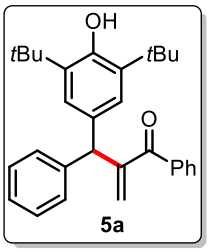

Colourless solid; mp = 130-132 ºC; ***Rf*** = 0.62 (pet. ether: ethyl acetate = 95:5);

^{1}H NMR (400MHz, $CDCl_3$) δ = 7.84 - 7.80 (m, 2 H), 7.56 - 7.50 (m, 1 H), 7.46 - 7.41 (m, 2 H), 7.34 - 7.27 (m, 3 H), 7.27 - 7.25 (m, 1 H), 7.23 - 7.18 (m, 1 H), 7.05 (s, 2 H), 5.85 (s, 1 H), 5.63 (s, 1 H), 5.48 (app. d, *J* = 0.9 Hz, 1 H), 5.08 (s, 1 H), 1.40 ppm (s, 18 H);

^{13}C NMR (100MHz, $CDCl_3$) δ = 197.1, 152.3, 151.8, 142.2, 137.6, 135.6, 132.3, 131.5, 129.7, 129.2, 128.3, 128.1, 127.5, 126.3, 125.8, 52.2, 34.4, 30.3 ppm;

HRMS (ESI-TOF) m/z: $[M+H]^+$ calcd for $C_{30}H_{35}O_2$ 427.2632; found 427.2623.

2-((3,5-Di-*tert*-butyl-4-hydroxyphenyl)(*p*-tolyl)methyl)-1-phenylprop-2-en-1-one (5b):

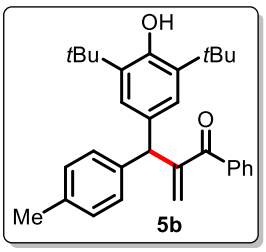

Colourless solid; mp = 131-132 ºC; ***Rf*** = 0.57 (pet. ether: ethyl acetate = 95: 5);

^{1}H NMR (400MHz, $CDCl_3$) δ = 7.82 (d, *J* = 7.3 Hz, 2 H), 7.56 - 7.50 (m, 1 H), 7.43 (t, *J* = 7.3 Hz, 2 H), 7.14 (q, *J* = 8.2 Hz, 4 H), 7.05 (s, 2 H), 5.82 (s, 1 H), 5.59 (s, 1 H), 5.48 (s, 1 H), 5.07 (s, 1 H), 2.32 (s, 3 H), 1.40 ppm (s, 18 H);

^{13}C NMR (100MHz, $CDCl_3$) δ = 197.2, 152.3, 151.9, 139.2, 137.6, 135.8, 135.5, 132.2, 131.6, 129.7, 129.1, 129.0, 128.1, 127.2, 125.7, 51.9, 34.3, 30.3, 21.0 ppm;

HRMS (ESI-TOF) m/z: $[M+H]^+$ calcd for $C_{31}H_{37}O_2$ 441.2788; found 441.2780.

2-((3,5-Di-*tert*-butyl-4-hydroxyphenyl)(4-methoxyphenyl) methyl)-1-phenylprop-2-en-1-one (5c):

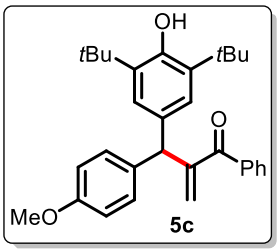

Colorless thick liquid; ***Rf*** = 0.42 (pet. ether: ethyl acetate = 95:5);

^{1}H NMR (400MHz, $CDCl_3$) δ = 7.83 - 7.80 (m, 2 H), 7.55 - 7.50 (m, 1 H), 7.45 - 7.40 (m, 2 H), 7.17 (d, *J* = 8.2 Hz, 2 H), 7.04 (s, 2 H), 6.85 (d, *J* = 8.7 Hz, 2 H), 5.81 (s, 1 H), 5.57 (s, 1 H), 5.47 (app. d, *J* = 0.9 Hz, 1 H), 5.06 (s, 1 H), 3.79 (s, 3 H), 1.39 (s, 18 H);

^{13}C NMR (100MHz, $CDCl_3$) δ = 197.2, 158.0, 152.3, 152.0, 137.6, 135.6, 134.3, 132.2, 131.8, 130.1, 129.7, 128.1, 127.1, 125.6, 113.7, 55.2, 51.5, 34.3, 30.3;

HRMS (ESI-TOF) m/z: $[M+Na]^+$ calcd for $C_{31}H_{36}O_3Na$ 479.2557; found 479.2548.

2-((3,5-Di-*tert*-butyl-4-hydroxyphenyl)(3,4,5-trimethoxyphenyl)methyl)-1-phenyl prop-2-en-1-one (5d):

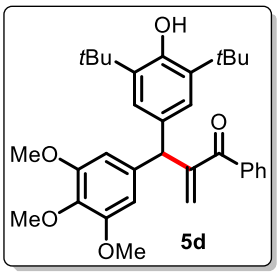

White solid; mp = 133-135 ºC; ***Rf*** = 0.30 (pet. ether: ethyl acetate = 8:2);

^{1}H NMR (400MHz, $CDCl_3$) δ = 7.85 - 7.81 (m, 2 H), 7.57 - 7.51 (m, 1 H), 7.46 - 7.41 (m, 2 H), 7.07 (s, 2 H), 6.49 (s, 2 H), 5.83 (s, 1 H), 5.54 (s, 1 H), 5.49 (app. d, *J* = 0.9 Hz, 1 H), 5.10 (s, 1 H), 3.81 (s, 3 H), 3.80 (s, 6 H), 1.41 ppm (s, 18 H);

^{13}C NMR (100MHz, $CDCl_3$) δ = 197.1, 153.0, 152.4, 151.6, 137.7, 137.4, 136.4, 135.7, 132.4, 131.1, 129.7, 128.2, 127.1, 125.7, 106.3, 60.8, 56.0, 52.5, 34.4, 30.3 ppm;

HRMS (ESI-TOF) m/z: $[M+Na]^+$ calcd for $C_{33}H_{40}O_5Na$ 539.2768; found 539.2759.

2-((4-Chlorophenyl)(3,5-di-*tert*-butyl-4-hydroxyphenyl)methyl)-1-phenylprop-2-en-1-one (5e):

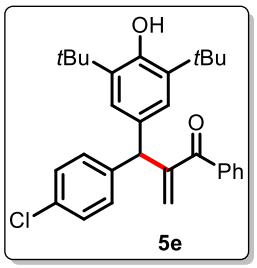

White solid; mp = 132-133 ºC; ***Rf*** = 0.43 (pet. ether: ethyl acetate = 95:9);

^{1}H NMR (400MHz, $CDCl_3$) δ = 7.82 - 7.79 (m, 2 H), 7.56 - 7.51 (m, 1 H), 7.46 - 7.41 (m, 2 H), 7.28 (d, *J* = 8.7 Hz, 2 H), 7.19 (d, *J* = 8.7 Hz, 2 H), 7.01 (s, 2 H), 5.86 (s, 1 H), 5.60 (s, 1 H), 5.48 (d like, *J* = 1.4 Hz, 1 H), 5.10 (s, 1 H), 1.39 ppm (s, 18 H);

^{13}C NMR (100MHz, $CDCl_3$) δ = 196.9, 152.5, 151.3, 140.9, 137.4, 135.8, 132.4, 132.1, 131.0, 130.5, 129.7, 128.5, 128.2, 127.7, 125.6, 51.6, 34.4, 30.3 ppm;

HRMS (ESI-TOF) m/z: $[M+H]^+$ calcd for $C_{30}H_{34}ClO_2$ 461.2242; found 461.2233.

Methyl 4-(2-benzoyl-1-(3,5-di-*tert*-butyl-4-hydroxy phenyl)allyl)benzoate (5f):

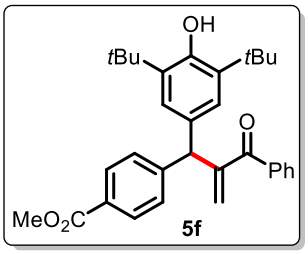

White solid; mp = 150-154 ºC; ***Rf*** = 0.45 (pet. ether: ethyl acetate = 9:1);

^{1}H NMR (400MHz , $CDCl_3$) δ = 7.99 (d, *J* = 8.2 Hz, 2 H), 7.82 - 7.79 (m, 2 H), 7.57 - 7.51 (m, 1 H), 7.47 - 7.41 (m, 2 H), 7.34 (d, *J* = 8.2 Hz, 2 H), 7.01 (s, 2 H), 5.89 (s, 1 H), 5.68 (s, 1 H), 5.48 (app. d, *J* = 1.4 Hz, 1 H), 5.11 (s, 1 H), 3.90 (s, 3 H), 1.39 ppm (s, 18 H);

^{13}C NMR (100MHz, $CDCl_3$) δ = 196.8, 167.0, 152.6, 151.0, 147.8, 137.4, 135.8, 132.4, 130.7, 129.7, 129.7, 129.2, 128.3, 128.2, 128.1, 125.7, 52.2, 52.0, 34.4, 30.3 ppm;

HRMS (ESI-TOF) m/z: $[M+H]^+$ calcd for $C_{32}H_{37}O_4$ 485.2686; found 485.2677.

2-((2-Bromophenyl)(3,5-di-*tert*-butyl-4-hydroxyphenyl) methyl)-1-phenylprop-2-en-1-one (5g):

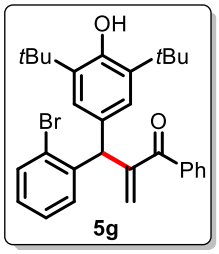

5g

Pale yellow solid; mp = 137-139 ºC; ***Rf*** = 0.57 (pet. ether: ethyl acetate = 95:5);

^{1}H NMR (400MHz , $CDCl_3$) δ = 7.84 - 7.81 (m, 2 H), 7.61 - 7.57 (m, 1 H), 7.56 - 7.51 (m, 1 H), 7.46 - 7.41 (m, 2 H), 7.27 - 7.21 (m, 1 H), 7.11 - 7.06 (m, 2 H), 7.05 (s, 2 H), 5.96 (s, 1 H), 5.92 (s, 1 H), 5.44 (d like, *J* = 1.4 Hz, 1 H), 5.10 (s, 1 H), 1.40 ppm (s, 18 H);

^{13}C NMR (50MHz, $CDCl_3$) δ = 196.4, 152.6, 149.9, 142.3, 137.6, 135.7, 133.1, 132.2, 130.6, 130.0, 129.6, 128.3, 128.1, 127.9, 127.1, 126.0, 125.5, 51.9, 34.4, 30.3 ppm;

HRMS (ESI-TOF) m/z: $[M+H]^+$ calcd for $C_{30}H_{34}BrO_2$ 505.1737; found 505.1729.

2-((3,5-Di-*tert*-butyl-4-hydroxyphenyl)(naphthalen-1-yl)methyl)-1-phenylprop-2-en-1-one (5h):

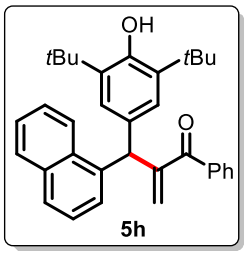

5h

White solid; mp = 145-147 ºC; ***Rf*** = 0.55 (pet. ether: ethyl acetate = 95:5);

^{1}H NMR (400MHz, $CDCl_3$) δ = 8.26 (d, *J* = 8.2 Hz, 1 H), 7.90 - 7.85 (m, 3 H), 7.75 (d, *J* = 8.2 Hz, 1 H), 7.57 - 7.49 (m, 3 H), 7.45 (d, *J* = 7.3 Hz, 2 H), 7.39 (t, *J* = 7.6 Hz, 1 H), 7.16 (s, 2 H), 7.10 (d, *J* = 7.3 Hz, 1 H), 6.43 (s, 1 H), 5.80 (s, 1 H), 5.33 (s, 1 H), 5.11 (s, 1 H), 1.42 ppm (s, 18 H);

^{13}C NMR (100MHz, $CDCl_3$) δ = 197.0, 152.6, 150.8, 139.3, 137.4, 135.7, 133.9, 132.4, 131.9, 131.7, 130.4, 129.9, 128.5, 128.3, 128.1, 127.8, 127.2, 127.1, 126.3, 126.2, 125.5, 125.2, 124.2, 48.2, 34.4, 30.4 ppm;

HRMS (ESI-TOF) m/z: $[M+Na]^+$ calcd for $C_{34}H_{36}O_2Na$ 499.2608; found 499.2597.

2-((3,5-Di-*tert*-butyl-4-hydroxyphenyl)(phenyl)methyl)-1-(*p*-tolyl)prop-2-en-1-one(5i):

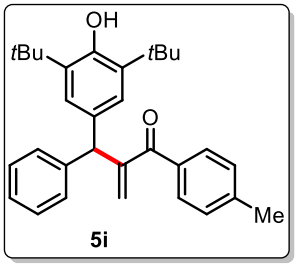

Thick liquid: ***Rf*** = 0.43 (pet ether: ethyl acetate = 95:9);

^{1}H NMR (400MHz, $CDCl_3$) δ = 7.76 (d, *J* = 8.2 Hz, 2 H), 7.33 - 7.27 (m, 3 H), 7.26 - 7.20 (m, 4 H), 7.05 (s, 2 H), 5.82 (s, 1 H), 5.63 (s, 1 H), 5.43 (s, 1 H), 5.08 (s, 1 H), 2.41 (s, 3 H), 1.40 ppm (s, 18 H);

^{13}C NMR (100MHz, $CDCl_3$) δ = 196.8, 152.3, 151.8, 143.1, 142.3, 135.6, 134.8, 131.8, 131.5, 129.9, 129.2, 128.8, 128.3, 126.8, 126.3, 125.8, 52.3, 34.3, 30.3, 21.6 ppm;

HRMS (ESI-TOF) m/z: $[M+H]^+$ calcd for $C_{31}H_{36}O_2$ 441.2788; found 441.2780.

2-((3,5-Di-*tert*-butyl-4-hydroxyphenyl)(phenyl)methyl)-1-(4-methoxyphenyl)prop-2-en-1-one (5j):

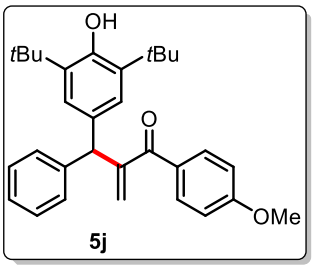

White solid; mp = 134-136 ºC; ***Rf*** = 0.38 (pet ether: ethyl acetate = 9:1);

^{1}H NMR (400MHz, $CDCl_3$) δ = 7.87 (d, *J* = 9.2 Hz, 2 H), 7.33 - 7.28 (m, 2 H), 7.27 - 7.24 (m, 2 H), 7.22 - 7.17 (m, 1 H), 7.04 (s, 2 H), 6.92 (d, *J* = 9.2 Hz, 2 H), 5.78 (s, 1 H), 5.61 (s, 1 H), 5.39 - 5.38 (m, 1 H), 5.07 (s, 1 H), 3.86 (s, 3 H), 1.39 ppm (s, 18 H);

^{13}C NMR (100MHz, $CDCl_3$) δ = 195.9, 163.1, 152.3, 151.8, 142.3, 135.5, 132.1, 131.5, 130.1, 129.2, 128.3, 126.3, 125.8, 125.8, 113.4, 55.4, 52.6, 34.3, 30.3 ppm;

HRMS (ESI-TOF) m/z: $[M+H]^+$ calcd for $C_{31}H_{37}O_3$ 457.2737; found 457.2730.

1-(4-Bromophenyl)-2-((3,5-di-*tert*-butyl-4-hydroxyphenyl)(phenyl)methyl)prop-2-en-1-one (5k):

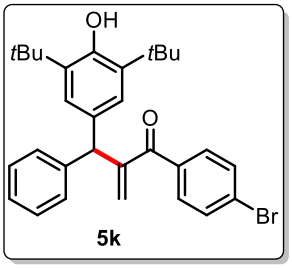

White solid; mp = 143-145 ºC; ***Rf*** = 0.47 (pet ether: ethyl acetate = 95:5);

^{1}H NMR (400MHz, $CDCl_3$) δ = 7.69 (d, *J* = 8.7 Hz, 2 H), 7.58 (d, *J* = 8.7 Hz, 2 H), 7.34 - 7.29 (m, 2 H), 7.26 - 7.19 (m, 3 H), 7.02 (s, 2 H), 5.81 (s, 1 H), 5.60 (s, 1 H), 5.48 (d like, *J* = 1.8 Hz, 1 H), 5.09 (s, 1 H), 1.40 ppm (s, 18 H);

^{13}C NMR (100MHz, $CDCl_3$) δ = 196.0, 152.4, 151.6, 142.0, 136.3, 135.7, 131.5, 131.2, 131.2, 129.1, 128.4, 127.4, 127.3, 126.4, 125.7, 52.3, 34.3, 30.3 ppm;

HRMS (ESI-TOF) m/z: $[M+Na]^+$ calcd for $C_{30}H_{33}BrO_2Na$ 527.1556; found 527.1550.

2-((3,5-Di-*tert*-butyl-4-hydroxyphenyl)(phenyl)methyl)undec-1-en-3-one (5l):

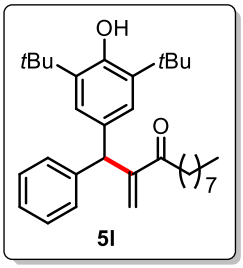

Thick liquid; ***Rf*** = 0.55 (pet. ether: ethyl acetate = 95:5);

^{1}H NMR (400MHz, $CDCl_3$) δ = 7.32 - 7.28 (m, 2 H), 7.23 - 7.17 (m, 1 H), 7.13 (d, *J* = 7.3 Hz, 2 H), 6.90 (s, 2 H), 6.22 (s, 1 H), 5.46 (s, 1 H), 5.35 (s, 1 H), 5.08 (s, 1 H), 2.69 (t, *J* = 7.3 Hz, 2 H), 1.57 - 1.52 (m, 2 H), 1.39 (s, 18 H), 1.32 - 1.24 (m, 10 H), 0.89 ppm (t, *J* = 6.7 Hz, 3 H)**;**

^{13}C NMR (100MHz, $CDCl_3$) δ = 201.8, 152.8, 152.2, 142.7, 135.5, 132.1, 129.0, 128.2, 126.2, 125.6, 125.5, 51.0, 38.6, 34.3, 31.8, 30.3, 29.4, 29.3, 29.1, 24.5, 22.6, 14.1 ppm;

HRMS (ESI-TOF) m/z: $[M+Na]^+$ calcd for $C_{32}H_{46}O_2Na$ 485.3390, found 485.3383.

4-(2-Benzoyl-4,5-dimethoxy-3-phenyl-*1H*-inden-1-ylidene)-2,6-di-*tert*-butylcyclohexa-2,5-dien-1-one (6a):

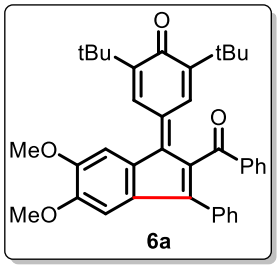

Yellow thick liquid; ***Rf*** = 0.43 (pet. ether: ethyl acetate = 9:1);

^{1}H NMR (500MHz , $CDCl_3$) δ = 7.81 (app. d, *J* = 2.3 Hz, 1 H), 7.59 (d, *J* = 7.2 Hz, 3 H), 7.20 - 7.13 (m, 3 H), 7.08 - 7.02 (m, 5 H), 6.99 (s, 1 H), 6.85 (app. d, *J* = 2.7 Hz, 1 H), 6.58 (s, 1 H), 3.73 (s, 3 H), 3.62 (s, 3 H), 1.12 (s, 9 H), 0.74 ppm (s, 9 H);

^{13}C NMR (125MHz , $CDCl_3$) δ = 196.8, 186.2, 150.3, 150.1, 149.0, 148.7, 148.5, 147.9, 137.5, 136.7, 135.4, 133.6, 132.9, 132.6, 130.4, 129.7, 128.9, 128.6, 128.5, 128.5, 128.4, 127.8, 111.2, 106.3, 56.3, 56.2, 35.9, 29.8, 29.2 ppm;

HRMS (ESI-TOF) m/z: $[M+H]^+$ calcd for $C_{38}H_{39}O_4$ 559.2843; found 559.2849.

4-(2-Benzoyl-4,6-dimethoxy-3-phenyl-*1H*-inden-1-ylidene)-2,6-di-*tert*-butylcyclohexa-2,5-dien-1-one (6b):

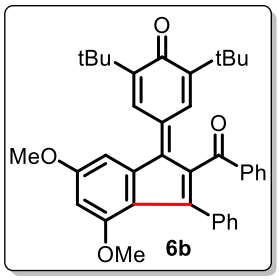

Yellow thick liquid; ***Rf*** = 0.5 (pet ether: ethyl acetate = 8.5:1.5);

^{1}H NMR (400MHz , $CDCl_3$) δ = 8.05 (app. d, *J* = 1.8 Hz, 1 H), 7.82 (d, *J* = 7.9 Hz, 2 H), 7.43 (t, *J* = 7.3 Hz, 1 H), 7.34 - 7.27 (m, 4 H), 7.20 - 7.15 (m, 4 H), 7.11 (app. d, *J* = 2.4 Hz, 1 H), 6.42 (s, 1 H), 3.92 (s, 3 H), 3.59 (s, 3 H), 1.38 (s, 9 H), 1.00 ppm (s, 9 H);

^{13}C NMR (100MHz , $CDCl_3$) δ = 197.1, 186.3, 161.4, 156.3, 150.4, 149.9, 148.6, 148.0, 138.8, 137.6, 134.7, 134.7, 133.4, 133.3, 130.5, 129.7, 128.8, 128.6, 128.3, 128.0, 127.0, 121.9, 107.1, 99.6, 55.7, 55.4, 35.9, 29.8, 29.2 ppm;

HRMS (ESI-TOF) m/z: $[M+H]^+$ calcd for $C_{38}H_{39}O_4$ 559.2843; found 559.2853.

(3-(3,5-Di-*tert*-butyl-4-hydroxyphenyl)-1-hydroxy-5,7-dimethoxy-1-phenyl-*1H*-inden-2-yl)(phenyl)methanone (7b):

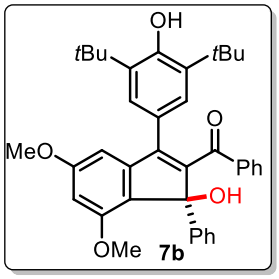

Colourless solid; mp = 154-156 ºC; ***Rf*** = 0.25 (pet. ether: ethyl acetate = 9:1);

^{1}H NMR (500MHz , $CDCl_3$) δ = 7.57 (d, *J* = 8.0 Hz, 2 H), 7.36 (d, *J* = 7.6 Hz, 2 H), 7.24 (t, *J* = 7.4 Hz, 2 H), 7.20 - 7.12 (m, 2 H), 7.06 (s, 2 H), 6.99 (t, *J* = 7.4 Hz, 2 H), 6.70 (s, 1 H), 6.45 (s, 1 H), 5.62 (s, 1 H), 5.20 (s, 1 H), 3.82 (s, 3 H), 3.68 (s, 3 H), 1.30 ppm (s, 18 H);

^{13}C NMR (125MHz , $CDCl_3$) δ = 196.9, 162.2, 156.3, 154.5, 151.7, 144.2, 142.6, 141.3, 137.5, 135.8, 131.9, 129.7, 129.2, 127.9, 127.4, 126.8, 126.4, 124.9, 124.1, 101.0, 100.2, 87.0, 55.9, 55.6, 34.1, 30.1 ppm;

HRMS (ESI-TOF) m/z: $[M+Na]^+$ calcd for $C_{38}H_{40}O_5Na$ 599.2768; found 599.2768.

(*Z*)-2-((4-hydroxyphenyl) (phenyl)methyl)-1,3-diphenylprop-2-en-1-one (8a):[15]

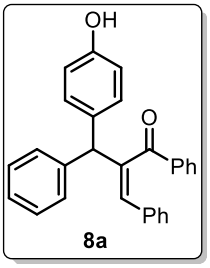

White solid; mp = 67-69 ºC; ***Rf*** = 0.32 (pet. ether: ethyl acetate = 8:2);

^{1}H NMR (200MHz, $CDCl_3$) δ = 7.68 (d, *J* = 7.5 Hz, 2 H), 7.25 – 7.19 (m, 4 H), 7.18 – 7.05 (m, 6 H), 6.97 (s like, 5 H), 6.66 (d, *J* = 8.2 Hz, 2 H), 6.45 (s, 1 H), 5.26 (s, 1 H), 5.07 ppm (s, 1 H);

^{13}C NMR (100MHz, $CDCl_3$) δ = 200.0, 154.4, 143.9, 141.3, 135.9, 135.7, 134.2, 132.9, 130.8, 129.6, 129.5, 128.8, 128.4, 128.2, 128.1, 127.7, 126.7, 115.4, 55.4 ppm;

HRMS (ESI-TOF) m/z: $[M+Na]^+$ calcd for $C_{28}H_{22}O_2Na$ 413.1512; found 413.1508.

3.2.6.5 X-ray Crystallography:

X-ray intensity data measurements of all the compounds were carried out on a Bruker D8 VENTURE Kappa Duo PHOTON II CPAD diffractometer equipped with Incoatech

Comp No.	Compound Structure	ORTEP Diagram
3i	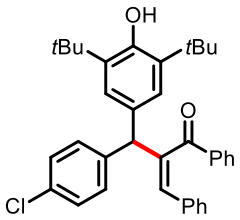 **CCDC 1817114**	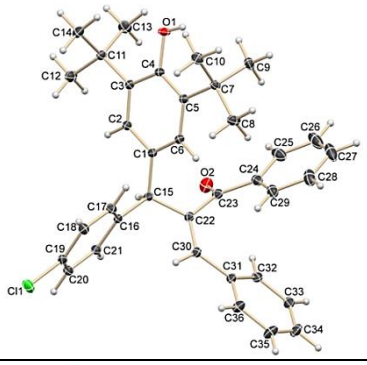
5h	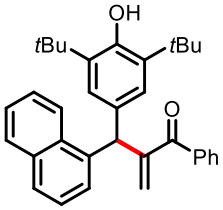 **CCDC 1817116**	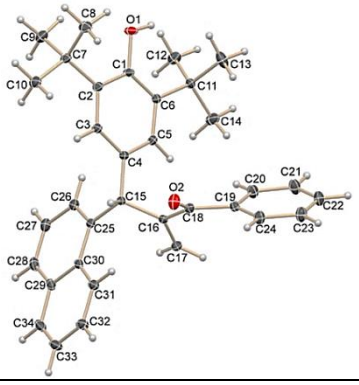
5j	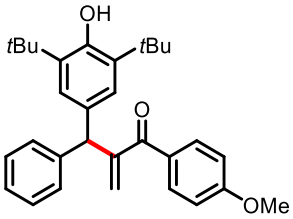 **CCDC 1817117**	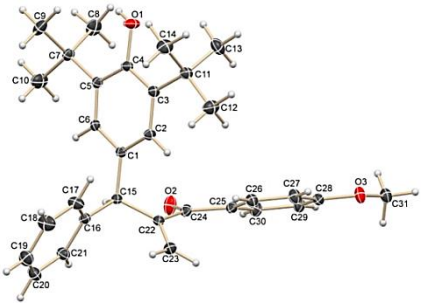
7b	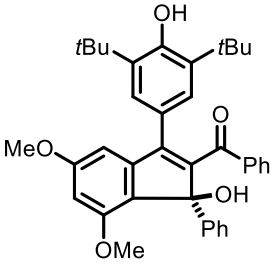 **CCDC 1817115**	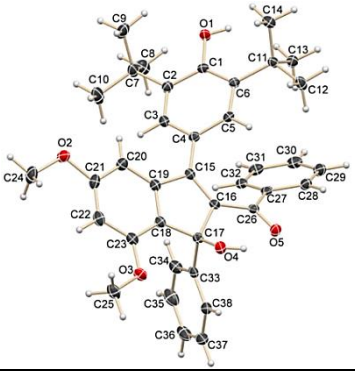

multilayer mirrors optics with graphite-monochromatized radiation. The intensity measurements were carried out with Mo micro-focus sealed tube diffraction source (MoK_{α}= 0.71073Å) at 100(2) K temperature. The X-ray generator was operated at 50 kV and 1.4 mA for Mo source. A preliminary set of cell constants and an orientation

matrix were calculated from three sets of 36 frames. Data were collected with ω scan width of 0.5° at different settings of φ and 2θ keeping the sample-to-detector distance fixed at 5.00 cm. The X-ray data collection was monitored by APEX3 program (Bruker, 2016).[13] All the data were corrected for Lorentzian, polarization and absorption effects using SAINT and SADABS programs (Bruker, 2016). SHELX-97 was used for structure solution and full matrix least-squares refinement on F^2.[14] All the hydrogen atoms were placed in geometrically idealized positions and constrained to ride on their parent atoms. An*ORTEP* III [15] view of both compounds were drawn with 50% probability displacement ellipsoids and H atoms are shown as small spheres of arbitrary radii.

Crystal Data	**3g**	**5h**
Formula	$C_{36}H_{37}ClO_2$	$C_{34}H_{36}O_2$
Mr	537.10	476.63
Temp. (K)	100(2) K	100(2) K
Wavelength	0.71073 Å	0.71073 Å
Crystal Syst., Sp. Gr	Triclinic, *P -1*	Monoclinic, $P2_1/c$
Unit cell dimensions	a = 9.9603(5) Å; α= 81.911(2)^o b = 12.4411(7) Å; β=86.691(2)^o c = 12.4653(7) Å; γ = 71.216(2)^o	a = 5.9965(2) Å; b = 35.6863(12) Å; β = 101.0680(10)^o c = 12.4237(4) Å
Volume (Å^3)	1447.72(14)	2609.13(15)
Z	2	4
D_c, Mg/m^3	1.232	1.213
μ/mm^{-1}	0.163	0.073
F(000)	572	1024
Crystal size (mm^3)	0.400 x 0.320 x 0.200	0.340 x 0.260 x 0.080
$\theta_{min\text{-}max}$	2.701 to 30.539^o	2.392 to 30.509^o
***h, k, l* (min, max)**	(-14, 14), (-17, 17), (-17, 17)	(-7, 8), (-50, 50), (-17, 17)
Number of reflections	74746	38577

unique reflections	8578 [R(int) = 0.0278]	15810 [R(int) = 0.0234]
Completeness at θ_{max}	96.9 %	99.9 %
Ab. Correct.	multi-scan	multi-scan
T_{min}	0.938	0.975
T_{max}	0.968	0.994
Refinement method	Full-matrix least-squares on F^2	Full-matrix least-squares on F^2
Number of parameters	359	331
Goodness-of-fit (S)	1.023	1.037
Final R indices [I>2sigma(I)]	R1 = 0.0351, wR2 = 0.0936	R1 = 0.0406, wR2 = 0.1057
R indices (all data)	R1 = 0.0359, wR2 = 0.0943	R1 = 0.044, wR2 = 0.1085
$\Delta\rho_{max}$, $\Delta\rho_{min}$(eÅ^{-3})	+0.435, -0.313 e.Å^{-3}	+0.435, -0.231 e.Å^{-3}
CCDC No.	**1817114**	**1817116**

Crystal Data	**5j**	**7b**
Formula	C_{31} H_{36} O_3	C_{38} H_{40} O_5, 0.5(CH_2Cl_2)
Mr	456.60	619.16
Temp. (K)	100(2) K	100(2) K
Wavelength	0.71073 Å	0.71073 Å
Crystal Syst., Sp. Gr	Triclinic, *P -1*	Orthorhombic, P_{bcn}
Unit cell dimensions	a = 10.0553(3) Å; α = 86.3840(10)^o b = 10.7561(4) Å; β = 69.6050(10)^o c = 13.7858(5) Å; γ = 71.3680(10)^o	a = 32.1927(10) Å; b = 18.4712(5) Å; c = 11.9350(4) Å
Volume (Å^3)	1322.34(8)	7097.0(4)
Z	2	8
D_c, *Mg/m^3*	1.147	1.159

***μ/mm*$^{-1}$**	0.072	0.148
F(000)	492	2632
Crystal size (mm^3)	0.180 x 0.090 x 0.050	0.370 x 0.250 x 0.110
$\theta_{min\text{-}max}$	2.615 to 30.509^o	2.781 to 25.000^o
***h, k, l* (min, max)**	(-13, 14), (-15, 15), (-19, 19)	(-38, 38), (-21, 21), (-14, 12)
Number of reflections	42514	62638
unique reflections	8052 [R(int) = 0.0276]	6215 [R(int) = 0.0243]
Completeness at θ_{max}	99.7 %	99.5 %
Ab. Correct.	multi-scan	multi-scan
T_{min}	0.987	0.947
T_{max}	0.996	0.984
Refinement method	Full-matrix least-squares on F^2	Full-matrix least-squares on F^2
Number of parameters	315	417
Goodness-of-fit (S)	1.026	1.040
Final R indices [I>2sigma(I)]	R1 = 0.0411, wR2 = 0.1030	R1 = 0.0374, wR2 = 0.0917
R indices (all data)	R1 = 0.0458, wR2 = 0.1063	R1 = 0.0404, wR2 = 0.0932
Extinction coefficient	-	-
$\Delta\rho_{max}$, $\Delta\rho_{min}$(eÅ^{-3})	+0.384, -0.220 e.Å^{-3}	+0.214, -0.201 e.Å^{-3}
CCDC No.	**1817117**	**1817115**

3.2.7 Selected Spectral Data

^{1}H NMR spectra of 1,3-diphenylprop-2-yn-1-yl acetate (2a) (200 MHz, $CDCl_3$):

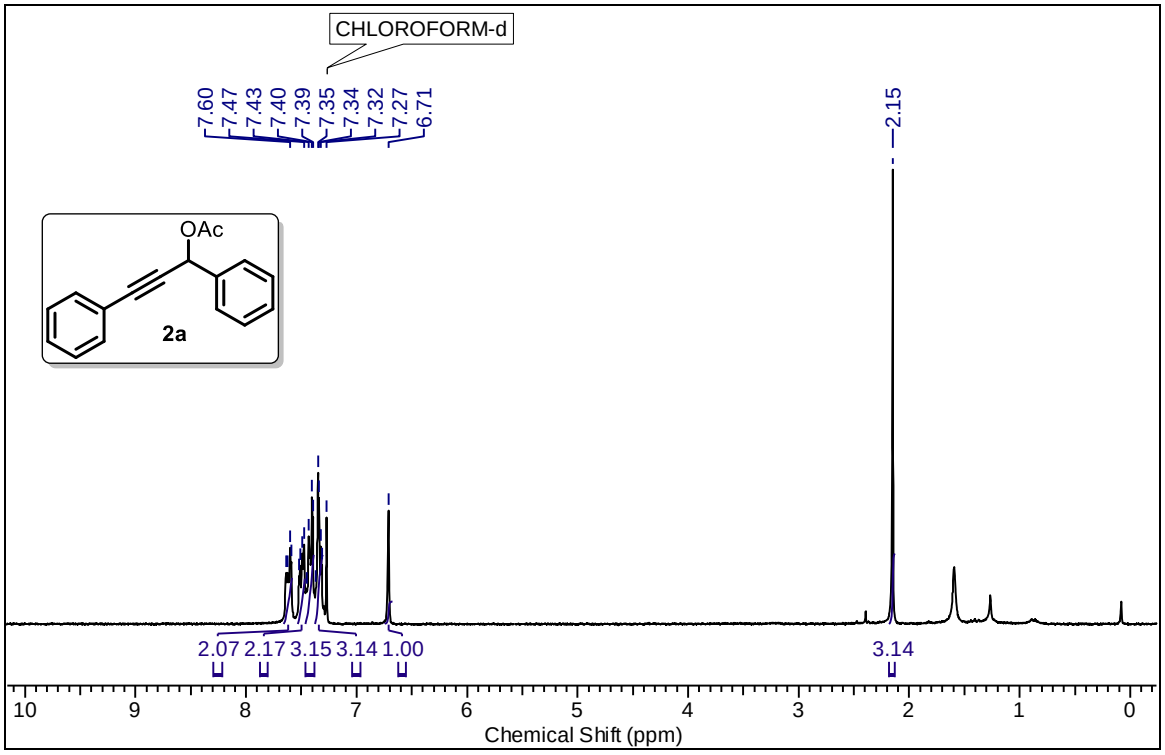

^{1}H NMR spectra of 1-(naphthalen-1-yl)-3-phenylprop-2-yn-1-yl acetate (2b) (200 MHz, $CDCl_3$):

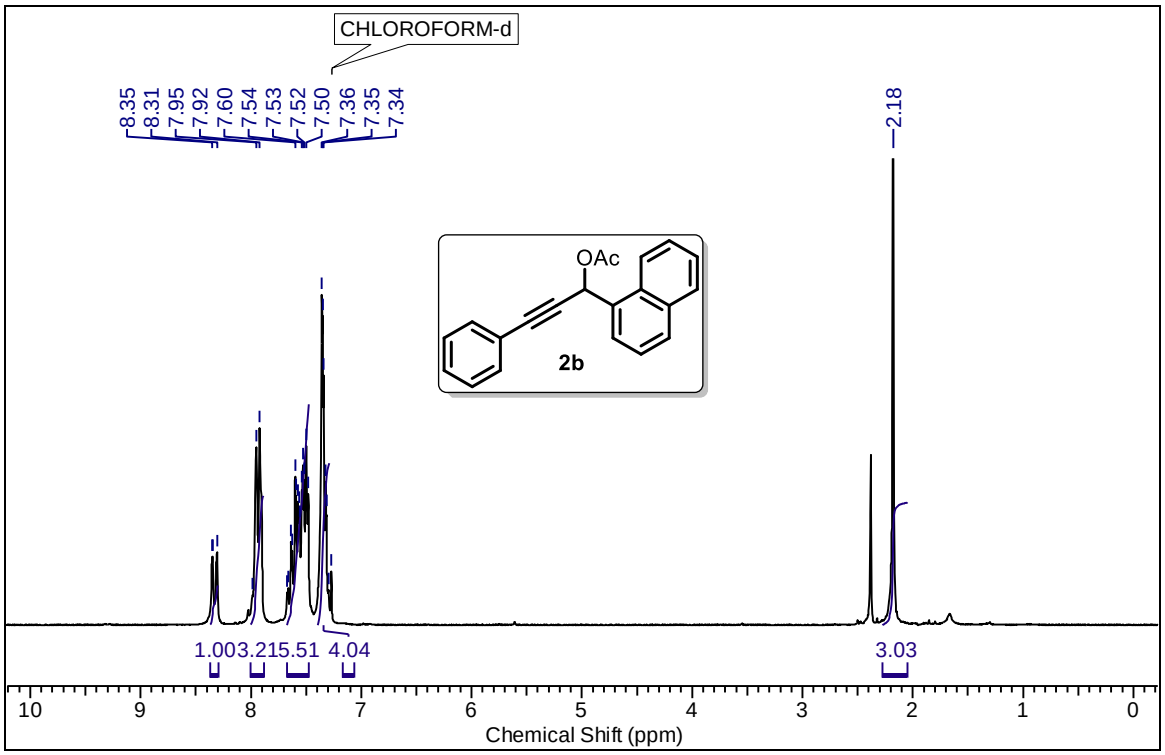

^{1}H NMR spectra of 1-(4-(*tert*-butyl)phenyl)non-1-yn-3-yl acetate (2c) (200 MHz, $CDCl_3$):

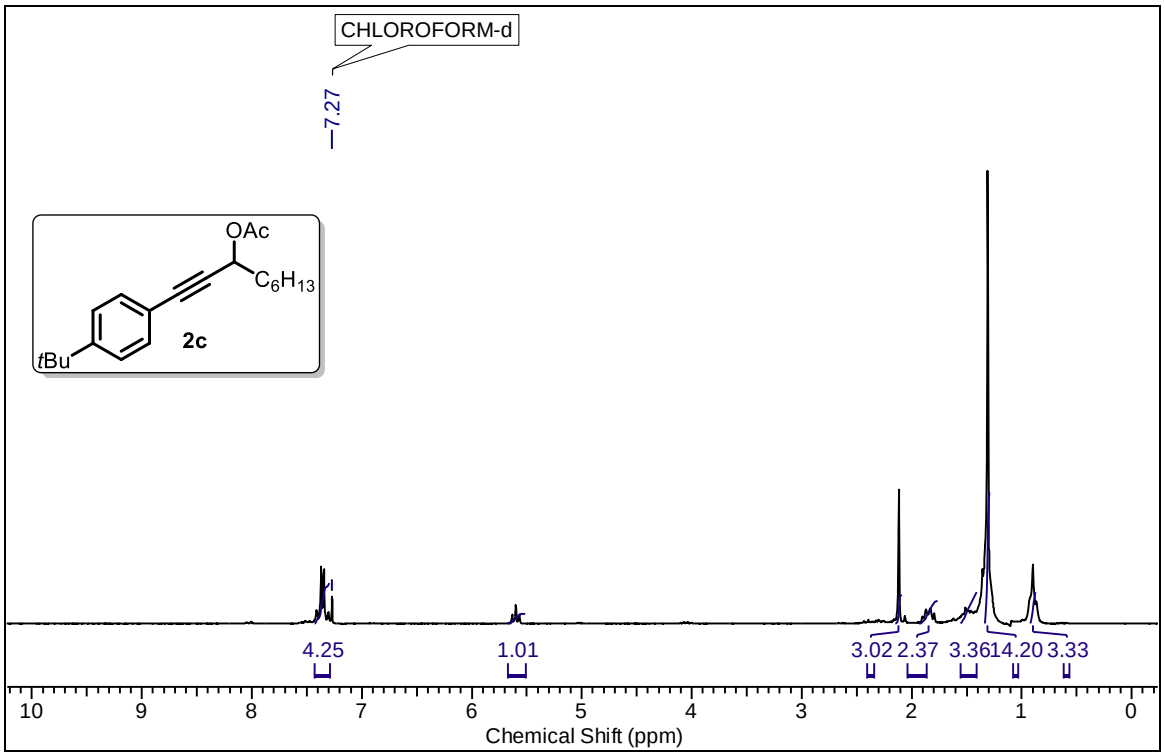

^{1}H NMR spectra of 3-phenylprop-2-yn-1-yl acetate (4a) (200 MHz, $CDCl_3$):

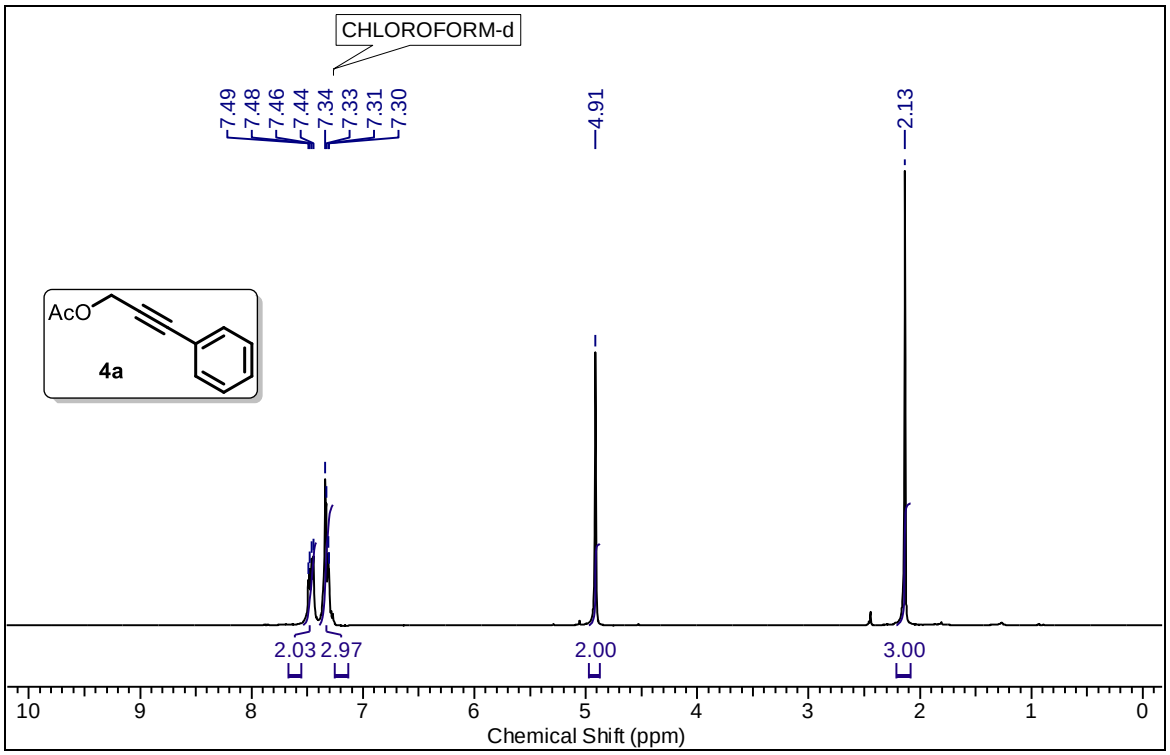

^{1}H NMR spectra of undec-2-yn-1-yl acetate (4e) (200 MHz, $CDCl_3$):

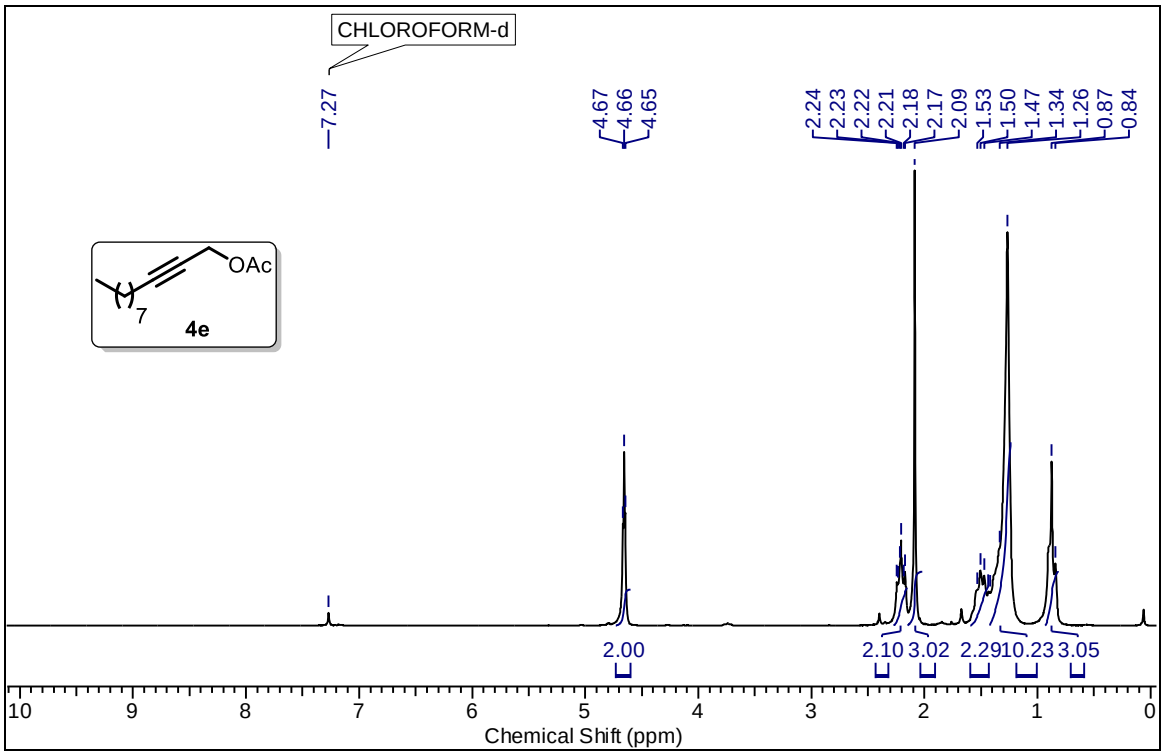

^{13}C NMR spectra of undec-2-yn-1-yl acetate (4e) (50 MHz, $CDCl_3$):

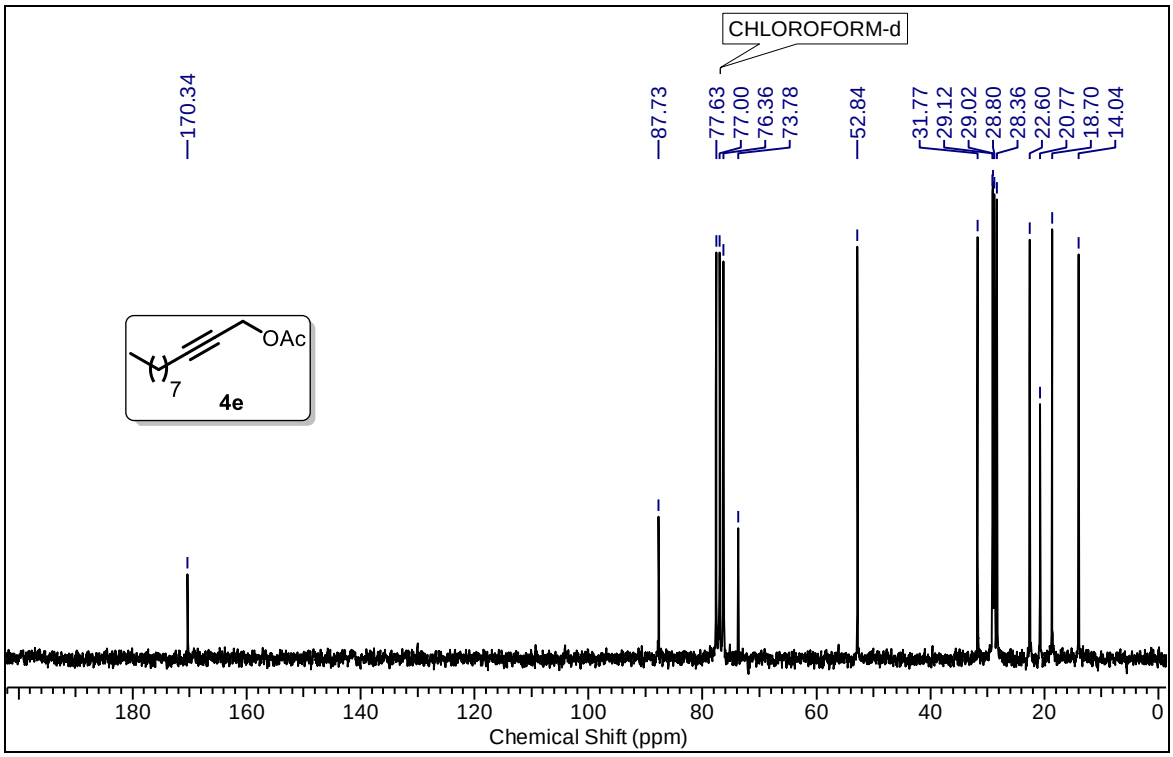

^{1}H NMR spectra of (*Z*)-2-((3,5-Di-*tert*-butyl-4-hydroxyphenyl)(phenyl)methyl)-1,3-diphenylprop-2-en-1-one (3a) (400 MHz, $CDCl_3$):

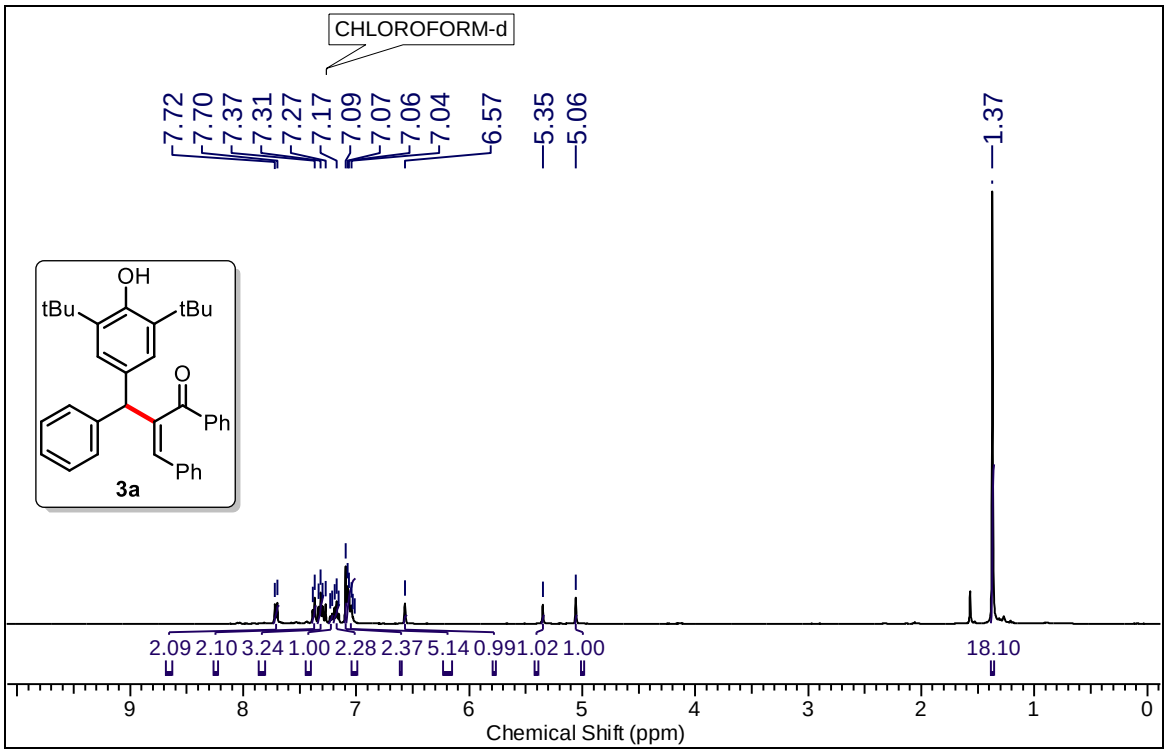

^{13}C NMR spectra of (*Z*)-2-((3,5-Di-*tert*-butyl-4-hydroxyphenyl)(phenyl)methyl)-1,3-diphenylprop-2-en-1-one (3a) (100 MHz, $CDCl_3$):

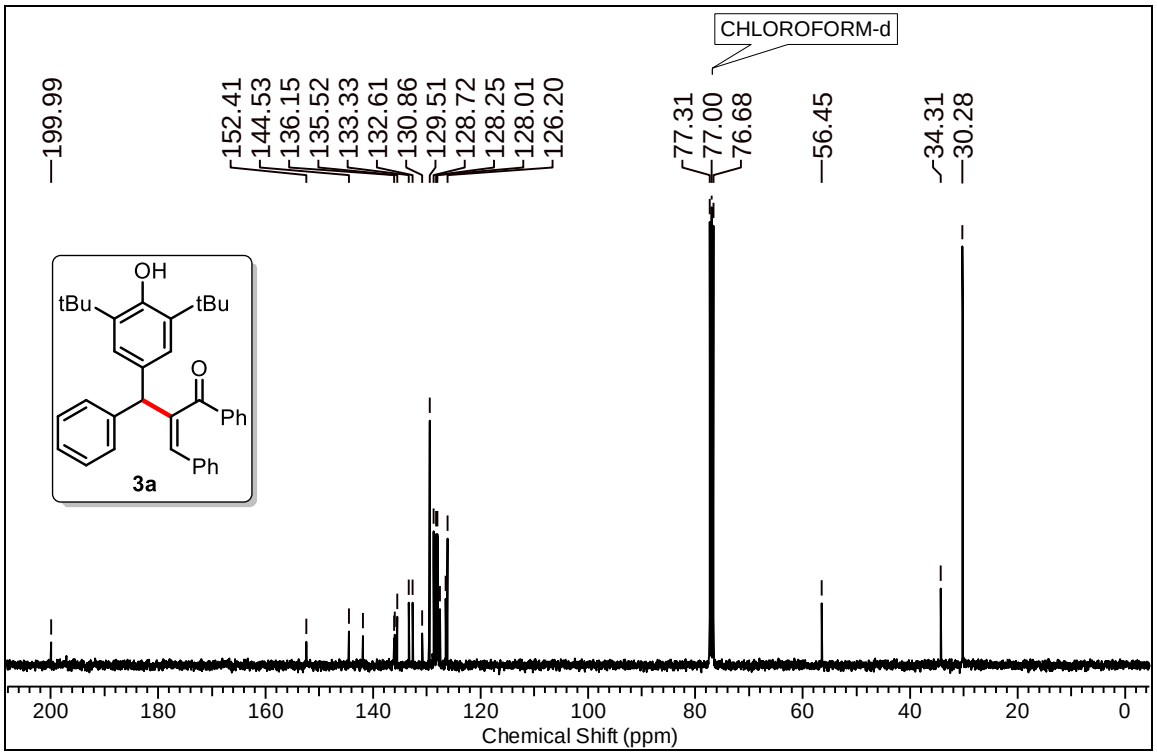

^{1}H NMR spectra of (*Z*)-2-((3,5-Di-*tert*-butyl-4-hydroxyphenyl)(4-methoxyphenyl) methyl)-1,3-diphenylprop-2-en-1-one (3c) (400 MHz, $CDCl_3$):

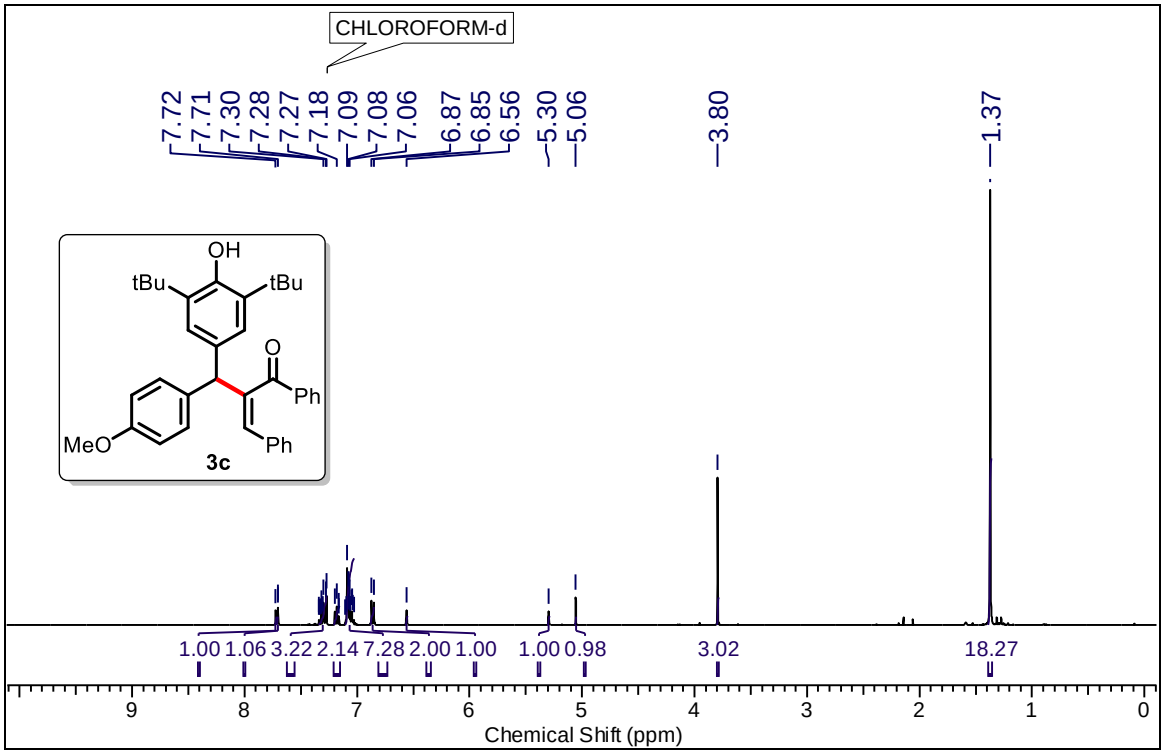

^{13}C NMR spectra of (*Z*)-2-((3,5-Di-*tert*-butyl-4-hydroxyphenyl)(4-methoxyphenyl) methyl)-1,3-diphenylprop-2-en-1-one (3c) (100 MHz, $CDCl_3$):

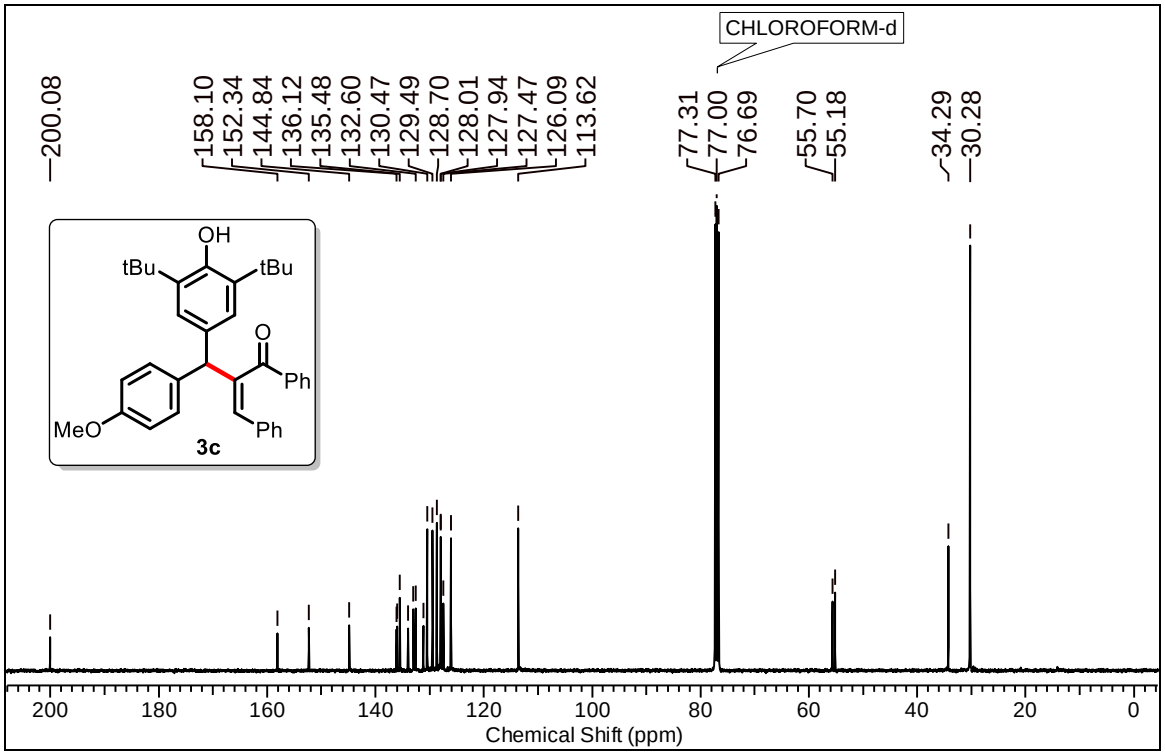

^{1}H NMR spectra of (*Z*)-2-((3,5-Di-*tert*-butyl-4-hydroxyphenyl)(3,4,5-trimethoxy phenyl)methyl)-1,3-diphenylprop -2-en-1-one (3e) (400 MHz, $CDCl_3$):

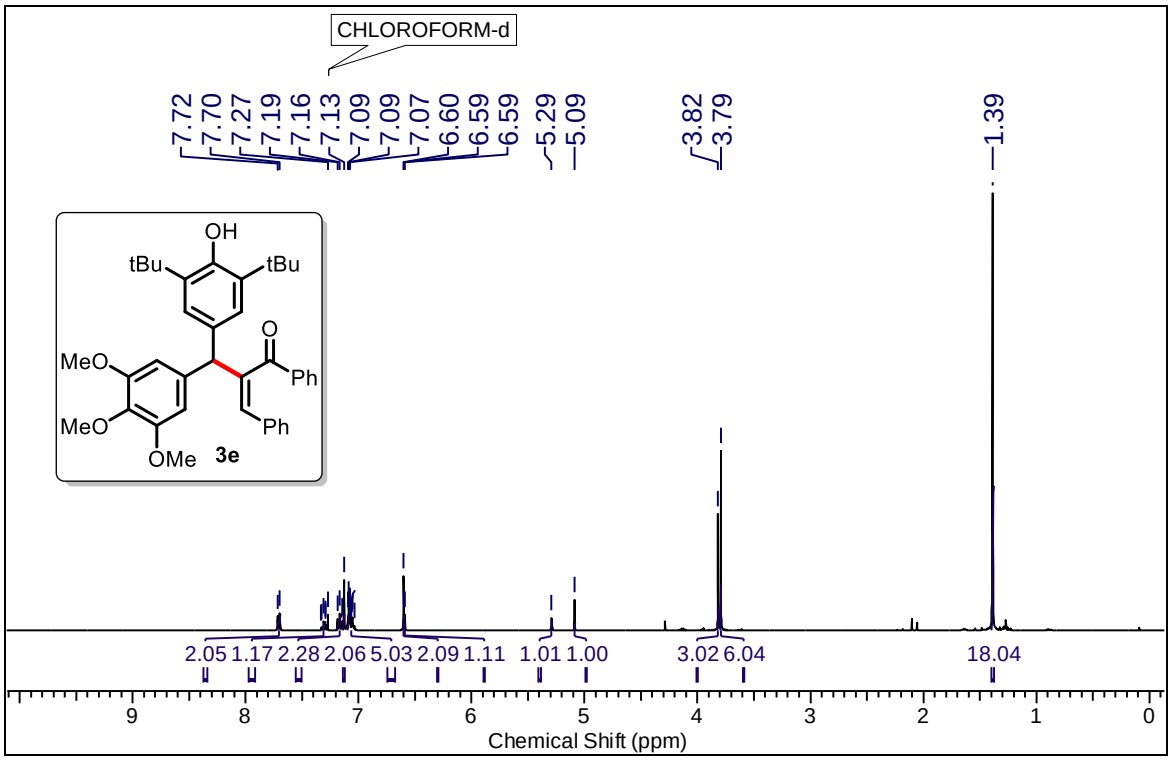

^{13}C NMR spectra of (*Z*)-2-((3,5-Di-*tert*-butyl-4-hydroxyphenyl)(3,4,5-trimethoxy phenyl)methyl)-1,3-diphenylprop-2-en-1-one (3e) (100 MHz, $CDCl_3$):

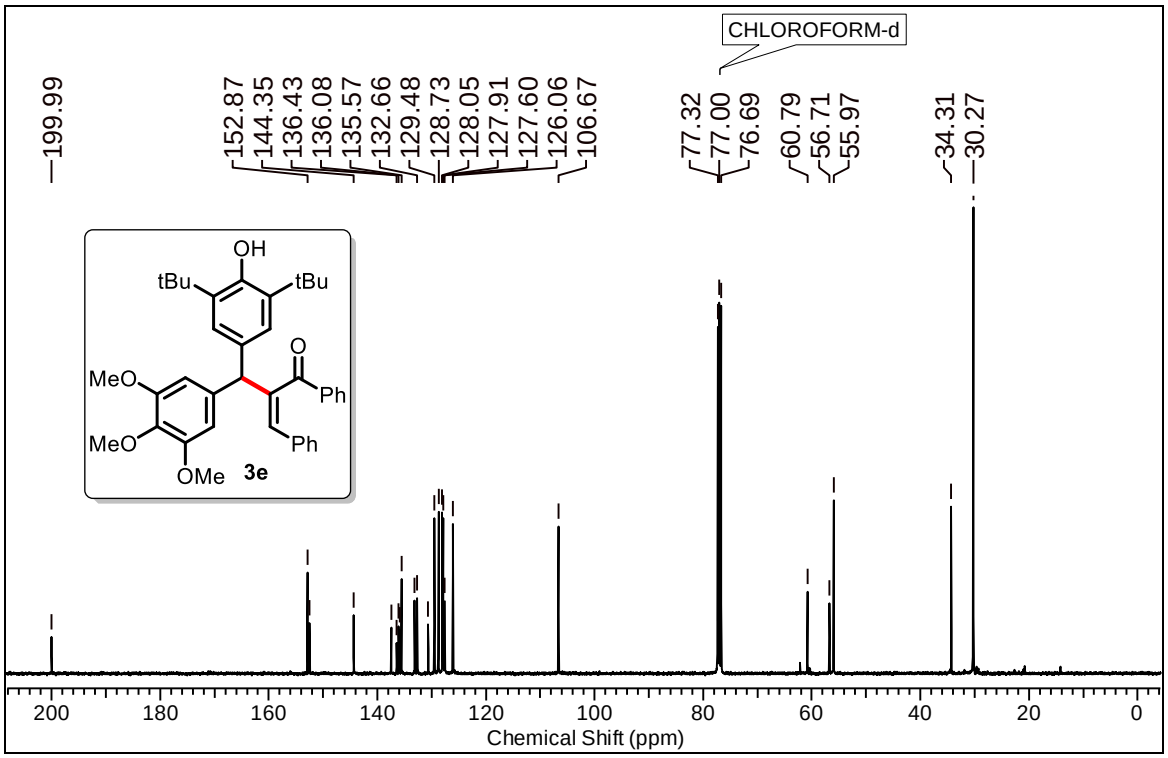

^{1}H NMR spectra of (*Z*)-2-((3,5-Di-*tert*-butyl-4-hydroxyphenyl)(naphthalen-1-yl) methyl)-1,3-diphenylprop-2-en-1-one (3g) (400 MHz, $CDCl_3$):

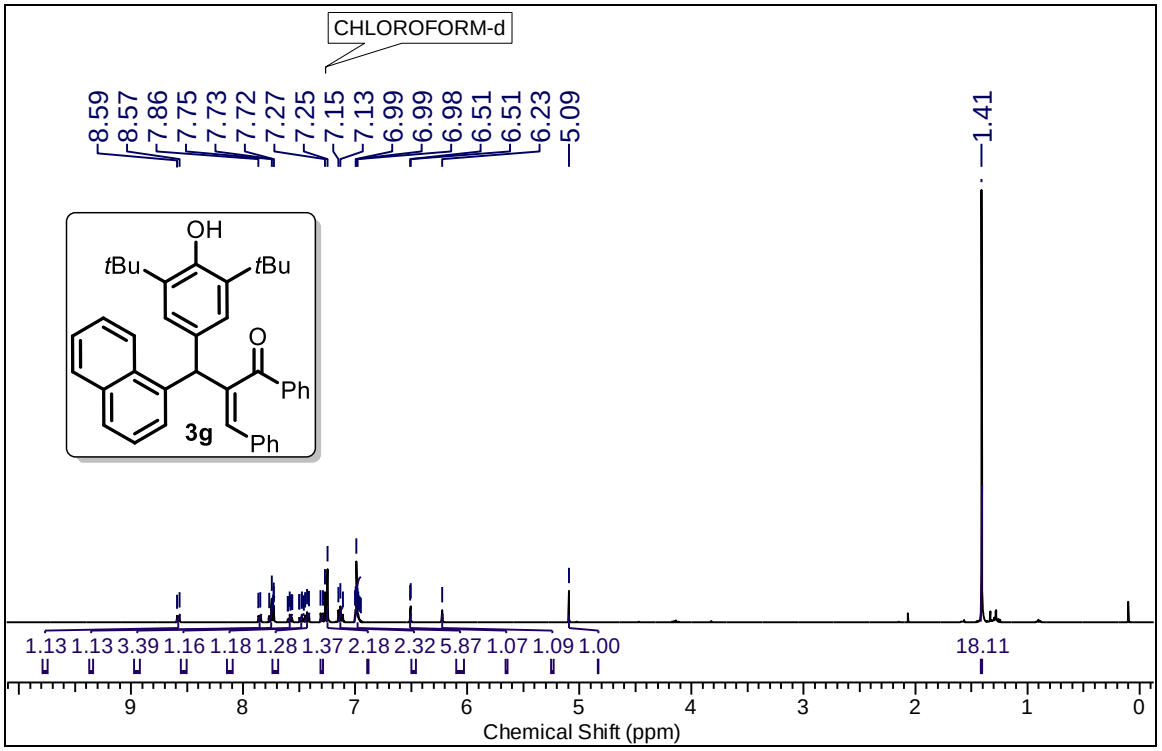

^{13}C NMR spectra of (*Z*)-2-((3,5-Di-*tert*-butyl-4-hydroxyphenyl)(naphthalen-1-yl) methyl)-1,3-diphenylprop-2-en-1-one (3g) (100 MHz, $CDCl_3$):

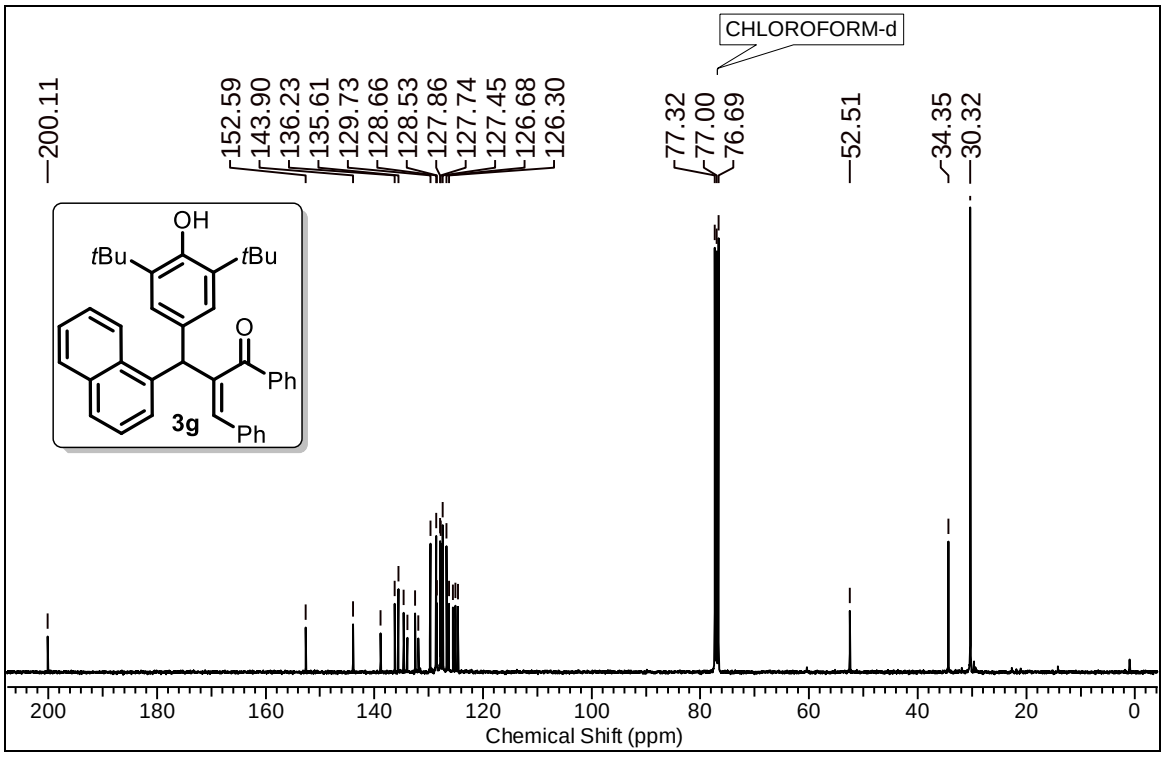

^{1}H NMR spectra of Methyl (*Z*)-4-(2-Benzoyl-1-(3,5-di-*tert*-butyl-4-hydroxy phenyl)-3-phenylallyl)benzoate (3h) (400 MHz, $CDCl_3$):

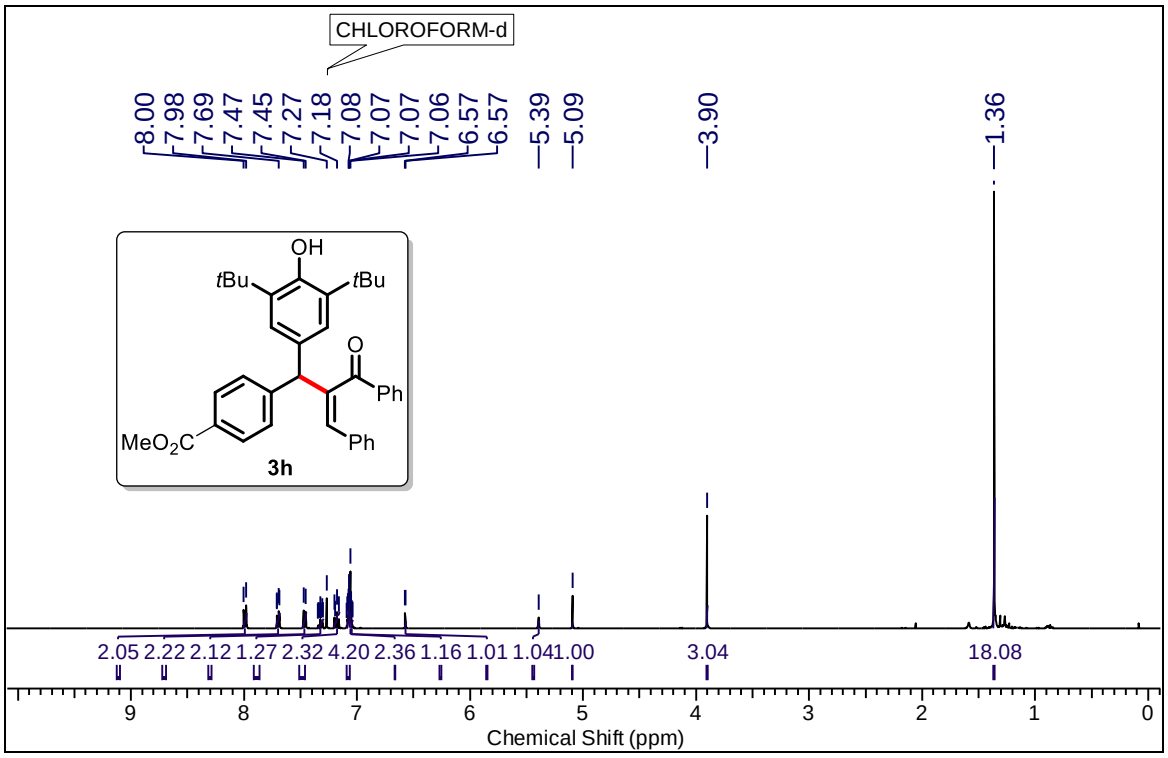

^{13}C NMR spectra of Methyl (*Z*)-4-(2-benzoyl-1-(3,5-di-*tert*-butyl-4-hydroxy phenyl)-3-phenylallyl)benzoate (3h) (100 MHz, $CDCl_3$):

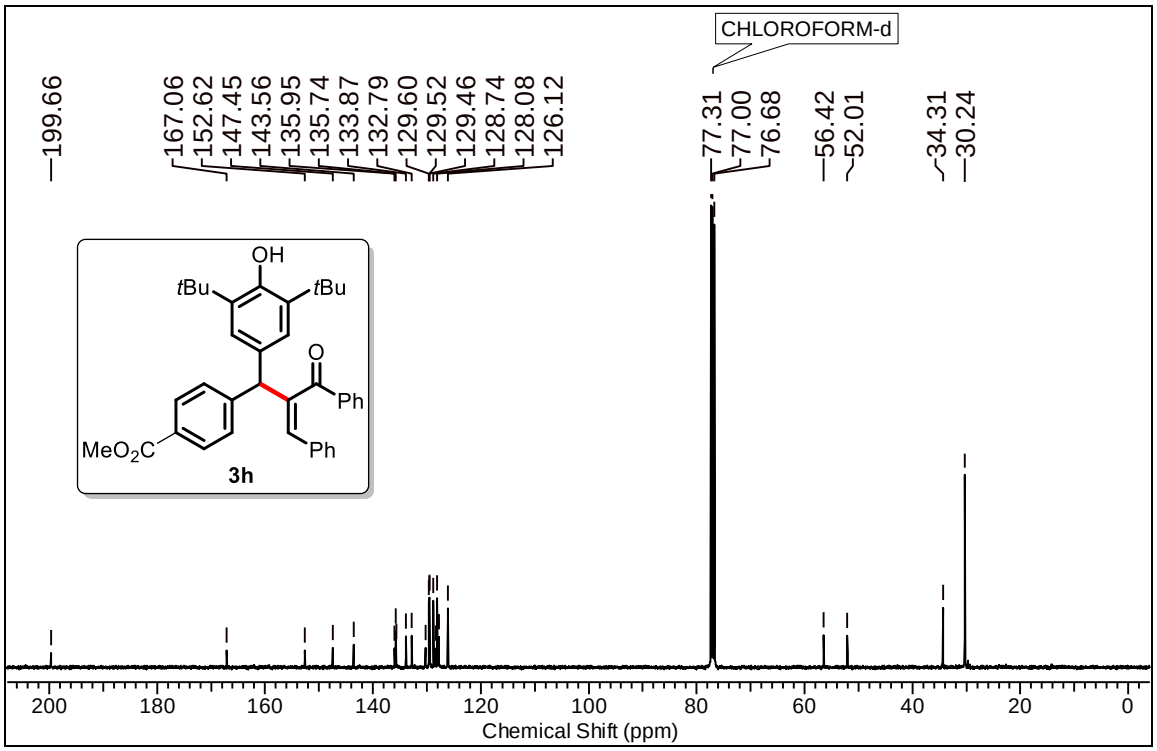

^{1}H NMR spectra of (*Z*)-2-(Benzo[d][1,3]dioxol-5-yl(3,5-di-*tert*-butyl-4-hydroxy phenyl)methyl)-1,3-diphenylprop-2-en-1-one (3j) (400 MHz, $CDCl_3$):

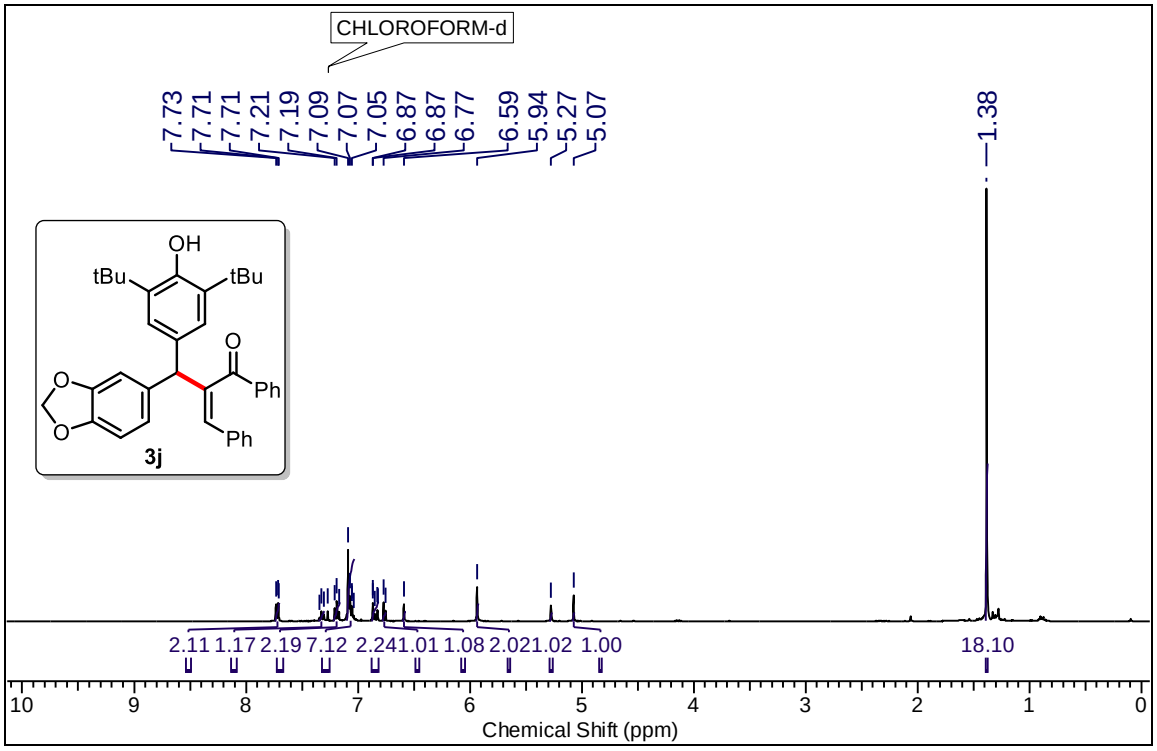

^{13}C NMR spectra of (*Z*)-2-(Benzo[d][1,3]dioxol-5-yl(3,5-di-*tert*-butyl-4-hydroxy phenyl)methyl)-1,3-diphenylprop-2-en-1-one (3j) (100 MHz, $CDCl_3$):

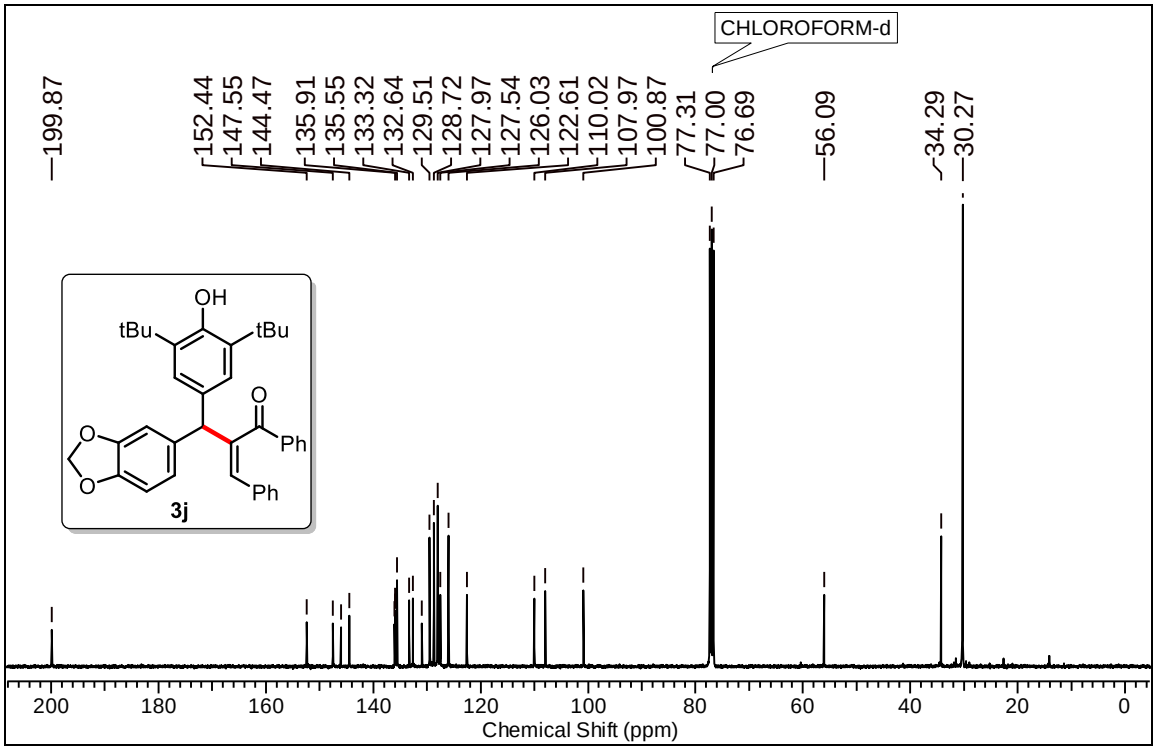

^{1}H NMR spectra of (*Z*)-2-((4-Chlorophenyl)(3,5-di-*tert*-butyl-4-hydroxyphenyl) methyl)-1-phenylbut-2-en-1-one (3k) (400 MHz, $CDCl_3$):

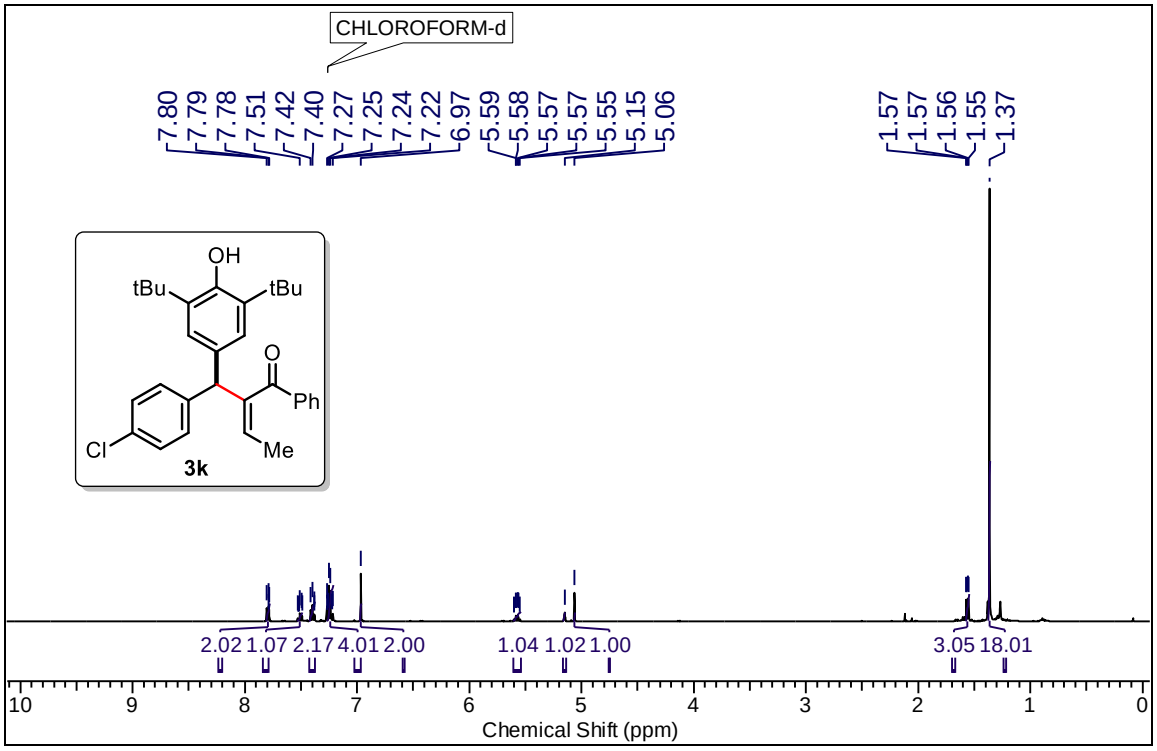

^{13}C NMR spectra of (*Z*)-2-((4-Chlorophenyl)(3,5-di-*tert*-butyl-4-hydroxyphenyl) methyl)-1-phenylbut-2-en-1-one (3k) (100 MHz, $CDCl_3$):

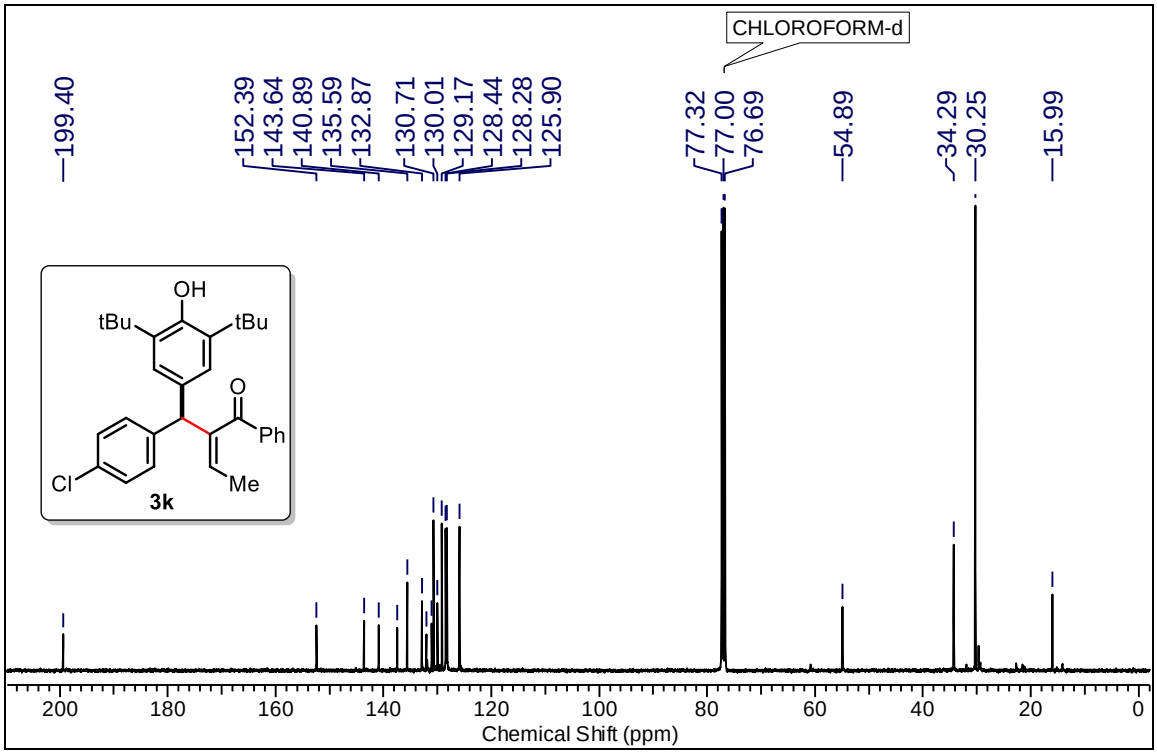

^{1}H NMR spectra of (*Z*)-2-((3,5-Di-*tert*-butyl-4-hydroxyphenyl)(phenyl)methyl)-4-methyl-1-phenylpent-2-en-1-one (3m) (400 MHz, $CDCl_3$):

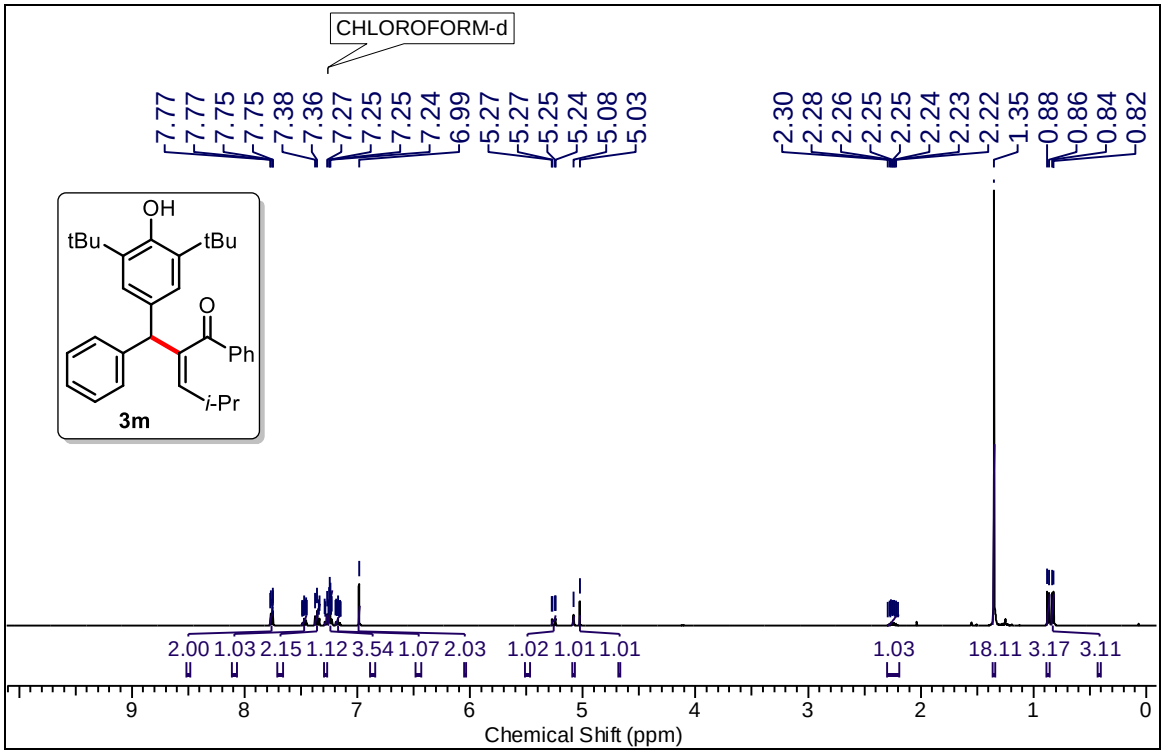

^{13}C NMR spectra of (*Z*)-2-((3,5-Di-*tert*-butyl-4-hydroxyphenyl)(phenyl)methyl)-4-methyl-1-phenylpent-2-en-1-one (3m) (100 MHz, $CDCl_3$):

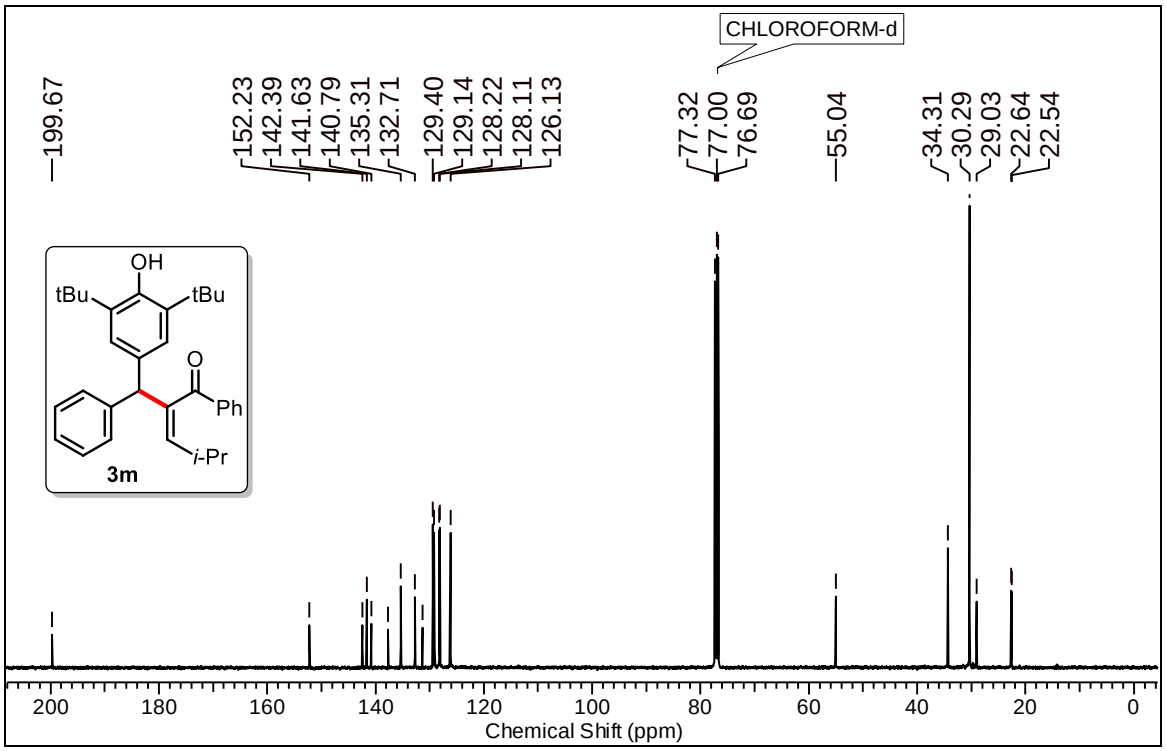

^{1}H NMR spectra of (*Z*)-2-((3,5-Di-*tert*-butyl-4-hydroxyphenyl)(phenyl)methyl) -1-phenyloct-1-en-3-one (3p) (400 MHz, $CDCl_3$):

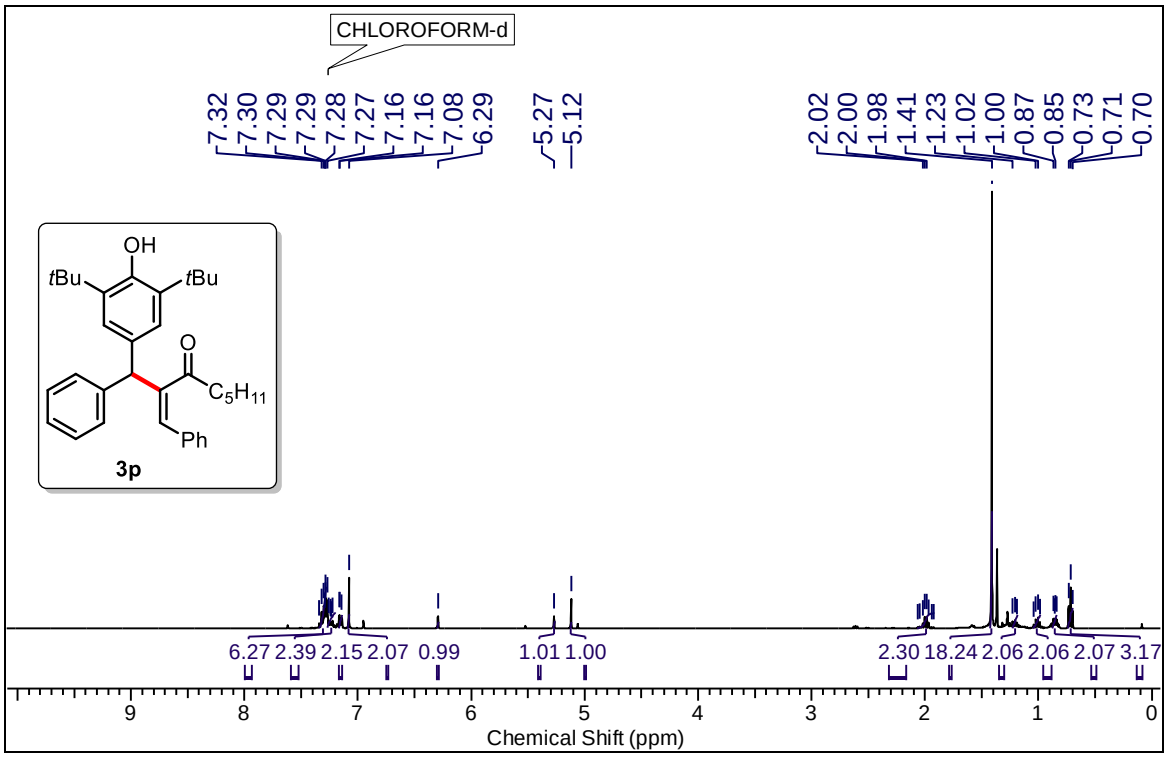

^{13}C NMR spectra of (*Z*)-2-((3,5-Di-*tert*-butyl-4-hydroxyphenyl)(phenyl)methyl) -1-phenyloct-1-en-3-one (3p) (100 MHz, $CDCl_3$):

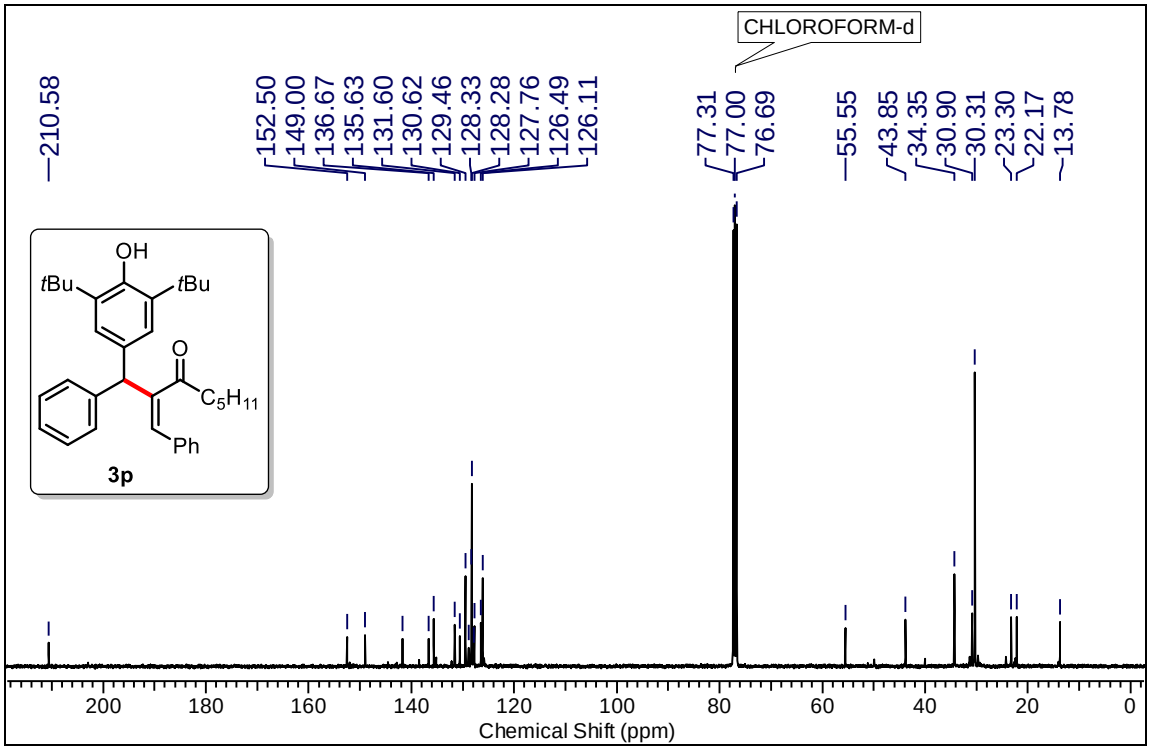

^{1}H NMR spectra of (*Z*)-2-((4-Hydroxy-3,5-dimethylphenyl)(phenyl)methyl)-1,3-diphenylprop-2-en-1-one (3q) (400 MHz, $CDCl_3$):

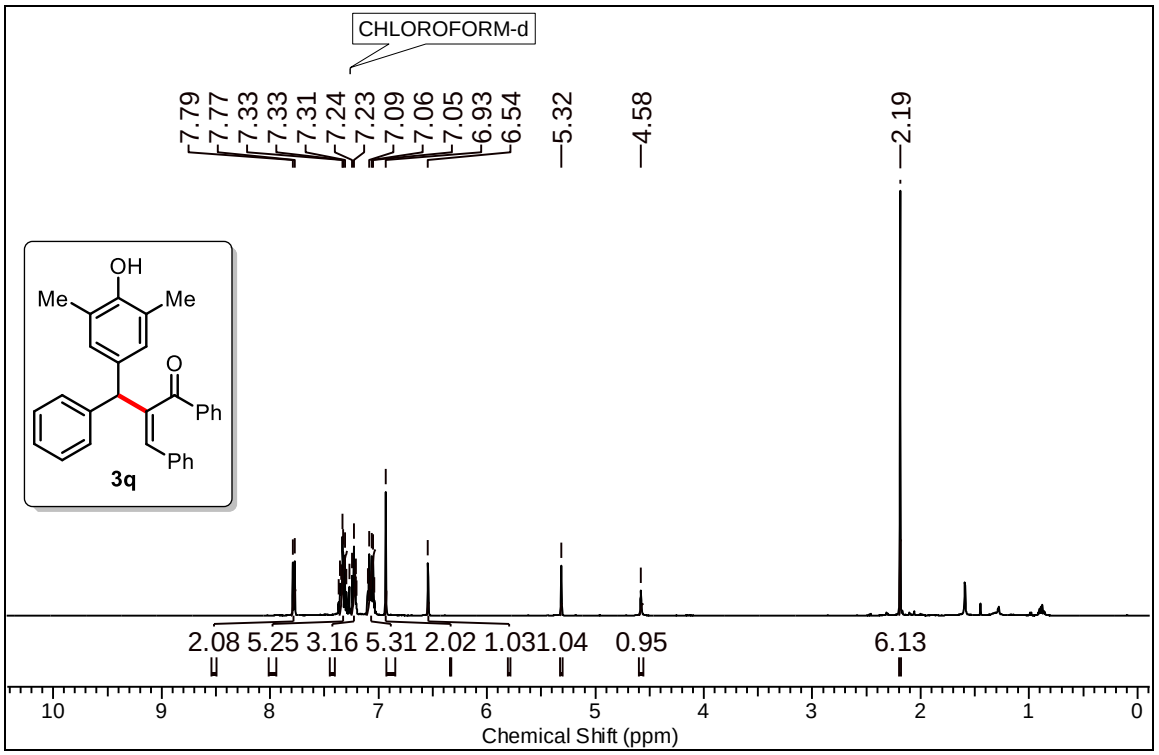

^{13}C NMR spectra of (*Z*)-2-((4-Hydroxy-3,5-dimethylphenyl)(phenyl)methyl)-1,3-diphenylprop-2-en-1-one (3q) (100 MHz, $CDCl_3$):

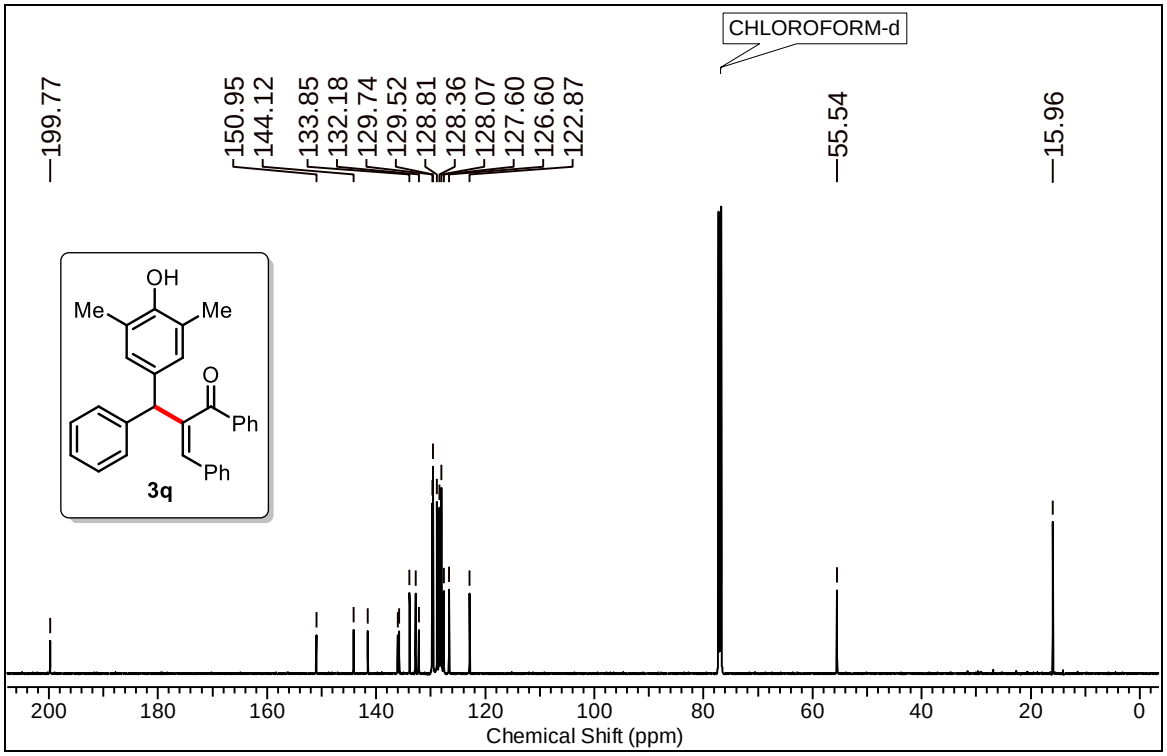

^{1}H NMR spectra of 2-((3,5-Di-*tert*-butyl-4-hydroxyphenyl)(*p*-tolyl)methyl)-1-phenyl prop-2-en-1-one (5b) (400 MHz, $CDCl_3$):

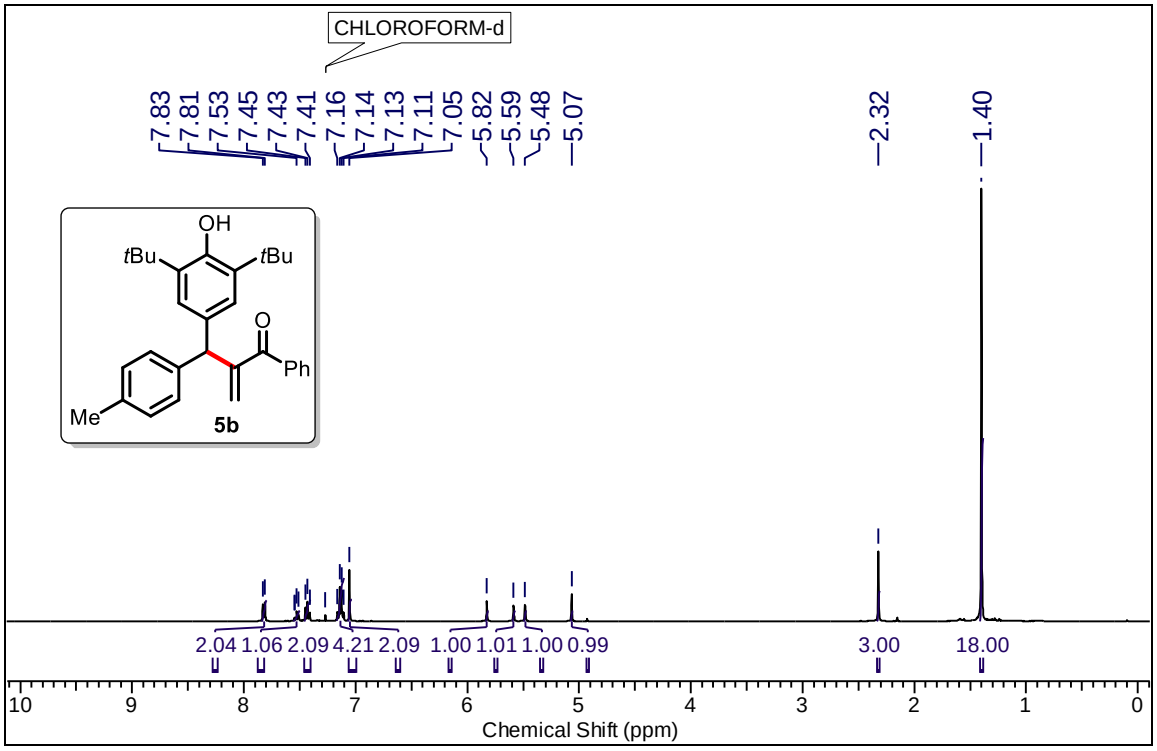

^{13}C NMR spectra of 2-((3,5-Di-*tert*-butyl-4-hydroxyphenyl)(*p*-tolyl)methyl)-1-phenyl prop-2-en-1-one (5b) (100 MHz, $CDCl_3$):

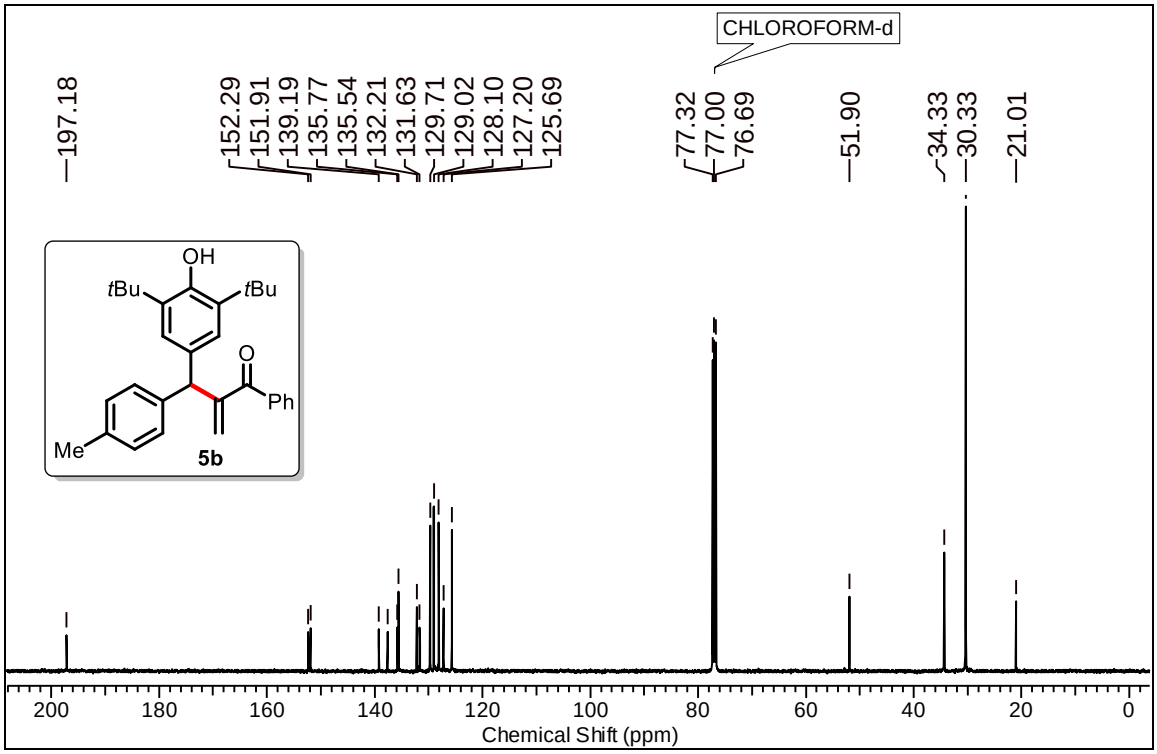

^{1}H NMR spectra of 2-((3,5-Di-*tert*-butyl-4-hydroxyphenyl)(3,4,5-trimethoxyphenyl) methyl)-1-phenyl prop-2-en-1-one (5d) (400 MHz, $CDCl_3$):

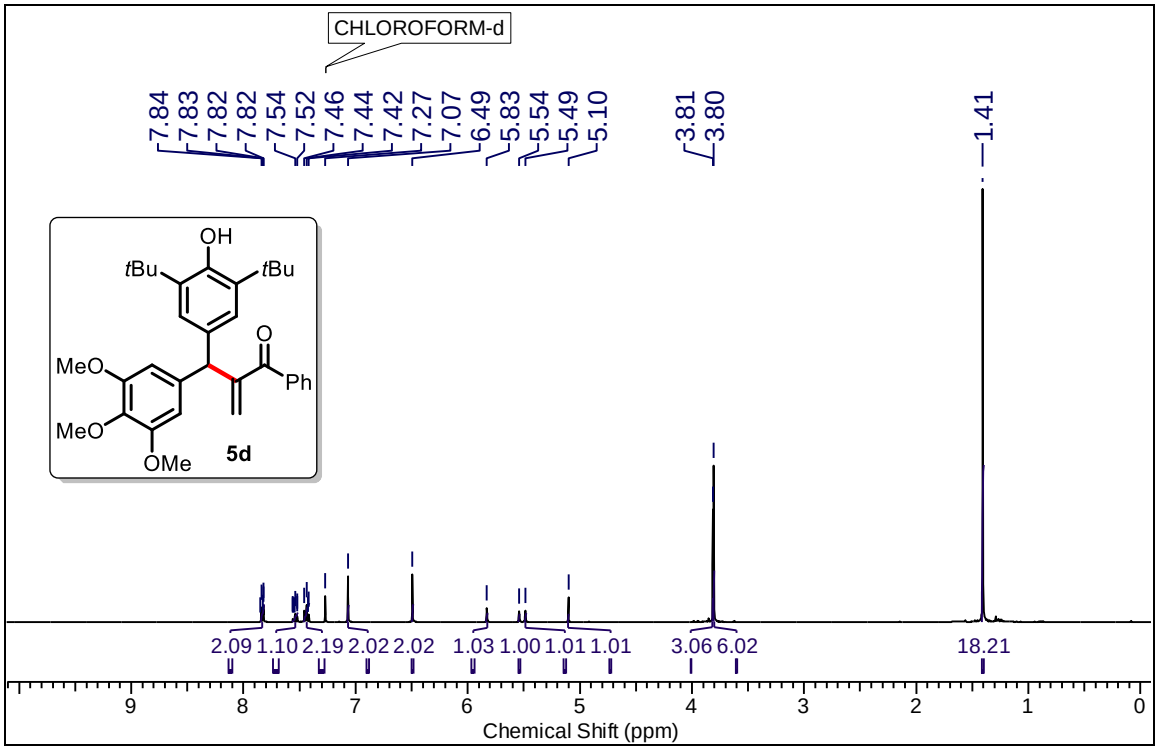

^{13}C NMR spectra of 2-((3,5-Di-*tert*-butyl-4-hydroxyphenyl)(3,4,5-trimethoxyphenyl) methyl)-1-phenyl prop-2-en-1-one (5d) (100 MHz, $CDCl_3$):

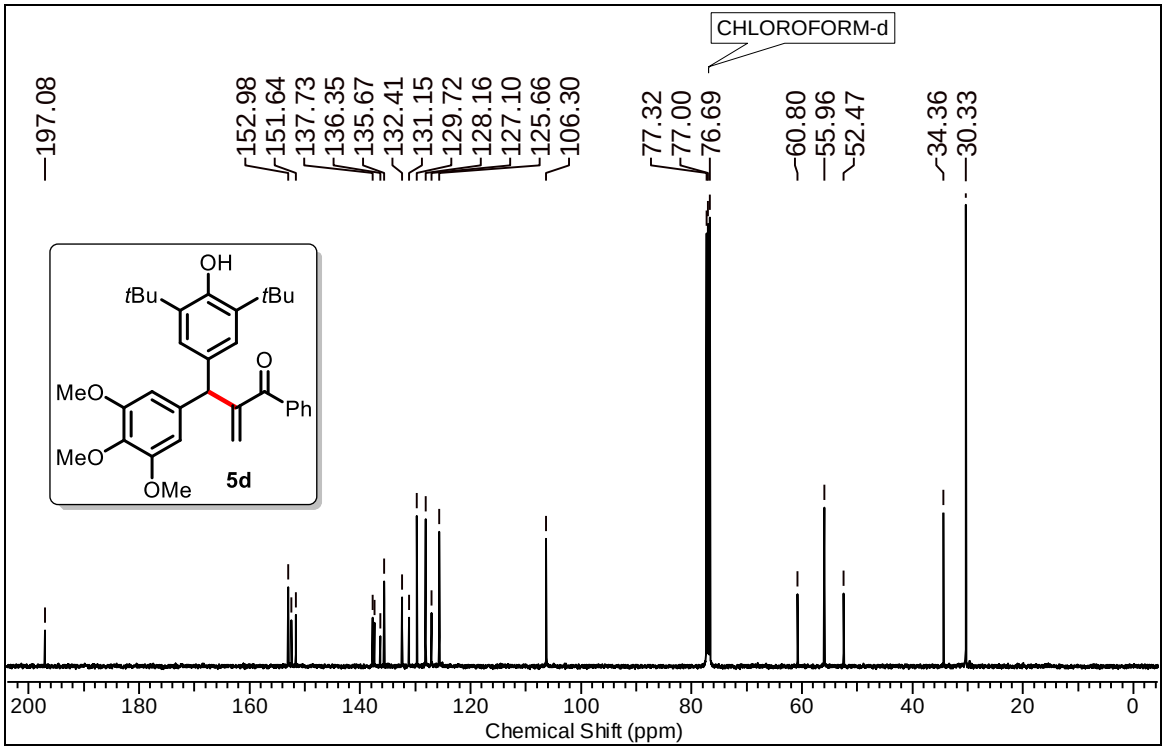

^{1}H NMR spectra of 2-((4-Chlorophenyl)(3,5-di-*tert*-butyl-4-hydroxyphenyl)methyl)-1-phenylprop-2-en-1-one (5e) (400 MHz, $CDCl_3$):

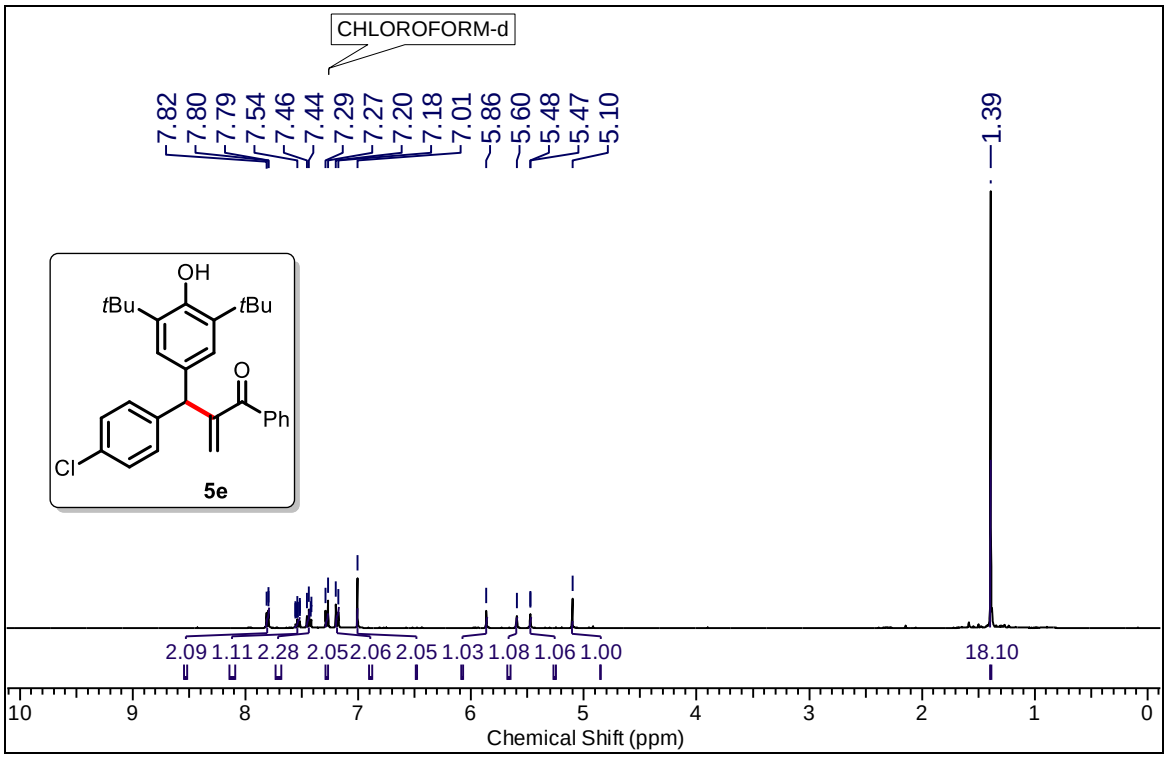

^{13}C NMR spectra of 2-((4-Chlorophenyl)(3,5-di-*tert*-butyl-4-hydroxyphenyl)methyl)-1-phenylprop-2-en-1-one (5e) (100 MHz, $CDCl_3$):

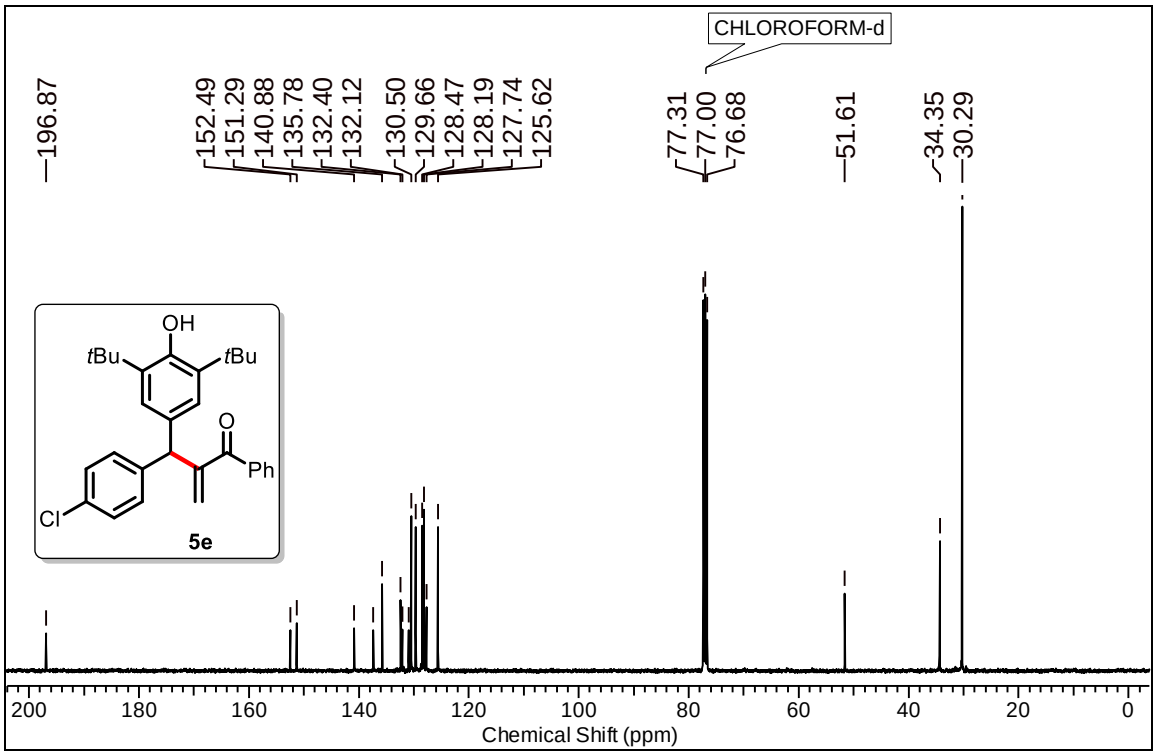

^{1}H NMR spectra of 2-((3,5-Di-*tert*-butyl-4-hydroxyphenyl)(phenyl)methyl)-1-(4-methoxyphenyl)prop-2-en-1-one (5j) (400 MHz, $CDCl_3$):

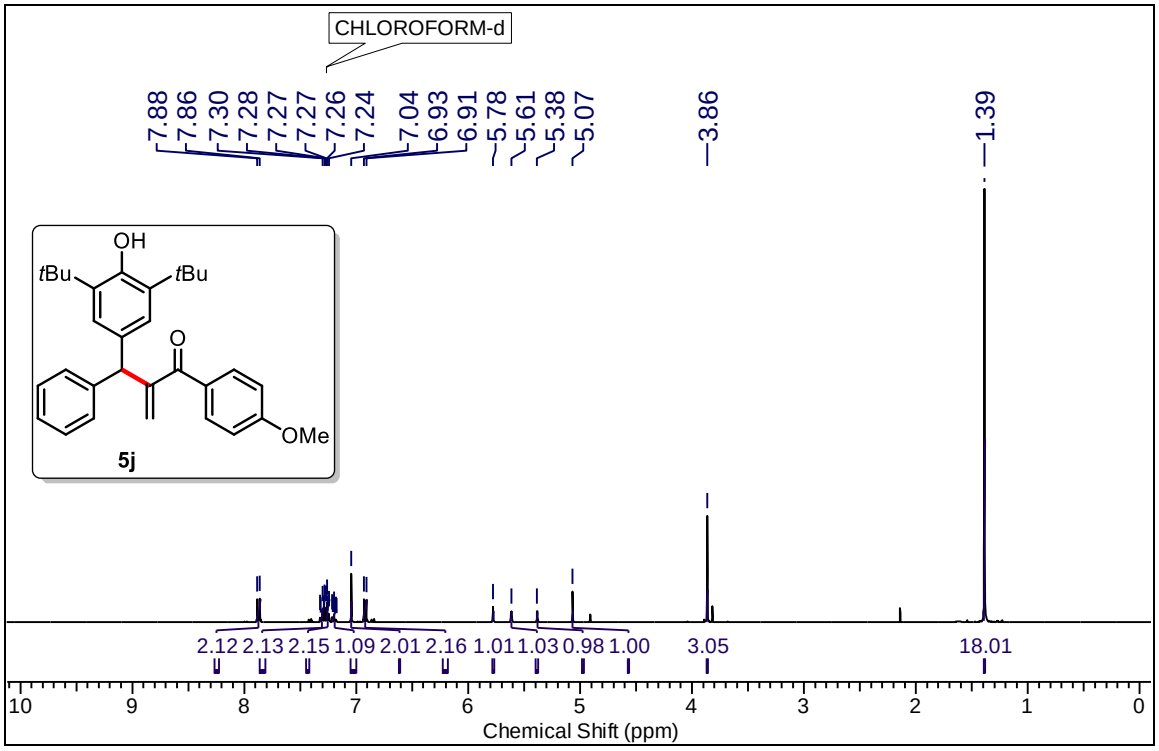

^{13}C NMR spectra of 2-((3,5-Di-*tert*-butyl-4-hydroxyphenyl)(phenyl)methyl)-1-(4-methoxyphenyl) prop-2-en-1-one (5j) (100 MHz, $CDCl_3$):

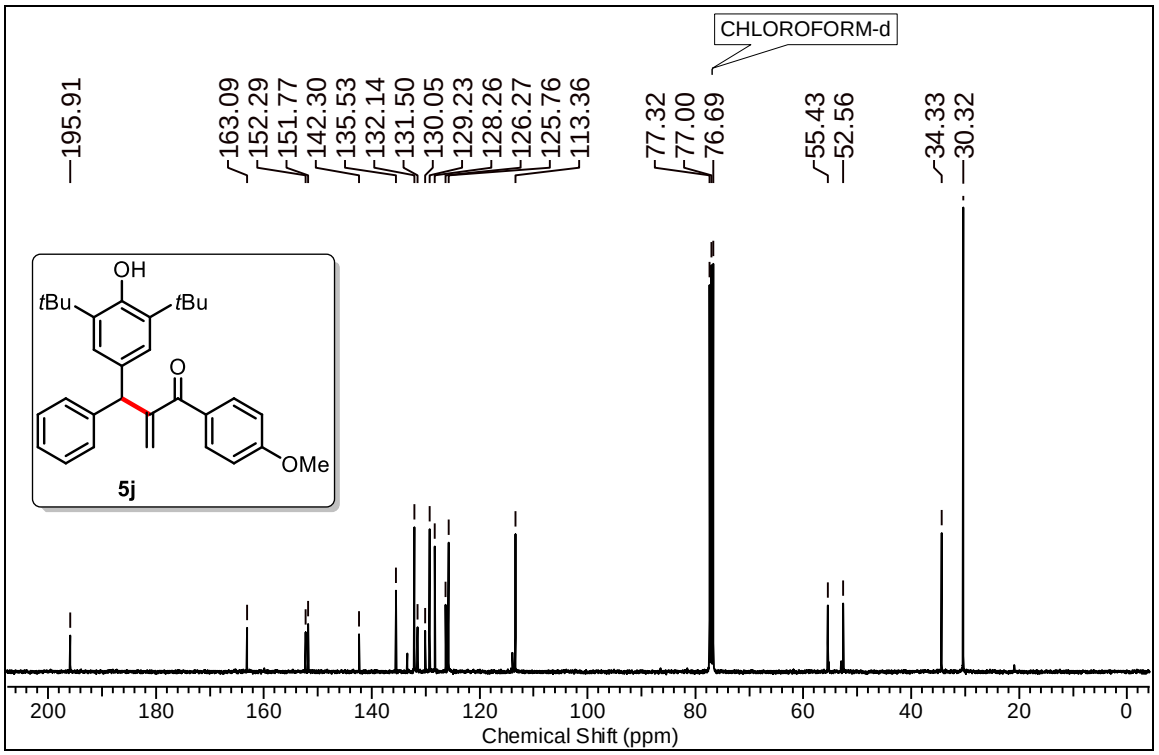

^{1}H NMR spectra of 2-((3,5-Di-*tert*-butyl-4-hydroxyphenyl)(phenyl)methyl)undec-1-en-3-one (5l) (400 MHz, $CDCl_3$):

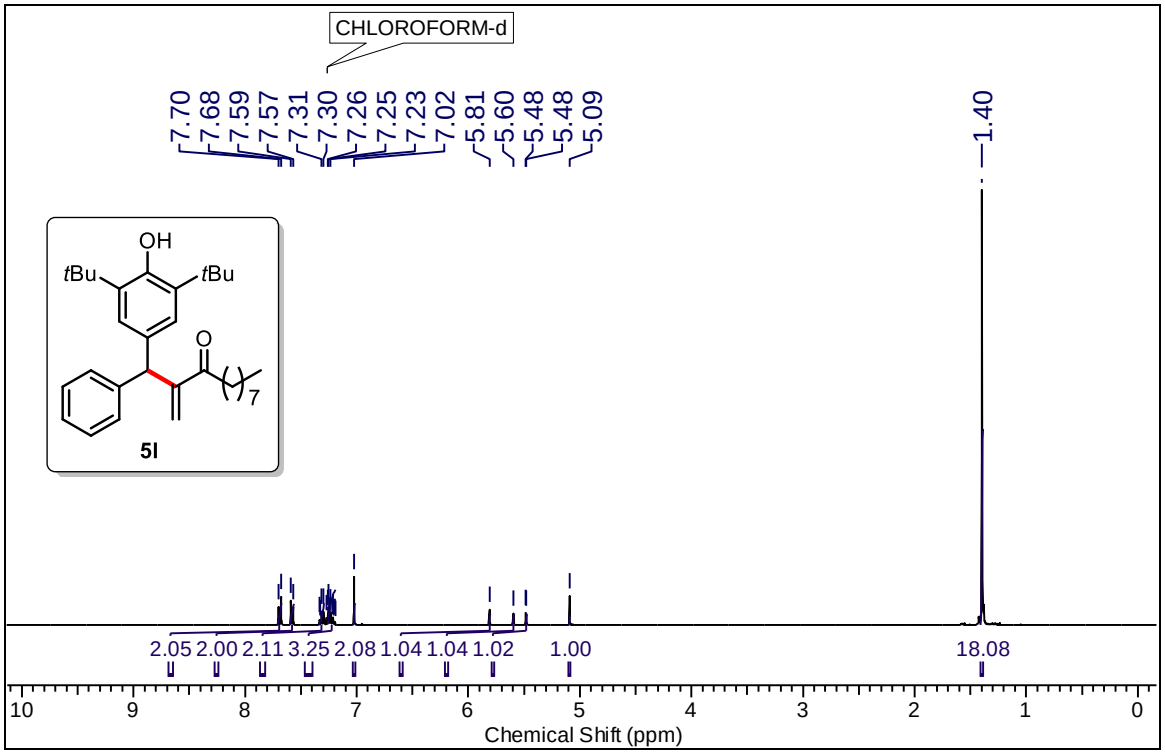

^{13}C NMR spectra of 2-((3,5-Di-*tert*-butyl-4-hydroxyphenyl)(phenyl)methyl)undec-1-en-3-one (5l) (100 MHz, $CDCl_3$):

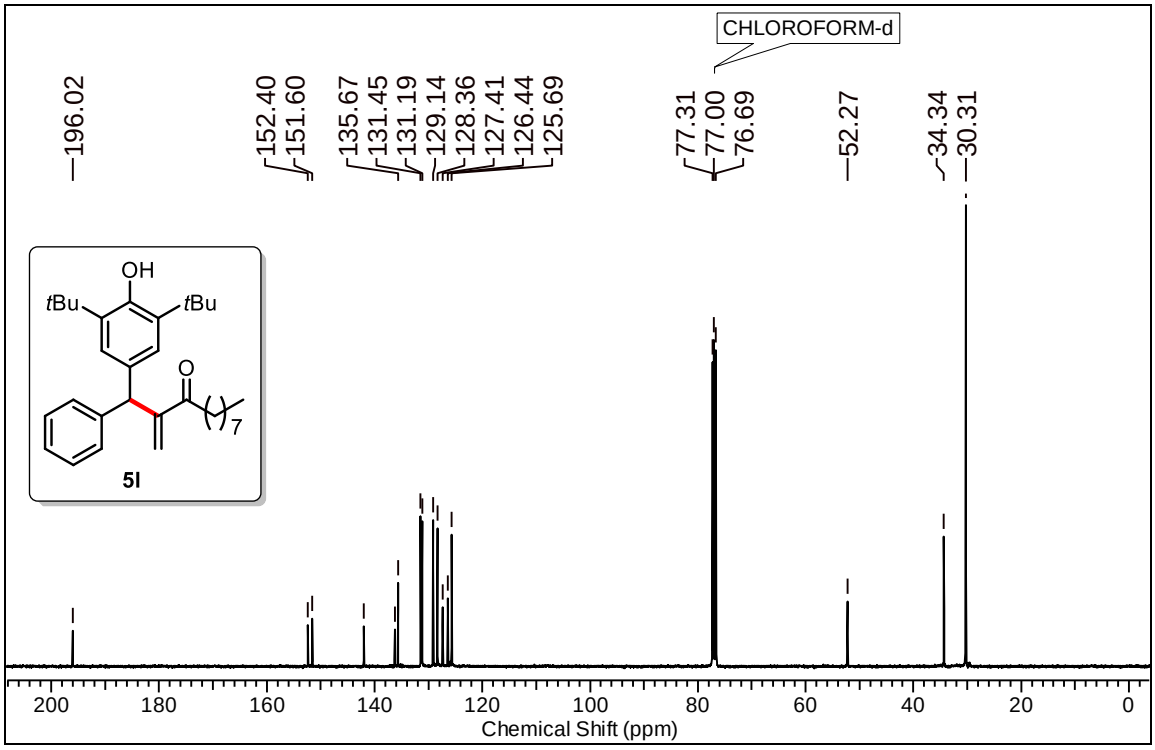

^{1}H NMR spectra of 4-(2-Benzoyl-4,6-dimethoxy-3-phenyl-*1H*-inden-1-ylidene)-2,6-di-*tert*-butyl cyclohexa-2,5-dien-1-one (6b) (400 MHz, $CDCl_3$):

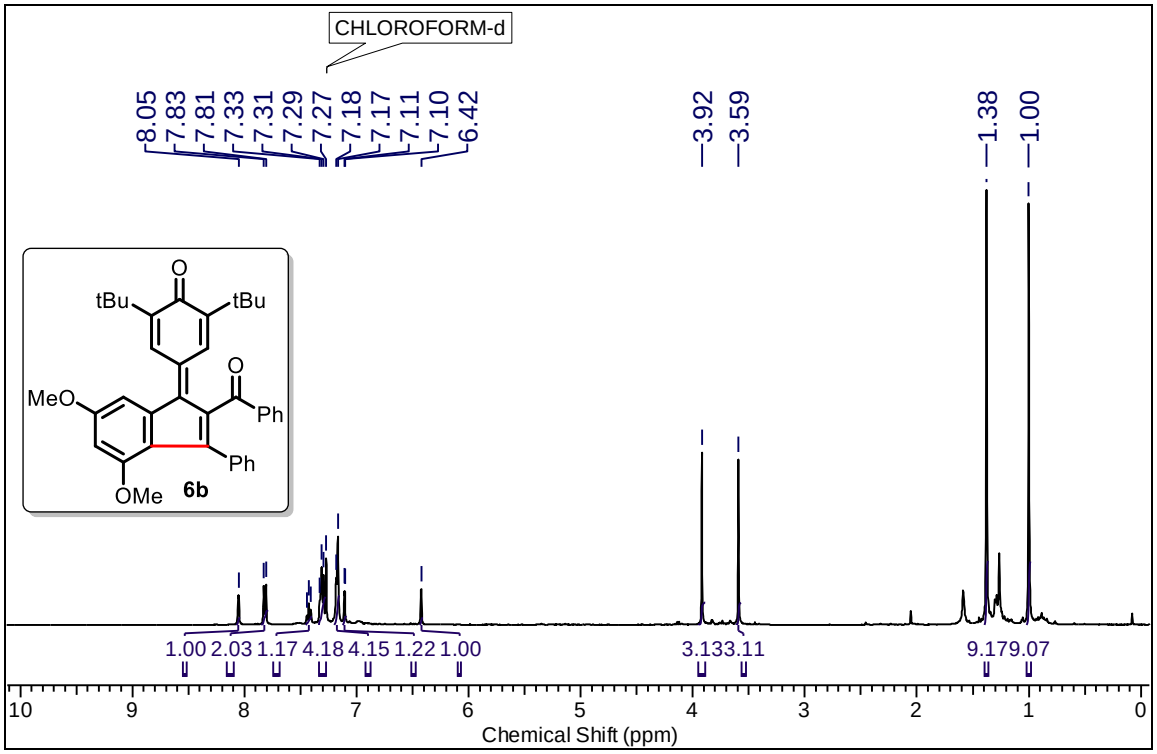

^{13}C NMR spectra of 4-(2-Benzoyl-4,6-dimethoxy-3-phenyl-*1H*-inden-1-ylidene)-2,6-di-*tert*-butyl cyclohexa-2,5-dien-1-one (6b) (100 MHz, $CDCl_3$):

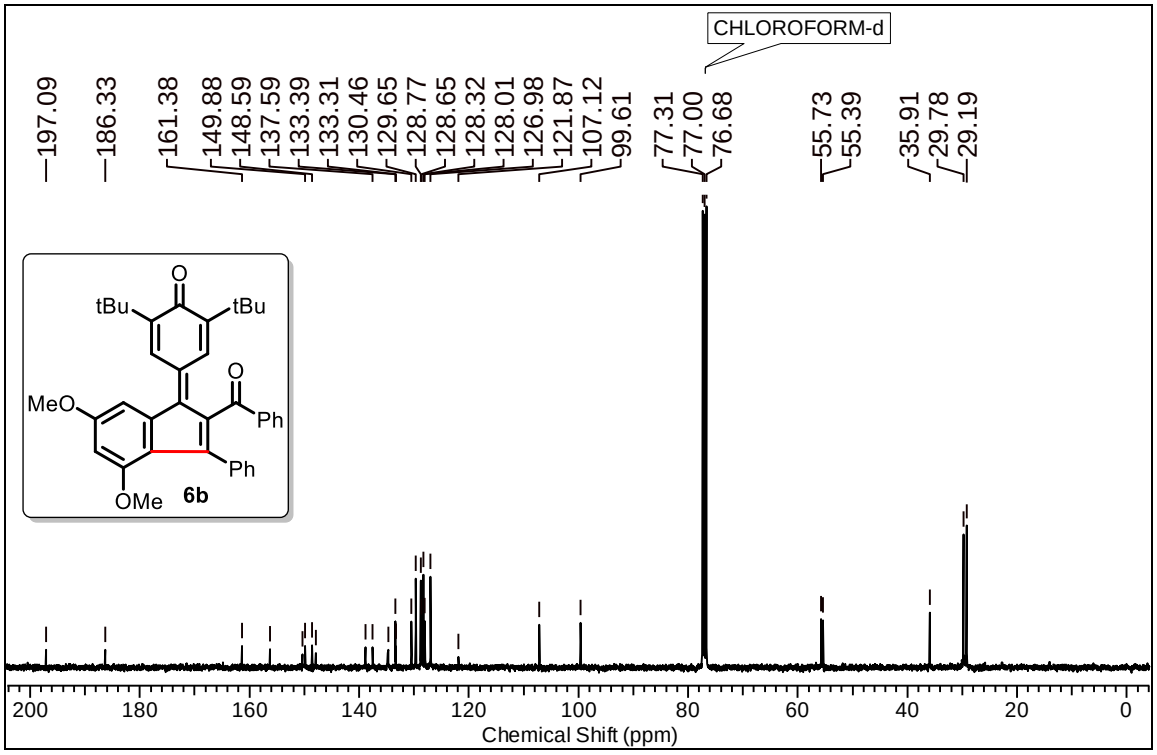

^{1}H NMR spectra of (3-(3,5-Di-*tert*-butyl-4-hydroxyphenyl)-1-hydroxy-5,7-dimethoxy-1-phenyl-*1H*-inden-2-yl)(phenyl)methanone (7b) (400 MHz, $CDCl_3$):

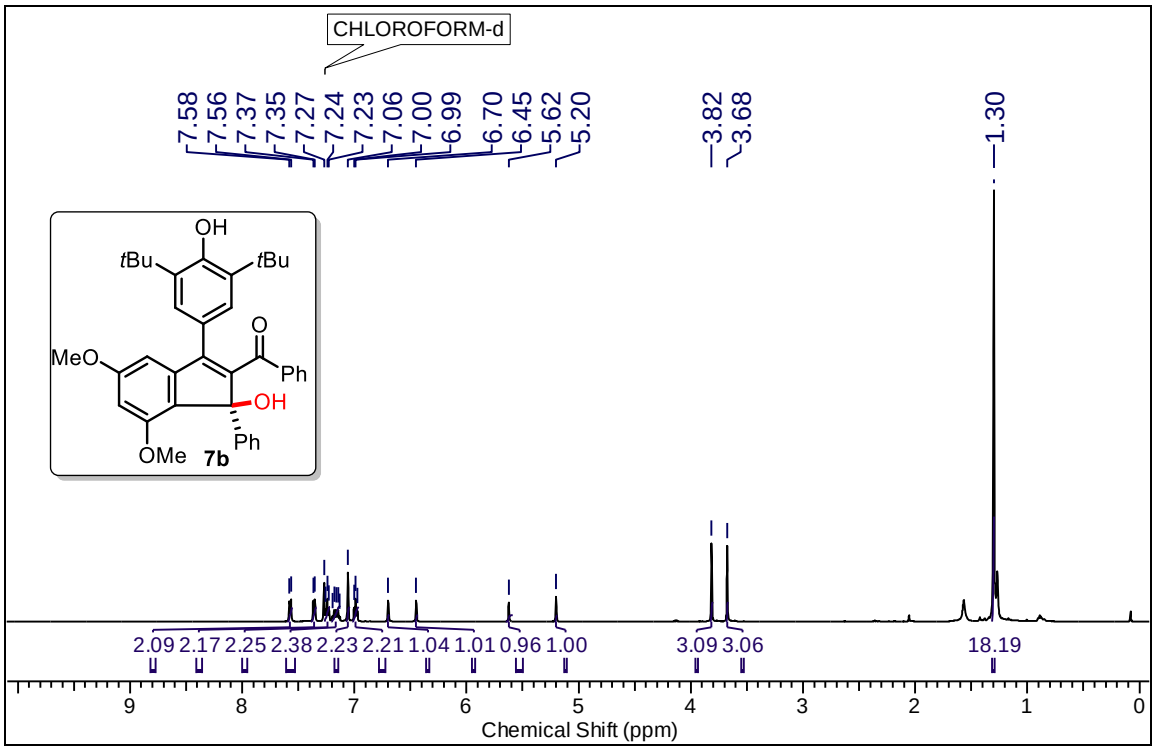

^{13}C NMR spectra of (3-(3,5-Di-*tert*-butyl-4-hydroxyphenyl)-1-hydroxy-5,7-dimethoxy-1-phenyl-*1H*-inden-2-yl)(phenyl)methanone (7b) (100 MHz, $CDCl_3$):

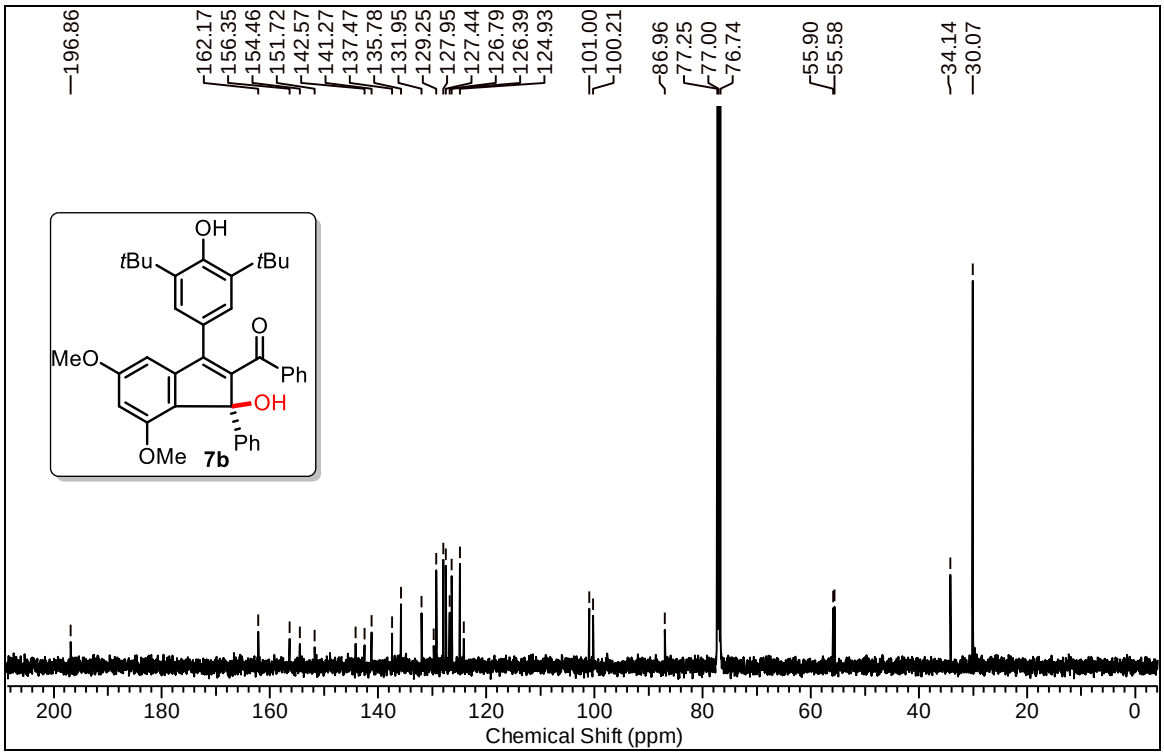

^{1}H NMR spectra of (Z)-2-((4-Hydroxyphenyl)(phenyl)methyl)-1,3-diphenylprop-2-en-1-one (8a) (400 MHz, $CDCl_3$):

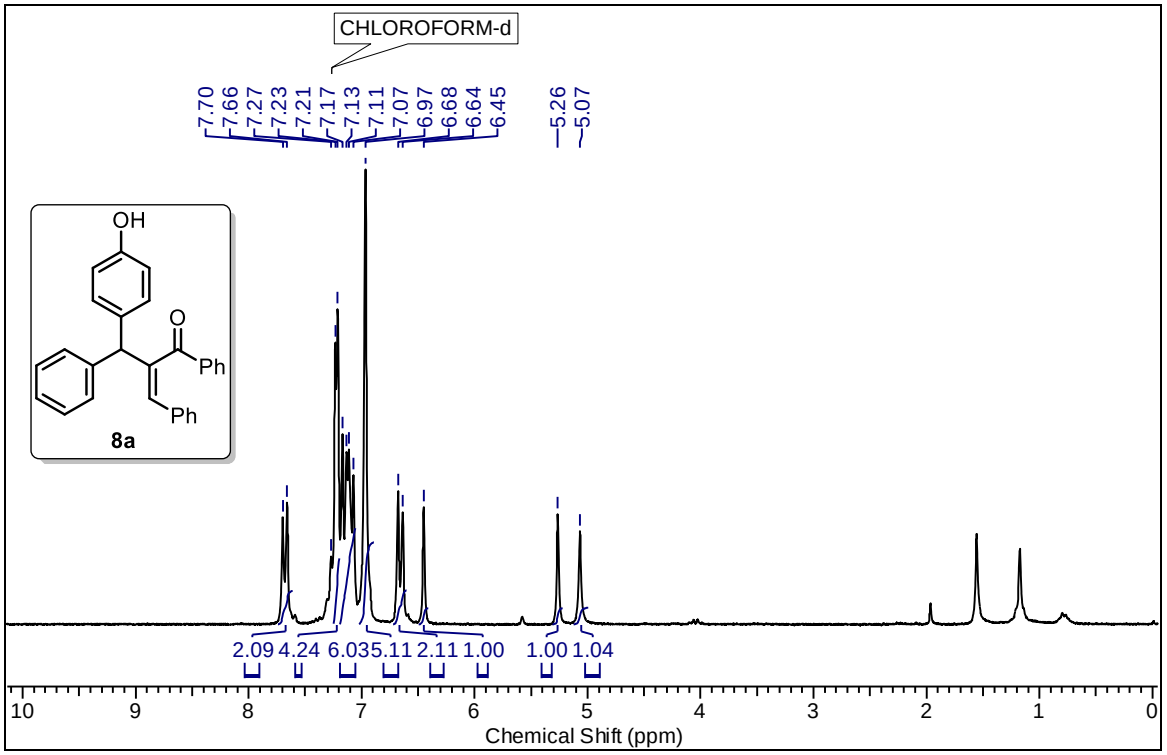

^{13}C NMR spectra of (Z)-2-((4-Hydroxyphenyl)(phenyl)methyl)-1,3-diphenylprop-2-en-1-one (8a) (100 MHz, $CDCl_3$):

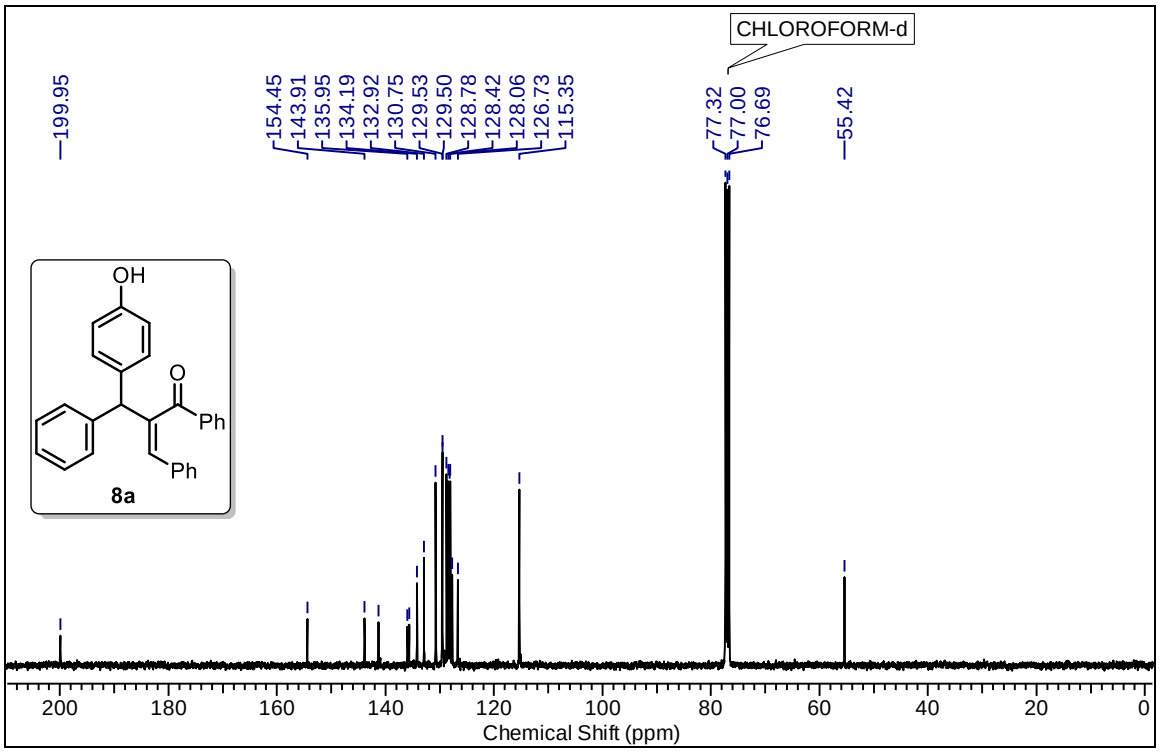

3.2.8 References

[1] Selected reviews on gold catalysis: a) Shiroodi, R. K.; Gevorgyan, V. *Chem. Soc. Rev.* **2013**, *42*, 4991-5001; b) Tejedor, D.; Méndez-Abt, G.; Cotos, L.; García-Tellado, F. *Chem. Soc. Rev.* **2013**, *42*, 458-471; c) Rudolph, M.; Hashmi, A. S. K. *Chem. Soc. Rev.* **2012**, *41*, 2448-2462; d) Corma, A.; Leyva-Pérez, A.; Sabater, M. J. *Chem. Rev.* **2011**, *111*, 1657-1712; e) Wang, S.; Zhang, G.; Zhang, L. *Synlett* **2010**, *2010*, 692-706; f) Shapiro, N. D.; Toste, F. D. *Synlett* **2010**, *2010*, 675-691; g) Hashmi, A. S. K. *Chem. Rev.* **2007**, *107*, 3180-3211; h) A. S. K. Hashmi, M. Rudolph, *Chem. Soc. Rev*. **2008**, *37*, 1766 – 1775.

[2] a) Ahlers, A.; de Haro, T.; Gabor, B.; Fürstner, A. *Angew. Chem. Int. Ed.* **2016**, *55*, 1406-1411; b) Wang, Z.; Zheng, H.; Yang, J.; Xie, X.; She, X. *Adv. Synth. Catal.* **2015**, *357*, 2082-2088; c) Wang, Y.-M.; Kuzniewski, C. N.; Rauniyar, V.; Hoong, C.; Toste, F. D. *J. Am. Chem. Soc.* **2011**, *133*, 12972-12975; d) Li, Z.; Brouwer, C.; He, C. *Chem. Rev.* **2008**, *108*, 3239-3265; e) Rettenmeier, E.; Hansmann, M. M.; Ahrens, A.; Rübenacker, K.; Saboo, T.; Massholder, J.; Meier, C.; Rudolph, M.; Rominger, F.; Hashmi, A. S. K. *Chem. - Eur. J.* **2015**, *21*, 14401-14409; f) Wang, L.-J.; Zhu, H.-T.; Wang, A.-Q.; Qiu, Y.-F.; Liu, X.-Y.; Liang, Y.-M. *J. Org. Chem*. **2014**, *79*, 204-212; g) Mauleón, P.; Krinsky, J. L.; Toste, F. D. *J. Am. Chem. Soc.* **2009**, *131*, 4513-4520; h) Marion, N.; de Fremont, P.; Lemiere, G.; Stevens, E. D.; Fensterbank, L.; Malacria, M.; Nolan, S. P. *Chem. Commun.* **2006**, 2048-2050.

[3] a) Correa, A.; Marion, N.; Fensterbank, L.; Malacria, M.; Nolan, S. P.; Cavallo, L. *Angew. Chem. Int. Ed.* **2008**, *47*, 718-721; b) Shapiro, N. D.; Toste, F. D. *J. Am. Chem. Soc.* **2008**, *130*, 9244-9245; c) Amijs, C. H.; López-Carrillo, V.; Echavarren, A. M. *Org. Lett.* **2007**, *9*, 4021-4024; d) Johansson, M. J.; Gorin, D. J.; Staben, S. T.; Toste, F. D. *J. Am. Chem. Soc.* **2005**, *127*, 18002-18003.

[4] a) Lemiere, G.; Gandon, V.; Cariou, K.; Fukuyama, T.; Dhimane, A.-L.; Fensterbank, L.; Malacria, M. *Org. Lett.* **2007**, *9*, 2207-2209; b) Wang, S.; Zhang, L. *J. Am. Chem. Soc.* **2006**, *128*, 14274-14275; c) de Haro, T.; Nevado, C. *Chem. Commun.* **2011**, *47*, 248-249; d) Ji, Y.-L.; Lin, J.-H.; Xiao, J.-C.; Gu, Y.-C. *Eur. J. Org. Chem.* **2014**, *2014*, 7948-7954; e) Oh, C. H.; Kim, J. H.; Oh, B. K.; Park, J. R.; Lee, J. H. *Chem. - Eur. J.* **2013**, *19*, 2592-2596.

[5] Yu, M.; Zhang, G.; Zhang, L. *Org. Lett.* **2007**, *9*, 2147-2150.

[6] Yu, Y.; Yang, W.; Rominger, F.; Hashmi, A. S. K. *Angew. Chem. Int. Ed.* **2013**, *52*, 7586-7589.

[7] Manoni, E.; Daka, M.; Mastandrea, M. M.; Nisi, A. D.; Monari, M.; Bandini, M. *Adv. Synth. Catal.* **2016**, *358*, 1404-1409.

[8] a) Rathod, J.; Sharma, B. M.; Mali, P. S.; Kumar, P. *Synthesis* **2017**, *49*, 5224-5230; b) sharma B. M.; Shinde, D. R.; Jain, R.; Begari, E.; Satbhaiya, S.; Gonnade, R. G.; Kumar P. Kumar, P. *Org. Lett.* **2018**, *20*, 2787-2791.

[9] a) Onishi, Y.; Nishimoto, Y.; Yasuda, M.; Baba, A. *Org. Lett.* **2014,** *16*, 1176-1179; b) Sengupta, D.; Saha, J.; De, G.; Basu, B. *J. Mater. Chem. A*, 2014, **2**, 3986-3992.

[10] a) Wang, X.; Zhou, Y.; Qiu, L.; Yao, R.; Zheng, Y.; Zhang, C.; Bao, X.; Xu, X. *Adv. Synth. Catal.* **2016,** *358*, 1571-1576; b) Tsukano, C.; Yamamoto, S.; Takemoto Y. *Chem. Pharm. Bull*. **2015**, *63*, 710-719; c) Cheng, X.; Yu, Y.; Mao, Z.; Chen, J.; Huang; X. *Org. Biomol. Chem*. **2016**, 14, 3878-3882.

[11] Chu, W. D.; Zhang, L. F.; Bao, X.; Zhao, X.-H.; Zeng, C.; Du, J. Y.; Zhang, G. B.; Wang, F. X.; Ma, X. Y.; Fan, C. A. *Angew. Chem. Int. Ed.* **2013**, *52*, 9229-9233.

[12] Carlos; J.-B.; Parra, A.; López, A.; Fabio, C.-A.; Daniel; C.-S.; Cárdenas, D. J.; Tortosa, M. *ACS Catal.* **2016**, *6*, 442-446.

[13] Bruker (2016). *APEX3*, *SAINT* and *SADABS*. Bruker AXS Inc., Madison, Wisconsin, USA.

[14] Sheldrick, G. M. *Acta Crystallogr*. **2008**, *A64*, 112-122.

[15] Farrugia, L. J. *J. Appl. Cryst.* **1997**, *30*, 565.

List of Publications:

1) Modular Synthesis of Biaryl-Substituted Phosphine Ligands: Application in Microwave-Assisted Palladium-Catalyzed C–N Cross-Coupling Reactions, Chandani Singh , **Jayant Rathod** , Vishwajeet Jha, Armen Panossian, Pradeep Kumar * Frédéric R. Leroux*. *Eur. J. Org. Chem.* **2015**, 6515-6525.

2) Highly active recyclable SBA-15-EDTA-Pd catalyst for Mizoroki-Heck, Stille and Kumada C–C coupling reactions, **Jayant Rathod**, Priti Sharma, Punam Pandey, A. P. Singh*, Pradeep Kumar*. *J. Porous Mater.* **2017**, *24*, 837–846.

3) Tf_2NH-Catalyzed 1,6-Conjugate Addition of Vinyl Azides with *p*-Quinone Methides: A Mild and Efficient Method for the Synthesis of *β*-Bis-Arylamides**,** **Jayant Rathod**, Brijesh M. Sharma, Pramod S. Mali, Pradeep Kumar* *Synthesis* **2017**; 49, 5224-5230.

4) Synthesis of heterogeneous Ru(II)-1,2,3-triazole catalyst supported over SBA-15: application to the hydrogen transfer reaction and unusual highly selective 1,4-disubstituted triazole formation *via*multicomponent click reaction , **Jayant Rathod**, Priti Sharma, A. P. Singh,* Pradeep Kumar* Yoel Sasson* *Catal. Sci. Technol.* **2018**, *8*, 3246-3259.

5) Harnessing Nucleophilicity of Allenol Ester with *p*-Quinone Methides via Gold Catalysis: Application to the Synthesis of Diarylmethine-Substituted Enones, Brijesh M. Sharma, **Jayant Rathod**, Rajesh G. Gonnade, Pradeep Kumar* *J. Org. Chem.* **2018**, *83*, 9353–9363.

6) Tf_2NH catalyzed 1,6-conjugate addition of 2-hydroxy-*p*-quinone methides with *β*-Functionalized Ketones: Access to 2,3,4,9-Tetrahydro-1*H*-xanthenones and 4*H*-Chromene Derivatives, Shruti Satbhaiya, Nilesh S. Khonde, **Jayant Rathod** Rajesh Gonnade, Pradeep Kumar* *Eur. J. Org. Chem.* **2019**, 3127-3133.

Jayant B. Rathod

Division of Organic Chemistry

National Chemical Laboratory,

Dr. Homi Bhabha road, Pune, (India), 411 008.

Mobile No.: +91 9689625412

Email ID: jbrathod1990@gmail.com

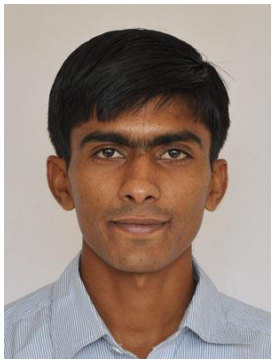

Jayant B. Rathod was born in 1990 in Surat (Gujarat), India. He completed his graduation in chemistry from M. M. Science College Morbi, in 2010 and post-graduation in Organic chemistry from the Department of Chemistry Saurashthra University Rajkot in 2012. He was university rank holder during his M.Sc. He has been awarded the CSIR fellowship for pursuing his Ph.D. degree in organic chemistry division of CSIR-National Chemical Laboratory under the guidance of Dr. Pradeep Kumar. His research interest focuses around the development of highly selective C-N and C−C bond-forming reactions as well as development of methodology under microwave condition and application of heterogeneous catalysis.

Supervised/Trained

Trained 1 under graduate and 2 post graduate students during PhD tenure:

Reprint of Publications

JOC The Journal of Organic Chemistry
Cite This: J. Org. Chem. 2018, 83, 9353−9363
Article
pubs.acs.org/joc

Harnessing Nucleophilicity of Allenol Ester with *p*-Quinone Methides via Gold Catalysis: Application to the Synthesis of Diarylmethine-Substituted Enones

Brijesh M. Sharma,[†,‡] Jayant Rathod,[†,‡] Rajesh G. Gonnade,[‡,§] and Pradeep Kumar*[,†,‡]

[†]Division of Organic Chemistry, CSIR-National Chemical Laboratory, Pune 411008, India
[‡]Academy of Scientific and Innovative Research (AcSIR), New Delhi 110025, India
[§]Physical and Materials Chemistry Division, CSIR-National Chemical Laboratory, Pune 411008, India

Supporting Information

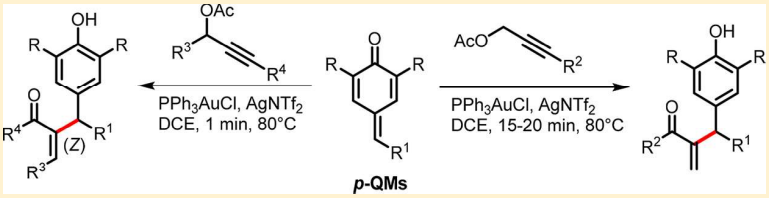

ABSTRACT: A gold(I)-catalyzed protocol for intermolecular 1,6-conjugate addition of nucleophilic allenol ester generated in situ through [3,3]-sigmatropic rearrangement with *p*-quinone methides (*p*-QMs) has been developed. The gold catalyst plays a dual role by the π-acid-triggered activation of alkynes and at the same time as a Lewis acid for activation of *p*-QMs toward nucleophilic attack. This method enables rapid access to a wide range of densely functionalized diarylmethine-substituted enones, a Morita-Baylis-Hillman (MBH) product with high selectivity, excellent yields, and broad substrate scope.

INTRODUCTION

In recent years, there has been a tremendous upsurge of interest in the homogeneous gold-catalyzed activation of C−C triple bond and allenes for constructing novel molecular architectures or structural core of natural products/analogs in a cascade fashion.[1] The gold-catalyzed [3,3]-sigmatropic rearrangement of propargylic acetate to allenol ester followed by electrophilic activation by gold(I)/(III) complexes toward nucleophilic attack, encompassing both inter-[2] and intramolecular[3] variants, are among the most exploited reactions (Figure 1, path I). However, to date, there are only a few reports which deal with inherent nucleophilicity of in situ generated allenol ester[4] toward intermolecular electrophilic addition through gold-catalyzed [3,3]-sigmatropic rearrangement reaction in C−C bond formation (Figure 1, path II). In this direction, recently Zhang and co-workers first reported an intermolecular addition of the nucleophilic allenol ester with electrophilic *N*-iodosuccinimide (NIS) for the synthesis of α-iodoenones.[5] Later, Hashmi and co-workers exquisitely demonstrated the gold-catalyzed intermolecular trapping of the allenol ester with electrophilic oxocarbenium ions generated from acetal derivatives for $C(sp^3)-C(sp^2)$ bond formation.[6] In this line, Bandini and co-workers further reported the gold-catalyzed α-alkylation of allylic alcohols by trapping allenol ester as shown in Figure 1.[7]

In recent years, the *p*-QMs motifs have received considerable attention owing to their Michael acceptor property toward various nucleophiles under Lewis or Brønsted acid catalysis.[8,9] In 2016, Lin and co-workers[10] demonstrated the intermolecular 1,6-conjugate arylation of *p*-QMs with electron-rich aromatic compounds for the synthesis of unsymmetrical triarylmethanes under $BF_3{\cdot}OEt_2$ catalysis.

Similarly Anand et al.[11] and Li et al.[12] reported 1,6-conjugate allylation of *p*-QMs using $B(C_6F_5)_3$ and $Bi(OTf)_3$ respectively. Further Angle[13] and China Raju[14] exquisitely demonstrated Lewis acid catalyzed intramolecular cyclization reaction on *p*-QMs utilizing terminators such as allyl silanes and β-keto esters appended to *p*-QMs. Recently our group has also reported acid-catalyzed 1,6-conjugate addition reaction of *p*-QMs with vinyl azides and butenolides.[15] To the best of our knowledge, the gold-catalyzed activation of alkynes along with *p*-QMs toward 1,6-conjugate addition has not yet been explored. In continuation with our ongoing research interest for exploring the electrophilicity of *p*-QMs and its nucleophilic repertoire, we envisioned that incipient allenol ester, generated from a propargylic acetate (path-II) through a π-acid-triggered cascade, could serve as a nucleophilic source (Figure 1). Herein, we report the gold-catalyzed intermolecular 1,6-conjugate addition of nucleophilic allenol ester with *p*-QMs to furnish a variety of unsymmetrical diarylmethine-substituted enones.

RESULTS AND DISCUSSION

To test our hypothesis for gold-catalyzed intermolecular nucleophilic addition, *p*-QMs **1a** and the propargylic ester **2a**

Received: May 21, 2018
Published: June 20, 2018

DOI: 10.1021/acs.joc.8b01294
J. Org. Chem. 2018, 83, 9353−9363

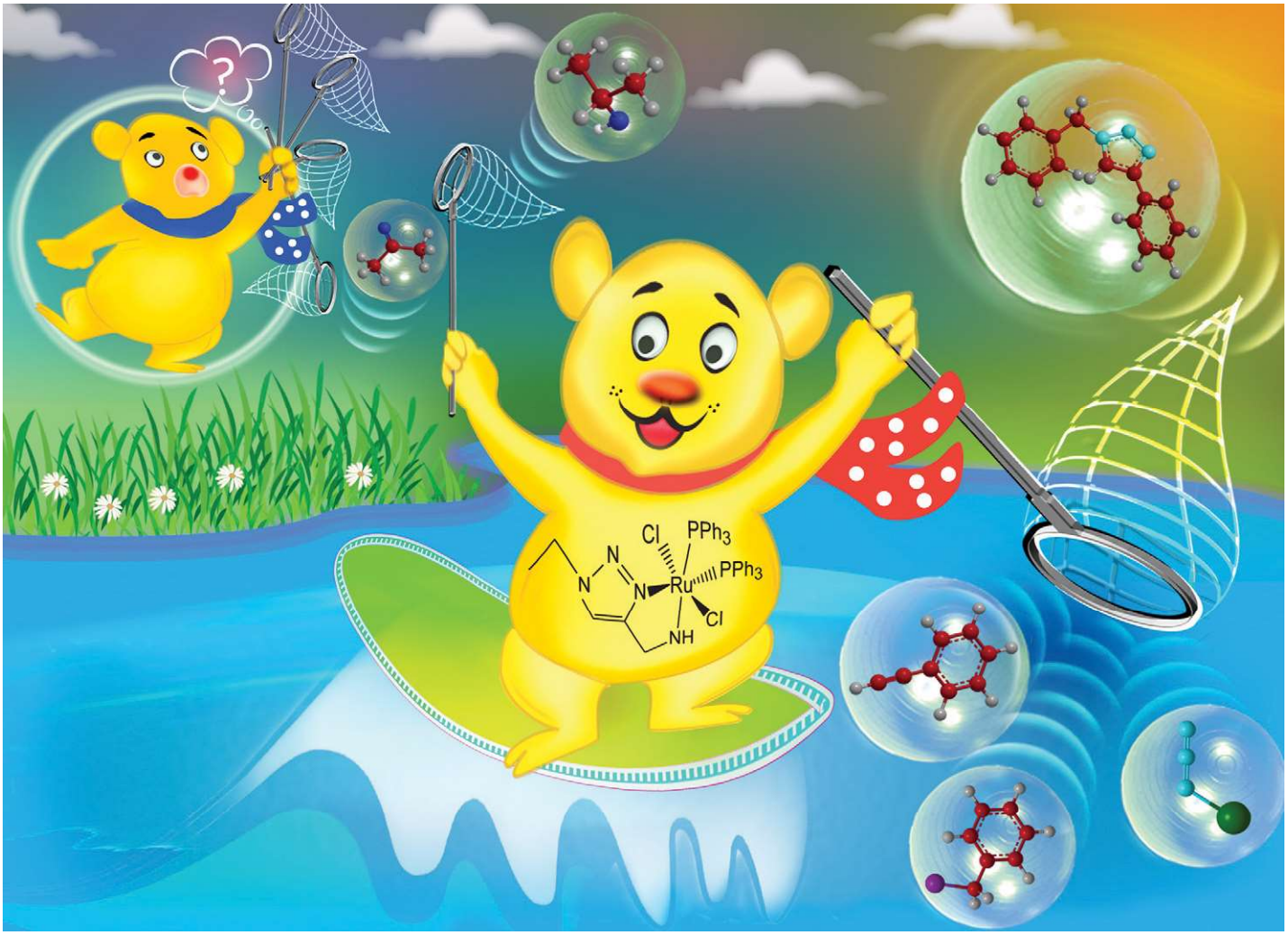

Showcasing collaborative research from Prof. Yoel Sasson group at the Hebrew University, Jerusalem, Israel and Dr. A. P. Singh & Dr. Pradeep Kumar group from CSIR-NCL, Pune, India.

Synthesis of heterogeneous Ru(II)-1,2,3-triazole catalyst supported over SBA-15: application to the hydrogen transfer reaction and unusual highly selective 1,4-disubstituted triazole formation *via* multicomponent click reaction

We demonstrated an efficient protocol for ligand synthesis and covalent tethering to a solid support in a single step using "click chemistry". Exclusively, SBA-15-Tz-Ru(II)TPP screening in multicomponent cycloaddition reaction exhibits remarkable reactivity in water for the regioselective synthesis of 1,4-disubstituted 1,2,3-triazole with excellent yields in one pot.

As featured in:

See A. P. Singh, Pradeep Kumar, Yoel Sasson *et al.*, *Catal. Sci. Technol.*, 2018, **8**, 3246.

ROYAL SOCIETY OF CHEMISTRY

rsc.li/catalysis

Registered charity number: 207890

Catalysis Science & Technology

PAPER

View Article Online
View Journal | View Issue

Cite this: *Catal. Sci. Technol.*, 2018, 8, 3246

Synthesis of heterogeneous Ru(II)-1,2,3-triazole catalyst supported over SBA-15: application to the hydrogen transfer reaction and unusual highly selective 1,4-disubstituted triazole formation *via* multicomponent click reaction†

Priti Sharma, ‡[a] Jayant Rathod,‡[c] A. P. Singh,*[b] Pradeep Kumar*[c] and Yoel Sasson*[a]

Received 26th December 2017,
Accepted 8th April 2018

DOI: 10.1039/c7cy02619f

rsc.li/catalysis

In the present study, we demonstrate a simple and efficient method for ligand formation and covalent anchoring to a heterogeneous support *via* click reaction. The complex tris(triphenylphosphine)ruthenium(II) dichloride [$RuCl_2(PPh_3)_3$] anchored over the click modified ligand of SBA-15 forms a new highly efficient heterogeneous SBA-15-Tz-Ru(II)TPP catalyst. Solid state ^{13}C, ^{29}Si, and ^{31}P CP-MAS NMR spectra provide evidence for the formation of the heterogeneous catalyst. SBA-15-Tz-Ru(II)TPP catalyst was screened for the multicomponent click cycloaddition reaction in water medium as a green solvent and it exhibited unusual and excellent selectivity for the formation of 1,4-disubstituted triazole product under mild reaction condition. In addition, SBA-15-Tz-Ru(II)TPP catalyst also catalyzed the hydrogen transfer reaction of various carbonyl compounds with excellent catalytic activity to give the corresponding alcohols. The heterogeneous catalyst can be recycled and reused several times (five) without a loss in reactivity.

Introduction

In recent years, the "click chemistry" reaction has grown exceptionally with enhanced attention from worldwide researchers owing to its applications in various fields, such as medicine,[1] materials and polymers.[2] Click chemistry is associated with several advantages, such as a simple and mild reaction procedure, atom efficient, and compatibility with broad range of functional groups.[3] Apart from the extensive applications of click chemistry in various fields, novel ligand design and modification *via* 1,2,3-triazole have added a new dimension in the area of coordination chemistry. In click chemistry, a high level of selectivity has been demonstrated exclusively for either 1,4 or 1,5-substituted 1,2,3-triazole with excellent yields, with further application as coordination ligands with various metal complexes.[4] In a remarkable work, Hecht *et al.* utilized click chemistry and its chelating ability to produce a transition metal complex *via* coordination [clickates based on 2,6-bis(1,2,3-triazol-4-yl)pyridines].[5] In addition, Sarkar and his co-workers designed and synthesized novel ligands *via* click reaction (1,2,3-triazole) for metal complex coordination and spin crossover complexes.[6] In a book chapter, Crowley *et al.* documented the extension of the applicable light of *click-triazole* in coordination chemistry.[7] With the fact that 1,2,3-triazole shows good capability with metal complexes in coordination chemistry due to its homogeneous nature, it suffers the drawback of recyclability. In our recent work, we have shown that the substituted 1,2,3-triazole can replace the traditional ligand and coordinate with metal complexes *via* nitrogen-donor ligands in an efficient way.[8] In the same context, we tried to design a new ligand with a covalent attachment to the heterogeneous support in a single step *via* 1,2,3-triazole formation (click reaction) (Schemes 1 and 2). Further, in the field of heterogeneous catalysis,[9] precisely, mesoporous materials like SBA-15 are preferred candidates for functionalization owing to their high hydrothermal stability, large pore size and thick walls, which can be easily functionalized using the free hydroxyl group of mesoporous SBA-15 (Scheme 2).[10]

In the literature, copper-catalyzed click reactions generally proceed with a two-component reaction system using an

[a] *Casali Center of Applied Chemistry, Institute of Chemistry, The Hebrew University of Jerusalem, Jerusalem, Israel. E-mail: ysasson@huji.ac.il*
[b] *Catalysis Division, CSIR-National Chemical Laboratory, Dr. Homi Bhabha Road, Pune 411008, India. E-mail: ap.singh@ncl.res.in*
[c] *Division of Organic Chemistry, CSIR-National Chemical Laboratory, Dr. Homi Bhabha Road, Pune-411008, India. E-mail: pk.tripathi@ncl.res.in*

† Electronic supplementary information (ESI) available: ^{31}P NMR of catalyst SEM-EDX analysis, TEM images, TEM-EDX, XPS result, P XPS, ^{1}H NMR of Intermediate 4-phenyl-1*H*-1,2,3-triazole, ICP, HR-XPS, analytical data of multi component click cycloaddition products. See DOI: 10.1039/c7cy02619f

‡ Equal contribution.

Synthesis J. Rathod et al. Paper

Tf_2NH-Catalyzed 1,6-Conjugate Addition of Vinyl Azides with *p*-Quinone Methides: A Mild and Efficient Method for the Synthesis of β-Bis-Arylamides

Jayant Rathod[a,b]
Brijesh M. Sharma[a,b]
Pramod S. Mali[c]
Pradeep Kumar*[a,b]

[a] Division of Organic Chemistry, CSIR-National Chemical Laboratory, Dr. Homi Bhabha Road, Pune-411008, India
pk.tripathi@ncl.res.in
[b] Academy of Scientific and Innovative Research (AcSIR), New Delhi-110025, India
[c] Central NMR Facility, National Chemical Laboratory, Pune-411008, India

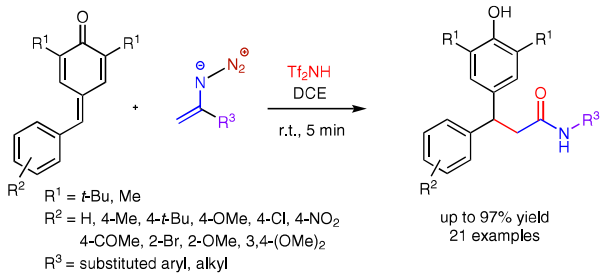

Received: 19.07.2017
Accepted after revision: 19.07.2017
Published online: 22.08.2017
DOI: 10.1055/s-0036-1588546; Art ID: ss-2017-n0227-op

Abstract Tf_2NH-catalyzed tandem 1,6-conjugate addition/Schmidt type rearrangement using vinyl azides and *p*-quinone methides to access a variety of β-bis-arylated amides is reported. The method is quick, efficient, mild, and high yielding with broad substrate scope.

Key words vinyl azide, *p*-quinone methide, Brønsted acid, 1,6-conjugate addition, rearrangement, β-bis-arylamides

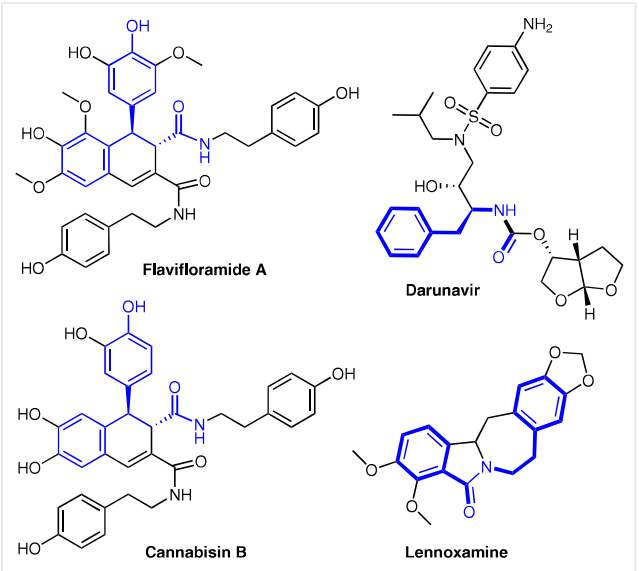

Figure 1 Privileged pharmaceutically active and naturally occurring amides

The β-bis-arylamides framework is a privileged structure embedded in various pharmaceutically active drugs and natural products (Figure 1). The bio-significance of β-bis-aryl amides propelled extensive endeavor towards their synthesis and development of novel and scalable protocols. Various synthetic approaches for β-bis-aryl amides have been documented in the literature,[1] however, the majority of them suffer either from the use of transition metal and expensive metal catalyst, long reaction times, harsh reaction conditions, and tedious workup. Therefore, development of mild and metal-free catalytic conditions for this reaction is highly desirable.

In recent years, the *p*-quinone methide derivatives gained attraction among synthetic organic chemistry, due to its unique reactivity[2] and its ability for 1,6-conjugate addition with a variety of nucleophiles.[3] *p*-Quinone methide motif serves as an important reactive intermediate in various natural product syntheses[4] and biosynthetic transformations.[5] Recently, *p*-quinone methides (*p*-QMs) were extensively studied for addition reaction, using the Lewis acid, organocatalytic, and transition-metal-catalyzed transformations.[6] Anand and co-workers have thoroughly investigated the chemistry of *p*-quinone methides for 1,6-conjugate addition with a variety of nucleophiles[7] using Lewis acid, N-heterocyclic carbene, bis(amino)cyclopropenylidene, and transition metal as a catalyst. Fan, Tortosa, and their co-workers including many other groups have studied the asymmetric Michael addition of *p*-quinone methides with malonates, enamines, borane thioester, and glycine Schiff base.[8,9] Lin and co-workers independently studied the reaction of *p*-quinone methide[10] catalyzed by the Lewis acid for the construction of unsymmetrical triarylmethanes.[10a] Bifunctional Pd complex and thiourea-catalyzed [3 + 2] annulation of *p*-QMs and vinylcyclopropanes is reported to give spirocycles with excellent diastereoselectivity.[10b] Construction of spirocycles via tandem 1,6-addition/cyclization with vinyl *p*-QMs was reported by Fan and

EurJOC European Journal of Organic Chemistry

FULL PAPER

DOI: 10.1002/ejoc.201500962

Modular Synthesis of Biaryl-Substituted Phosphine Ligands: Application in Microwave-Assisted Palladium-Catalyzed C–N Cross-Coupling Reactions

Chandani Singh,[a] Jayant Rathod,[a] Vishwajeet Jha,[b] Armen Panossian,[b] Pradeep Kumar,*[a] and Frédéric R. Leroux*[b]

Keywords: Synthetic methods / Homogeneous catalysis / Palladium / Cross-coupling / Microwave chemistry / Biaryls / Phosphines

Biaryl-substituted monophosphine-based ligands have been synthesized by transition-metal-free "ARYNE" cross-coupling reaction of aryllithiums with 1,2-dibromobenzene and subsequent regioselective functionalization through bromine–lithium interconversion. These ligands were employed in palladium-catalyzed C–N bond-forming reactions. The reaction was found to be general with wide substrate applicability. A wide variety of both primary and secondary amines were successfully coupled with an array of differently substituted halobenzenes under microwave irradiation to give the expected products in good to excellent yields. A number of biaryl-substituted phosphine ligands screened for the coupling reaction showed that steric bulk and the electronic properties of substituents on phosphorus play a crucial role in governing the catalytic activity of C–N cross-coupling reactions.

Introduction

In last few years there has been tremendous upsurge of interest among the synthetic chemists in developing diverse methods for palladium-catalyzed C–N bond-forming reactions. Consequently, this synthetic transformation has gained utmost importance with its widespread use across various disciplines, such as the synthesis of key intermediates for fine chemicals, building blocks for pharmaceuticals, conducting polymers, and photographic materials. Despite significant advances in palladium-catalyzed C–N coupling reactions, many reported methods have limitations and suffer from drawbacks, such as generality of methods, tedious steps, expensive catalytic system, compatibility with various functional groups, selectivity, and rather long reaction time. In view of these issues, it is highly desirable to develop a general catalytic system, which could be readily accessible with a wide substrate scope in Pd-catalyzed amination reactions.

Monodentate phosphines that possess a binaphthyl skeleton – MOP-type ligands – have been extensively employed in asymmetric catalysis, including C–N bond forming reactions.[1–8] Among other methods reported, several new and bulky ligands,[9–13] which include electron-rich phosphines[14–20] and N-heterocyclic carbenes,[21–30] have been reported for Pd-catalyzed amination reactions. Buchwald and co-workers developed a new class of biaryl monophosphine ligands that were found to be useful in many cross-coupling reactions.[31] To find a catalytic system that incorporates improved and better features, various strategies that use catalysts based on multiple Pd sources and ligands have been developed by various research groups.[32–39] In addition, a more comprehensive approach to catalyst design that uses a multi-ligand system has also been employed for cross-coupling methodologies.[40–43]

As a part of our ongoing research program on C_1-symmetric biaryl-based phosphine ligands[44–48] and their application for various catalytic reactions, we report here the concise synthesis of biaryl-based phosphine ligands and demonstrate their application in Pd-catalyzed C–N bond-forming reactions.

Results and Discussion

Synthesis of Biaryl Monophosphines

Dialkylbiaryl-substituted phosphine ligands have been efficiently used in palladium-catalyzed amination reactions. It has been shown that they can favorably influence the reaction time, catalyst loading and reaction conditions. According to the reaction mechanism, steric bulk and electron-donor ability of the dialkylbiaryl-substituted phosphine ligands facilitate the formation of an active L_2Pd^0 and thus oxidative addition under mild conditions. Another

[a] Organic Chemistry Division, CSIR – National Chemical Laboratory,
Homi Bhabha Road, Pune 411008, India
E-mail: pk.tripathi@ncl.res.in
http://www.ncl-india.org/
[b] CNRS-University of Strasbourg (ECPM), UMR CNRS 7509, COHA,
25 Rue Becquerel, 67087 Strasbourg, France
E-mail: frederic.leroux@unistra.fr
http://www.coha-lab.org

Supporting information for this article is available on the WWW under http://dx.doi.org/10.1002/ejoc.201500962.

J Porous Mater (2017) 24:837–846
DOI 10.1007/s10934-016-0323-8

Highly active recyclable SBA-15-EDTA-Pd catalyst for Mizoroki-Heck, Stille and Kumada C–C coupling reactions

Jayant Rathod[1] · Priti Sharma[2] · Punam Pandey[1] · A. P. Singh[2] · Pradeep Kumar[1]

Published online: 22 November 2016

Abstract Highly efficient SBA-15-EDTA-Pd(11) heterogeneous catalyst was synthesized by covalent anchoring Pd-EDTA complex over organo-modified surface of SBA-15. SBA-15-EDTA-Pd(11) catalyst was found to exhibit excellent catalytic activity in appreciable yield for Heck, Stille and Kumada cross-coupling reactions. Catalytic system exhibited excellent activity for completion of reaction, isolation, Pd loading (0.87 mmol%) and yields of products as compared to earlier reported heterogeneous supported Pd catalysts. Covalently anchored heterogeneous SBA-15-EDTA-Pd(11) catalyst can be recycled for more than five times without noticeable loss in activity and selectivity.

Keywords SBA-15-EDTA-Pd · Heterogeneous · Mizoroki-Heck coupling · Stille reaction · Kumada reaction · C–C bond formation

1 Introduction

Palladium catalyzed Heck, Stille and Kumada cross-coupling reactions are the most fundamental and practical method for carbon–carbon bond formation of aryl halides with various nucleophiles in organic synthesis [1–3]. Several reports have been published on coupling reaction for the synthesis of symmetrical and unsymmetrical binary compounds; leading components for natural products, engineering materials, conducting polymers, molecular wires, liquid crystals [4], C–C bond formation and retro-synthesis [5].

Various supported heterogeneous palladium catalysts have been reported in the literature which includes palladium supported over polymer/dendrimer, palladium on carbon, palladium supported metal oxides, clays, molecular sieves, mesopores and nanopores etc. [6–10]. For the heterogeneous support ordered mesoporous material SBA-15; high surface areas, easily accessible surface sites, uniform pore sizes and good stability constitute the basis of promising suitable substitute as mesoporous support [11–13]. Heterogeneous surfaces should be modified by organic functional groups for anchoring metals and complexes for better application purpose and at the same time leaching of active moieties could be diminished by covalently anchoring over support.

As a part of our continuous effort to explore potential of SBA-15-EDTA-Pd(11) heterogeneous catalytic system; we have reported earlier synthesis and characterization of SBA-15-EDTA-Pd(11) and its application for Suzuki and Sonogashira coupling reactions [14]. The physical properties of SBA-15-EDTA-Pd(11) measured are as follows; N% = 2.5, Pd% = 6.2, BET surface area = 363 $m^2\ g^{-1}$ (elemental analysis of Pd is based on ICP-OES analysis). Catalyst displayed good reactivity on low catalytic loading

Jayant Rathod and Priti Sharma have contributed equally to this work.

Electronic supplementary material The online version of this article (doi:10.1007/s10934-016-0323-8) contains supplementary material, which is available to authorized users.

✉ Pradeep Kumar
pk.tripathi@ncl.res.in

[1] Division of Organic Chemistry, CSIR-National Chemical Laboratory, Dr. Homi Bhabha Road, Pune 411008, India

[2] Catalysis Division, CSIR-National Chemical Laboratory, Dr. Homi Bhabha Road, Pune 411008, India